Investigations into the Functions of Immunoglobulin-like Cell Adhesion Molecules During Vertebrate Neural Development

Submitted by

Heather Jane Yeomans

for the degree of

Doctor of Philosophy

Centre for Developmental Genetics

Department of Biomedical Science

November 2001

Summary

During neural development, each neuron sends an axon out from its cell body. Extending axons are guided by interactions between environmental factors and axonal receptors for these factors. It has been suggested that certain proteins of the immunoglobulin-like superfamily are among the molecules involved in axon guidance. In particular, TAG-1, L1 and NrCAM have previously been implicated in the guidance of dorsal spinal commissural axons at the ventral midline region known as the floor plate. To establish whether these molecules have such roles in mice, the dorsal spinal axons of *TAG-1*, *L1* or *NrCAM* mutant mouse embryos were traced. There were no significant differences between the results from mutant embryos and their wild type counterparts. This indicated that these three proteins are individually not essential for the normal development of mouse dorsal spinal projections. However, results from *TAG-1/L1* double mutant embryos suggested that TAG-1 and L1 might affect the ability of commissural axons to extend out of the floor plate. Analysis of *ephrin B3* mutant embryos indicated that ephrin B3 might also be important for floor plate exit.

As the *TAG-1* null mutation includes a *lacZ* construct, this reporter gene was used to further investigate the roles of TAG-1. Its expression was used to determine distribution of *TAG-1* gene activity in the developing mouse nervous system. As the pattern of reporter expression was found to be comparable with that of TAG-1 protein, the *TAG-1* null allele was used as a marker for TAG-1-expressing cells in mutant embryos. Most of the structures that normally express TAG-1 seemed to be unaffected by an absence of the protein. However, the hypoglossal nerve was significantly less likely to extend towards the tongue in *TAG-1* null homozygous embryos than in heterozygotes. This suggested that TAG-1 might be important for the guidance of hypoglossal axons.

Acknowledgements

I would like to thank some of the many people who have made this thesis possible:

- my supervisor Andy Furley, for his ideas, support, enthusiasm and faith in my ability.

- Brent Kiernan, who contributed as much to the DiI injection of dorsal spinal commissural axons as I did, and without whom those results would probably not have been analysed.

- Marty Grumet for *NrCAM* mutant mice, Nick Gale for *ephrin B3* mutant mice, and Jane Johnson for *math-1* mutant mice.

- all of those in Sheffield who looked after the mouse colonies; Andy Furley, Brent Kiernan, Rosie Summers and Rin Yoshida, for carrying out so much of the genotyping

- Esther Stoeckli, for instructing me in the ways of labelling dorsal spinal commissural axons with DiI.

- various housemates, including Jane, Phil, Stu, Chris, and Sarah, for their patience, encouragement and entertainment.

- Rob.

- and, last but not least, my long-suffering parents.

Contents

Please note that throughout this thesis, the term "*TAG-1* null mutant" has been applied to embryos or mice carrying the either one copy (heterozygotes) or two copies (homozygotes) of the *TAG-1* null allele. Thus, "heterozygous null" mutants are those that carry one copy of the null allele.

List of Figures

List of Tables

Selected Abbreviations* and Definitions

ANOVA	analysis of variance
BMP	bone morphogenetic protein
bp	base pairs
CAM	cell adhesion molecule
DAB	3,3"-diaminobenzidine tetrahydrochloride (used to visualise labelling by horseradish-peroxidase conjugated antibodies)
dATP	deoxyadenosine triphosphate
DCC	Deleted in colorectal cancer (a receptor for netrin proteins).
dCTP	deoxycytidine triphosphate
dGTP	deoxyguanidine triphosphate
DiI	1,1'-dioctadecyl-3,3,3',3'-tetramethylindocarbocynine perchlorate
DMF	dimethyl formamide
dTTP	deoxythymidine triphosphate
ECM	extracellular matrix
EDTA	ethylenediaminetetraacetic acid
EGTA	ethylene glycol-bis(ß aminoethyl ether)-N,N,N',N'-tetraacetic acid
ephrin B3 mutant mice	mice either heterozygous or homozygous for the *ephrin B3* null mutation
FITC	fluorescein isothiocyanate
FNIII	fibronectin type III domain
HGF	hepatocyte growth factor
Ig domain	immunoglobulin-like domain
IgCAM	immunoglobulin-like cell adhesion molecule
IgSF	immunoglobulin-like super-family
lacZ	the bacterial gene that encodes ß-galactosidase

L1 null mutant mice	mice either heterozygous or homozygous for the *L1* null mutation
NCAM	neural cell adhesion molecule
NgCAM	neural-glial cell adhesion molecule
NrCAM	NgCAM-related cell adhesion molecule
NrCAM null mutant mice	mice either heterozygous or homozygous for the *NrCAM* null mutation
PBS	phosphate buffered saline
PCR	polymerase chain reaction
Rpm	revolutions per minute
RPTP	receptor protein tyrosine phosphatase
SDS	sodium dodecyl silphate
TAG-1	transiently expressed axonal glycoprotein 1
TAG-1 null mutant mice	mice either heterozygous or homozygous for the *TAG-1* null mutation, which is shown in figure 1.7 C
TAG^{A} mutant mice	mice either heterozygous or homozygous for the *TAG-1* truncation, which is shown in figure 1.7 B
TAX-1	the human homologue of TAG-1
TRITC	tetremethyl rhodamine isothiocyanate
TUNEL	TdT-mediated dUTP-biotin nick end labelling
VEMA	ventral midline antigen
X-gal	5-bromo-4-chloro-3-indolyl-ß-$_{D}$-galactopyranoside

* For the anatomical abbreviations used in chapter 5, see appendix 5A.

1 Introduction

1.1 Axon Guidance

The vertebrate nervous system is a highly complex network. It is estimated that there are as many as 10^{11} neurons in the human brain, and this figure does not include neurons of the spinal cord or peripheral nervous system. The neurons of the brain make around 10^{14} connections, or synapses (Garrity and Zipursky, 1995), and so form the basis of a large number of neural pathways. It is along such routes that all nervous information is passed. The fact that these pathways are highly similar between individuals of the same species suggests that neural development is precisely controlled.

Each neuron consists of a cell body and a number of processes known as neurites. Cajal and Harrison both showed that the longest of these, which is called the axon, extends from the cell body to a target during development (Cajal, 1909; Harrison, 1910). Weiss proposed that axon outgrowth was undirected, that targets were reached at random, and that non-functional connections were subsequently pruned back (Weiss, 1936). More recent work has shown that it is indeed possible to eliminate surplus connections, on the basis of a lack of neuronal activity (Purves and Lichtman, 1980).

Activity-dependent refining of neuronal connections is important for the development of a properly wired nervous system. However it is now known that initial axonal outgrowth, which occurs before the onset of electrical activity, actually lays down a relatively specific network of neuronal connections (Goodman and Shatz, 1993). Sperry's "chemoaffinity hypothesis" first suggested that extending axons are guided by relative affinities for different areas, being directed by gradients of chemical signals (Sperry, 1963). Such gradients are indeed found in the developing nervous system. They may be established either by release of a molecular "cue" from a distinct source, as is the case with netrins in the spinal cord, or by graded expression of the molecule by a field of cells, as for ephrin ligands across the retina (Tessier-Lavigne and Goodman, 1996). It is now known that some axon guidance cues can also work in a more discrete way than Sperry envisaged. For example, extending axons can turn to grow along certain nerve fibres and yet avoid others (the "labelled pathway hypothesis": Goodman *et al.*, 1984; Bastiani *et al.* 1984; Raper *et al.*, 1983a, 1983b, 1984), and can respond to individual "guidepost cells" (Bentley and Caudy, 1983). Axon guidance cues have often been assigned to one of four categories, being thought of as either long range or short range signals, and molecules of either type having either positive or negative effects upon axon growth (Figure 1.1; Tessier-Lavigne and Goodman, 1996, Jessell and Sanes, 2000). However, it is now known that certain single guidance molecules

function as both long- and short-range cues. For example, netrin-1 can be membrane bound (Serafini *et al.*, 1994) or diffusible (Kennedy *et al.*, 1994), and slit appears to act as both a long and short range repellent (Kidd *et al.*, 1999; Simpson *et al.*, 2000). Furthermore, single guidance molecules can function as both positive and negative signals, as has been demonstrated for Semaphorin 1 (Wong *et al.*, 1997), Semaphorin 3A (Song *et al.*, 1998; Tuttle and O'Leary, 1998), Netrin-1 (Colamarino and Tessier-Lavigne, 1995; Ming *et al.*, 1997, 2001; Hong *et al.*, 1999; Höpker *et al.*, 1999), Slit-2 (Nguyen Ba-Charvet *et al.*, 1999, 2001; Wang *et al.*, 1999 a; Zinn and Sun, 1999) and myelin-associated glycoprotein (Ming *et al.*, 2001). Therefore, distinctions between the four modes of action shown in figure 1.1 are not always clear (Mueller, 1999; Jessell and Sanes, 2000).

To generate a different guidance cue for each decision point in the nervous system would require more genes than are contained in the human genome (Treubert and Brümmendorf, 1998). Instead it seems that an armoury of different molecules are used at particular times, in precise combinations and in specific contexts. In order to respond to environmental cues, the leading edge of the axon, referred to as the growth cone (Cajal, 1909), bears numerous receptor molecules. When activated, such receptors initiate intracellular signalling events, which subsequently cause the growth cone to proceed either towards or away from the cue (Gomez *et al.*, 2001).

Of the many cell surface receptor molecules, those that are able to mediate adhesion by their interactions are classified as cell adhesion molecules (CAMs). Some CAMs recognise components of the extracellular matrix (ECM), as for example do the integrins (figure 1.2). Others interact with counter-receptors on other cells, either using a different sort of molecule or using another CAM of the same type, as is commonly the case for cadherins. Certain proteins of the immunoglobulin-like superfamily (IgSF) can act both as ECM receptors and as counter-receptors for molecules, including themselves, on other cells. Many of the CAMs implicated in axon guidance belong to the IgSF (i.e. are 'IgCAMs'), and it is on this group of proteins that the present study concentrates.

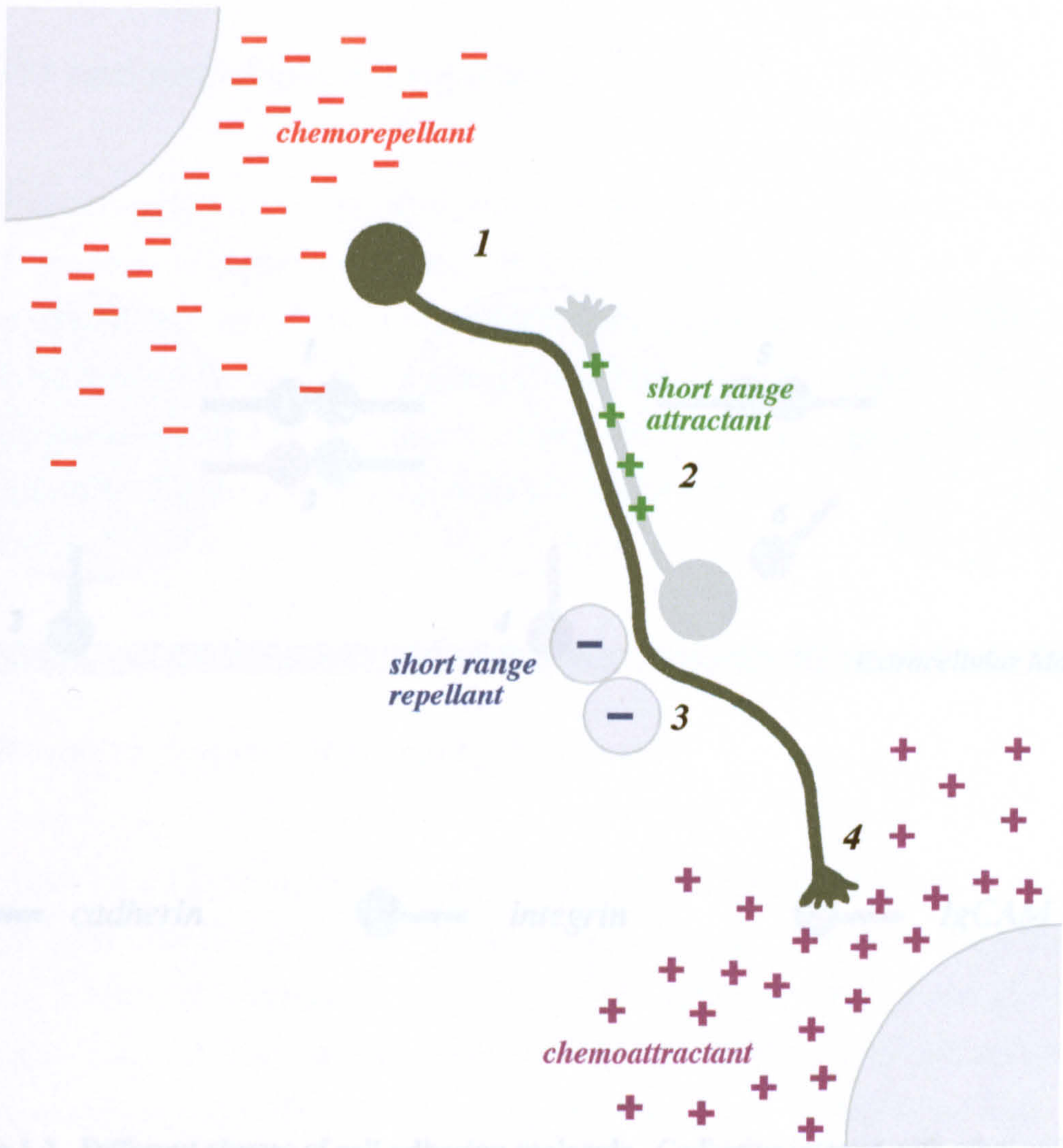

Figure 1.1. Four major mechanisms of axon guidance. The four types of axon guidance force are shown schematically, with respect to the dark grey neuron. Axons can be guided by long range chemorepulsive cues (1) , depicted here as diffusing from the source on the left. Such chemorepulsive factors may include semaphorins (Messersmith *et al.*, 1995; Puschel et al., 1995; Bagnard *et al.*, 2000), netrins (Colamarino and Tessier-Lavigne, 1995; Hopker *et al.*, 1999), slits (Li *et al.*, 1999; Nguyen Ba-Charvet *et al.*, 1999) and bone morphogenetic proteins (BMPs; Augsburger *et al.*, 1999). There can be contact-mediated attraction (2), for example during the fasciculation along other axons that is mediated by proteins such as NCAM (Thanos *et al.*, 1984) or L1 (Stoeckli and Landmesser, 1995). There can also be contact-mediated repulsion (3), such as that caused by ephrin ligands (reviewed in O'Leary and Wilkinson, 1999), some semaphorins (Yu *et al*, 1998) and slits (Kidd *et al.*, 1999). Axons may also be guided by long-range chemoattractant molecules (4), such as netrins (Kennedy *et al.*, 1994; Serafini *et al.*, 1996), some semaphorins (Bagnard *et al.*, 2000) and hepatocyte growth factor (HGF; Ebens *et al.*, 1996; Caton *et al.*, 2000). Using Tessier-Lavigne and Goodman, 1996; Varela-Echavarría and Guthrie, 1997; Jessell and Sanes, 2000.

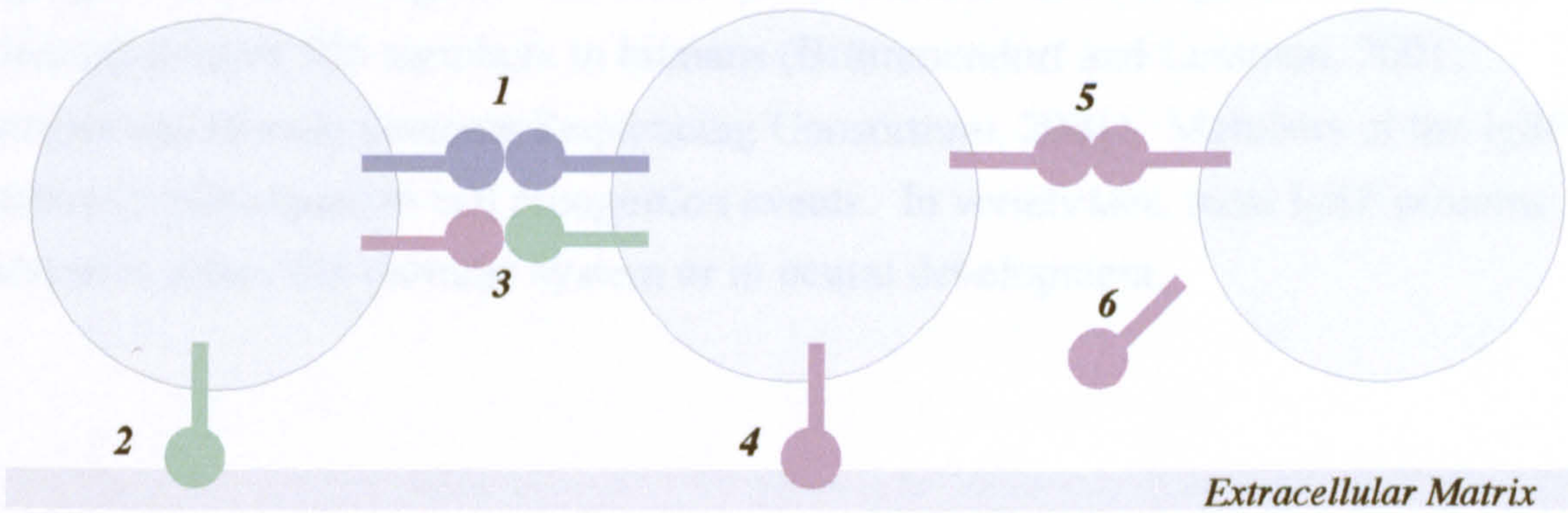

Figure 1.2 Different classes of cell adhesion molecule. Cadherins interact with other cadherins, to mediate cell to cell contact (1). Integrins interact with components of the extracellular matrix (2), or with IgCAMs on the surfaces of other cells (3). IgCAMs can interact with cell-surface integrin (3), components of the extracellular matrix (4) or other IgCAMs (5). Some IgCAMs are also secreted (6).

1.2 Neural IgSF Molecules

1.2.1 The immunoglobulin-like superfamily

The IgSF is currently the largest superfamily of proteins. It is represented in organisms ranging from yeast to higher vertebrates (Brümmendorf and Rathjen, 1995), and is estimated to have 765 members in humans (Brümmendorf and Lemmon, 2001; International Human Genome Sequencing Consortium, 2001). Members of the IgSF commonly participate in cell recognition events. In vertebrates, most IgSF proteins function in either the immune system or in neural development.

1.2.2 Structural features of neural IgSF molecules

As is the case for all IgSF members, those of the nervous system contain immunoglobulin-like (Ig) domains. These domains are generally defined by the presence of two cysteine residues, which are separated by between 55 and 75 other amino acids. The two cysteine residues form a disulphide bond with one another, to give a characteristic loop. The intra-cysteine residues, many of which are also conserved, form a secondary structure of ß-pleated sheets. These fold into a so-called "Greek Key" conformation (Williams and Barclay, 1988; Vaughn and Bjorkman, 1996), and allow the immunoglobulin-like domain to be assigned to a particular sub-type. Initially, Ig domains were classified either as "C1", "C2" or "V"-type, according to their similarity to either the constant or variable regions of antibodies, and most of the neural Ig domains were assigned to the C2 set (Williams and Barclay, 1988). More recently, the Ig domains found in many neural cell surface molecules have been reclassified as belonging to an "I" set, so called as the domains appear to in fact be intermediate between the C and V categories (Harpaz and Chothia, 1994; Chothia and Jones, 1997). However, it has also been suggested that the I-type immunoglobulin domains are actually merely a subset of the V class (Vaughn and Bjorkman, 1996). For the purposes of this thesis, the neural Ig domains which were originally referred to as C2-type will be shown as I-type, and the few neural Ig domains defined originally as V-type will still be classified as such (Williams and Barclay, 1988; Chothia and Jones, 1997).

In addition, many of the neural IgSF molecules contain "fibronectin type III" (FNIII) domains, which are so called because of their similarity to particular regions of the ECM molecule fibronectin (Brümmendorf and Rathjen, 1995; Chothia and Jones, 1997). These regions have the same Greek Key structure as Ig domains (Vaughn and Bjorkman, 1996; Cota *et al.*, 2000), and are sometimes even referred to as Ig-like structures of the same class as the "C2" type domains (Bork *et al.*, 1994).

As can be seen in figure 1.3, different combinations of these two types of domains are used to generate a large number of molecules. These molecules can be grouped into sub-families according to the combination of domains that they contain, with some sub-family members also showing up to 60% homology in their amino acid sequences (Holm *et al.*, 1996; Ogawa *et al.*, 1996). It should be noted that figure 1.3 is a stylised diagram, showing the proteins' constituent domains rather than their native conformations. The binding abilities of axonin-1 domain-deletion constructs indicated that the first four Ig-like domains might in fact form a "horseshoe-like" conglomerate (Rader *et al.* 1996; as in figure 1.4 B). Crystallography has since shown that this is indeed the case for axonin-1 (Freigang *et al.*, 2000), and for part of hemolin, an insect Ig-like molecule (Su *et al.*, 1998). Rotary shadowing electron microscopy (Hall *et al.*, 2000) and negative stain electron microscopy (Schürmann *et al.*, 2001) seem to provide evidence that the N-terminal Ig domains of L1 form a similar shape. Rotary shadowing electron microscopy has also led to the suggestion that axonin-1 shows additional folding (Rader *et al.*, 1996; figure 1.4 C), although whether L1 can have such a conformation remains unclear. It could be that IgCAMs exist in multiple conformations *in vivo*, and that the ability to switch between isoforms is important for their binding to other proteins (Freigang *et al.*, 2000; Schürmann *et al.*, 2001).

1.2.3 Meet the family

N-CAM, the first IgCAM to be characterised (Hoffman *et al.*, 1982), and its closest relations all have five "I" type Ig-like domains, and either one or two FNIII domains (figure 1.3 A). TAG-1-like sub-family molecules all have six I-type Ig domains and four FNIII regions. TAG-1-like proteins, as with those of the N-CAM-like sub-family, can be either attached to the cell surface by a glycosylphosphatidyl-inositol (GPI) anchor, or secreted (figure 1.3 B; Furley *et al.*, 1990; Karagogeos *et al*, 1991; Ruegg *et al.*, 1989; Wolff *et al.*, 1989). L1-like molecules also have six I-type Ig regions, but

D

E

F

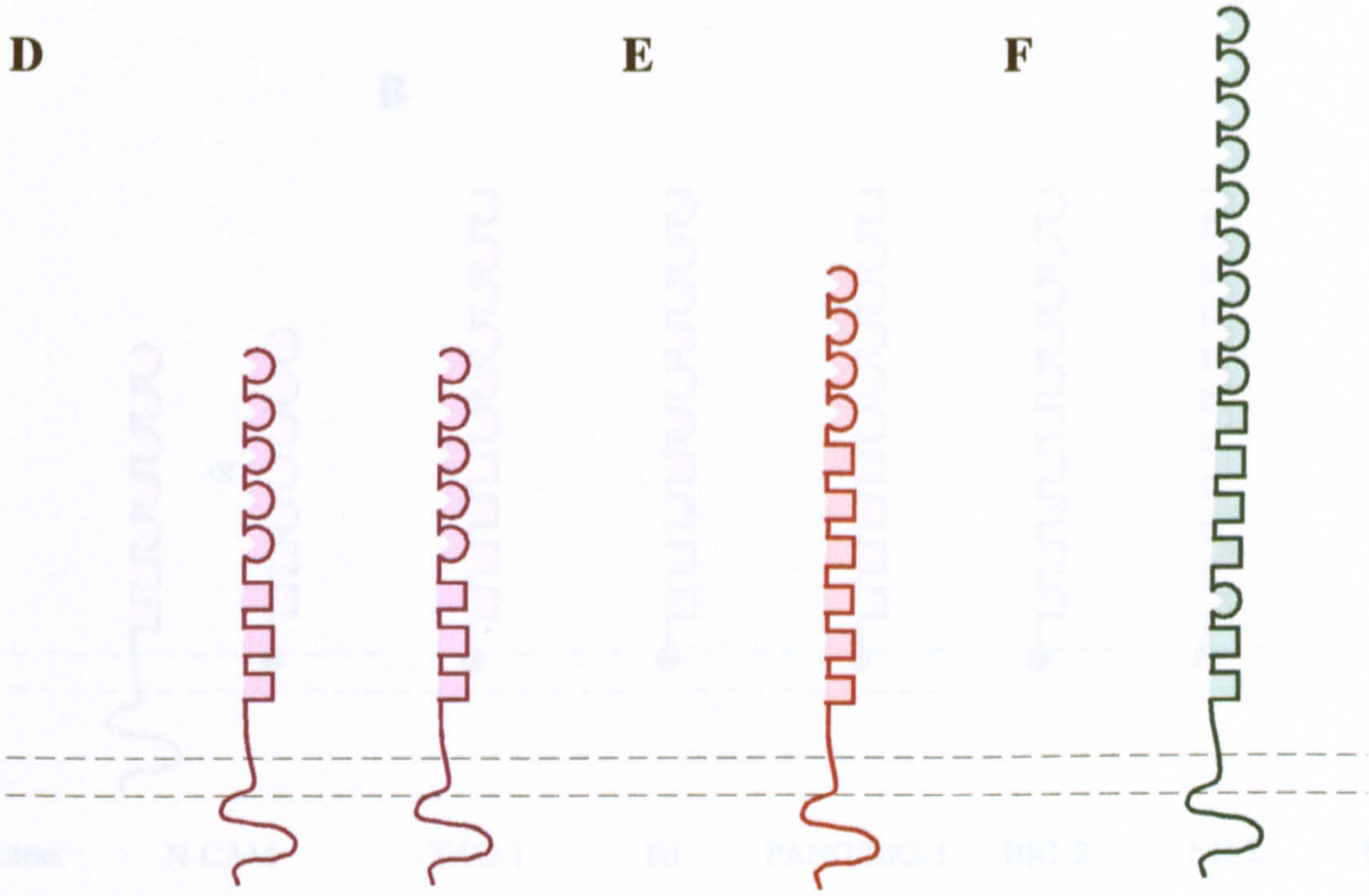

rat/mouse: rRobo-1 rRobo-2 DCC

chick: neogenin

human: hRobo-1 hRobo-2 DCC DSCAM

G

H

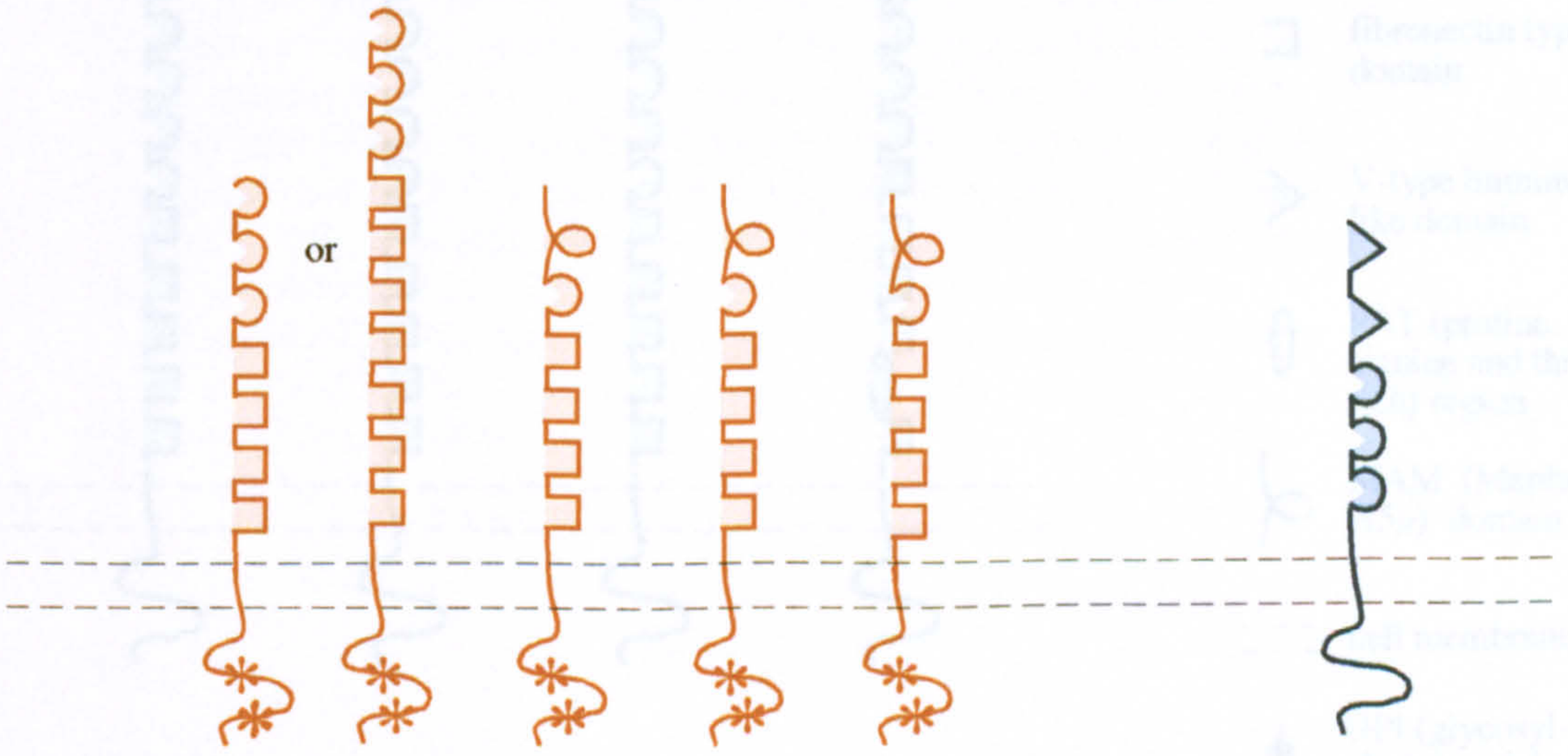

rat/mouse: PTPσ PTPκ PTPμ PTPψ DM-GRASP/BEN/SC1

chick: CRYPα DM-GRASP/BEN/SC1

human: DM-GRASP/BEN/SC1

Figure 1.3, continued. For key, see previous page. D: Robo proteins. E: DCC (Deleted in Colorectal Cancer). F: DSCAM (Downs Syndrome Cell Adhesion Molecule). G: Type II receptor protein tyrosine phosphatases (R-PTPs). PTPσ can occur in one of two forms. H: DM-GRASP, which is also known as BEN and SC1. For references, see text.

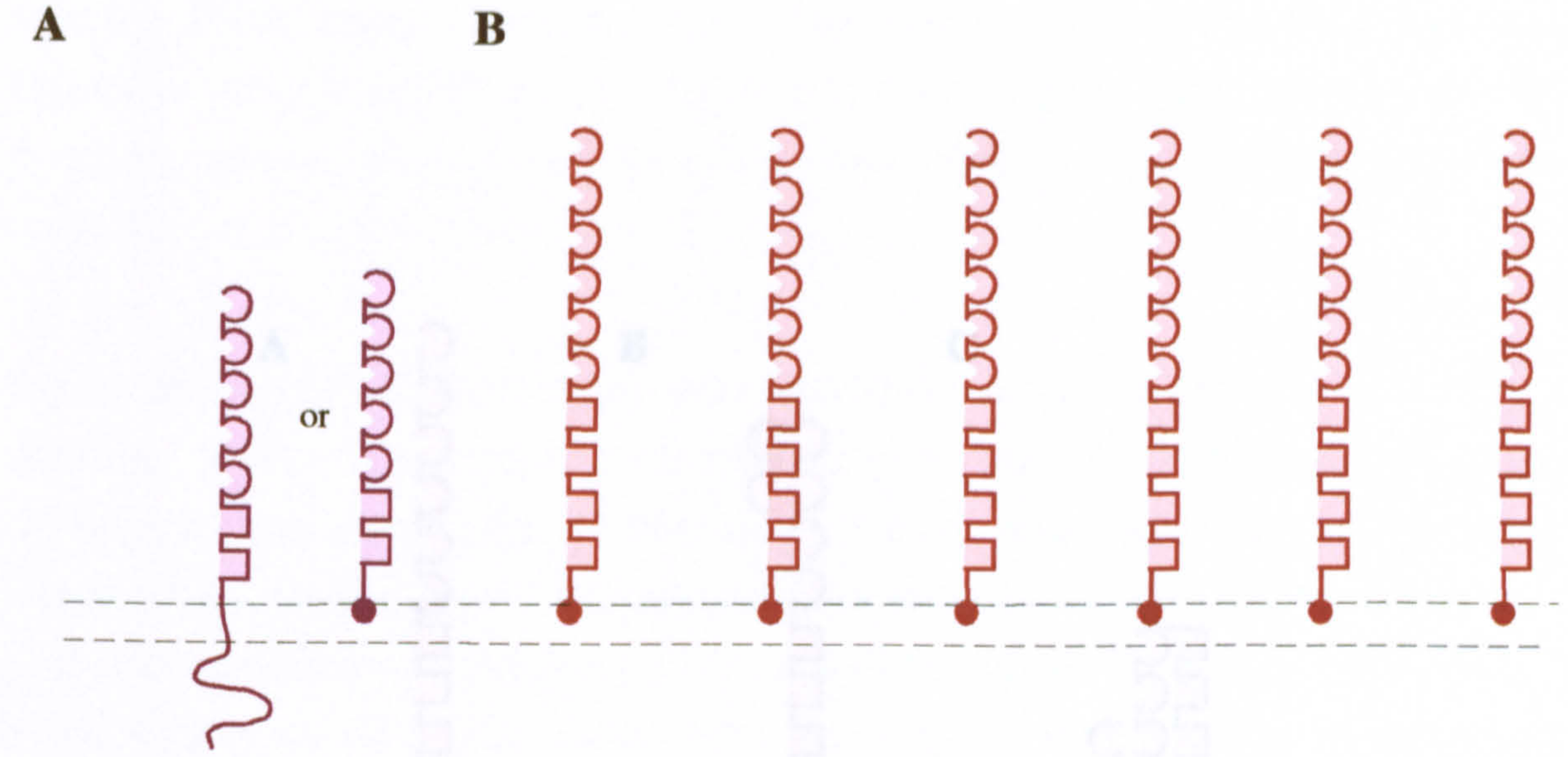

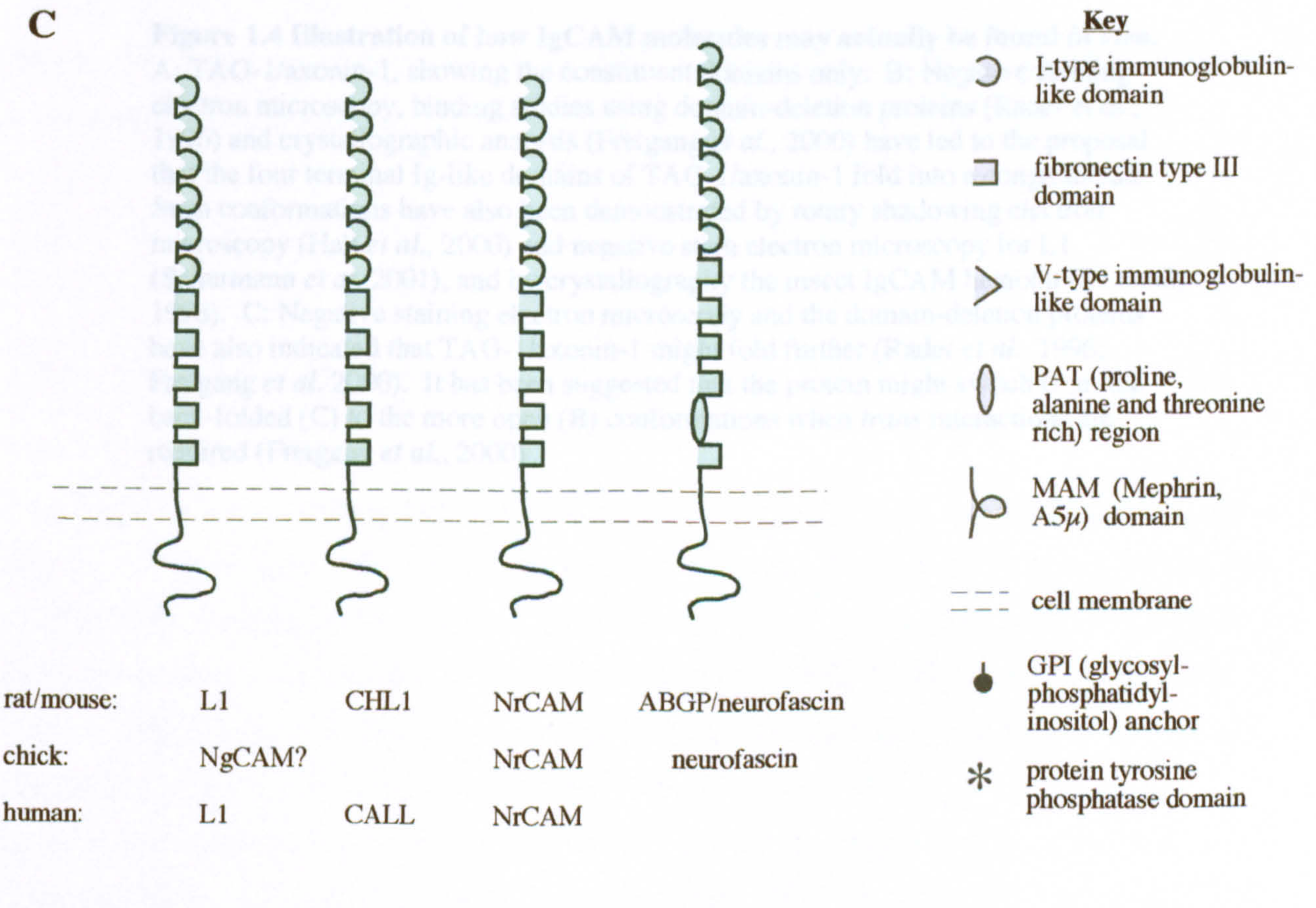

Figure 1.3 Selected vertebrate members of the Immunoglobulin-like superfamily that have been implicated in development of the nervous system. A: NCAM, which can occur either as a trans-membrane or GPI-anchored protein. B: The TAG-1-like subfamily. All members are attached to the membrane by a GPI-linkage, although at least two are also secreted. C: The L1-like subfamily. Continues overleaf. For references, see text.

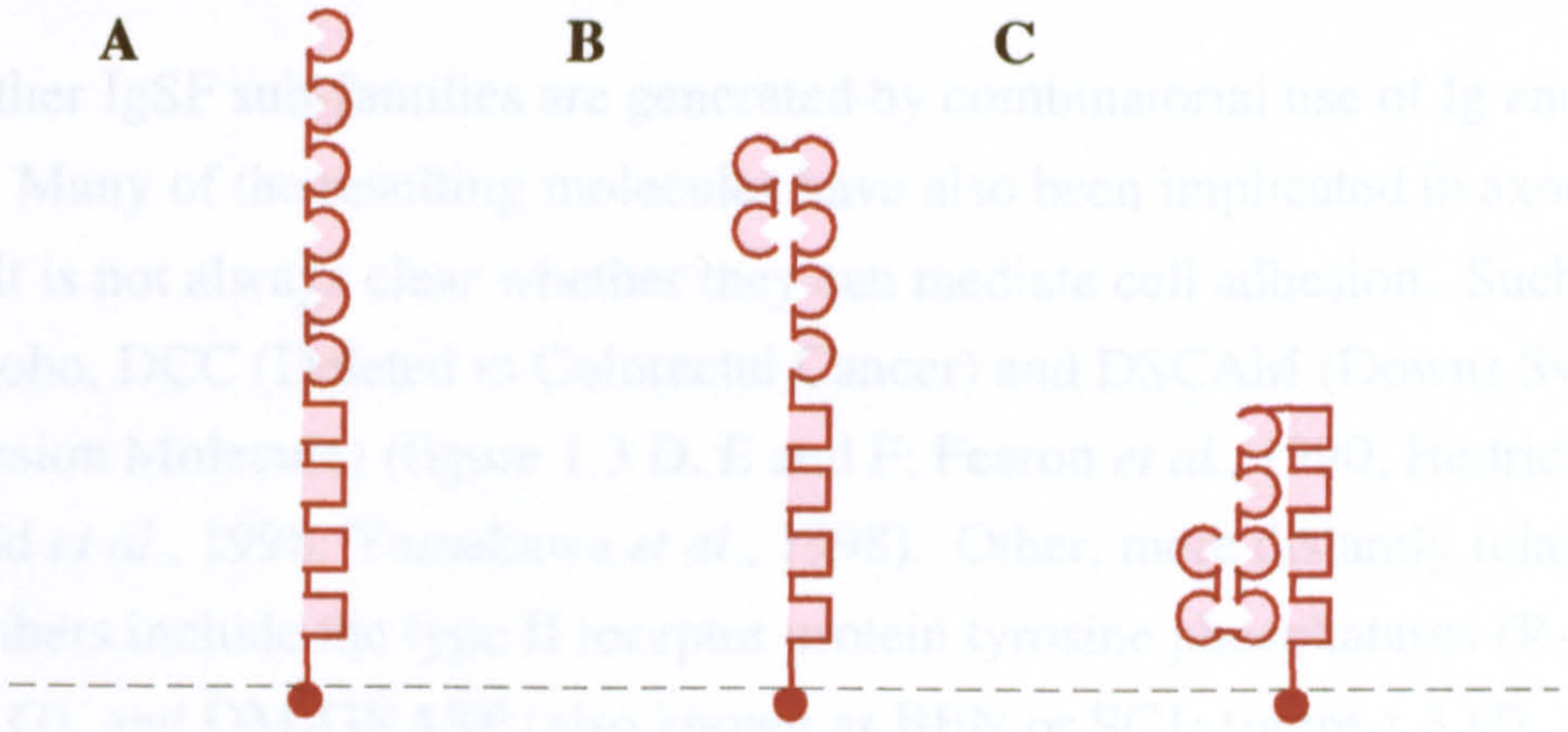

Figure 1.4 Illustration of how IgCAM molecules may actually be found *in vivo*. A: TAG-1/axonin-1, showing the constituent domains only. B: Negative staining electron microscopy, binding studies using domain-deletion proteins (Rader *et al.*, 1996) and crystallographic analysis (Freigang *et al.*, 2000) have led to the proposal that the four terminal Ig-like domains of TAG-1/axonin-1 fold into a conglomerate. Such conformations have also been demonstrated by rotary shadowing electron microscopy (Hall *et al.*, 2000) and negative stain electron microscopy for L1 (Schurmann *et al.* 2001), and by crystallography the insect IgCAM hemolin (Su *et al.*, 1998). C: Negative staining electron microscopy and the domain-deletion proteins have also indicated that TAG-1/axonin-1 might fold further (Rader *et al.*, 1996; Freigang *et al.* 2000). It has been suggested that the protein might switch from the back-folded (C) to the more open (B) conformations when *trans* interactions are required (Freigang *et al.*, 2000)

have five FNIII domains rather than four. They have transmembrane and cytoplasmic sequences rather than GPI anchors (figure 1.3 C), although in some circumstances the metalloproteinases might release the extracellular portions of L1-like molecules from cells (Beer *et al.*, 1999; Gutwein *et al.*, 2000).

Several other IgSF sub-families are generated by combinatorial use of Ig and FNIII domains. Many of the resulting molecules have also been implicated in axon guidance, although it is not always clear whether they can mediate cell adhesion. Such proteins include Robo, DCC (Deleted in Colorectal Cancer) and DSCAM (Downs Syndrome Cell Adhesion Molecule) (figure 1.3 D, E and F; Fearon *et al.*, 1990; Hedrick *et al.*, 1994; Kidd *et al.*, 1998; Yamakawa *et al.*, 1998). Other, more distantly related neural IgSF members include the type II receptor protein tyrosine phosphatases (R-PTPs; figure 1.3 G), and DM-GRASP (also known as BEN or SC1; figure 1.3 H). The former are distinguished by cytoplasmic phosphatase activity, while the latter includes immunoglobulin regions of the V-type (Burns *et al.*, 1991; Tanaka *et al.*, 1991, Desai *et al.*, 1997; Stoker and Dutta, 1998).

Much of this thesis will focus upon the TAG-1- and L1-like proteins, and their roles in development of the mouse nervous system.

1.2.4 The TAG-1-like sub-family

The TAG-1-like subfamily contains at least six different molecules (figure 1.3 B), and is represented in at least three vertebrate classes. The rodent molecule TAG-1 (Furley *et al.*, 1990) has homologues in zebrafish (Warren et al., 1999) and chicken. In the latter case, the protein is known as axonin-1 (Ruegg *et al.*, 1989; Zuellig *et al.*, 1991). The human homologue of TAG-1 is known as TAX-1, although the gene is also sometimes referred to as *CNTN2* (Tsiotra *et al.*, 1993; Hasler *et al.*, 1993). F3, which is also known as Contactin, has been characterised in rodents (Gennarini *et al.*, 1989) and its chicken homologue is known as F11 (Rathjen *et al.*, 1987 a; Brümmendorf *et al.*, 1989). There is also a human homologue of F3, the gene for which is often referred to as *CNTN1* (Berglund and Ranscht, 1994; Ried *et al.*, 1994). BIG-1, which is also known as PANG, has been characterised in rodents (Yoshihara *et al.*, 1994) and humans. In the latter, gene is known as called *CNTN3* (Mock *et al.*, 1996). BIG-2 has been described

in rodents (Yoshihara *et al.*, 1995). NB-2 has been identified in rodents (Ogawa *et al.*, 1996), and humans, in which the gene is called *CNTN5* (Kamei *et al.*, 1998). It has also recently been identified as FAR-2 in chicken (Plagge *et al.*, 2001). Humans also possess a homologue of the sixth rodent TAG-1-like protein, NB-3 (also referred to as *CNTN6*: Ogawa *et al.*, 1996; Kamei *et al.*, 2000). Amino acid sequence homology has recently indicated that there may also be TAG-1-like molecule in *Drosophila melanogaster* (A.J.W. Furley, personal communication).

Vertebrate TAG-1-like proteins share between 40% and 60% amino acid sequence homology with one another (Brümmendorf and Rathjen, 1995; Holm *et al.*, 1996; Ogawa *et al.*, 1996; Kamei *et al.*, 2000). All have been implicated in neural development, and TAX-1 has also recently been suggested to play a role in glial tumour migration (Rickman *et al.*, 2001).

1.2.5 The L1-like sub-family

Members of the L1-like sub-family show less homology with one another than those of the TAG-1-like sub-group, sharing around 40% amino acid sequence similarity (Brümmendorf and Rathjen, 1995). In rodents, the L1-like sub-family currently has four members: L1 (previously also known as NILE in rat: Rathjen and Schachner, 1984; Bock *et al.*, 1985), Neurofascin (also known as ABGP: Davis *et al.*, 1993), NrCAM (Moscoso and Sanes, 1995), and CHL1 (Close Homologue of L1: Holm *et al.*, 1996). Neurofascin has been identified in chicken (Rathjen *et al.*, 1987 a). NrCAM (also referred to as Bravo) has been characterised in chicken (Grumet *et al.*, 1991) and human (Lane *et al*, 1996). The human homologue of CHL1 is known as CALL (Wei *et al.*, 1998).

L1 has also been identified in other species. However, the identity of L1 homologues in other vertebrate classes is not always clear. Zebrafish appear to have two L1 homologues, L1.1 and L1.2 (Tongiorgi *et al.*, 1995). The chicken homologue of L1 is commonly thought to be NgCAM (Grumet and Sakurai, 1996), which is often assumed to be identical to the chick molecule G4 (Rathjen *et al.*, 1987; Kuhn *et al.*, 1991). However, there are notable differences between these proteins (Rathjen *et al.*, 1987 b; Burgoon *et al.*, 1991; Kayyem *et al.*, 1992; for discussion, see chapter 3, Grumet 1992,

and Sonderegger and Rathjen, 1992). Thus there could in fact be at least five classes of vertebrate L1-like molecules (Holm *et al.*, 1996), rather than four (Hortsch, 2000).

The L1-like sub-family of neural IgCAMs is also represented in invertebrates, by the *Drosophila melanogaster* molecule neuroglian (Bieber *et al.*, 1989), the *Hirudo medicinalis* (leech) protein Tractin (Huang *et al.*, 1997), and the LAD-1 protein of *Caenorhabditis elegans* (Chen *et al.*, 2001).

The human *L1* gene has been studied in particular detail, as it has been implicated in a number of X-linked neurological conditions. Symptoms commonly presented by *L1* hemizygous male patients include corpus callosum agenesis, mental retardation, adducted thumbs, spastic paraplegia and hydrocephalus (reviewed in Wong *et al.*, 1995; Brümmendorf *et al*, 1998; Kamiguchi *et al.*, 1998), collectively referred to as the CRASH syndrome (Fransen *et al.*, 1998). L1 might also have a role in the ability of axons to regenerate (Becker *et al.*, 1998), and both L1 and NrCAM have been implicated in tumour development (Izumoto *et al.*, 1996; Sehgal *et al.*, 1998)

1.3 A web of interactions

1.3.1 Interactions of IgCAMs *in vitro*

Variations on the basic structural theme of immunoglobulin-like and fibronectin-type III domains afford a battery of cell surface molecules, many of which are found on axons. As is true of all cell surface molecules, the neural Ig-like proteins function by interacting with other molecules. In order to understand these proteins it is important to characterise their interactions (Volkmer *et al.*, 1996). The interactions of TAG-1- and L1- like sub-family members have been studied extensively, and figure 1.5 summarises some of the findings (see figure legend for details).

Evidence for interactions has been obtained in a number of different ways. Some associations have been demonstrated by the ability of tagged proteins to attach to particular substrates (as in Lustig *et al.*, 1999), or by the aggregation of inert spheres conjugated with the molecules of interest (e.g. Grumet and Edelman, 1988; as in figure 1.6 A). Others have been identified on the basis of cell binding assays, using cells that naturally expressed only certain cell surface molecules (Kadmon *et al.*, 1990), or that have been specifically transfected with molecules of interest (e.g. Felsenfeld *et al.*, 1994; Buchstaller *et al.*, 1996; as in figure 1.6 B). Some interactions have been inferred from the ability of molecules to be co-immunoprecipitated from cell or tissue extracts (e.g. L1 and NCAM: Kadmon *et al.*, 1990; axonin-1 and NgCAM: Buchstaller *et al.*, 1996; NrCAM and Neurofascin, Volkmer *et al.*, 1996). Others have been suggested by the ability of proteins to co-localise within living cell membranes (e.g. L1 and NCAM: Pollerberg *et al.*, 1987; axonin-1 and NgCAM: Stoeckli *et al.*, 1996).

1.3.2 Interactions of IgCAMs *in vivo*

Thus an interaction between proteins *in vitro* does not necessarily mean that the same association occurs *in vivo*. Many of the techniques used to study IgCAM interactions *in vitro* have inadequacies, and results from different assay systems can seem to be contradictory. For example, NgCAM and axonin-1 could be said to interact on the basis of bead aggregation assays (Kuhn *et al.*, 1991), but seem unable to bind when expressed by cells (Buchstaller *et al.*, 1996). It has been proposed that this potential discrepancy

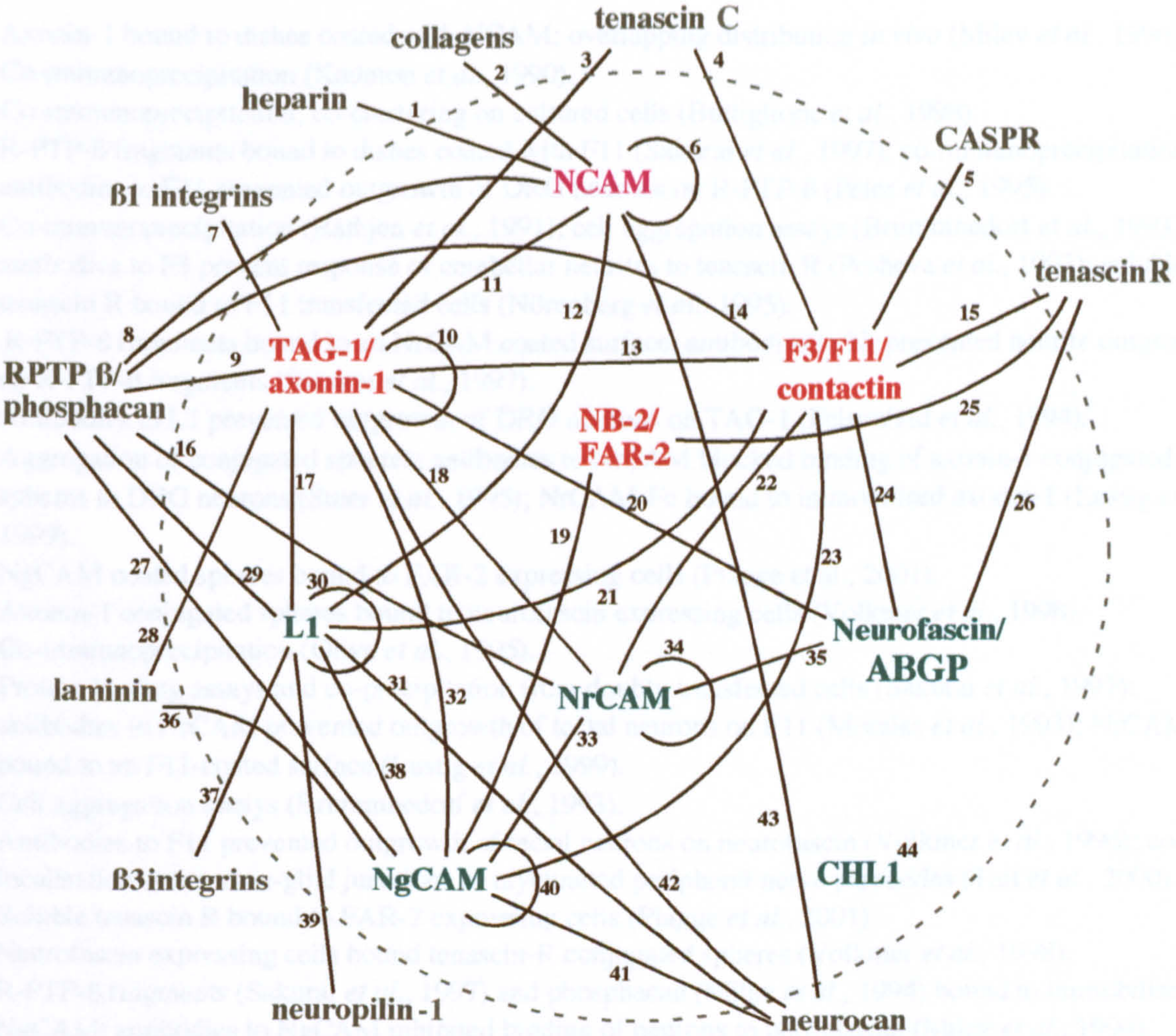

Figure 1.5 Possible interactions of N-CAM, L1-like and TAG-1-like members of the immunoglobulin-like superfamily. IgSF members are within the circle. Interactions of BIG-1, BIG-2, and NB-3 are not yet well documented. Numbers direct the reader to the experimental details and references below or overleaf. Note that the nature of interactions varies. For example, one line may represent a predominantly *cis* interaction, and another an interaction that occurs in *trans*; some assays indicate that the interaction mediates growth as well as adhesion, where as others do not.

1) An antibody to NCAM prevented attachment of cells to heparin (Cole *et al.*, 1985; Cole *et al.*, 1986).
2) Soluble NCAM bound to immobilised collagens (Probstmeier *et al.*, 1989)
3) Axonin-1 bound to immobilised tenascin-C; co-localisation *in vivo* (Milev *et al.*, 1996).
4) F11 bound to immobilised tenascin-C (Zisch *et al.*, 1992).
5) Co-immunoprecipitation; co-expression *in vivo* (Peles *et al.*, 1997).
6) Aggregation of NCAM-containing lipid vesicles (Hoffman and Edelman, 1983); cell aggregation assays (Felsenfeld *et al.*, 1994).
7) Antibodies to β1 integrins prevented outgrowth of tectal neurons on TAG-1 (Felsenfeld *et al.*, 1994).
8) R-PTP-ß fragments (Sakurai *et al.*, 1997) and phosphacan (Milev et al., 1994) bound to immobilised NCAM; antibodies to NCAM inhibited binding of neurons to phosphacan (Milev *et al.*, 1994).
9) Phosphacan bound to immobilised axonin-1; overlapping distribution *in vivo* (Milev, *et al.*, 1996).
10) Cell aggregation assays (Rader et al., 1993; Felsenfeld *et al.*, 1994), although bead aggregation assays have also suggested that TAG/axonin-1 might NOT bind homophilically (Kuhn *et al.*, 1991).

11) Axonin-1 bound to dishes coated with NCAM; overlapping distribution *in vivo* (Milev *et al.*, 1996).
12) Co-immunoprecipitation (Kadmon *et al.*, 1990).
13) Co-immunoprecipitation; co-clustering on cultured cells (Buttiglione *et al.*, 1998).
14) R-PTP-ß fragments bound to dishes coated with F11 (Sakurai *et al.*, 1997); co-immunoprecipitation; antibodies to F11 prevented outgrowth of DRG neurons on R-PTP-ß (Peles *et al.*, 1995).
15) Co-immunoprecipitation (Rathjen *et al.*, 1991); cell aggregation assays (Brummendorf *et al.*, 1993); antibodies to F3 prevent response of cerebellar neurites to tenascin R (Pesheva *et al.*, 1993); soluble tenascin R bound to F11 transfected cells (Nörenberg *et al.*, 1995).
16) R-PTP-ß fragments bound to an NrCAM coated surface; antibodies to Nr prevented neurite outgrowth on R-PTP-ß fragments (Sakurai *et al.*, 1997).
17) Antibodies to L1 prevented outgrowth of DRG neurons on TAG-1 (Felsenfeld *et al.*, 1994).
18) Aggregation of conjugated spheres; antibodies to NrCAM blocked binding of axonin-1 conjugated spheres to DRG neurons (Suter *et al.*, 1995); NrCAM-Fc bound to immobilised axonin-1 (Lustig *et al.*, 1999).
19) NgCAM coated spheres bound to FAR-2 expressing cells (Plagge et al., 2001).
20) Axonin-1 conjugated spheres bound to neurofascin expressing cells (Volkmer *et al.*, 1998).
21) Co-immunoprecipitation (Olive *et al.*, 1995).
22) Protein binding assays and co-precipitation from doubly transfected cells (Sakurai *et al.*, 1997); antibodies to NrCAM prevented outgrowth of tectal neurons on F11 (Morales *et al.*, 1993); NrCAM-Fc bound to an F11-coated surface (Lustig *et al.*, 1999).
23) Cell aggregation assays (Brummnedorf *et al.*, 1993).
24) Antibodies to F11 prevented outgrowth of tectal neurons on neurofascin (Volkmer *et al.*, 1996); co-localisation at the axon-glial junctions of myelinated peripheral nerve paranodes (Tait *et al.*, 2000).
25) Soluble tenascin R bound to FAR-2 expressing cells (Plagge *et al.*, 2001).
26) Neurofascin expressing cells bound tenascin-R conjugated spheres (Volkmer *et al.*, 1998).
27) R-PTP-ß fragments (Sakurai *et al.*, 1997) and phosphacan (Milev *et al.*, 1994) bound to immobilised NgCAM; antibodies to NgCAM inhibited binding of neurons to phosphacan (Milev *et al.*, 1994).
28) Axonin-1 bound to dishes coated with laminin (Milev *et al.*, 1996).
29) Phosphacan bound to immobilised L1; antibodies to L1 inhibited binding of neurons to phosphacan (Milev *et al.*, 1994).
30) Aggregation of conjugated spheres (Kuhn *et al*, 1991; Kadmon *et al.*, 1990) and transfected cells (Felsenfeld *et al.*, 1994).
31) L1 bound to a neurocan-coated surface (Oleszewski et al., 1999).
32) Antibodies to NgCAM prevented outgrowth of DRG neurons on axonin-1 (Kuhn *et al*, 1991); NgCAM expressing cells bound axonin-1-conjugated beads (Buchstaller *et al.*, 1996); antibody co-capping experiments (Rader *et al.*, 1993).
33) NrCAM-Fc bound to an NgCAM coated surface (Lustig *et al.*, 1999), although conjugated spheres did not aggregate (Morales et al., 1993; Suter et al., 1995).
34) Cell aggregation assays, aggregation of conjugated spheres (Mauro *et al.*, 1992); aggregation of conjugated spheres (Morales *et al.*, 1993); NrCAM-Fc bound to an NrCAM coated surface (Lustig *et al.*, 1999).
35) Antibodies to NrCAM prevented outgrowth of tectal neurons on neurofascin (Volkmer *et al.*, 1996), although conjugated spheres did not aggregate (Morales *et al.*, 1993).
36) NgCAM bound to a laminin-coated surface; aggregation of conjugated spheres, which was inhibited by antibodies to either molecule; antibodies to NgCAM inhibited neuronal attachment to laminin (Grumet *et al.*, 1993 a).
37) Antibodies to $\alpha_V\beta_3$ integrins perturbed adhesion of myeloma cells to L1 (Montgomery *et al.*, 1996).
38) Antibodies to NgCAM prevented outgrowth of chick neurites on L1 (Lemmon *et al.*, 1989).
39) Co-immunoprecipitation (Castellani *et al.*, 2000).
40) Aggregation of conjugated spheres (Grumet and Edelman, 1988).
41) Neurocan bound to an NgCAM-coated surface (Friedlander *et al.*, 1994)
42) Neurocan bound to an axonin-1-coated surface (Milev *et al.*, 1996).
43) Neurocan bound to an NCAM-coated surface (Friedlander *et al.*, 1994).
44) Cells transfected with CHL1 do not aggregate with one another, or with cells transfected with L1 (Hillenbrand *et al.*, 1999).

can be explained if NgCAM and axonin-1 normally interact in *cis* (within the same plasma membrane) rather than in *trans* (between adjacent plasma membranes) (Rader *et al.*, 1996). Cells would theoretically present the proteins in their native orientations, whereas the molecules could be held in non-physiological orientations when conjugated to inert beads. In the latter situation, binding domains could be abnormally exposed, such that *trans* interactions become possible (Rader *et al.*, 1996; figure 1.6). Thus the ability of IgCAMs to mediate adhesion of inert beads does not always mean that the molecules interact when expressed on opposing surfaces *in vivo*.

The understanding of IgCAM function is further complicated by the fact that their interactions vary with context. For example, *trans* homophilic binding of L1 is greatly enhanced when L1 can also interact in *cis* with NCAM (Kadmon *et al.*, 1990), but is inhibited when L1 can interact with the proteoglycan neurocan (Grumet *et al.*, 1993 b; Oleszewski *et al.*, 2000). L1-like subfamily members seem to exist in a number of differentially spliced isoforms, and these do not necessarily all have the same properties. There are splice variants of NgCAM (Buchstaller *et al.*, 1996), NrCAM (Kayyem *et al.*, 1992) and Neurofascin, the latter having at least fifty different isoforms (Hassel *et al.*, 1997). It has recently been proposed that the *Drosophila* IgCAM DSCAM may have more than thirty-eight thousand differentially spliced isoforms (Schmucker *et al.*, 2000). Differently spliced versions of NCAM (Small *et al.*, 1988) and neurofascin (Hassel *et al.*, 1997) have distinct patterns of expression, suggesting that differential splicing might generate proteins with specific functions. Indeed, at least some splice variants have distinct binding properties. For example, isoforms of Neurofascin which include the PAT domain show a greater affinity for NrCAM conjugated spheres than those that do not (Volkmer *et al.*, 1996), the extensive O-linked glycosylation of this domain being thought to alter the shape of the molecule (Volkmer *et al.*, 1998).

Figure 1.6 Possible explanation for apparent discrepancies in assays of axonin-1 - NgCAM binding. A: inert beads with axonin-1 and NgCAM attached to them are able to aggregate (Kuhn et *al.*, 1991, yet cells expressing the proteins do not aggregate (Buchstaller *et al.*, 1996; Felsenfeld *et al.*, 1994 for the proposed rodent homologues TAG-1 and L1 (B). This apparent difference may be explained by an interaction between axonin-1 and NgCAM in *cis* (C), as has been suggested by co-clustering (Stoeckli *et al.*, 1996; Kunz *et al.*, 1996; Malhorta *et al.*, 1998). Physical attachment of proteins to inert beads could present the molecules in such a way that they could interact (D), where as expression by living cells would present the molecules more physiologically, such that they could not interact (E). After Rader *et al.*, (1996).

1.4 Neural IgSF proteins and neurite outgrowth *in vitro*

While the ability to mediate adhesion and the ability to affect neurite outgrowth are not necessarily linked (Lemmon *et al.*, 1992; Doherty *et al.*, 1995), certain TAG-1- and L1-like cell adhesion proteins do seem to influence both outgrowth and adhesion. TAG-1- and L1-like cell adhesion molecules often have expression patterns that are suggestive of roles in axon guidance (e.g. Dodd *et al.*, 1988), and *in vitro* experiments such as cell and explant culture have shown that several of these proteins can indeed have effects upon neurite outgrowth. Neurons have been grown on substrates of IgCAMs bound to nitro-cellulose or plastic surfaces (e.g. TAG-1: Furley *et al.*, 1990; L1, NgCAM: Lemmon *et al.*, 1989; L1, NCAM: Kadmon *et al.*, 1990; NgCAM, axonin-1: Stoeckli *et al.*, 1996), or upon cells that express the molecules of interest (e.g. F3: Gennarini *et al.*, 1991; NCAM: Saffell *et al.*, 1994; NgCAM: Buchstaller *et al.*, 1996). However, care must be taken when interpreting such results. Even if IgCAMs do interact with certain binding partners when real neurons are involved, their interaction can have different outcomes in different situations. For example, the interaction between F11 and the extracellular matrix molecule tenascin-R (TN-R; also known as restrictin) seems to mediate outgrowth of tectal neurons, and yet cause repulsion of neurons from the cerebellum (Nörenberg *et al.*, 1995). It may also be that a response to, or a response mediated by, IgCAMs can be altered by electrical activity, as has been shown to be the case for the sensitivity of growth cones to components of the extracellular matrix (Harris and Holt, 2001; Ming *et al.*, 2001).

It is thus difficult to predict the precise role of an IgCAM *in vivo* from its behaviour *in vitro*. Increasingly, studies involve direct investigation of the roles of IgCAMs *in vivo*. So far the most common approach has been to prevent the molecule of interest from functioning normally, and to observe the effects of this perturbation.

1.5 Neural IgSF proteins and neurite outgrowth *in vivo*

1.5.1 Perturbation of neural IgSF protein function *in ovo*

Protein function can be perturbed in a number of ways. Chicken embryos are particularly amenable to *in ovo* manipulation, as it is possible to reseal eggs and to allow development to continue after a perturbation event. The effects of interference can then be studied at later stages. For example, such experiments have provided direct evidence that the IgCAMs axonin-1, NgCAM and NrCAM are involved in guidance of dorsal spinal commissural axons at the ventral midline of the spinal cord (Stoeckli and Landmesser, 1995; Lustig *et al.*, 1999; Fitzli *et al.*, 2000). The neural tubes of developing chicken embryos were injected with antibodies to these IgCAMs, or with soluble versions of axonin-1 (Stoeckli and Landmesser, 1995) and NrCAM (Lustig *et al.*, 1999). Development was allowed to continue in the presence of the function-blocking antibodies, or soluble IgCAMs that would have presumably inhibited the function of axonal IgCAMs by competitively interacting with their binding partners. As will be discussed in more detail later (see chapter 3), subsequent tracing of commissural axons revealed that these perturbations of IgCAM function did indeed seem to affect the ability of dorsal spinal axons to fasciculate with one another, and also alter their ability to enter the midline region known as the floor plate (Stoeckli and Landmesser, 1995; Lustig *et al.*, 1999; Fitzli *et al.*, 2000).

1.5.2 Perturbation of neural IgSF protein function *in ovo:* caveats

However, such results are not completely conclusive. For example, soluble IgCAMs could theoretically interact with binding partners and activate them, rather than necessarily being competitive inhibitors. Soluble L1 (Doherty *et al.*, 1995) and F3 (Durbec *et al.*, 1992; Rougon *et al.*, 1994) have indeed been shown to promote outgrowth in such a way *in vitro*. Furthermore, function-blocking antibodies may not always have the intended effect (Grenningloh and Goodman, 1992). Inhibition of one interaction/function of a molecule does not mean that all are inhibited. For example, it has been suggested that antibodies which prevent a *trans* interaction could leave a *cis* interaction unhindered (Buchstaller *et al.*, 1996). An antibody to certain integrins has been shown to prevent binding to vitronectin, and yet promote interactions with laminin

and collagens (Neugebauer and Reichardt, 1991). In some cases, antibodies that prevent at least some intermolecular interactions can also stimulate cell-signalling events (Schuch *et al.*, 1989).

As commented by Stoeckli and Landmesser (1995), the total absence of a molecule is needed to avoid ambiguity. While GPI anchored proteins such as TAG-1 may be removed from a cell surface using the enzyme phosphatidyl-inositol phospholipase C (PI-PLC) (Stoeckli *et al.*, 1996), this method cannot target a specific GPI-linked molecule. Anti-sense oligonucleotides, which act to prevent mRNA translation, have so far been used to perturb IgCAM function with limited success (Buchstaller *et al.*, 1996). Currently the most definite and specific way of ensuring that there is no functioning version of a protein is to interfere with its gene. Genetic mutations have been used to study the roles of IgCAM proteins in both invertebrate and vertebrate systems.

1.5.3 Mutations in genes encoding invertebrate neural IgSF proteins

Mutagenesis screens have led to the isolation of mutant alleles of several invertebrate neural IgSF genes. Such studies have led to the identification of three Robo proteins in *Drosophila melanogaster* (Seeger *et al.*, 1993; Kidd *et al.*, 1998 b; Simpson *et al.*, 2000) and of the related protein Sax-3 in *Caenorhabditis elegans* (Zallen *et al.*, 1998). Animals with loss-of-function mutations in *robo* or *sax-3* show excessive crossing of the midline of the nervous system by axons, leading to suggestions that these proteins normally prevent inappropriate crossing (Seeger *et al.*, 1993; Kidd *et al.*, 1998 a,b; Zallen *et al.*, 1998). *Drosophila* embryos with mutations in the *DSCAM* gene have disorganised connective tracts and incorrect targeting of Bolwig's nerve, implicating the DSCAM protein in the guidance of both CNS longitudinal axons and Bolwig's nerve sensory axons (Schmucker *et al.*, 2000). The phenotypes that result from manipulation of the *fasII* gene indicate that fasciclin II has roles in formation of the *Drosophila* MP1, vMP2 and FN3 fascicles (Grenningloh *et al.*, 1991; Lin *et al.*, 1994) and in the ability of motor neurons to contact their specific target muscles (Lin and Goodman, 1994; Davis *et al.*, 1997). The study of mutant flies has also led to suggestions that fasciclin II is important for growth and stabilisation of synapses (Schuster *et al.*, 1996) and for memory formation (Cheng *et al.*, 2001). Mutation of the gene encoding neuroglian has implicated this molecule in correct motor neuron guidance (Hall and Bieber, 1998), and

mutation of the gene encoding frazzled has implicated this Drosophila homologue of DCC both in the guidance of motor neurons and the formation of commissures (Kolodziej *et al.*, 1996).

Combining mutations in *Drosophila* IgCAM genes with those in other genes has also afforded information on how IgCAM proteins might relate to other axon guidance mechanisms. For example, neuroglian seems to affect the functioning of *Drosophila* EGF and FGF receptors (García-Alonso *et al.*, 2000). The roles of fasciclin II in the fasciculation and guidance of motor axons appears to be finely balanced with those of the molecule beaten path (Fambrough *et al.*, 1996), semaphorins (Winberg *et al.*, 1998) and netrins (Winberg *et al.*, 1998; Yu *et al.*, 1998).

1.5.4 Mutations in genes encoding vertebrate neural IgSF proteins

In the mouse, mutagenesis can be targeted to genes of interest. Thus mice with mutations in the appropriate genes have been used to investigate the roles of vertebrate IgCAMs *in vivo*. *NCAM* mutant mice were initially shown to have smaller brains, with a particular reduction in the size of the olfactory bulbs (Cremer *et al.*, 1994). Subsequently *NCAM* mutant mice have been found to have defects in olfactory neuron precursor migration, and in the development of their hippocampal projections (Cremer *et al.*, 1997). They also display behavioural problems, with abnormal levels of aggression (Stork *et al.*, 1997) and, under certain circumstances, an inability to maintain a normal circadian rhythm (Shen *et al.*, 1997). In all of these cases, mutant mice were compared with those that are wild type for the *NCAM* gene, indicating that NCAM normally functions in these situations. Similarly, studies of *L1* mutant mice have implicated this IgCAM in a number of processes, including the guidance of corticospinal axons (Cohen *et al.*, 1997) and axons of the corpus callosum (Demyanenko *et al.*, 1999), both at the midline of the developing brain. L1 also seems to be involved in correct development of the brain ventricles (Dahme *et al.*, 1997; Demyanenko *et al.*, 1999; Fransen *et al.*, 1998), the cerebellar vermis (Fransen *et al.*, 1998) and the cyto-architecture of the spleen (Wang *et al.*, 2000). Mutation of the gene encoding NrCAM has implicated this protein in postnatal development of the lens (Moré *et al.*, 2001) and cerebellum (Sakurai *et al.*, 2001). Mutation of the gene for F3 (contactin) indicates that this molecule is important for development of certain aspects of cerebellar cyto-architecture (Berglund *et al.*, 1999). Analysis of these mutant mice

also implicates F3 in the localisation of potassium channels to the axo-glial junctions of peripheral myelinated nerves, and thus also in the ability of these nerves to conduct nervous impulses efficiently (Boyle *et al.*, 2001).

1.5.5 The present study

1.5.5.1 Mice with mutations in the *TAG-1* gene

A major part of this thesis is an investigation into the roles of TAG-1 in the developing nervous system, through analysis of embryonic and immature *TAG-1* mutant animals. An independent study of *TAG-1* null mutant mice has recently reported that adenosine A1 receptors are upregulated in the adult hippocampus, and that animals have an increased susceptibility to epileptogenic drugs. However, effects of the mutation upon neural development were not described (Fukimauchi *et al.*, 2001).

Two separate mutations were made in the mouse *TAG-1* gene (A.J.W. Furley; see also materials and methods). In the "TAG^{A}" mutation, a neomycin resistance cassette was inserted into the *TAG-1* gene by homologous recombination. As the initial leader sequence was left intact, and the remaining Ig-encoding exons are within the same reading frame, the inserted cassette is spliced over. Truncated TAG-1 proteins are expressed on the surface of affected cells (figure 1.7; A.J.W. Furley, personal communications). The absent Ig domains are some of those shown to be essential for the interaction of axonin-1 with NgCAM or NrCAM (Rader *et al*, 1996; Fitzli *et al.*, 2000; figure 1.8), such that TAG^{A} homozygous mutant mice can be assumed to express TAG-1 that cannot bind to L1 or NrCAM. Separate lines of mice with this mutation were maintained on C57Bl/6 and 129Sv strain backgrounds. Mice homozygous for this mutation on either genetic background were born at normal Mendelian frequencies, and displayed no overt defects.

Completely null *TAG-1* mutant mice were also generated. These animals lack all TAG-1 protein (verified by B.W. Kiernan and A.J.W. Furley, data not shown), as the mutation involves deletion not only of coding exons but also of the *TAG-1* leader sequence (A.J.W. Furley, personal communication; figure 1.7). This mutation was maintained separately in mice of either a mixed genetic background or of a pure

A Wild type *TAG-1* gene

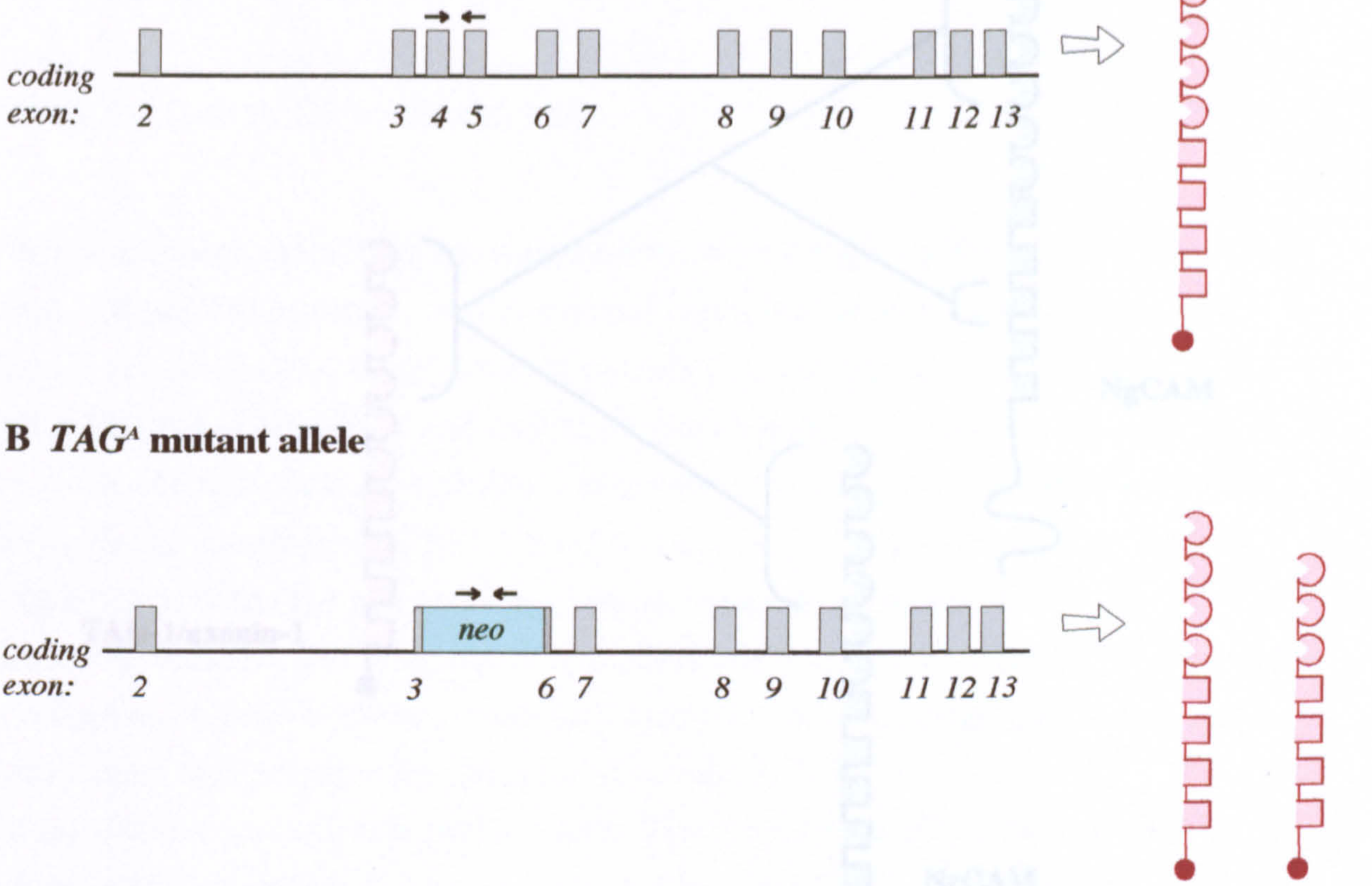

B *TAG^A* mutant allele

C *TAG-1* null allele

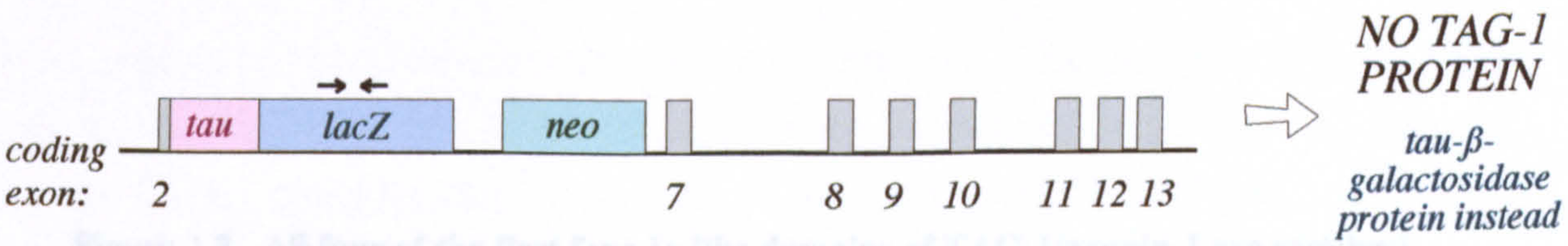

Figure 1.7 *TAG-1* alleles and their products. A: The wild type *TAG-1* gene, which encodes full-length TAG-1 protein. B: The *TAG^A* mutant allele. Insertion of a neomycin resistance cassette deleted part of exon 3 through to part of exon 6, preventing the production of full length TAG-1 protein. However, the leader sequence of exon 2 remains intact, and transcription can continue from this either with exon 7, giving TAG-1 protein that lacks the first two immunoglobulin-like domains, or with exon 9, giving TAG-1 protein that lacks the first three immunoglobulin-like domains (A.J.W. Furley. personal communication). Both of these truncated TAG-1 proteins should be unable to interact with L1 or NrCAM (Rader *et al.*, 1996; Fitzli *et al.*, 2000; see figure 1.8). C: the TAG-1 null mutant allele. As the leader sequence of exon 2 has been deleted, no TAG-1 protein is produced (A.J.W. Furley and B.W. Kiernan, personal communication). Instead, the *tau-lacZ* gene construct is transcribed, giving a reporter protein that has ß-galactosidase activity and that is transported along axons. Arrows represent the oligonucleotide primers used to determine the genotypes of mice (see methods).

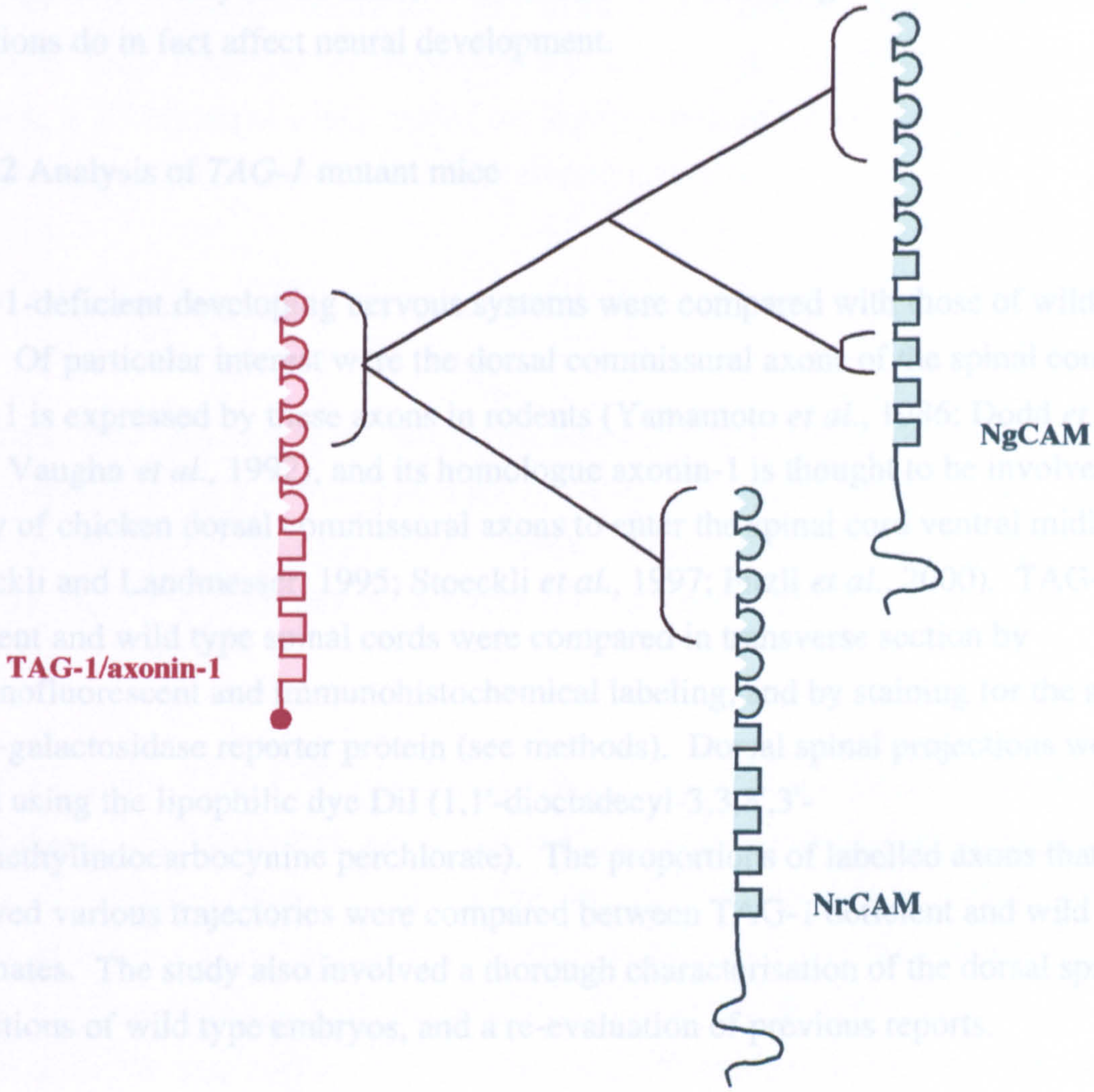

Figure 1.8 All four of the first four Ig-like domains of TAG-1/axonin-1 are required for its interactions with either NgCAM or NrCAM. Binding sites have been determined by assessing the interactions of proteins that lack certain domains. Regions of axonin-1 that are important for binding of this protein to NgCAM were determined by Rader *et al.*, 1996. Regions of NgCAM required for binding to axonin-1 were identified by Kunz *et al.*, 1998. The third fibronectin type II domain of NgCAM was required for association with axonin-1, although this does not necessarily mean that this domain itself interacts with axonin-1 (De Angelis *et al.*, 1999). The regions of axonin-1 and NrCAM that are involved in the interaction of these two molecules were identified by Fitzli *et al.*, 2000. The results of Rader *et al.* and Fitzli *et al.* imply that proteins produced from the *TAG*^{A} mutant allele are unable to interact with either NrCAM or the rodent NgCAM-like molecule L1.

C57Bl/6 strain. In both cases, mice were born at expected Mendelian frequencies and outwardly appeared to be unaffected by the mutation. This thesis describes analyses of *TAG-1* mutant embryos and mice, with the aim of establishing whether *TAG-1* mutations do in fact affect neural development.

1.5.5.2 Analysis of *TAG-1* mutant mice

TAG-1-deficient developing nervous systems were compared with those of wild type mice. Of particular interest were the dorsal commissural axons of the spinal cord. TAG-1 is expressed by these axons in rodents (Yamamoto *et al.*, 1986; Dodd *et al.*, 1988; Vaughn *et al.*, 1992), and its homologue axonin-1 is thought to be involved in the ability of chicken dorsal commissural axons to enter the spinal cord ventral midline (Stoeckli and Landmesser, 1995; Stoeckli *et al.*, 1997; Fitzli *et al.*, 2000). TAG-1-deficient and wild type spinal cords were compared in transverse section by immunofluorescent and immunohistochemical labeling, and by staining for the activity of a ß-galactosidase reporter protein (see methods). Dorsal spinal projections were also traced using the lipophilic dye DiI (1,1'-dioctadecyl-3,3,3',3'-tetramethylindocarbocynine perchlorate). The proportions of labelled axons that followed various trajectories were compared between TAG-1 deficient and wild type littermates. The study also involved a thorough characterisation of the dorsal spinal projections of wild type embryos, and a re-evaluation of previous reports.

Other aspects of neural development were also analysed. The inclusion of a *tau-lacZ* gene within the *TAG-1* null mutation meant that all structures that would ordinarily express TAG-1 could be stained for ß-galactosidase activity. This allowed the expression pattern of TAG-1 to be documented comprehensively. It also allowed a general survey of the ways in which expressing structures were affected by a lack of TAG-1 protein. Particular attention was paid to cells whose development has previously been suggested to involve TAG-1. For instance, TAG-1 is normally expressed by neurons of the facial (VIIth cranial) nerve nucleus during a period of caudal migration. In mouse embryos homozygous for mutations in the *krox-20* or *ebf-1* transcription factor genes, a premature cessation of TAG-1 expression by facial nerve neurons coincides with a truncated caudal migration (Garel *et al.*, 2000). Axonin-1 has been implicated in the fasciculation of axons in the chicken hindlimb (Xue and Honig, 1999), which appears to be important for correct innervation (Landmesser and Honig, 1986; Honig and Rutishauser, 1996). Therefore both the developing facial nerve nucleus and extending limb nerves were examined. The cerebellum, which shows some

failure of granule cell migration in adult *TAG-1* mutant mice (K. Ohyama and R. Yoshida, personal communication) was also examined for gross defects during its maturation. Other structures were studied in particular detail following the initial survey of ß-galactosidase expressing structures. For example, TAG-1 had not previously been implicated in development of the hypoglossal (XIIth cranial) nerve, but appearance of this nerve when stained for ß-galactosidase activity raised the possibility that its axons might require TAG-1 for correct extension.

1.5.5.3 Mice with mutations in *L1*, *NrCAM* or *ephrin B3*

This thesis also provides novel data on the neural development of mouse embryos with null mutations in the genes encoding the IgCAMs L1 (courtesy of P. Soriano; Cohen *et al.*, 1997) or NrCAM (courtesy of M. Grumet; Sakurai *et al.*, 2001), or in the gene encoding the cell surface molecule ephrin B3 (courtesy of N. Gale; Kullander *et al*, 2001 b).

As is the case for TAG-1, L1 is expressed by dorsal spinal commissural axons (Dodd *et al.*, 1988), and its homologue appears to be required for correct development of these axons in the chicken (Stoeckli and Landmesser, 1995; Stoeckli *et al.*, 1997). Male mice that are hemizygous for the X-linked mutation in *L1* are smaller than normal, have sunken and lacrimous eyes, are unable to breed, and often drag their hind limbs. This latter feature has been attributed to incomplete decussation of the corticospinal tract (Cohen *et al.*, 1997), a pathway that carries impulses from the brain to the spinal cord, and which normally crosses the mid-line of the caudal hind-brain (Kalil, 1984; Gribnau *et al.*, 1986). Thus it was conceivable that L1 might also be involved in the decussation of dorsal spinal commissural axons. Previous immunofluorescent labelling of spinal cord sections showed that some dorsal spinal axons do decussate in *L1* hemizygous mutant embryos (Cohen *et al.*, 1997), but it was not shown whether this was true of all of the axons. Therefore the dorsal spinal projections of *L1* mutant embryos were also traced using DiI, and differences between hemizygous and wild type embryos were analysed statistically. The possibility that TAG-1 and L1 might act redundantly was also investigated. The dorsal spinal projections of *L1/TAG-1* double mutant embryos were traced with DiI and compared to those of wild type embryos. A broader analysis was also conducted: whole embryos devoid of full-length TAG-1 and L1 proteins were stained for ß-galactosidase activity, and the structures that normally express TAG-1 were compared.

The IgCAM NrCAM is also expressed by rodent dorsal spinal commissural axons, with specific localisation to axonal surfaces that are actually within the commissure. It is also expressed by the rodent spinal cord ventral midline, or floor plate, beneath which the decussating axons extend (Lustig *et al.*, 2001). Like axonin-1, NrCAM seems to have a role in guiding dorsal spinal commissural axons at the chicken floor plate (Stoeckli and Landmesser, 1995; Stoeckli *et al.*, 1997). Thus, although *NrCAM* homozygous mutant mice show no overt defects (Sakurai *et al.*, 2001), it was conceivable that NrCAM might influence spinal commissural axon guidance. In order to investigate this possibility, the dorsal spinal axons of *NrCAM* homozygous mutant embryos were labelled. So too were those of *ephrin B3* mutant embryos, as ephrin B3 is also expressed in the floor plate (Gale *et al.*, 1996 a; Bergemann *et al.*, 1998; Imondi *et al.*, 2000), and at least one population of commissural axons re-decussates aberrantly the *ephrin B3* null mutants (Kullander *et al.*, 2001 b).

In summary, this thesis describes analysis of the dorsal spinal commissural axons of a number of lines of mutant mice. Although dorsal spinal projections of other *NrCAM* mutant embryos have since been studied elsewhere (Moré *et al.*, 2001), this thesis provides the first reports of DiI analysis of these projections in *TAG-1*, *L1* or *ephrin B3* null mutant embryos. It also constitutes the first general description of the neural development of *TAG-1* mutant embryos.

2 Materials and Methods

2.1 Production of mutant mice and embryos

2.1.1 Generation of single mutant animals

TAG-1 mutant mice were generated by A.J.W. Furley. The *TAG-1* gene was mutated by homologous recombination in embryonic stem cells (as in Mansour *et al.*, 1990; see Capecchi 2001 for review). As indicated in figure 1.7, the TAG^{A} mutation involved partial deletion of the gene, such that truncated TAG-1 proteins were still produced and expressed at the cell surface (A.J.W. Furley, personal communication). The *TAG-1* null mutation also involved deletion of the gene's leader sequence, such that no TAG-1 protein was produced (B.W. Kiernan and A.J.W. Furley, personal communications). Initially, both mutations were maintained within mice of a mixed strain background. Subsequently the null mutation was backcrossed, for at least 6 generations, onto a C57Bl/6 genetic background. The TAG^{A} mutation was backcrossed onto a C57Bl/6 genetic background for at least 10 generations, and was also maintained separately on a 129/SvEv background. All of these lines of mice were viable, and without obvious deficiencies. Mutant embryos were obtained from pregnant females mated as shown in figure 2.1. Cross 2.1 A was used to obtain litters that contained all three TAG^{A} or *TAG-1* null mutant genotypes, so that "blind" analyses could be performed. Crosses 2.1 B, C and D were used subsequently, to increase the numbers of samples of particular genotypes more effectively.

L1 mutant mice were a gift from P. Soriano. Their generation is described in Cohen *et al.*, 1997. For the present study they were maintained on a 129/SvEv strain background, and mutant embryos were obtained from pregnant heterozygous females, mated as shown in figure 2.2. The cross shown is the only one that could be used, as hemizygous males are effectively sterile (Cohen *et al.*, 1997).

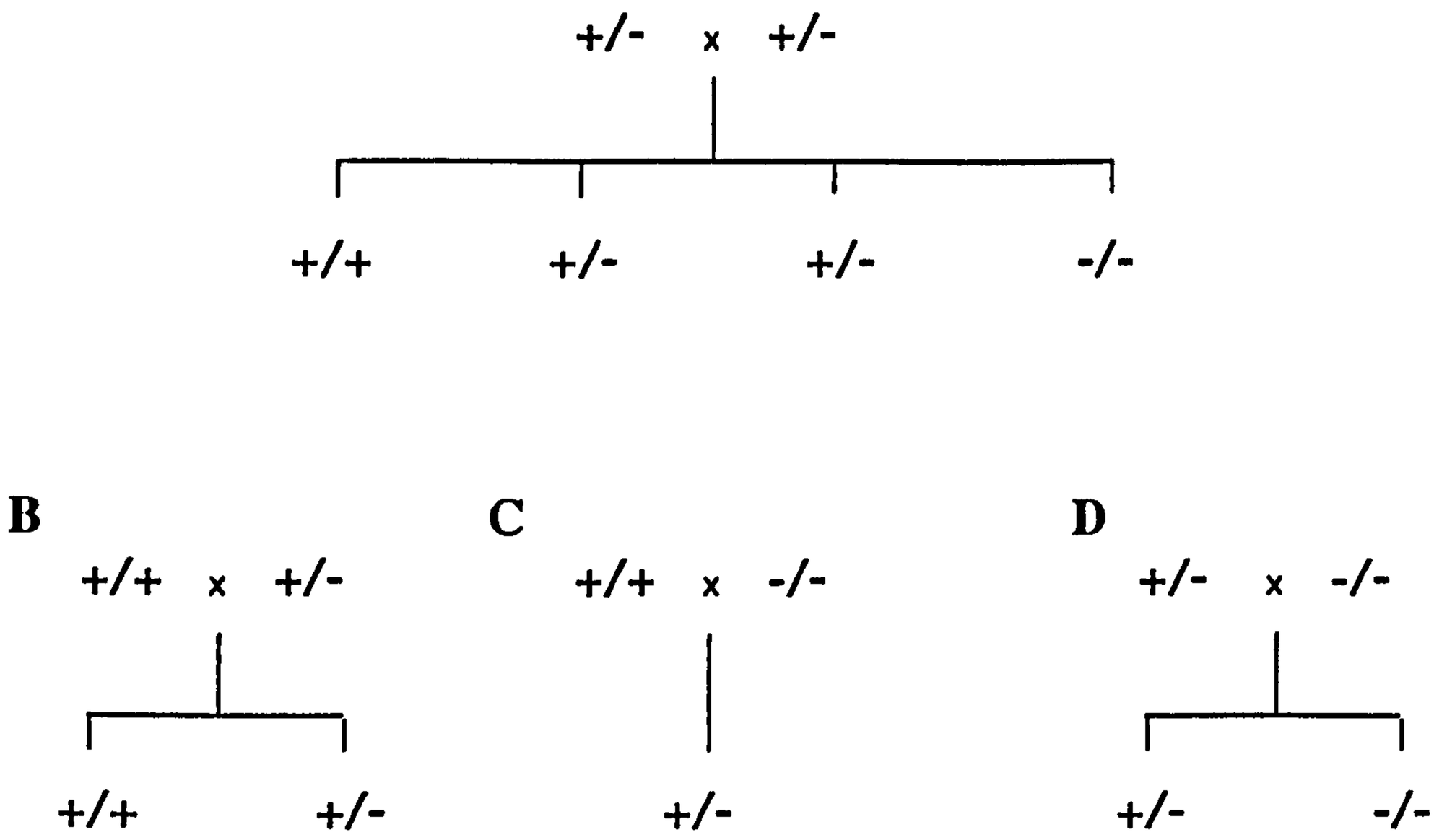

Figure 2.1 Crosses used to obtain *TAG-1, NrCAM* and *ephrin B3* mutant embryos.
A: heterozygote x heterozygote matings were used to obtain litters that contained all three genotypes. This allowed embryos of all genotypes to be analysed together, "blindly". Crosses B, C and D were also used, according to which embryos were required and which mice were available. So too were crosses of mice with others of the same genotype, to produce embryos all of that genotype.

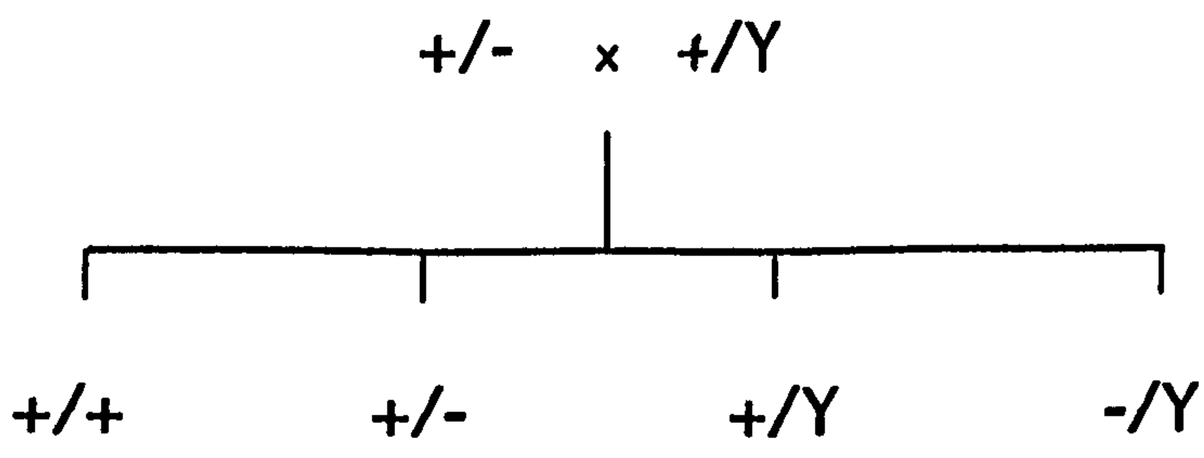

Figure 2.2 Cross used to obtain *L1* mutant embryos. The *L1* gene is X-linked, so hemizygous males completely lack L1 protein. As such mice are largely unable to mate (Cohen *et al.*,1997), homozygous female embryos could not be generated.

NrCAM mutant mice were a gift from M. Grumet. Their generation is described in Sakurai *et al.*, 2001. For the present study they were maintained on a mixed strain background, and mutant embryos were obtained from pregnant females mated as shown in figure 2.1. Again, cross A was used to obtain litters that contained all three genotypes, to allow unbiased analysis, and crosses B, C and D were used subsequently, as required.

Ephrin B3 mice were a gift from N. Gale. Their generation is described in Kullander *et al.*, 2001 b, and for the present study they were maintained on a mixed strain background. Heterozygous and homozygous mutant embryos were obtained from pregnant females mated as shown in figure 2.1 and described above for *TAG-1* and *NrCAM* mutant mice.

Math-1-lacZ transgenic mice were a gift from J. Johnson. Their generation is described in Helms and Johnson, 1998, and for the present study they were maintained on a C57Bl/6 strain background. These mice express *lacZ* under the control of ectopic *math-1* regulatory sequences, such that endogenous *math-1* gene expression is unaffected. Thus cells that would normally express the Math-1 transcription factor still do so, and in addition contain the *lacZ* gene product, ß-galactosidase. Math-1 is normally expressed in the cells of the dorsal spinal cord that give rise to TAG-1-positive D1 interneurons (Liem *et al.*, 1997; Helms and Johnson, 1998; Lee *et al.*, 1998; Gowan *et al.*, 2001). Therefore staining of *math-1-lacZ* transgenic embryos for ß-galactosidase provides a TAG-1-independent method of marking D1 interneurons. *Math-1-lacZ* transgenic mice were mated with those carrying the TAG^A mutation. This provided a method for staining the D1 interneurons of TAG^A homozygous mutant embryos, which would not otherwise contain ß-galactosidase activity and which were not recognised by the 4D7 antibody (figure 3.6).

2.1.2 Generation of double mutant animals

TAG-1/L1 double mutant embryos were also generated. For DiI labeling of dorsal spinal axons (see below), the TAG^A mutant allele was used. This was to ensure that embryos were all of the same genetic background. At the time of the investigation, the TAG^A and *L1* mutations were both being maintained on a pure 129/SvEv strain background, but the *TAG-1* null mutation was being maintained on mixed and C57Bl/6 genetic backgrounds. Thus *TAG-1* null */L1* double mutant embryos would have had a heterogeneous genetic background, and littermates would not all have had the same genes. This is likely to have affected the results obtained, as the *L1* mutant phenotype is known to be more severe when on a C57Bl/6 genetic background than when on a 129/SvEv genetic background (Dhame *et al.*, 1997). The use of TAG^A mutant animals meant that embryos differed from one another only at the *TAG-1* and *L1* loci, so that any differences in phenotype could be attributed to the IgCAM deficiencies. TAG^A */L1* double mutant embryos were most commonly obtained as illustrated in figure 2.3.

For other analyses of double mutant embryos, the *TAG-1* null mutation was used. Although not as precise an approach, the use of this mutation did mean that embryos could be stained for ß-galactosidase activity. This allowed TAG-1-expressing structures to be stained more easily and more reliably than by whole mount immunohistochemistry (see below). As *L1*/TAG^A double heterozygous (or "trans-heterozygous") mice were already being bred for the matings shown in figure 2.3, it proved easier to mate these with *TAG-1* null animals than to begin to breed *L1/TAG-1* null trans-heterozygotes. As illustrated in figure 2.4, the embryos that lacked wild type TAG-1 protein thus carried one *TAG-1* null and one TAG^A allele. This had the additional benefit that double mutant and control embryos contained equivalent amounts of ß-galactosidase, which allowed their staining to be compared more objectively than if some embryos had been carrying two *tau-lacZ* alleles.

A

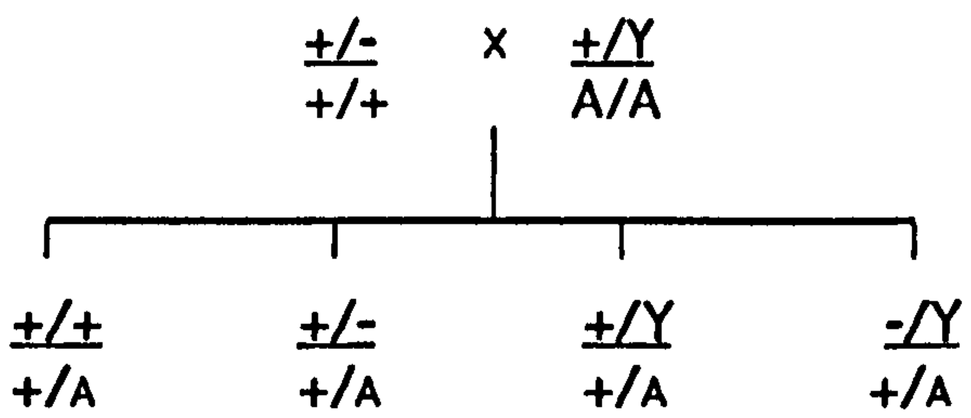

B

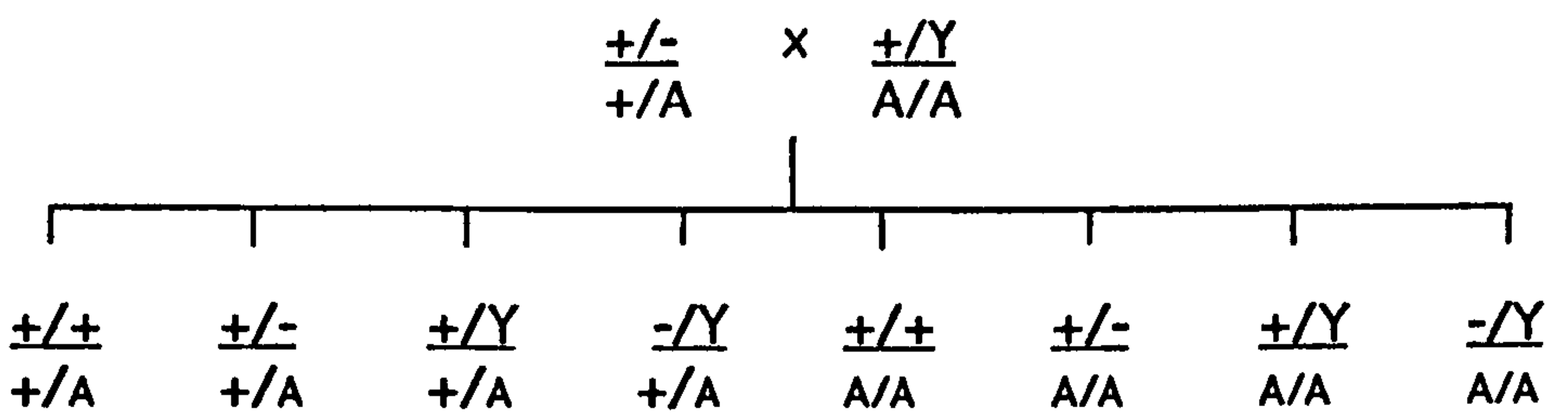

C

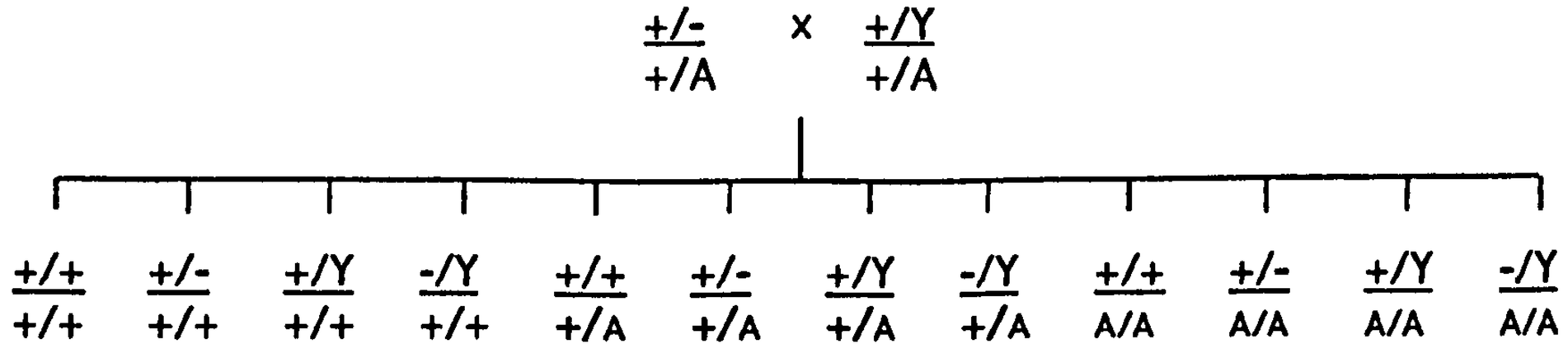

Figure 2.3 Crosses used to obtain *L1/TAG-1* double mutant embryos for DiI analysis. Such embryos were used as described in chapters 3 and 4. In each case, genotype with regards to *L1* is shown above the line, and genotype with regards to *TAG-1* is shown below the line. "A" denotes the TAG^{A} allele, which encodes truncated TAG-1 proteins (see figure 1.7). Whether cross A, B or C was used depended on the mice that were available.

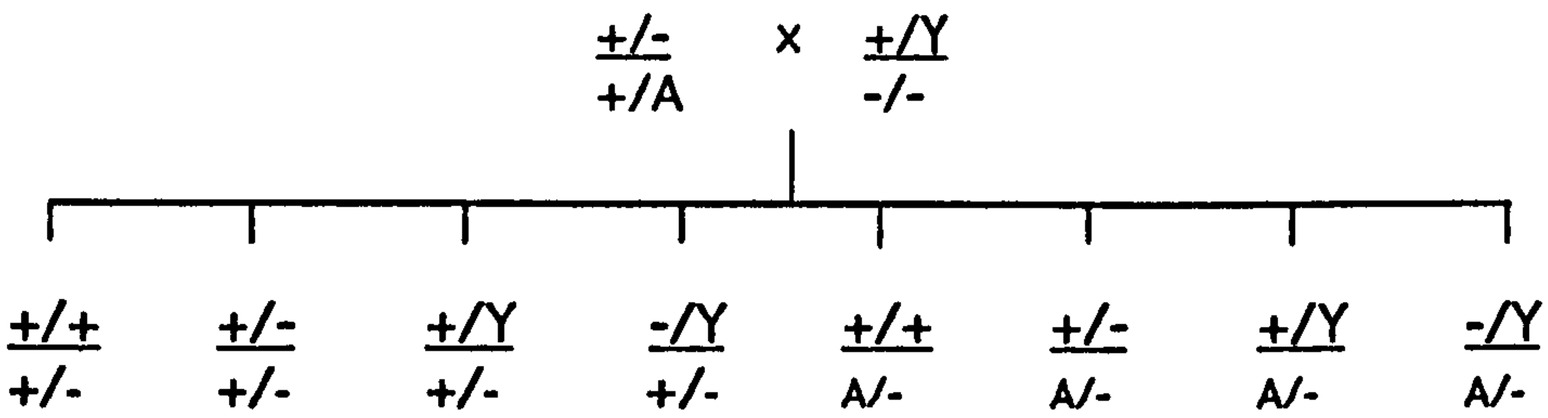

Figure 2.4 The cross used to obtain *L1/TAG-1* double mutant embryos to be stained for ß-galactosidase activity. Other crosses were used occasionally, according to which mice were available. In each case the genotype above the line is that for *L1*, and the one beneath the line is for *TAG-1*. All of the resulting embryos carry a null TAG-1 allele, so can be stained for ß-galactosidase activity. "A" denotes the TAG^A allele. This encodes truncated TAG-1 proteins (A.J.W. Furley, personal communication), so "A/-" embryos have no full-length TAG-1 protein.

2.1.3 Harvesting of animals

For analysis of embryos, pregnant females were killed by an overdose of anaesthetic (pentobarbitone) the appropriate number of days after mating: the time of vaginal plug discovery was referred to as E0.5. The uterus was transferred to cold PBS (phosphate buffered saline; Sigma), and embryos were removed under a Zeiss Stemi SV6 dissecting microscope. Although it was usual for embryos of a single litter to show slight age differences (Kaufman 1992), embryos were not used if they were judged to be abnormally under-developed. There did not appear to be any relationship between the occurrence of such embryos and genotype (data not shown). The developmental ages of embryos were confirmed using Hogan *et al.*, 1994. For instance, an embryo that was nominally E11.5 would not be used as such if it did not have a pigmented retina.

Post-natal mice were anaesthetised by exposure to carbon dioxide, and killed by decapitation. Their brains were removed in cold PBS, under a Zeiss Stemi SV6 dissecting microscope.

2.1.4 Genotyping of animals

When necessary, the genotypes of animals were determined by polymerase chain reaction (PCR). Embryonic sacs or other small pieces of tissue were incubated overnight at 50°C in 100 - 500 µl lysis buffer (100mM NaCl, 10mM Tris (pH 8), 1mM EDTA and 1% SDS in de-ionised water), to which had been added 0.2 mg/ml proteinase K (Promega). DNA was purified from the resulting mixture by the addition of twice the sample volume of phenol-chloroform, mixing vigorously for 10 minutes, and then centrifuging at 13000 rpm for 10 minutes. The resulting supernatant was removed and put through a second phenol-chloroform extraction, and then 1 µl was added to 19µl PCR reaction mixture. This reaction mixture consisted of 20mM tris-HCl (pH 8.4), 50mM KCl, 2.25mM $MgCl_2$,

0.2mM of each of the deoxyribonucleoside triphosphates dATP, dCTP, dGTP and dTTP, 0.5μM of each of 4 diagnostic oligonucleotide primers, and 2.5 units *Taq* DNA polymerase (GibcoBRL), in sterile water. In each case, one pair of oligonucleotide primers was used to detect the wild type allele, and another pair used to detect the mutant allele. The primers used to diagnose genotypes of TAG^{A}, *TAG-1* null and *L1* mutant animals are shown in figure 2.5 A-D. PCR was performed using a Hybaid "PCR Express" PCR machine. Reaction conditions were 3 minutes at 94°C, followed by 30 cycles of 30 seconds at 94°C, 30 seconds at 59°C, 1 minute at 72°C, and a final stage of 3 minutes at 72°C. PCR products were run on 2% agarose gels containing 0.5 μg/ml ethidium bromide, for 40 minutes at 80 volts. Ultra-violet illumination of gels revealed the extents to which DNA bands had migrated. As the different primer sets produced DNA of distinctive sizes, the bands obtained from a PCR reaction could be used to diagnose the genotype of the original tissue (as shown in figure 2.5 E and F).

A wild type *TAG-1* gene

GGA GGA GAG AGA CCC CGT GAA A
ACA CGA AGT GAC GCC CAT CCG T

B neomycin-resistance gene

TGG AGA GGC TAT TCG GCT ATG AC
AGC AAG GTG AGA TGA CAG GAG ATC

C *lacZ* gene

CTG GAT AAC GAC ATT GGC GTA AG
AGA TCC CAG CGG TCA AAA CAG

D wild type *L1* gene

GGT GCA AGG GTG ACA TTC ACG T
TGC TCT CCA CCT CAT CCA GTT CAG

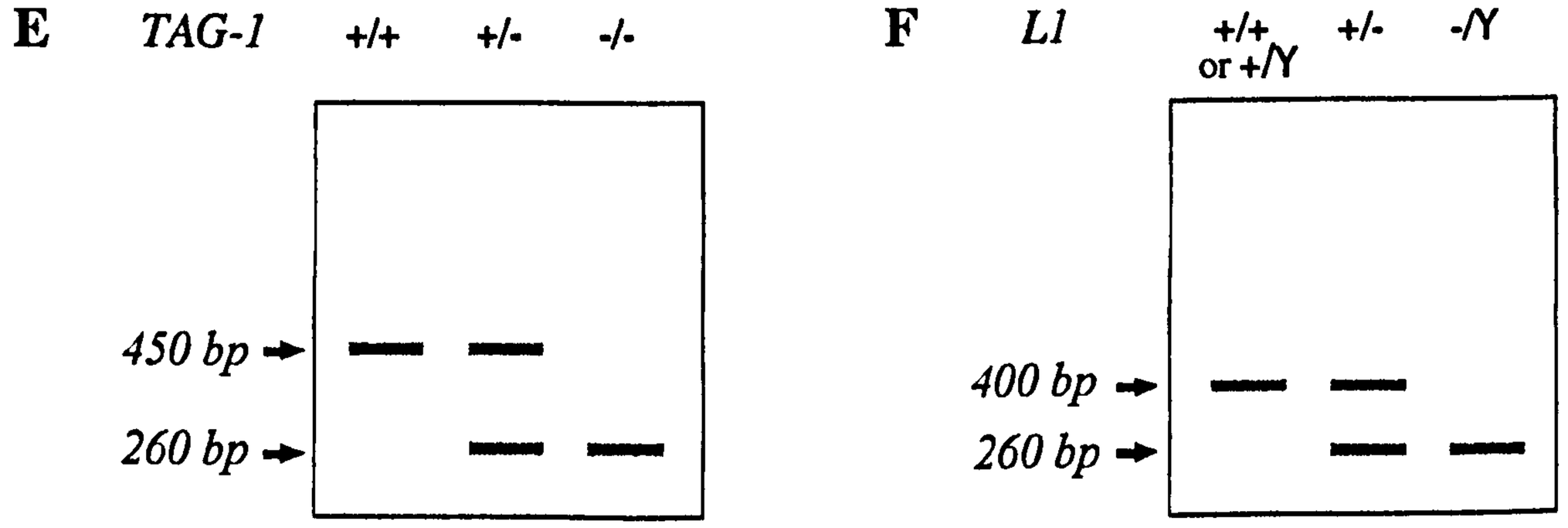

Figure 2.5 Diagnostic oligonucleotide primers used to determine the genotypes of mutant mice. Two primers are used to detect each allele. A PCR reaction to diagnose the genotypes of *TAG-1* mutant animals would use primers A (to detect the wild type gene) and B (to detect the mutant allele). The primers shown in A give a DNA product of 450 base pairs (bp), while the primers shown in B give a product of 260 bp. These migrate for different distances when run on an agarose gel, such that the genotype could be determined as illustrated in E. A PCR reaction to genotype *TAG-1* null mutant animals would use primers A and either B or C, as the mutant allele contains both the neomycin resistance and *lacZ* genes (figure 1.7). A PCR reaction to genotype *L1* mutant animals would use the primers shown in D, which gives a product of 400 bp, to detect the wild type *L1* gene. The primers shown in B were used to detect the mutant allele, as it includes a neomycin resistance cassette (Cohen *et al.*, 1997). When the reaction products had been run on an agarose gel, genotypes could be determined as illustrated in F. The regions to which the A, B and C primer sets anneal are shown in figure 1.6 A, B and C respectively. Other genotyping reactions are not illustrated as they were always performed by other members of the laboratory.

2.2 Immunohistochemistry

2.2.1 Whole-mount immunohistochemistry

For whole-mount immunohistochemistry, embryos or pieces of embryos were fixed in 4% paraformaldehyde (in 0.12M phosphate buffer, pH 7.4), at 4°C for approximately two hours. Samples were then washed at least three times in PBS, each wash lasting for a minimum of one hour. The function of endogenous hydrogen peroxidase enzyme, such as is within red blood cells, was blocked by an overnight incubation at 4°C in a solution of 0.1 % hydrogen peroxide in PT_x (PBS with 1% $Triton_{x100}$; Sigma). After this blocking step, the hydrogen peroxide solution was removed and samples were washed at least three times in PT_x, each wash lasting for a minimum of one hour. The samples were then incubated overnight in blocking solution (PT_x with 10% heat-inactivated goat serum: GibcoBRL goat serum, heat inactivated at 56°C for 30 minutes) at 4°C. After this step, which serves to reduce the non-specific binding of antibodies, embryos or pieces were incubated at 4°C, with agitation, in primary antibody solution. This solution consisted of a 1/5 dilution of the required hybridoma supernatant in PT_xH (PT_x with 1 % heat-inactivated goat serum). The supernatant was either 2H3, which recognises a 155kd neurofilament protein (Dodd *et al.*, 1988), or 4D7, which recognises TAG-1 (Yamamoto *et al.*, 1986; Dodd *et al.*, 1988). After at least four days the primary antibody was removed. Samples were washed at least three times in PT_xH, each wash lasting at least one hour and involving agitation of the samples. Tissue was then incubated at 4°C with agitation in a solution of the appropriate horseradish peroxidase–conjugated secondary antibody, diluted 1/200 in PT_xH. If the primary antibody had been 2H3, a goat anti-mouse IgG secondary antibody was used (Biosource International, or Jackson ImmunoResearch); if the primary antibody had been 4D7, a goat anti-mouse IgM secondary antibody was used (Biosource International).

After at least three days, samples were washed briefly in PT_xH. They were then washed at least twice in 0.1 M Tris buffer (pH 7.2), each wash lasting at least one hour and involving agitation of the tissue. Samples were then immersed in a solution of 1 mg/ml DAB (3,3"-

diaminobenzidine tetrahydrochloride), which had been made up as 1 x 6mg DAB buffer tablet (Merck) per 6ml distilled water and filtered before use. This pre-incubation lasted for at least two hours, and was carried out at room temperature and in darkness. Samples were then incubated in more of the DAB solution, to which had been added 0.03% hydrogen peroxide. This incubation in "activated" DAB was also carried out at room temperature and in darkness, but only for as long as was necessary for a brown reaction product to develop. When labelling had developed sufficiently, active DAB solution was removed and samples were washed a number of times in PBS. Samples were examined using a Zeiss Stemi SV6 dissecting microscope. When required, samples were photographed using either an MC-100 camera attachment and Kodak Ektachrome 64T film, or a Nikon Coolpix 990 digital camera. In the former case, pictures were scanned electronically using a Nikon LS-2000 scanner. Figures were prepared using Adobe Photoshop and Canvas 7.

2.2.2 Immunohistochemical and immunofluorescent labelling of sections

Other embryos were sectioned before labelling. Following fixation and rinses in PBS as described above, embryos were cryo-preserved. This involved incubation in a solution of 30% sucrose in PBS, at 4°C for a minimum of one night. Once saturated with sucrose solution, embryos or pieces of embryos were mounted onto chucks using OCT compound (BDH) and stored at -20°C until sectioning. Tissue was sectioned using a Bright cryostat, and 15 μm sections were collected on glass slides (Superfrost Plus, BDH).

Sections to be labelled were re-hydrated using PT_x. Those to be used for immunohistochemistry were incubated in a solution of 0.1 % hydrogen peroxide in PT_x, at 4°C for approximately 30 minutes, to block the function of endogenous hydrogen peroxidase. Those to be used for immunofluorescence, and those that had been rinsed in PT_x after the hydrogen peroxidase blockage step, were then incubated at 4°C for a

minimum of two hours in blocking solution (10% heat-inactivated goat serum in PT_x). Sections were then incubated in primary antibody solutions, overnight at 4°C. The 4D7 and 2H3 antibodies were used as described above. 324, a rat monoclonal IgG antibody to L1 (Boehringer Mannheim; Rathjen and Schachner, 1984), was used at 1/50 in PT_xH. 838. a rabbit polyclonal antibody to NrCAM (courtesy of M. Grumet; Lustig *et al.*, 2001), was used at 1/300 in PT_xH. R.331, a rabbit polyclonal antibody to BMP7, was used at 1/500 in PT_xH that had been specifically adjusted to pH 6.4 (Dale *et al.*, 1997). Sections were rinsed at least three times in PT_xH, and incubated for at least one hour at 4°C in a solution of the appropriate secondary antibody.

Secondary antibodies were used at a dilution of 1/200 in PT_xH. For immunohistochemical labelling, horseradish peroxidase-conjugated secondary antibodies were applied. For the 4D7 and 2H3 primary antibodies, the secondary antibodies used were as described above. For 838 or R.331, a goat anti-rabbit secondary antibody was used (Biosource International or Boehringer Mannheim), and for 324, a goat anti-rat secondary antibody was used (Sigma). Following this incubation, sections were rinsed at least three times in PT_xH or PBS, and incubated for at least 30 minutes in 0.1M Tris buffer (pH 7.2). They were then covered in a solution of 1 mg/ml DAB (without hydrogen peroxide, prepared as above) in darkness for at least 30 minutes. Samples were then incubated in DAB solution to which had been added 0.03% hydrogen peroxide. This incubation was conducted at room temperature in darkness, progress of the reaction being checked frequently using a Zeiss Stemi SV6 dissecting microscope. When labelling had developed sufficiently, active DAB solution was removed and sections were rinsed a number of times in PBS. Cover slips were applied to the slides, using a mounting medium of approximately 2:1 glycerol to carbonate buffer. Sections were examined using a Zeiss Axiophot microscope. When required they were photographed, using either an MC-100 camera attachment with Kodak Ektachrome 64T film, or a Nikon Coolpix 990 digital camera. In the former case, pictures were scanned electronically using a Nikon LS-2000 scanner. Figures were prepared using Adobe Photoshop and Canvas 7. Unless otherwise stated, the sections shown were from inter-limb levels of the spinal cord.

For immunofluorescent labelling, the appropriate classes of fluorescently- conjugated secondary antibodies were applied, and the incubation was carried out in darkness. Secondary antibodies were either fluorescein isothiocyanate (FITC) or tetremethyl rhodamine isothiocyanate (TRITC) conjugates (Biosource International), according to which colour of fluorescence was required. After at least three washes in PT_xH and/or PBS, cover slips were applied. A mounting medium of 2:1 glycerol: carbonate buffer, to which had been added the "anti-fade" compound p-phenylenediamine (Sigma; one small crystal per 1.5 ml) was used. Sections were examined under an Olympus BX60 fluorescent microscope and photographed with an Olympus PM C35DX camera, Olympus PM 30 Exposure Control Unit and Kodak Ektachrome P1600 film. Pictures were scanned electronically using a Nikon LS-2000 scanner, and figures were prepared using Adobe Photoshop and Canvas 7. Unless otherwise stated, the sections shown in figures were from inter-limb levels of the spinal cord.

2.3 DiI injection of spinal cord preparations

2.3.1 Injection of open book preparations

While antibody labelling can demonstrate whether some axons do cross the midline, it cannot show whether other axons also fail to decussate (figure 2.6). In contrast to antibodies, which label bilaterally, axon tracers such as DiI (1,1'-dioctadecyl-3,3,3',3'-tetramethylindocarbocynine perchlorate) can be used unilaterally and allow commissural axons to be traced without interference of axons from the other side of the spinal cord. DiI injections were equally the work of the author and B.W. Kiernan.

Spinal cords were dissected from embryos in cold Leibovitz's L15 medium (GibcoBRL) that contained approximately 1% heat inactivated goat serum. Isolated spinal cords were slit along the roof plate and pinned out onto Sylgard coated petri dishes as "open books" (figure 2.7; Bovolenta and Dodd, 1990). The petri dishes contained a solution of 4% paraformaldehyde fixative (as above), such that incubation for at least two hours at 4°C caused the spinal cords to be fixed as open books. After this fixation, dishes were rinsed gently with PBS. Before they were unpinned, the PBS-covered open book preparations were injected with DiI (Molecular Probes), dissolved to be 2.5 mg/ml in DMF (di-methyl formamide; Sigma). Injections were made using glass micropipettes (1.2mm outer diameter, 0.69mm inner diameter, Clark Electrical Instruments) that had been pulled to fine points using a P-97 Flaming/Brown micropipette puller, Sutter Instrument Company. Pulled micropipettes were filled with DiI solution by capillary action, and attached to the end of rubber tubing (an "aspirator assembly"; Sigma). Small amounts of DiI were blown into the required regions of fixed spinal cord by mouth. Open book samples were then unpinned, transferred to micro-centrifuge tubes, and stored in darkness at 4°C for at least one week. One week was found to be sufficient time for DiI to diffuse along dorsal commissural axons such that trajectory could be determined (data not shown).

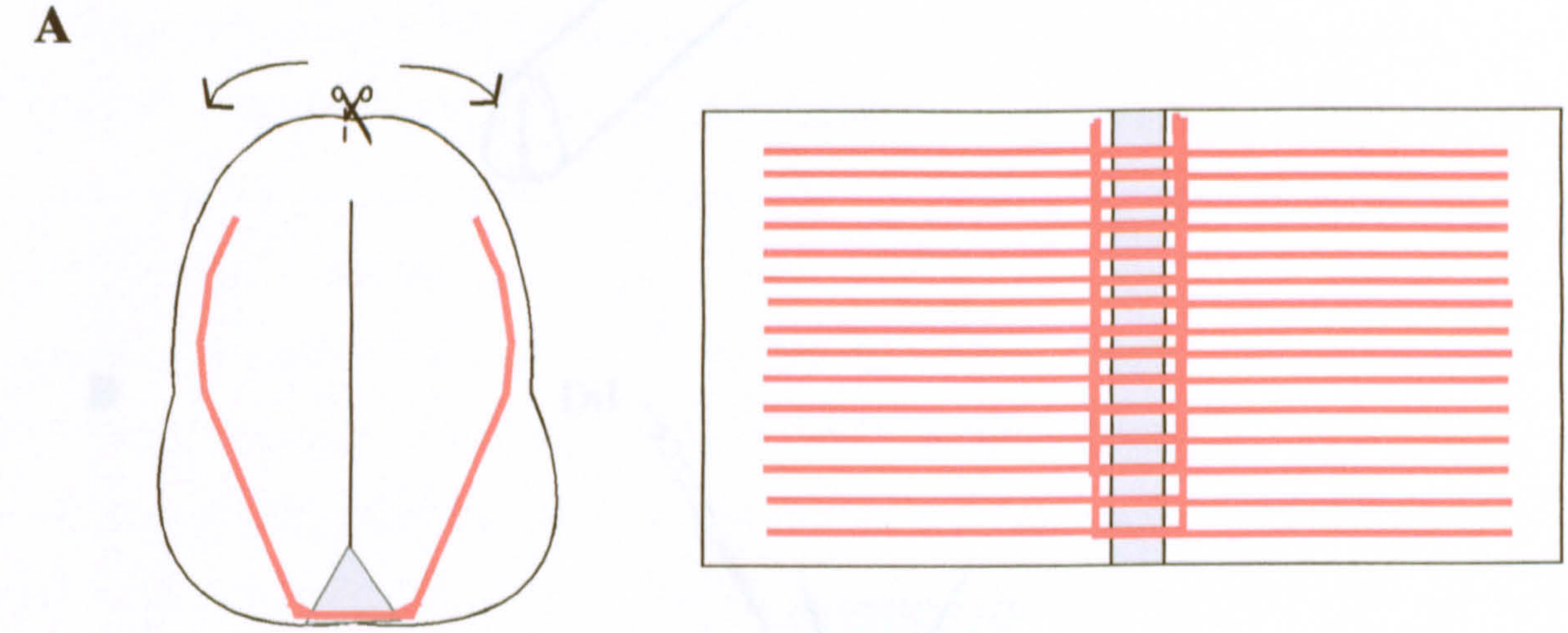

Figure 2.6 The sensitivity of DiI labeling in the spinal cord. Antibodies label bilaterally (A), such that it is not possible to trace individual axons. For example, if a length of spinal cord is cut along its dorsal mid-line to give an "open book" preparation (as indicated on the left and shown on the right), the labelling of all axons means that it is not clear whether axons are projecting ipsilaterally or contralaterally, or rostrally or caudally. In contrast, DiI is applied unilaterally (B). In "open book" preparations, it is possible distinguish between different projections as labelled fascicles must all originate from the same area. Scissors not to scale.

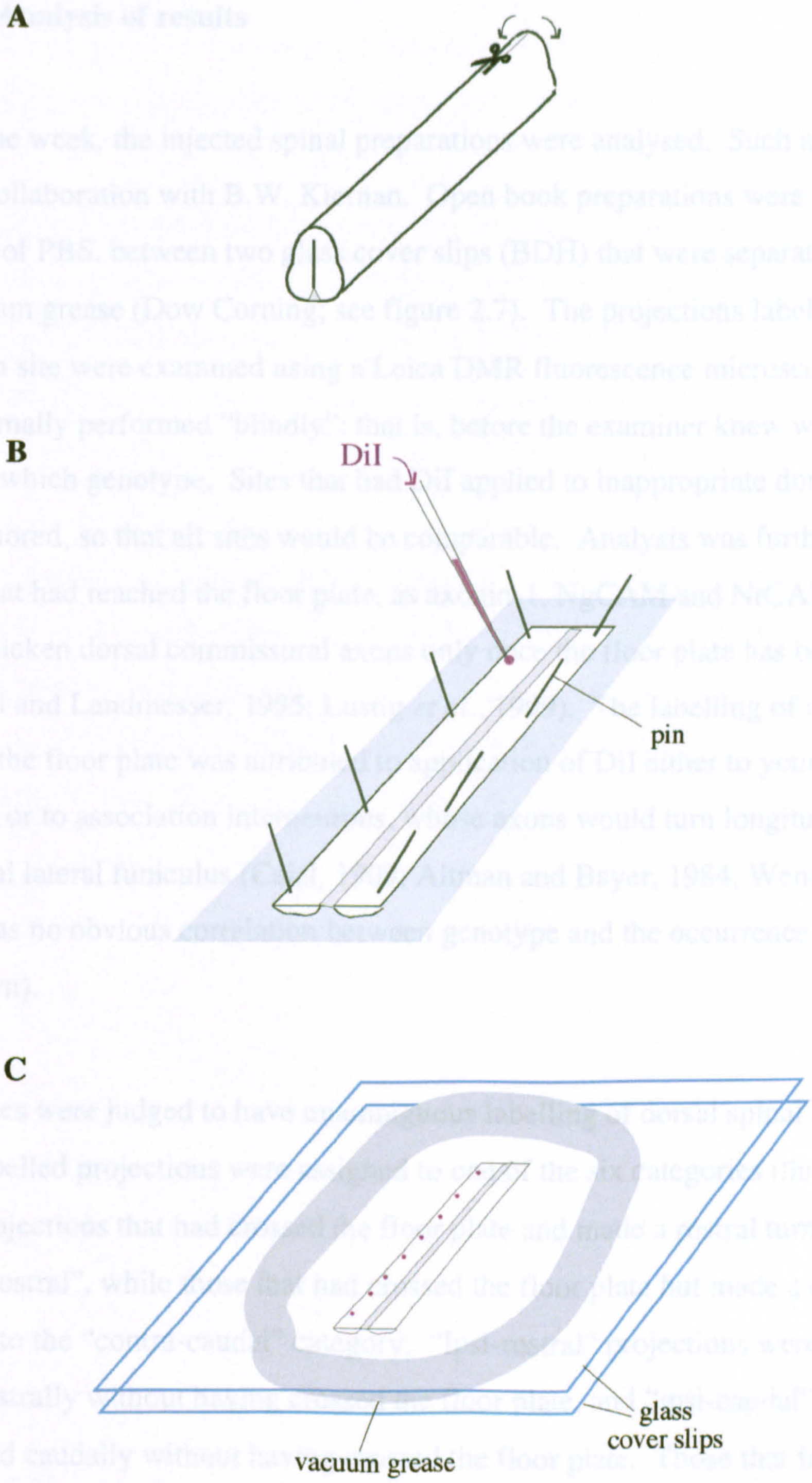

Figure 2.7 Preparation of samples for DiI analysis. A: spinal cords were removed from mouse embryos and slit longitudinally along the roof plate. B: Opened-out spinal cords were pinned down and fixed into an "open book" conformation. After fixation, the preparation was injected with DiI, using a glass micropippette. C: After at least a week, preparations were mounted, in a small volume of PBS, between glass cover slips that were separated by a ring of vacuum grease. This allowed the sample to be examined from both sides under a conventional fluorescence or confocal microscope.

2.3.2 Analysis of results

After one week, the injected spinal preparations were analysed. Such analysis was carried out in collaboration with B.W. Kiernan. Open book preparations were mounted in a small volume of PBS, between two glass cover slips (BDH) that were separated slightly by a ring of vacuum grease (Dow Corning; see figure 2.7). The projections labelled by each injection site were examined using a Leica DMR fluorescence microscope. This analysis was normally performed "blindly": that is, before the examiner knew which preparations were of which genotype. Sites that had DiI applied to inappropriate dorso-ventral locations were ignored, so that all sites would be comparable. Analysis was further restricted to axons that had reached the floor plate, as axonin-1, NgCAM and NrCAM are thought to guide chicken dorsal commissural axons only once the floor plate has been reached (Stoeckli and Landmesser, 1995; Lustig *et al.*, 1999). The labelling of axons that had not reached the floor plate was attributed to application of DiI either to younger commissural neurons, or to association interneurons, whose axons would turn longitudinally in the ipsilateral lateral funiculus (Cajal, 1909; Altman and Bayer, 1984; Wentworth, 1984). There was no obvious correlation between genotype and the occurrence of such axons (data not shown).

When sites were judged to have unambiguous labelling of dorsal spinal axons, proportions of the labelled projections were assigned to one of the six categories illustrated in figure 3.10. Projections that had crossed the floor plate and made a rostral turn were classed as "contra-rostral", while those that had crossed the floor plate but made a caudal turn were assigned to the "contra-caudal" category. "Ipsi-rostral" projections were those that had turned rostrally without having crossed the floor plate, and "ipsi-caudal" ones those that had turned caudally without having crossed the floor plate. Those that failed to turn, and instead continued to extend circumferentially into the contra-lateral spinal cord, were classed as "continuing". Axons that appeared to have been in the process of crossing the floor plate at the time of spinal cord fixation were said to be "in/at the floor plate". Where possible, the proportions of projections in each category were determined by counts of

labelled axon/fascicles. In other cases, proportions were estimated. The validity of this approach was tested by comparing estimates with those of another researcher, and also with those made from photographs of the sites (data not shown).

When required, samples were imaged using a Leica TCS SP confocal system and TCS NT/SP software, or were photographed using an Olympus BX60 fluorescent microscope, Olympus PM C35DX camera, Olympus PM 30 Exposure Control Unit, Kodak Ektachrome P1600 film. In the latter case, pictures were scanned electronically using a Nikon LS-2000 scanner. Figures were prepared using Adobe Photoshop and Canvas 7.

The mean proportion of axons in each category was calculated for all of the injection sites of each type. The proportions of axons within each category were displayed graphically using Microsoft Excel (Excel:mac, 2001). This software was also used to test the statistical significance of apparent differences, one-way ANOVA (analysis of variance) tests being judged to be the most appropriate (Dytham, 1999).

2.4 Staining for structures that contain ß-galactosidase

2.4.1 Staining for ß-galactosidase activity

Fresh samples (brains or embryos) were rinsed in PBS, and fixed for approximately one hour in fresh "*lacZ* fixative" (1% paraformaldehyde, 0.2% gluataraldehyde, 5mM EGTA and 0.02% $Triton_{x100}$, in PBS) at room temperature. After at least three washes in *lacZ* wash (1mM EGTA, 2mM $MgCl_2$ and 0.02% $Triton_{x100}$, in PBS), each lasting at least 30 minutes, ß-galactosidase activity was visualised. This involved an overnight incubation in *lacZ* staining solution (5mM potassium ferrocyanide (Sigma), 5mM potassium ferricyanide (Sigma), 0.01% sodium deoxycholate, and 0.02% $Triton_{x100}$, in PBS) to which had been added 1 mg/ml 5-bromo-4-chloro-3-indolyl-ß-$_D$-galactopyranoside (X-gal, Sigma). This incubation was carried out at room temperature, in darkness.

The following day, samples were rinsed thoroughly in PBS. They were then fixed overnight in 4% paraformaldehyde at 4°C, for better preservation of staining, and stored at 4°C in PBS.

2.4.2 Processing of stained samples

Samples stained for ß-galactosidase activity were subsequently processed in one of a number of ways. Brains and bisected brains were photographed using a Zeiss Stemi SV6 dissecting microscope with MC-100 camera attachment and Kodak Ektachrome 64T film. Stained structures were identified using Paxinos, 1985, Yamamoto *et al.*, 1986, Paxinos *et al.*, 1991, Fitzgerald, 1992, Wolfer *et al.*, 1994, Altman and Bayer, 1995 and Jacobowitz and Abbott, 1997.

Embryos were usually cleared. Clearing involved dehydration by successive overnight incubations in 70% ethanol, 100% methanol and fresh 100% methanol, before immersion in benzoyl benzoate: benzoyl alcohol mixture (ratio of 2:1, both from Sigma). This rendered the embryos transparent, allowing ß-galactosidase stained structures to be studied in more detail. Embryos were photographed using a Zeiss Stemi SV6 dissecting microscope with either an MC-100 camera attachment and Kodak Ektachrome 64T film, or a Nikon Coolpix 990 digital camera. Figures were prepared using Adobe Photoshop and Canvas 7. Stained structures were identified using Paxinos *et al.*, 1991, Kaufman, 1992 and Jacobowitz and Abbott, 1997. In the case of whole embryos, the phenotype of the hypoglossal nerve was scored, as illustrated in figures 6.2 and 6.3. The phenotypes recorded for mutant and control embryos were compared using a χ^2 test (Microsoft Excel:mac, 2001, as suggested by Dytham, 1999).

Embryos were also often sectioned. If they had been cleared, they were first "un-cleared" and re-hydrated, the dehydrating and clearing process described above being carried out in reverse. Regions of interest were pre-incubated in embedding mixture (made up as 2.25g gelatin dissolved in 50ml PBS, to which was added PBS up to a volume of 400ml, 135g albumin, and 90g sucrose), overnight for between 1 and 3 nights depending upon size of the tissue. After this, the sample was put onto a layer of the same embedding mixture, which had been set with 1 part in 10 of 25% glutaraldehyde, in the base of an embedding mould. More embedding /glutaraldehyde mixture was then added. Once the whole block had set, 100µm sections were made using a Series 1000 Vibratome Sectioning System. Sections were collected in 24-well plates containing PBS, and were examined using a Zeiss Stemi SV6 dissecting microscope. If high magnification was required, sections were mounted between two cover slips (as described above and shown in figure 2.7 for open book preparations) and examined using a Zeiss Axiophot microscope. Photographs were taken either using an MC-100 camera attachment and Kodak Ektachrome 64T film, or using a Nikon Coolpix 990 digital camera. In the former case, pictures were scanned electronically using a Nikon LS-2000 scanner. Figures were prepared using Adobe Photoshop and Canvas 7. Unless otherwise stated, the sections shown were from inter-limb levels of the spinal cord.

3 Roles of Immunoglobulin-like Cell Adhesion Molecules in Guidance of Dorsal Spinal Commissural Axons at the Rodent Floor Plate

3.1 Abstract

One of the most striking examples of IgCAM expression is that of commissural neurons of the dorsal spinal cord. In rodents, TAG-1 is expressed as the axons of dorsal commissural interneurons extend towards the midline and cross it, but not once they have turned longitudinally. In contrast L1 is expressed only during and after decussation (Dodd *et al.*, 1988). NrCAM is expressed by the decussating portions of commissural axons, and also by the midline region that the axons cross (Stoeckli and Landmesser, 1995; Lustig *et al.*, 1999, 2001). Perturbation of the functions of the corresponding chicken IgCAMs using antibodies (Stoeckli and Landmesser, 1995, Lustig *et al.*, 1999) has suggested that these molecules are important for the correct guidance of avian dorsal commissural axons.

This chapter describes an investigation into the roles of TAG-1, L1 and NrCAM in guidance of mammalian dorsal spinal projections. In addition to demonstrating that dorsal spinal neurons do not necessarily all decussate and turn rostrally, as had previously been implied, it shows that mutations in the*TAG-1*, *L1* or *NrCAM* genes alone do not have significant effects upon their guidance. However, it does seem that when both of the *TAG-1* and *L1* genes are mutated, the development of at least some dorsal spinal projections is perturbed. At E12.5, double mutant embryos had a greater proportion of axons "in or at the floor plate" than did wild type embryos. However, at E13.5, the spinal cords of double mutant embryos have a *smaller* proportion of their dorsal spinal axons within the midline. These results suggest that L1 and TAG-1 are in fact involved in the ability of dorsal spinal axons to cross the floor plate, but that other factors can compensate for their absence.

3.2 Introduction

3.2.1 Commissural neurons

Commissural neurons are those whose axons decussate: that is, those whose axons extend across the midline of the nervous system. The axons of commissural neurons make synaptic contacts with targets on the contralateral side of the nervous system to that of their cell body. Such connections between the two halves of the body are important for co-ordination of sensory input to, and of motor output from, the brain. If inappropriate decussations are made, or appropriate ones are not, function of the nervous system can be compromised. For example, inappropriate decussations seem to underlie "mirror movement" disorders, in which patients are unable to prevent both sides of the body from carrying out actions intended for just one side (Schott and Wyke, 1981; Yokoyama *et al.*, 2001). Axons of the corticospinal tract and/or corpus callosum fail to decussate in a number of retardation syndromes (Wong *et al.*, 1995, Brümmendorf *et al.*, 1998). Thus the ability of axons to grow across the midline of the developing nervous system is carefully controlled.

3.2.2 D1 interneurons

The spinal cord consists of a variety of populations of neurons (figure 3.1), and some of these are commissural (Wentworth, 1984). The axons of motor neurons, which extend out of the ventral horn of the spinal cord to peripheral targets such as muscles, do not decussate. The axons of interneurons, which are by far the most common spinal neurons (Jankowska and Lundberg, 1981), project entirely within the central nervous system and synapse on other neurons. If their axons extend across the midline of the spinal cord, to a target on the contralateral side of the nervous system, they are known as commissural interneurons. The majority of commissural axons decussate ventral to the lumen of the spinal cord, in the ventral commissure, although a few do decussate dorsal to the lumen, in the dorsal commissure (Cajal, 1909; Orlino *et al.*, 2000). If the axon of an interneuron

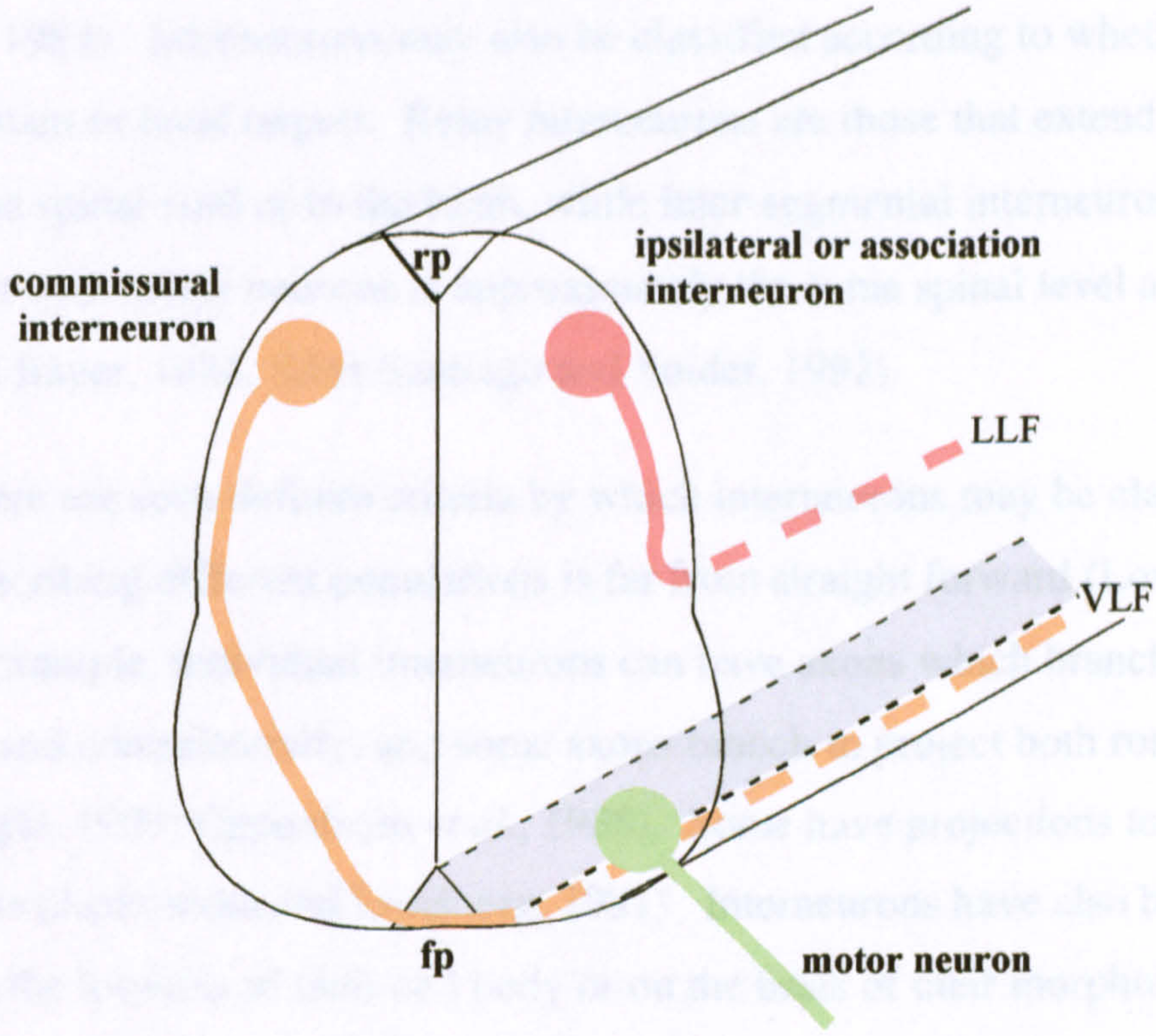

Figure 3.1. The major classes of neurons that originate in the spinal cord. Interneurons of either type may also be classified as relay interneurons if their axons project to distant regions of the spinal cord or to the brain, or as intersegmental interneurons if their axons extend to targets at approximately the same rostro-caudal level as the cell body. The axon of the commissural interneuron is shown extending rostrally in the ventral longitudinal fasciculus (VLF); the ipsilateral interneuron is shown extending rostrally in the lateral longitudinal fasciculus (LLF). rp- roof plate; fp- floor plate.

remains ipsilateral, that is, if it extends only on the same side of the nervous system as the cell body, the neuron is said to be an association interneuron (Altman and Bayer, 1984; Wentworth, 1984). Interneurons may also be classified according to whether their axons extend to distant or local targets. Relay interneurons are those that extend axons to distant regions of the spinal cord or to the brain, while inter-segmental interneurons are those that make contact with motor neurons at approximately the same spinal level as their cell body (Altman and Bayer, 1984; Silos-Santiago and Snider, 1992).

Although there are such definite criteria by which interneurons may be classified, the matter of describing different populations is far from straight forward (Lowrie and Lawson, 2000). For example, individual interneurons can have axons which branch to project both ipsilaterally and contralaterally, and some axons branch to project both rostrally and caudally (Cajal, 1909; Oppenheim *et al.*, 1988). Some have projections to both local and distant targets (Jankowska and Lundberg, 1981). Interneurons have also been classified according to the location of their cell body or on the basis of their morphology, in addition to their axonal projection (for example, Oppenheim *et al.*, 1988; Silos-Santiago and Snider, 1992, 1994; Eide *et al.*, 1999). However, differences in species and developmental stages used mean that is often extremely difficult to determine how such methods of classification relate to one another (Eide *et al.*, 1999), or to the adult situation (Oppenheim *et al.*, 1988). In the adult rat, axons of dorsal horn commissural neurons contribute to the spinothalamic (Tracey, 1985) and ventral spinocerebellar (Brown, 1981) tracts, while the axons of other adult dorsal horn neurons may contribute to the ipsilateral spinocervical and dorsal column pathways (Brown, 1981). However, interneuron cell bodies migrate considerably during development (Leber and Sanes, 1995), and the position of a mature neuron can often be quite different from the site of origin (Lee *et al.*, 1998; Pierani *et al.*, 2001).

More recent studies classify interneurons according to the transcription factors that they express during development, although relating early gene expression to ultimate axon trajectory remains difficult (Bermingham *et al.*, 2001). Using criteria of Lim homeobox transcription factor expression, there seem to be at least nine distinct classes of interneurons (figure 3.2 A). Five of these classes originate in the dorsal spinal cord (that is, the region

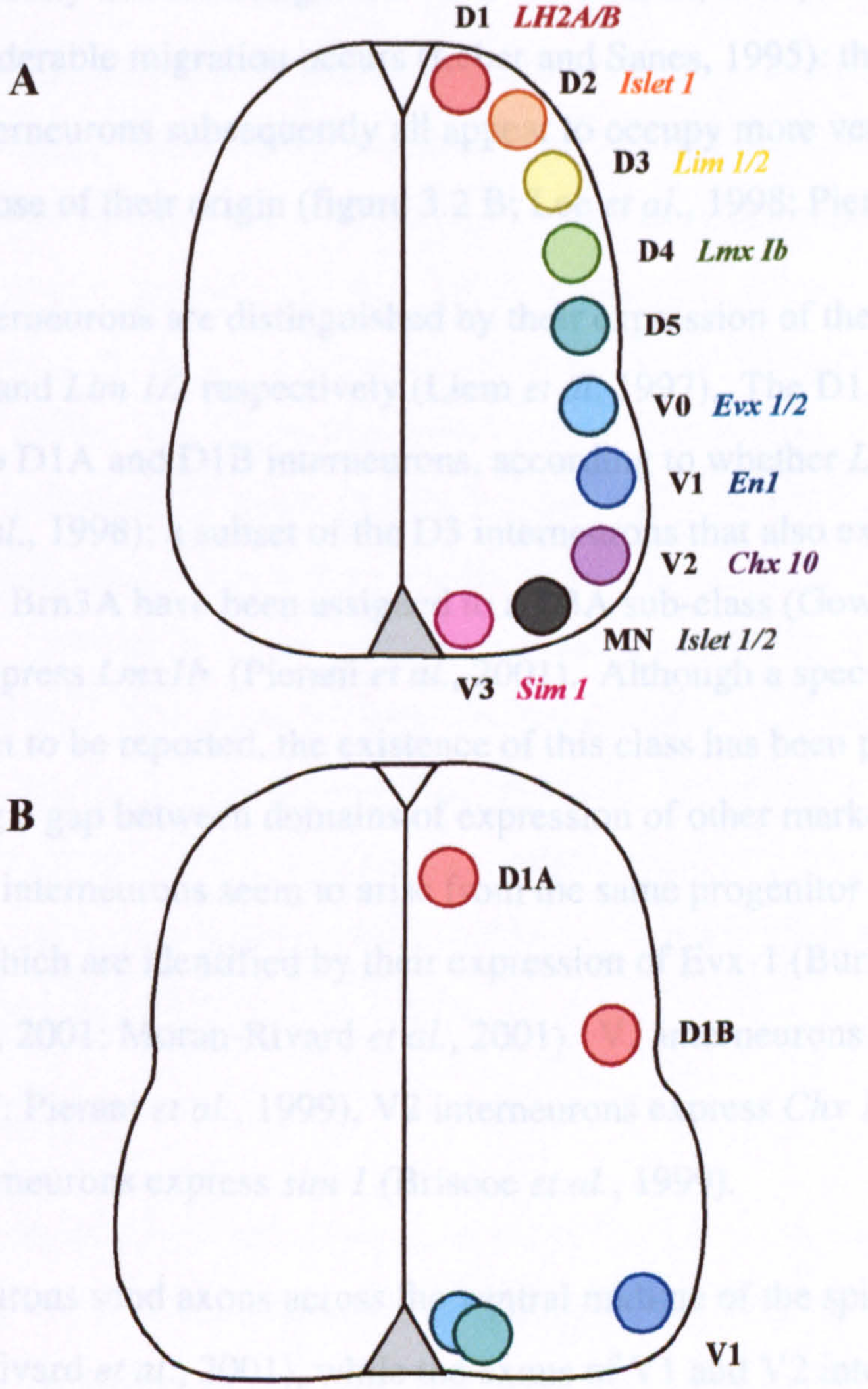

Figure 3.2 Different classes of developing spinal neurons.
A. There are at least 9 distinct populations of interneurons within the developing spinal cord: five dorsal (D1 to D5) and four ventral (V0 to V3). The ventral spinal cord also contains motor neurons (MN). The different classes of neurons are distinguished by the expression of characteristic transcription factors (shown above in italics), and the dorso-ventral region of the spinal cord in which they originate (shown above for approximately E10.5 spinal cord). Using Burril *et al.*, 1997; Liem *et al.*, 1997; Matise and Joyner, 1997; Lee *et al.*, 1998; Briscoe *et al.*, 1999, 2000; Pierani *et al.* 2001; Moran-Rivard *et al.*, 2001.
B. At least some of the populations occupy different regions of the spinal cord by E12.5. The D1 interneurons have migrated ventrally and form two distinct sub-groups (Lee *et al.*, 1998); the D5, V0 and V1 neurons also appear to have migrated to more ventral locations (Moran-Rivard *et al.*, 2001). The V2 interneurons are also thought migrate ventrally (Moran-Rivard *et al.*, 2001). The later positions of the other interneuron classes has not been reported.

dorsal to the *sulcus limitans*; Shoji *et al.*, 1996; Matise and Joyner, 1997), and are referred to as classes D1 to D5 (Lee and Jessell, 1999; Pierani *et al.*, 2001). The other four classes originate more ventrally and are designated V0 to V3 (Jessell, 2000). However, it should be noted that considerable migration occurs (Leber and Sanes, 1995): the cell bodies of D1, D5, V0 and V1 interneurons subsequently all appear to occupy more ventral regions of the spinal cord than those of their origin (figure 3.2 B; Lee *et al.*, 1998; Pierani *et al.*, 2001).

D1, D2 and D3 interneurons are distinguished by their expression of the Lim homeobox genes *LH2, islet 1* and *Lim 1/2* respectively (Liem *et al*, 1997). The D1 population can be further divided into D1A and D1B interneurons, according to whether *LH2A* or *LH2B* is expressed (Lee *et al.*, 1998); a subset of the D3 interneurons that also expresses the transcription factor Brn3A have been assigned to a D3A sub-class (Gowan *et al.*, 2001). D4 interneurons express *Lmx1b* (Pierani *et al.*, 2001). Although a specific marker of D5 interneurons has yet to be reported, the existence of this class has been predicted on the basis of there being a gap between domains of expression of other markers (Matise and Joyner, 1997). D5 interneurons seem to arise from the same progenitor population as the V0 interneurons, which are identified by their expression of Evx-1 (Burrill *et al.*, 1997; Pierani *et al.*, 1999, 2001; Moran-Rivard *et al.*, 2001). V1 interneurons express *En 1* (Burrill *et al.*, 1997; Pierani *et al.*, 1999), V2 interneurons express *Chx 10* (Briscoe *et al.*, 2000), and V3 interneurons express *sim 1* (Briscoe *et al.*, 1999).

D1 and V0 interneurons send axons across the ventral midline of the spinal cord (Liem *et al.*, 1997; Moran-Rivard *et al.*, 2001), while the axons of V1 and V2 interneurons project entirely within the ipsilateral spinal cord (Saueressig *et al.*, 1999; Moran-Rivard *et al.*, 2001). The nature of the D2, D3, D4, D5 and V3 axonal projections is not well documented, although lack of expression of the dorsal commissural neuron markers TAG-1 (Liem *et al.*, 1997) and Math-1 (Helms and Johnson, 1998; Lee *et al.*, 1998) implies that D2 and D3 axons remain ipsilateral. Thus D1 interneurons are so far the only neurons of dorsal origin that are known send axons across the floor plate.

3.2.3 Guidance of the axons of Dorsal Spinal Commissural Interneurons

3.2.3.1 From cell body to floor plate

The guidance of dorsal commissural interneuron axons has been studied extensively, and what are thought to be D1 axons are now known to be guided by a number of different molecular mechanisms (summarised in figure 3.3). Beginning at around E9 in the mouse embryo, the axons project ventrally (Holley, 1982; Altman and Bayer, 1984; Wentworth, 1984), apparently being forced away from the roof plate by the repulsive activity of BMP7 (Augsburger *et al.*, 1999). The axons then continue to extend ventrally and also medially, under the attractive influence of Netrin (Kennedy *et al.*, 1994; Serafini *et al.*, 1994, 1996), which is secreted by the floor plate and responded to via the axonal Ig-like receptor DCC (Keino-Masu *et al.*, 1996; de la Torre *et al.*, 1997; Stein *et al.*, 2001). There might also be other, as yet unidentified, floor plate attractant factors (Serafini *et al.*, 1996; Hummel *et al.*, 1999). The 400μm from cell body to floor plate is crossed in approximately twenty-four hours (Bovolenta and Dodd, 1990), with the first commissural axons reaching the floor plate at about E10, and later generated axons continuing to reach the floor plate during the following forty-eight hours (Wentworth, 1984).

3.2.3.2 Floor plate entry

Once at the floor plate, commissural axons must extend into this structure. Continued attraction by Netrin, and short-range attraction by F-Spondin (Burstyn-Cohen *et al.*, 1999) appear to encourage the axons to extend into the midline. It has also been suggested that certain IgCAMs might be involved in floor plate entry, as they are expressed in a highly specific manner. At the time of floor plate entry, dorsal spinal expression of TAG-1 appears to be unique to D1 interneurons (Vaughn et *al.*, 1992; Liem *et al.*, 1997). It is found on the surface of D1 cell bodies from the onset of their differentiation, and once axons begin to extend expression becomes restricted to these processes (Dodd *et al.*, 1988). When the axons have crossed the midline of the spinal cord, they too cease to express TAG-1, possibly due to the influence of the floor plate cells (Bovolenta and Dodd, 1991; Campbell and Peterson, 1993; Matise *et al.*, 1999; Zou *et al.*, 2000; figure 3.4 A, D, G, J

1. Cell body to floor plate

- Repulsion from roof plate by BMP7 (rat)
- Attraction to floor plate by netrins (mouse, chicken, rat)

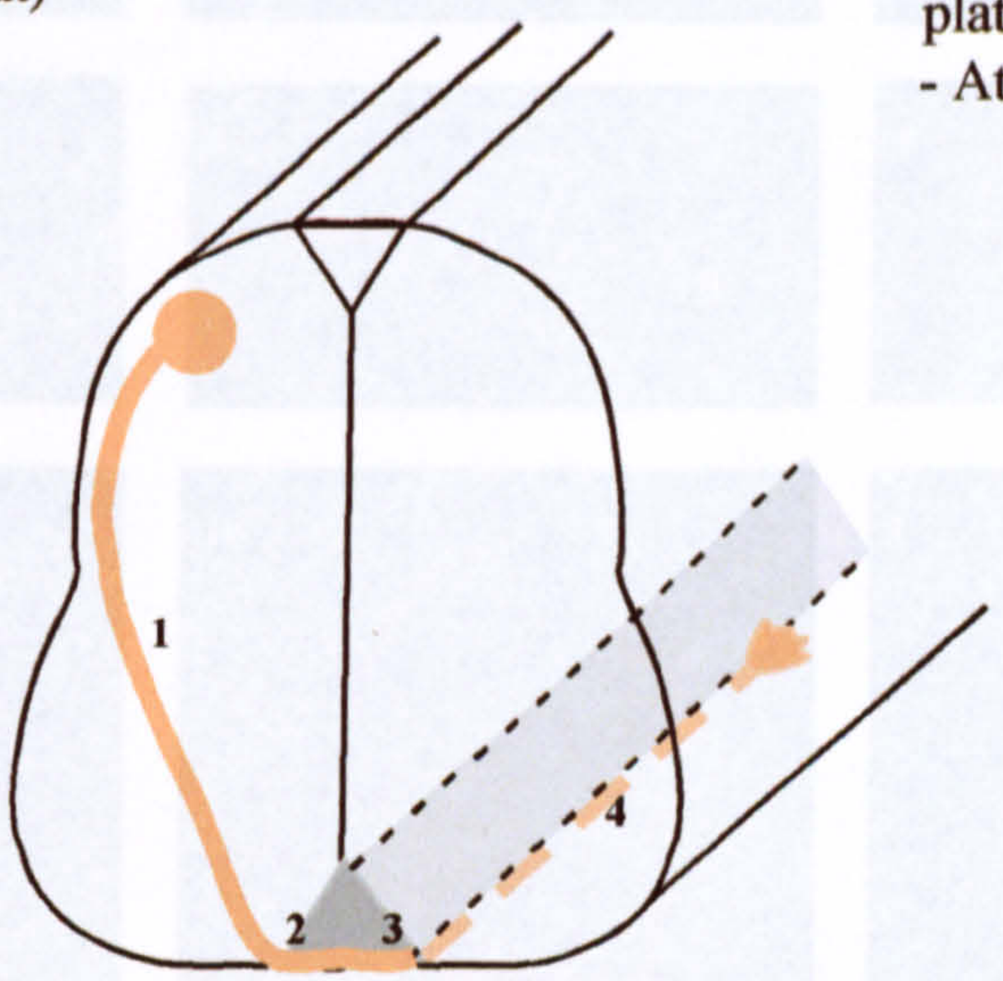

2. Floor plate entry

- Continued attraction by netrins
- Axons are unable to respond to the repulsive midline factor Sema 3B (mouse)
- Lack of axonal Eph B receptors (mouse)
- Masking of a repulsive cue by axonin-1 (TAG-1) - NrCAM interactions (chicken)
- Low axonal expression of Robo, receptor for the repulsive midline factor Slit (*Drosophila*)
- *Low axonal expression of L1 (mouse,rat)*

3. Floor plate exit

- Loss of attraction to netrins (rat), due to interaction of Robo with DCC (*Xenopus*)
- Axons acquire sensitivity to the repulsive midline factor Sema 3B (mouse)
- Increased axonal expression of Eph receptors mediates repulsion by midline ephrins (mouse)
- Increased axonal expression of Robo mediates repulsion by Slit (*Drosophila*)
- *Up regulation of axonal F11/F3/ contactin (chicken)*
  Up regulation of L1(mouse, rat)
- *Down regulation of axonal DM-GRASP, N-Cadherin* and *ß1 integrins (chicken)*
- *Down regulation of axonal TAG-1 (mouse, rat)*

4. Longitudinal extension

- Continued repulsion from the floor plate (as for floor plate exit)
- Attraction to floor plate by F-Spondin (chicken)
- Repulsion from more lateral regions by Slit-2 and Sema 3E(mouse)
- Fasciculation along other longitudinal axons (chicken)

Figure 3.3 Mechanisms that might guide dorsal commissural interneurons.
Four stages of dorsal commissural axon guidance are shown. Mechanisms suggested to be acting at each stage are listed, along with the species in which experiments were performed . Note that the change in surface Robo expression has not yet been demonstrated in vertebrates. Expression patterns which are of note, but which have not yet been shown to be of physiological relevance, are given in italics.
For references, see text.

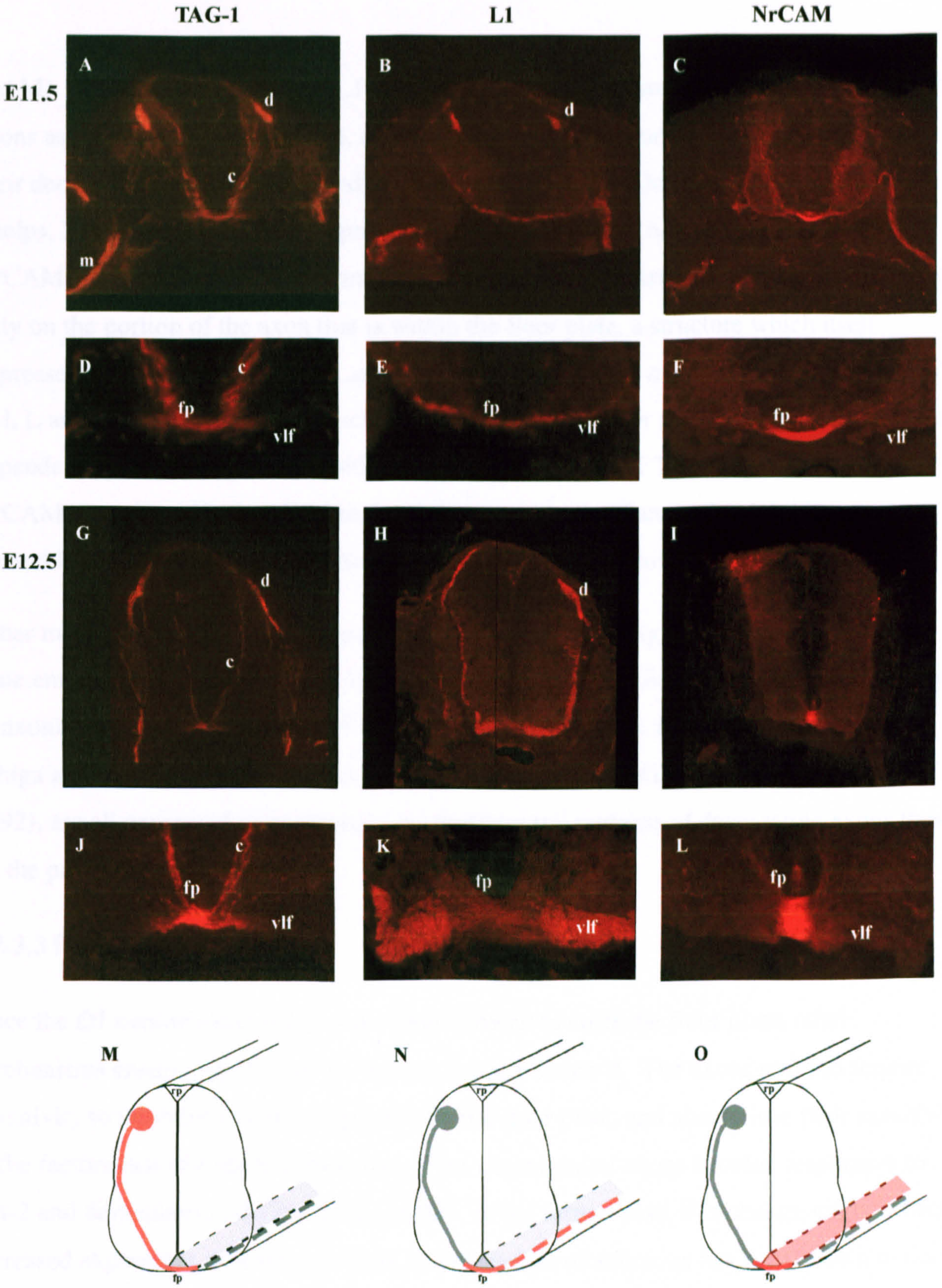

Figure 3.4 Expression of the IgCAMs TAG-1, L1 and NrCAM in E11.5 and E12.5 mouse spinal cord. Transverse sections were labelled using antibodies to TAG-1 (A, D, G and J), L1 (B, E, H and K) or NrCAM (C, F, I and J). A-F: expression of TAG-1, L1 and NrCAM in E11.5 spinal cord. D-F show the floor plate regions at a higher magnification. The antibody to TAG-1 has labelled commissural axons (c), from the dorsal origin to their decussation underneath the floor plate (fp). The area at which dorsal root ganglion axons enter the spinal cord is particularly strongly labelled (d; also labelled strongly for L1 in B), as are the motor axons extending into the periphery(m). L1 is strongly expressed by commissural axons underneath the floor plate and in the ventral longitudinal funiculus (vlf). Axons label most strongly for NrCAM underneath the floor plate. The floor plate cells themselves also express NrCAM (F).
At E12.5, the expression patterns are very similar to those at at E11.5 (G-L). The major difference is that many more axons can be seen beneath the floor plate and in the ventral longitudinal fasciculus, as more axons have decussated. M-O summarize expression of the three IgCAMs by dorsal commissural neurons. Red indicates strong surface expression.

and M). In contrast, the IgCAM L1 is only expressed on the surface of dorsal commissural axons as they reach the floor plate, and this expression continues as the axons complete their decussation and turn to extend in the ventral funiculus (Dodd *et al*, 1988; Tran and Phelps, 2000; Zou *et al.*, 2000; figure 3.4 B, E, H, K and N). Another L1-like protein, NrCAM, is also expressed by commissural axons, although surface levels appear to be high only on the portion of the axon that is within the floor plate, a structure which itself expresses NrCAM (Stoeckli and Landmesser, 1995; Lustig *et al.*, 1999, 2001; figure 3.4 C, F, I, L and O). Experiments in chick have suggested that floor plate entry is at least in part dependent upon these IgCAMs, with the chick homologues of TAG-1 (axonin-1), and NrCAM, seeming to be involved in the ability to overcome factors that inhibit entry (Stoeckli and Landmesser, 1995; Stoeckli *et al.*, 1997; see below).

Other molecules have expression patterns that are similarly suggestive of roles in floor plate entry, although their *in vivo* functions have not been studied in the same way as those of axonin-1, NgCAM and NrCAM. The IgCAM Neurofascin, ß1-integrins, N-cadherin (Shiga and Oppenheim, 1991), and possibly the IgCAM DM-GRASP (El-Deeb *et al.*, 1992), are all expressed more strongly on commissural portions of decussating axons than on the pre-commissural surfaces.

3.2.3.3 Floor plate exit

Once the D1 commissural axons have been allowed to enter the floor plate, other mechanisms ensure that they do not simply remain within it. The axons seem to acquire sensitivity to inhibitory factors expressed by the floor plate, and also to lose their sensitivity to the factors that had made it attractive. Post-commissural axons become responsive to Slit-2 and Semaphorin 3B (Zou *et al.*, 2000). In the former case, this change might reflect increased expression of Robo receptors on the surface of axons, as has been shown to occur in *Drosophila* (Kidd *et al.*, 1998 a, b; 1999; Brose *et al.*, 1999). Axonal expression of the Eph B1 receptor also seems to increase at the time of floor plate exit (Imondi *et al.*, 2000), possibly so that the axons can begin to be repelled by floor plate ephrin B3 (Gale et al., 1996; Bergemann *et al.*, 1998; Imondi *et al.*, 2000). In addition, post-decussation commissural axons cease to be attracted by Netrin (Shirasaki *et al.*, 1998). This seems to

involve silencing of Netrin receptor function by the newly active Robo receptors (Stein and Tessier-Lavigne 2001; see Dickson, 2001 for review). The down-regulation of axonal TAG-1, and the up-regulation of axonal L1, (Dodd *et al.*, 1988; Shiga and Oppenheim, 1991; figure 3.4) might also be involved in the loss of attraction and/or the onset of repulsion (Shirasaki *et al.*, 1995; Stoeckli and Landmesser, 1998). So too could be the reduced surface expression of ß1-integrins, N-cadherin (Shiga and Oppenheim, 1991) and DM-GRASP (El-Deeb *et al.*, 1992), and the concomitant increased expression of F11 (F3/contactin; Shiga and Oppenheim, 1991) as the axons exit the floor plate.

3.2.3.4 Longitudinal Extension

After decussation, extending spinal commissural axons commonly make a sharp turn to proceed longitudinally, growing alongside the floor plate, in the ventral funiculus of the spinal cord (Altman and Bayer, 1984; Oppenheim *et al.*, 1988). This longitudinal turn appears to require a balance of attractive and repulsive factors. Continued expression of the aforementioned receptors for repulsive floor plate factors, and the loss of sensitivity to floor plate attractants, ensures that commissural axons do not re-decussate (Kidd *et al.*, 1998b, 1999; Harris and Holt, 1999; Imondi *et al.*, 2000; Zou *et al.*, 2000; Stein *et al.*, 2001). A number of other mechanisms ensure that the axons are still able to extend alongside the floor plate, rather than being repelled into more lateral spinal cord. It appears that the floor plate continues to produce at least one attractive factor. F-spondin, a positive signal for neurite extension, is expressed at the time when commissural axons are extending longitudinally (Klar *et al.*, 1992; Burstyn-Cohen *et al.*, 1999). It has been shown that injection of antibodies to F-spondin reduces the ability of commissural axons to turn sharply, the axons appearing to be more reluctant to maintain contact with the floor plate (Burstyn-Cohen *et al.*, 1999). However, a longitudinal turn is still made, suggesting that F-spondin is not the only factor that prevents the axons from continuing to extend into more lateral tissue. Indeed, regions of the lateral spinal cord, such as the cell bodies of motor neurons, have been shown to express some of the same inhibitory factors as the floor plate (Wang *et al.*, 1999; Imondi *et al.*, 2000; Zou *et al.*, 2000). Thus the post-decussation D1 axons are effectively forced to extend in between the motor neurons and ventral midline (Zou *et al.*, 2000). In addition, it is thought that commissural axons specifically extend

along axons that already lie in the ventral funiculus. Such mechanisms have been proposed to involve NgCAM and NrCAM in the chicken (Stoeckli and Landmesser, 1995; Fitzli *et al.*, 2000), and FasII and connectin in the fruit fly (Rusch and Van Vactor, 2000; Simpson *et al.*, 2000).

3.2.4 The Roles of TAG-1, L1 and NrCAM in Guidance of Dorsal Commissural Axons at the Floor Plate

3.2.4.1 The Roles of Axonin-1, NgCAM and NrCAM in Guidance of Chick Dorsal Commissural Axons

As mentioned, experiments conducted on chick embryonic spinal cord have suggested that TAG-1, L1 and NrCAM may influence guidance of commissural axons at the floor plate. Stoeckli and Landmesser (1995) perturbed the function of what are thought to be the chicken homologues of these molecules: axonin-1, the homologue of TAG-1; the chick NrCAM; and NgCAM, which is arguably thought to be the equivalent of L1 (Sonderegger and Rathjen, 1992, and see below). Function-blocking antibodies or purified IgCAMs were injected into the central canals of chick spinal cords *in ovo*. Development was allowed to continue, with periodic repetition of the injection procedure to ensure that levels of the added proteins remained high. Effects on the developing commissural axons were visualised by injection of the dorsal commissural neuron cell bodies with DiI (1,1'-dilinoleyl-3,3,3',3'-tetramethylindocarbocyanine perchlorate), a lipophilic dye that diffuses along cell membranes and enables axons to be traced (Schlessinger *et al.*, 1977; Godement *et al.*, 1987). Antibodies to Ng-CAM caused defasciculation (a reduction in the tightness of bundling) of commissural axons, as illustrated in figure 3.5 A and B. Purified axonin-1 protein, which is thought to compete with endogenous axonin-1 for its usual binding partners (Stoeckli *et al.*, 1991), and antibodies to axonin-1, also caused defasciculation. In addition, when function of axonin-1 was perturbed, up to 50% of commissural axons failed to cross the midline. These axons were instead seen to turn longitudinally on the ipsilateral side of the floor plate, without having decussated (figure 3.5 B). Antibodies to Nr-CAM also caused defasciculation and failure of up to 50% of axons to enter the midline (Stoeckli and Landmesser, 1995).

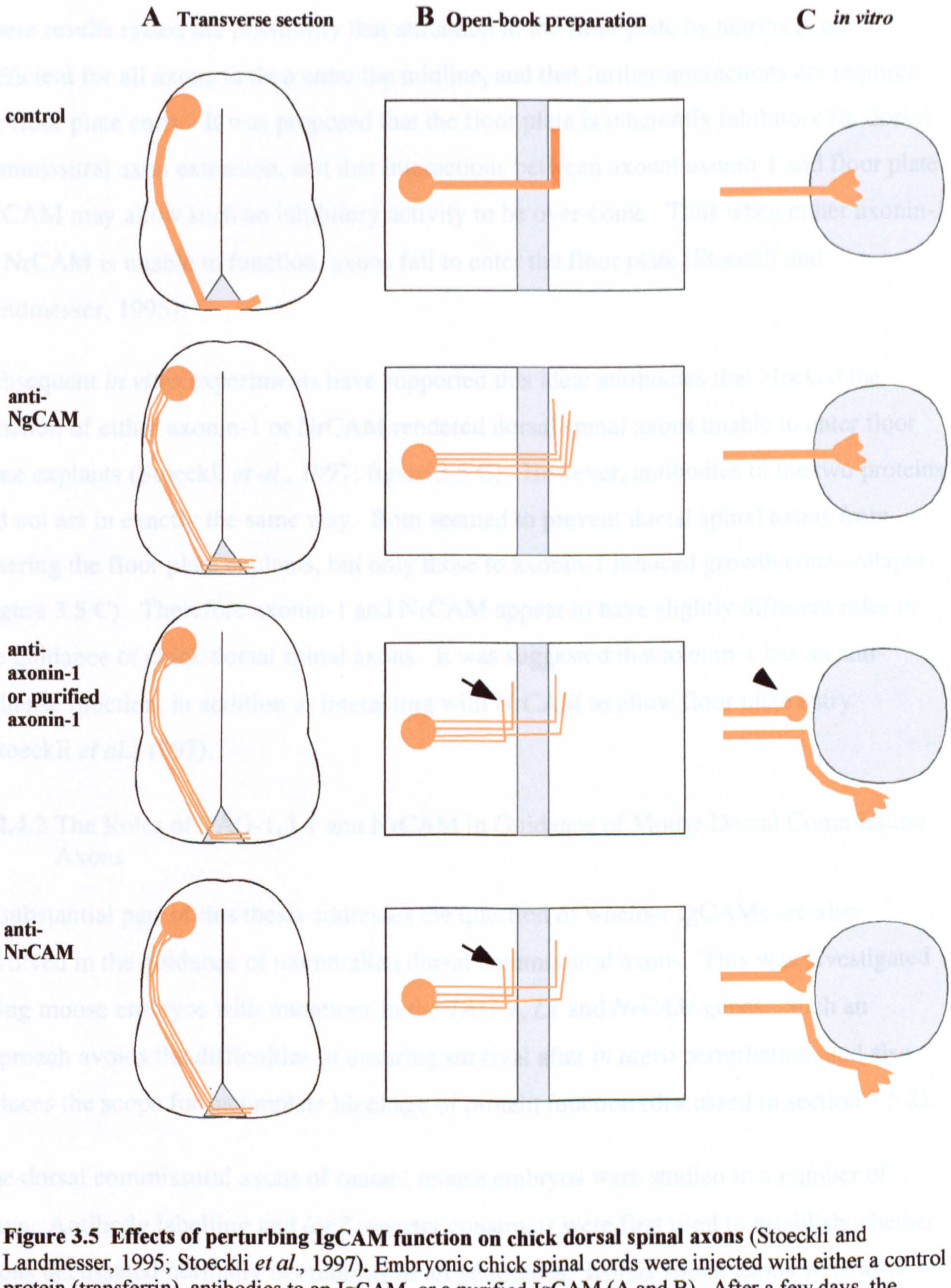

Figure 3.5 Effects of perturbing IgCAM function on chick dorsal spinal axons (Stoeckli and Landmesser, 1995; Stoeckli *et al*., 1997)**.** Embryonic chick spinal cords were injected with either a control protein (transferrin), antibodies to an IgCAM, or a purified IgCAM (A and B). After a few days, the spinal cords were dissected out and either sectioned transversely (A) or cut dorsally to give flat "open-book" preparations (B; see methods). Dorsal spinal neurons were traced using the lipophilic dye DiI. Antibodies to NgCAM caused a defasciculation not seen in control samples. Antibodies to axonin-1 or NrCAM, or purified axonin-1, also caused defasciculation, and in addition up to 50% of axons turned on the ipsilateral side of the floor plate (arrows; Stoeckli and Landmesser, 1995). The effect of IgCAM perturbation upon the ability of dorsal spinal axons to enter floor plate was also tested *in vitro* (C). In control experiments, or when anti-NgCAM antibodies were applied, axons from dorsal spinal cord were able to extend into floor plate tissue (grey). Antibodies to axonin-1 or NrCAM, or purified axonin-1, seemed to prevent floor plate entry. Anti-axonin-1 and purified axonin-1 also caused growth cone collapse (arrow head).

These results raised the possibility that attraction to the floor plate by netrins is not sufficient for all axons to then enter the midline, and that further interactions are required for floor plate entry. It was proposed that the floor plate is inherently inhibitory for dorsal commissural axon extension, and that interactions between axonal axonin-1 and floor plate NrCAM may allow such an inhibitory activity to be over-come. Thus when either axonin-1 or NrCAM is unable to function, axons fail to enter the floor plate (Stoeckli and Landmesser, 1995).

Subsequent *in vitro* experiments have supported this idea: antibodies that blocked the function of either axonin-1 or NrCAM rendered dorsal spinal axons unable to enter floor plate explants (Stoeckli *et al.*, 1997; figure 3.5 C). However, antibodies to the two proteins did not act in exactly the same way. Both seemed to prevent dorsal spinal axons from entering the floor plate explants, but only those to axonin-1 induced growth cone collapse (figure 3.5 C). Therefore axonin-1 and NrCAM appear to have slightly different roles in the guidance of chick dorsal spinal axons. It was suggested that axonin-1 has an anti-collapse function, in addition to interacting with NrCAM to allow floor plate entry (Stoeckli *et al.*, 1997).

3.2.4.2 The Roles of TAG-1, L1 and NrCAM in Guidance of Mouse Dorsal Commissural Axons

A substantial part of this thesis addresses the question of whether IgCAMs are also involved in the guidance of mammalian dorsal commissural axons. This was investigated using mouse embryos with mutations in the *TAG-1*, *L1* and *NrCAM* genes. Such an approach avoids the difficulties of ensuring survival after *in utero* perturbation, and also reduces the scope for incomplete blockage of protein function (discussed in section 1.5.2).

The dorsal commissural axons of mutant mouse embryos were studied in a number of ways. Antibody labelling and *lacZ* reporter constructs were first used to establish whether axons decussated normally in embryos of all genotypes. Dorsal spinal axons were also traced using the lipophilic dye DiI (Schlessinger *et al.*, 1977; Godement *et al.*, 1987; Bovolenta and Dodd, 1990; Stoeckli *et al.*, 1995; see methods), and the results from embryos of different genotypes were compared statistically (Dytham, 1999).

3.3 Results

3.3.1 Antibody labelling of dorsal commissural neurons

In accordance with previous reports, immunofluorescent and immunohistochemical labelling showed that wild type mouse dorsal spinal axons extend across the ventral midline of developing spinal cord (Yamamoto et al., 1986; Bovolenta and Dodd, 1990; figures 3.4 A-J; 3.6 A, C, E and G; 3.8 A, C; 3.9 A, C).

Antibodies were also used to label the dorsal spinal commissural neurons of mutant embryos.

3.3.1.1 Embryos with mutations in *TAG-1*

Figure 3.6 shows approximately transverse sections of E11.5 spinal cord from TAG^A homozygote and wild type embryos. Although the embryos were not sectioned in exactly the same plane, dorsal commissural neurons can be seen to extend underneath the floor plate in both cases (arrowheads). Furthermore, the expression patterns of neurofilament proteins, and the IgCAMs L1 and NrCAM, appear to be unaffected by the mutation. There is no specific labelling of TAG-1 (figure 3.6B) as the monoclonal antibody used does not seem to recognise the proteins produced by the TAG^A allele, although the truncated proteins can be labelled using a polyclonal antibody to TAG-1 (A.J.W. Furley, personal communication). *TAG-1* null mutant embryos were not studied by immunofluorescence, as they were reserved for more sensitive axon tracing techniques (see below).

3.3.1.2 Embryos with mutations in *L1* or *NrCAM*

Figure 3.7 presents transverse sections of E11.5 (a-f) and E12.5 (g-l) wild type and L1 mutant embryos that have been labelled by immunofluorescence. Again, all of the spinal cord sections have at least some labelled axons beneath the floor plate, and the expression of neurofilament proteins, TAG-1 and NrCAM appear unaffected by the mutation.

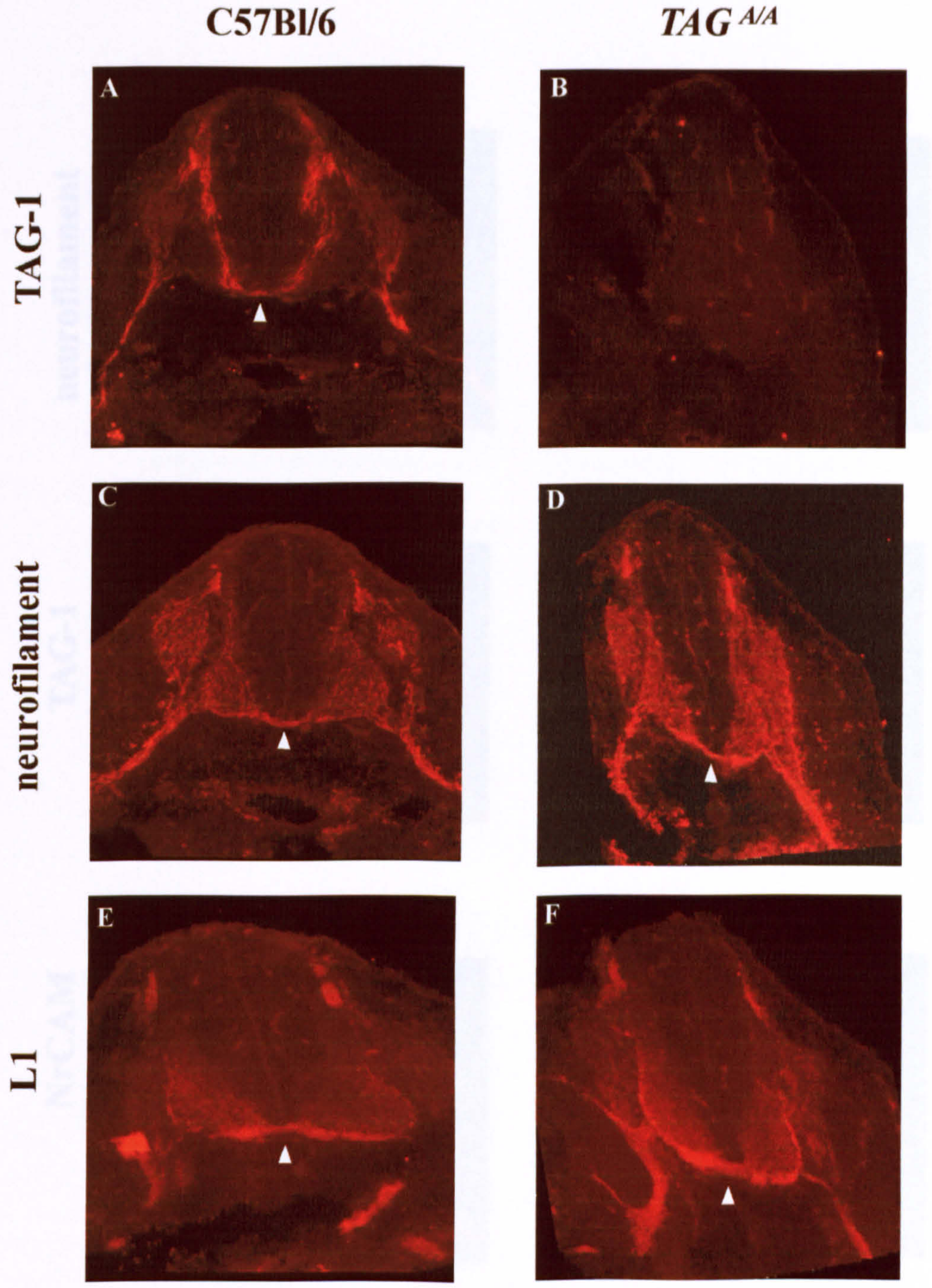

Figure 3.6 Comparison of transverse sections of E11.5 spinal cord which have either wild type (C57Bl/6) or truncated ($TAG^{A/A}$) TAG-1 protein. Sections were labelled with antibodies to the proteins indicated on the left. Arrowheads point to axons which are crossing the midline underneath the floor plate.

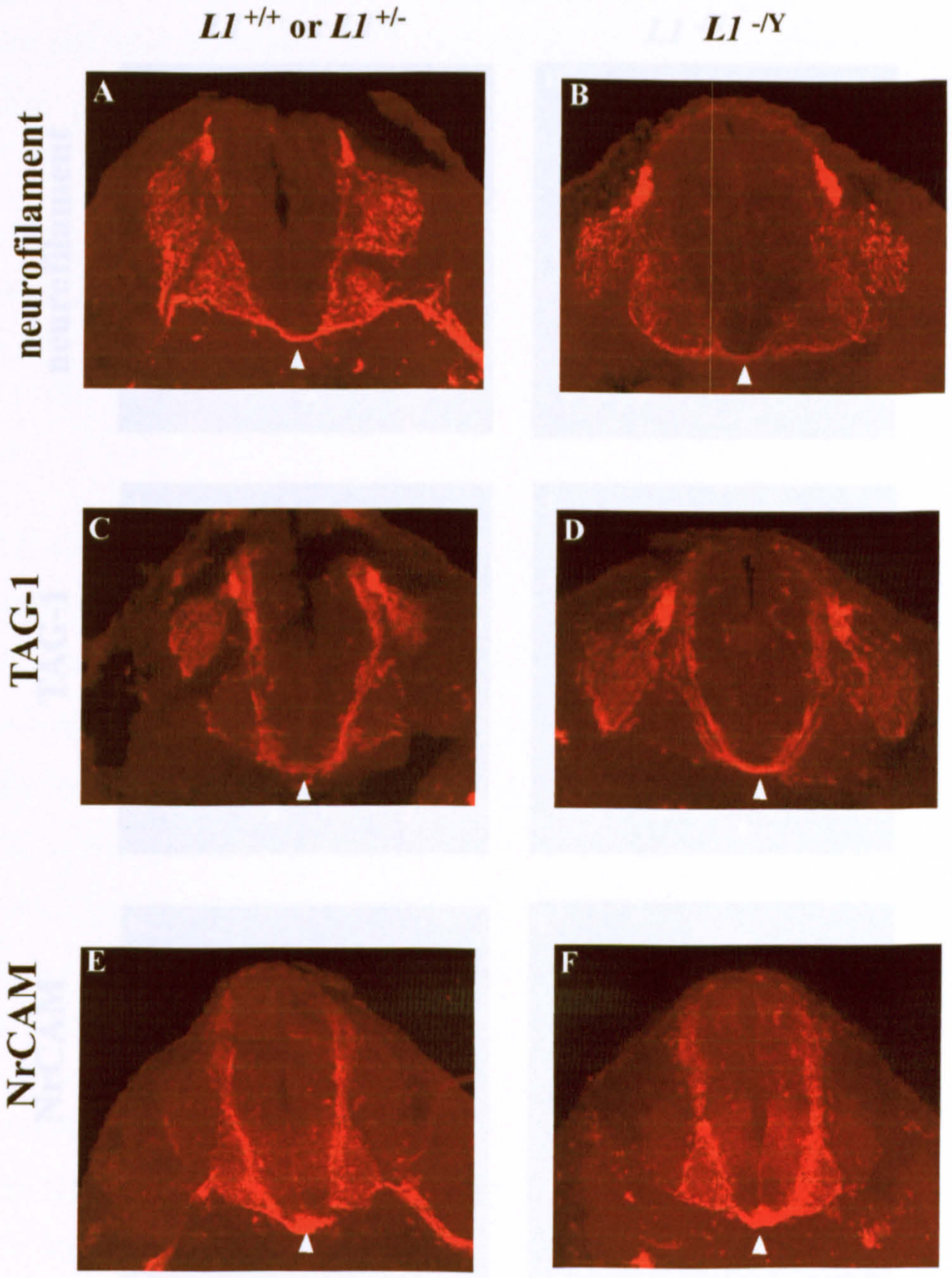

Figure 3.7 Comparison of transverse sections of E11.5 and E12.5 spinal cords taken from embryos that either did or did not have wild type L1 protein.
A - F: E11.5 spinal cord. Sections were labelled using antibodies to the proteins named on the left. Arrowheads indicate the presence of axons beneath the floor plate in all sections.

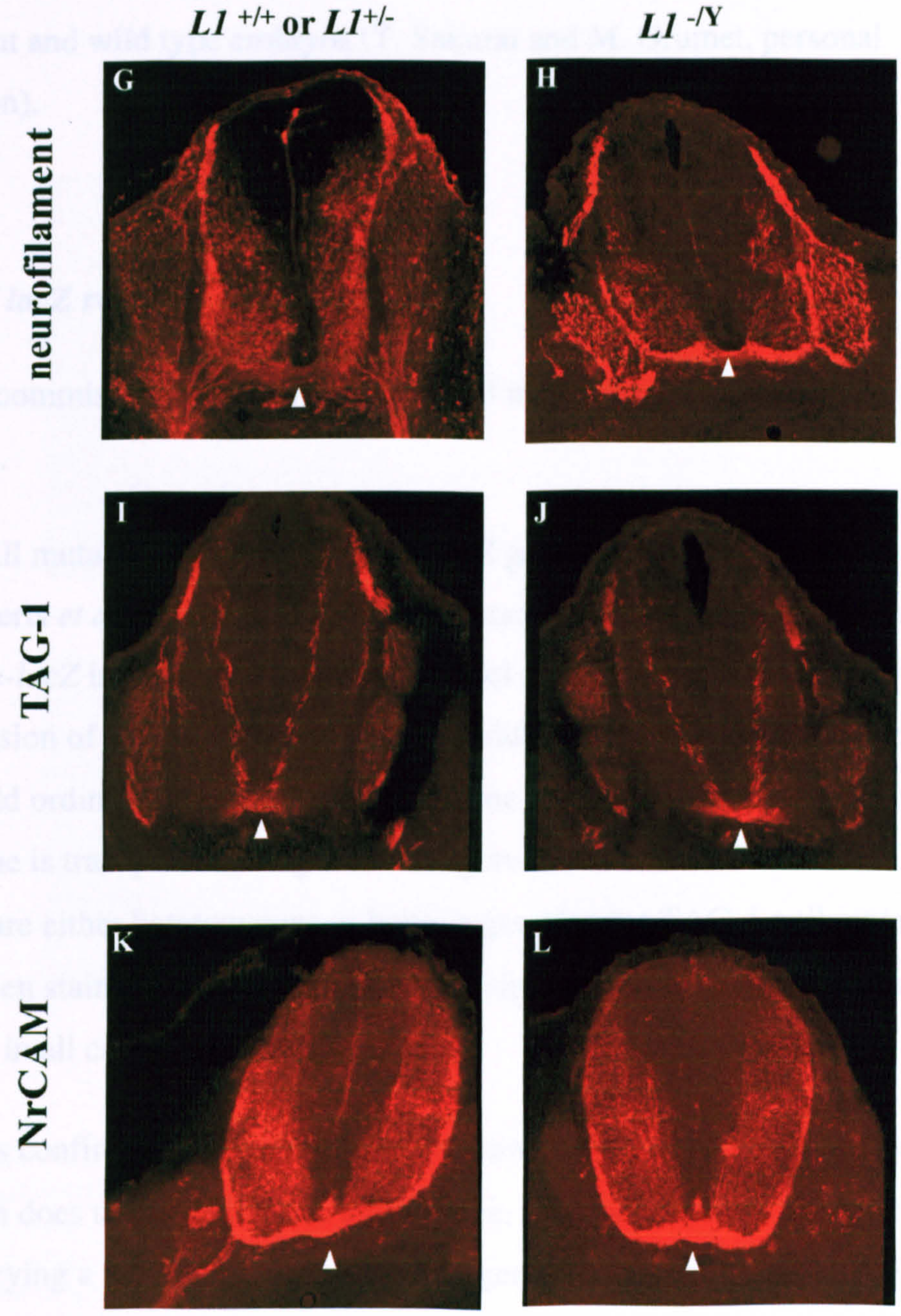

Figure 3.7 continued. G - L: E12.5 spinal cord. Sections were labelled using antibodies to the proteins named on the left. Arrowheads indicate the presence of axons beneath the floor plate in all sections.

Immunofluorescent labelling of spinal cord sections did not reveal any differences between *NrCAM* mutant and wild type embryos (T. Sakurai and M. Grumet, personal communication).

3.3.2 Use of *lacZ* reporter gene constructs

Dorsal spinal commissural neurons were labelled more specifically using one of two *lacZ* reporter genes.

The *TAG-1* null mutation incorporates a *tau-lacZ* gene construct (Callahan and Thomas, 1994; Mombaerts *et al.*, 1996; A.J.W. Furley, personal communication; see methods). This means that *tau-lacZ* is expressed under the control of the gene sequences that normally control expression of *TAG-1*. The tau-ß-galactosidase fusion protein is thus present in all cells that would ordinarily express TAG-1, and the tau component of the protein ensures that the enzyme is transported along axons. Figure 3.8 shows sections of E11.5 and E12.5 embryos that are either heterozygous or homozygous for the TAG-1 null mutation, and which have been stained for ß-galactosidase activity. Labelled axons can be seen beneath the floor plate in all cases (arrowheads).

This result was confirmed using embryos expressing only truncated TAG-1proteins. As the TAG^{A} mutation does not itself include a *lacZ* gene, mice with this mutation were mated with those carrying a *math-1-lacZ* reporter transgene (Helms and Johnson, 1998; see methods). This transgene allows essentially wild type embryos to express ß-galactosidase protein under the control of elements that regulate expression of the transcription factor Math-1. As Math-1 is normally expressed by D1 interneurons, staining for ß-galactosidase activity labels dorsal spinal commissural axons (Helms and Johnson, 1998). Matings of *math-1-lacZ* mice with those carrying the TAG^{A} mutation generated embryos which, when stained for ß-galactosidase activity, allowed direct comparisons of the D1 interneurons of embryos of different TAG^{A} genotypes (see methods). Figure 3.9 shows sections of E11.5 and E12.5 spinal cords stained for ß-galactosidase activity. Labelled axons can be seen to cross the ventral midline in embryos of all three genotypes (arrowheads). Although the

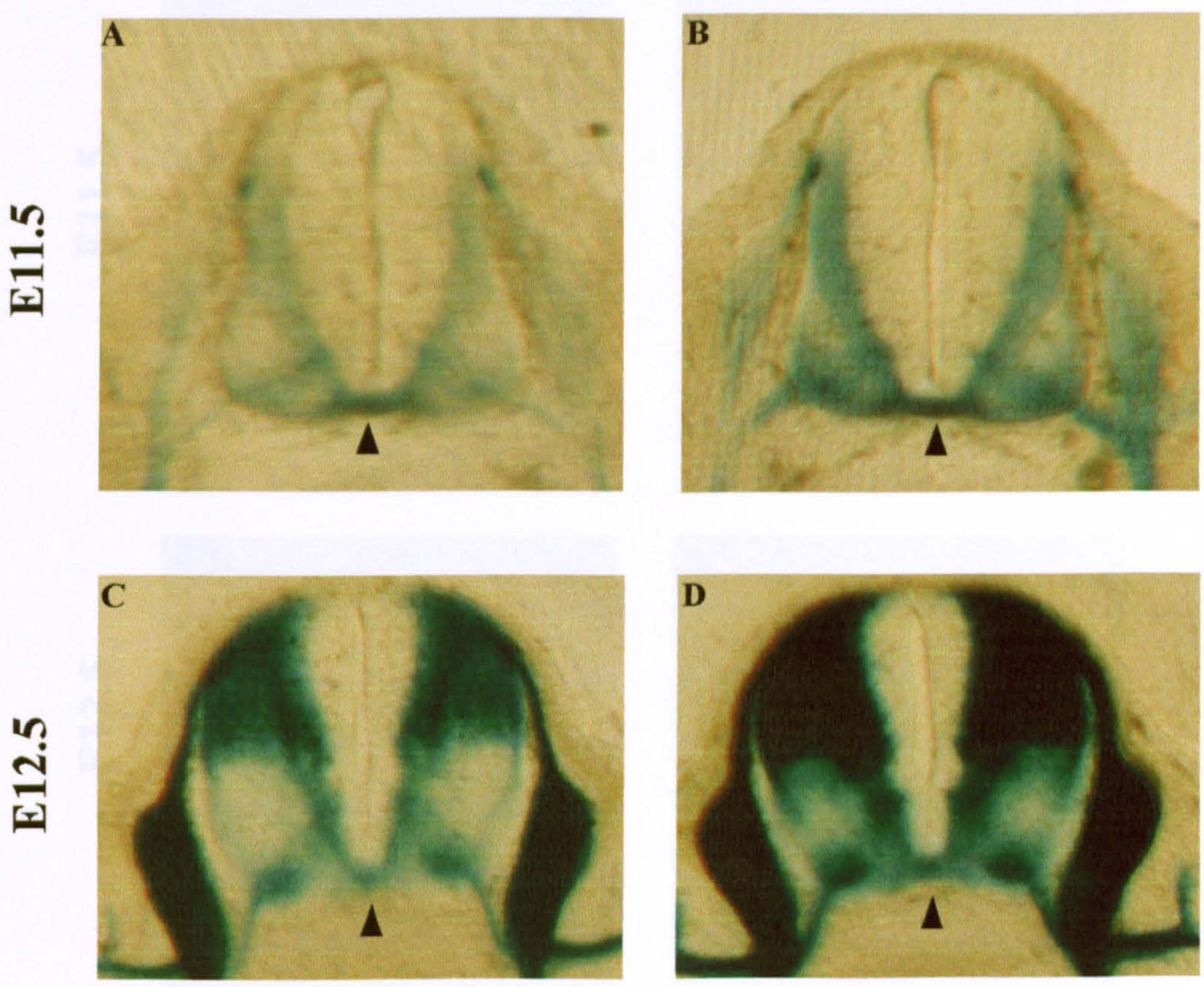

Figure 3.8 Sections of embryos with the *TAG-1* null mutation. Staining for ß-galactosidase activity specifically labelled cells that would normally express TAG-1. The stain is stronger in homozygote embryos as they have two copies of the *lacZ* gene, and so more ß-galactosidase protein. The staining is otherwise very similar in the heterozygous and homozygous embryos. Labelling differs from that obtained using antibodies (see figure 3.4), possibly reflecting perdurance of ß-galactosidase protein (see discussion). Arrow heads indicate axons crossing the ventral midline of the spinal cord.

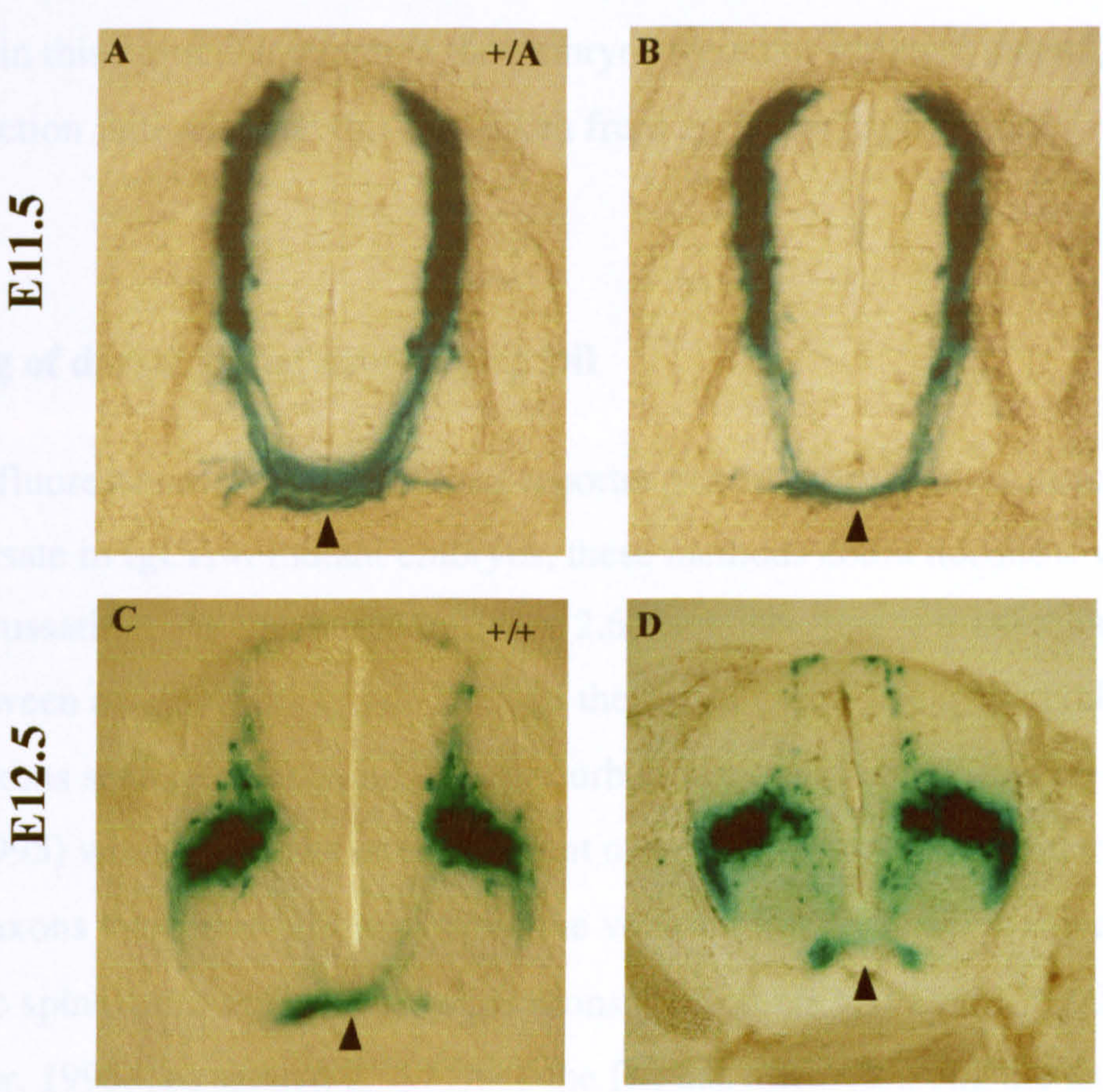

Figure 3.9 Sections of *TAG*^{A} mutant embryos that also have the *math-1-lacZ* transgene. Staining for ß-galactosidase activity specifically labelled the D1 interneurons (Helms and Johnson, 1998; Lee and Jessell, 1999). Arrowheads indicate axons crossing the ventral midline of the spinal cord. The difference between the ventral commissures shown in A and B is likely to reflect slightly different plans of sectioning. The differences between the staining of sections C and D is attributable to age variation. Although both nominally E12.5, the embryos were from different litters, and the littermates of "embryo D" were all developmentally more advanced than those of "embryo C" (data not shown). Such differences are not uncommon (Kaufman, 1992).

commissure appears thicker in the vibratome-sectioned E11.5 heterozygote than in the homozygote littermate, this can be attributed to differences in plane of section. The differences between the E12.5 embryos of different genotypes can be attributed to age differences, as in this particular example the embryos were not siblings; indeed, the shape of the E12.5 section indicates that this was taken from an "older" spinal cord.

3.3.3 Tracing of dorsal spinal axons using DiI

While immunofluorescent labelling and *lacZ* reporter gene constructs demonstrated that axons do decussate in IgCAM mutant embryos, these methods could not show whether *all* axons were decussating. As illustrated in figure 2.6, such labelling is bilateral and cannot distinguish between axons from the two sides of the spinal cord. The ipsilateral turning of up to 50% of axons seen in chicken IgCAM perturbation experiments (Stoeckli and Landmesser, 1995) would not have been apparent using this approach. In order to assess whether some axons were also failing to cross the ventral midline, DiI was injected unilaterally into spinal cord open book preparations (Bovolenta and Dodd, 1990; Stoeckli and Landmesser, 1995; see section 2.3). Once the DiI has diffused along the axons, the labelled projections were examined using conventional fluorescence and confocal microscopy. All DiI injections and subsequent analyses were carried out in collaboration with B.W. Kiernan.

In contrast to what might have been expected (e.g. Bovolenta and Dodd, 1990; Stoeckli and Landmesser, 1995), a number of different types of projection were labelled (figure 3.10). In addition to the well-documented "contra-rostral" projections, some axons turned caudally once they had left the floor plate (referred to subsequently as "contra-caudal" projections). Some axons did not turn at all, and instead appeared to "continue" into more lateral regions of the contralateral spinal cord. Other axons made a longitudinal turn, either rostrally or caudally, without having crossed the floor plate (here known as "ipsi-rostral" or "ipsi-caudal" respectively). A final group of axons was judged to be "in or at the floor plate": such axons had growth cones that appeared to have been in the process of

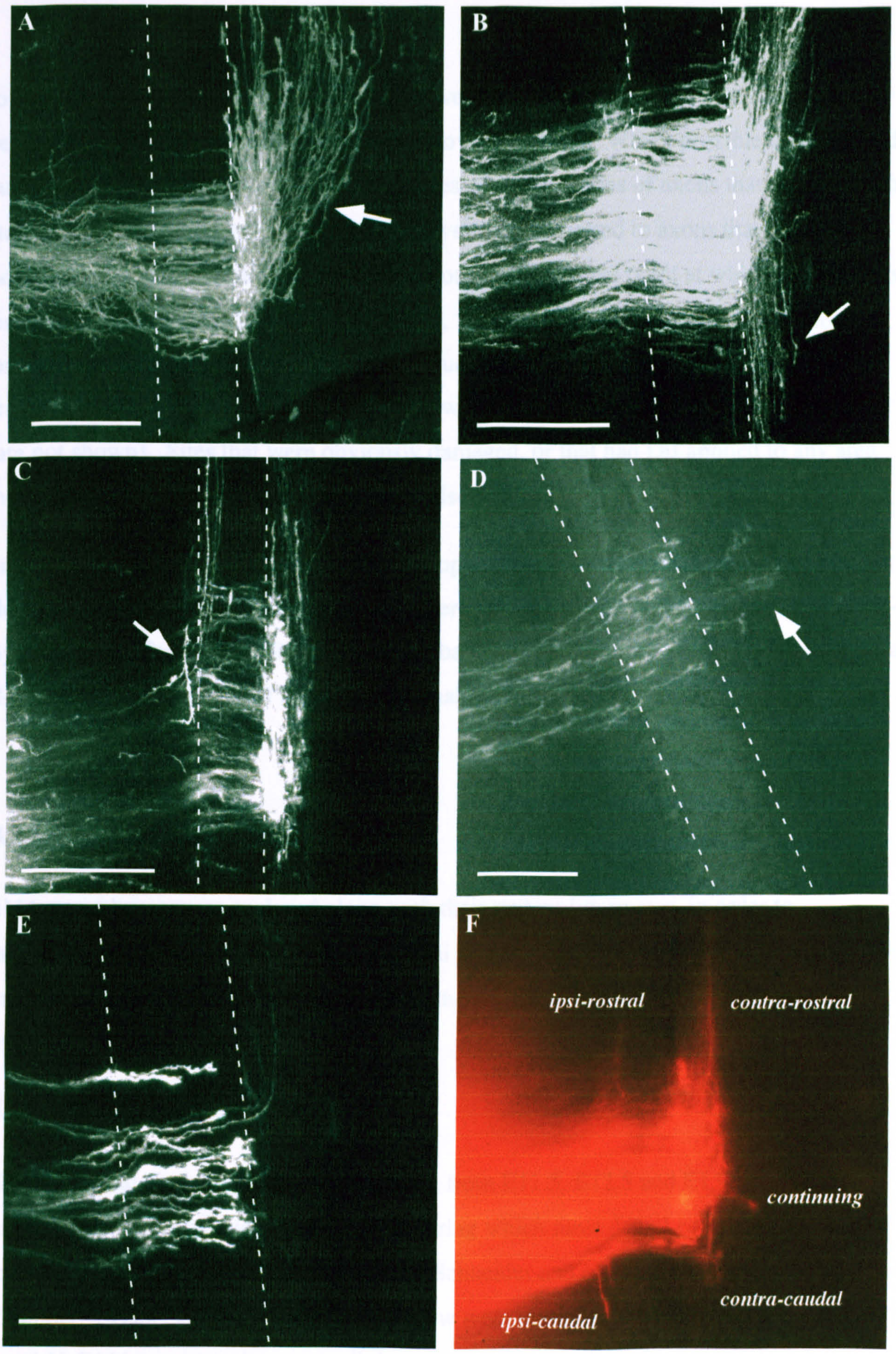

Figure 3.10 Examples of different trajectories taken by dorsal spinal projections.
A: site at which the majority of axons make a contra-rostral turn (would have been estimated as 98%). B: site at which approximately 40% of labelled axons make a contra-caudal turn (arrowed). C: site at which approximately 10% of axons make an ipsi-rostral turn (arrowed). D: site at which approximately 35% of axons continue to extend laterally (arrowed). E: site at which approximately 90% axons are in/at the floor plate. In all of these examples, the boundaries of the floor plate are represented by dashed lines, and the white bar is of a length equivalent to 100μm. F: site demonstrating that one injection can label axons in several categories. An estimate of proportions at this site would be 70% contra-rostral, 10% contra-caudal, 15% ipsi-rostral, 2% ipsi-caudal and 3% continuing to extend laterally.

crossing the floor plate when the spinal cord was fixed (figure 3.10 E). For each injection site, labelled fascicles were assigned to the above categories. Where possible this involved counting the labelled projections; in other cases, the proportions of axons that fell into each category were estimated (see methods). Analysis was restricted to axons that could be traced as far as the floor plate, as others had not yet reached the point at which the IgCAMs were thought to act (Stoeckli and Landmesser, 1995), and might even have been axons from different population of neurons. It was judged valid to discount such projections, as there did not appear to be any relationship between their occurrence and embryo genotype (data not shown). Sites that were obviously damaged, or that had DiI applied to any area other than the dorsolateral spinal cord, were also ignored.

For each experimental condition, the mean proportion of axons within each category was calculated. The statistical significance of differences was tested at the 5% level, using one-way ANOVAs (Dytham, 1999). Selected probabilities are given to three significant figures below, and a full summary of the statistical analysis is given as appendix 3.A.

3.3.4 Wild type dorsal spinal projections

Wild type embryos were analysed along with their mutant littermates, in order to characterise the normal pattern of dorsal spinal projections. Two different wild type strains were analysed, to provide controls of both of the genetic backgrounds used for mutant animals.

3.3.4.1 129/SvEv embryos

129/SvEv spinal cord preparations were taken from E11.5, E12.5 and E13.5 embryos, as these ages were expected to cover the time during which most dorsal commissural axons decussate (Bovolenta and Dodd, 1990, using Schneider and Norton, 1979; Silos-Santiago and Snider, 1992). The results described below were compiled from studies of the *TAG*^{A}, *L1* and *NrCAM* mutant embryos, as all three mutations were being maintained on the 129/SvEv strain background. As can be seen in figure 3.11, the majority of axons were

judged to have either made a contra-rostral turn or to have their growth cones in or at the floor plate. At E11.5, over 80% of axons appeared to be in/at the floor plate, while only 17% had made a contra-rostral turn. The percentage of axons judged to have growth cones within the floor plate fell over the next two days, with the difference between E11.5 and E12.5 embryos proving significant (p= 0.0220). The percentage of axons making a contra-rostral turn showed a concomitant increase, again with the difference between E11.5 and E12.5 proving significant (p= 0.000438). Although always below 5%, the percentage of axons making a contra-caudal turn was also increased between E11.5 and E12.5, changing by a statistically significant percentage (p= 0.0436). These results suggest that the E12.5 and E13.5 contra-rostral and contra-caudal categories comprise axons that were in/at the floor plate at E11.5. The proportions of axons making ipsi-rostral or ipsi-caudal turns, or continuing without turning, were below 5% at all three ages and showed no significant changes over time (see appendix 3A.1).

3.3.4.2 C57Bl/6 embryos

Embryos of a second wild type strain, C57Bl/6, were also analysed. The dorsal spinal axons of E12.5 and E13.5 C57Bl/6 embryos were traced as part of the study of *TAG-1* null mutant embryos (see below). These results were also compared with those from the 129Sv mouse embryos, to ensure that the occurrence of "non-contra-rostral" projections was not peculiar to the 129/SvEv strain. Figure 3.12 illustrates this comparison.

The C57Bl/6 spinal preparations were also found to have projections other than those that decussated and then turned rostrally. The proportions of "contra-caudal", "ipsi-rostral", "ipsi-caudal" and "continuing" projections did not differ significantly between embryos of the two strains, at either E12.5 or E13.5 (see appendix 3.A.2). Therefore it appears that mouse embryos other than those of the 129/SvEv strain have dorsal spinal axons which extend in ways previously regarded as "abnormal" (e.g. Bovolenta and Dodd, 1990; Stoeckli and Landmesser, 1995).

The 129/SvEv and C57Bl/6 strains are also similar in that embryos of both strains display an increase in the proportion of contra-rostral axons, and a concomitant decrease in the proportion of axons in or at the floor plate, between E12.5 and E13.5. This supports the

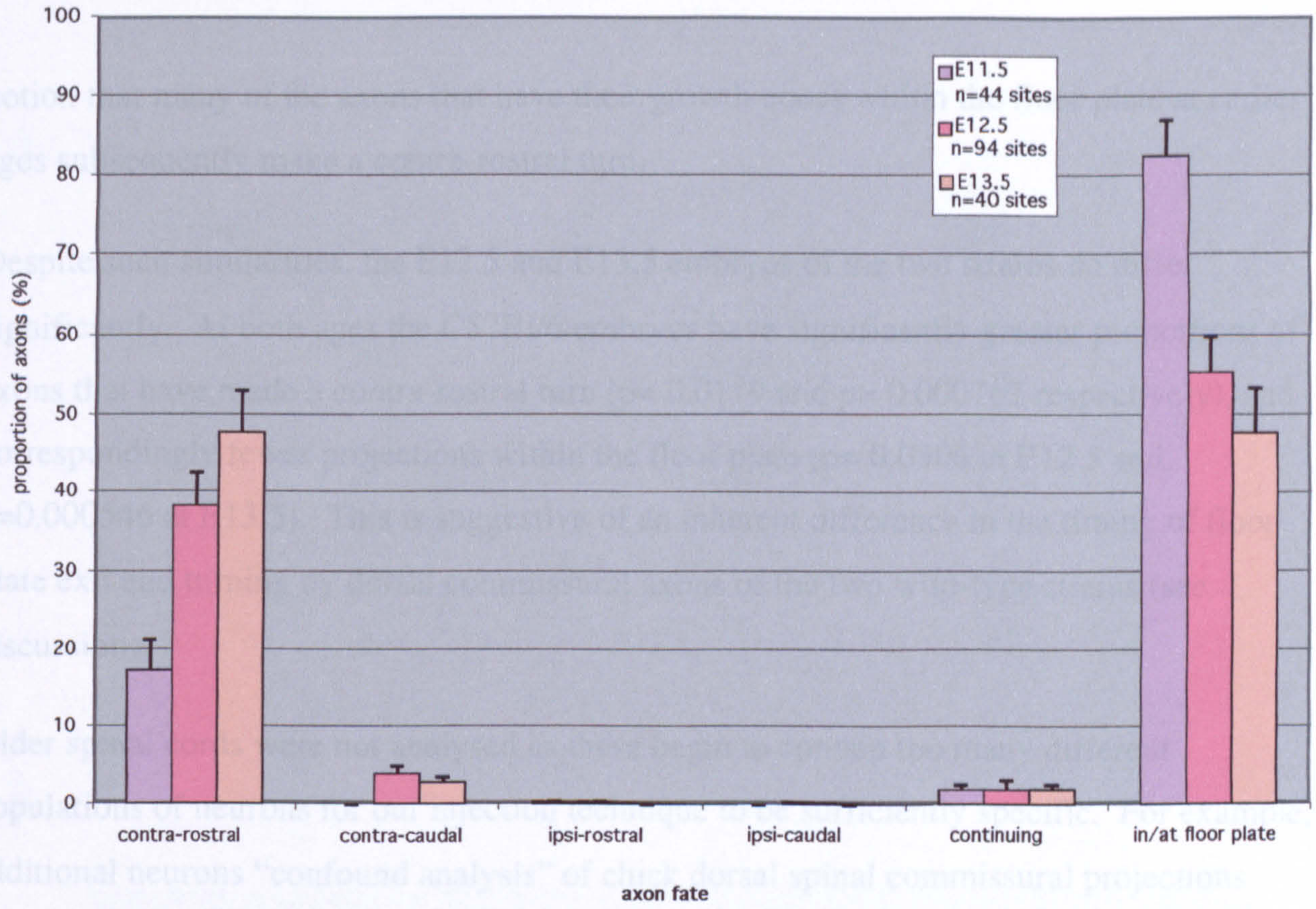

Figure 3.11 Mean proportions of axons within each category in 129/SvEv embryos of three different ages. Bars show standard errors.

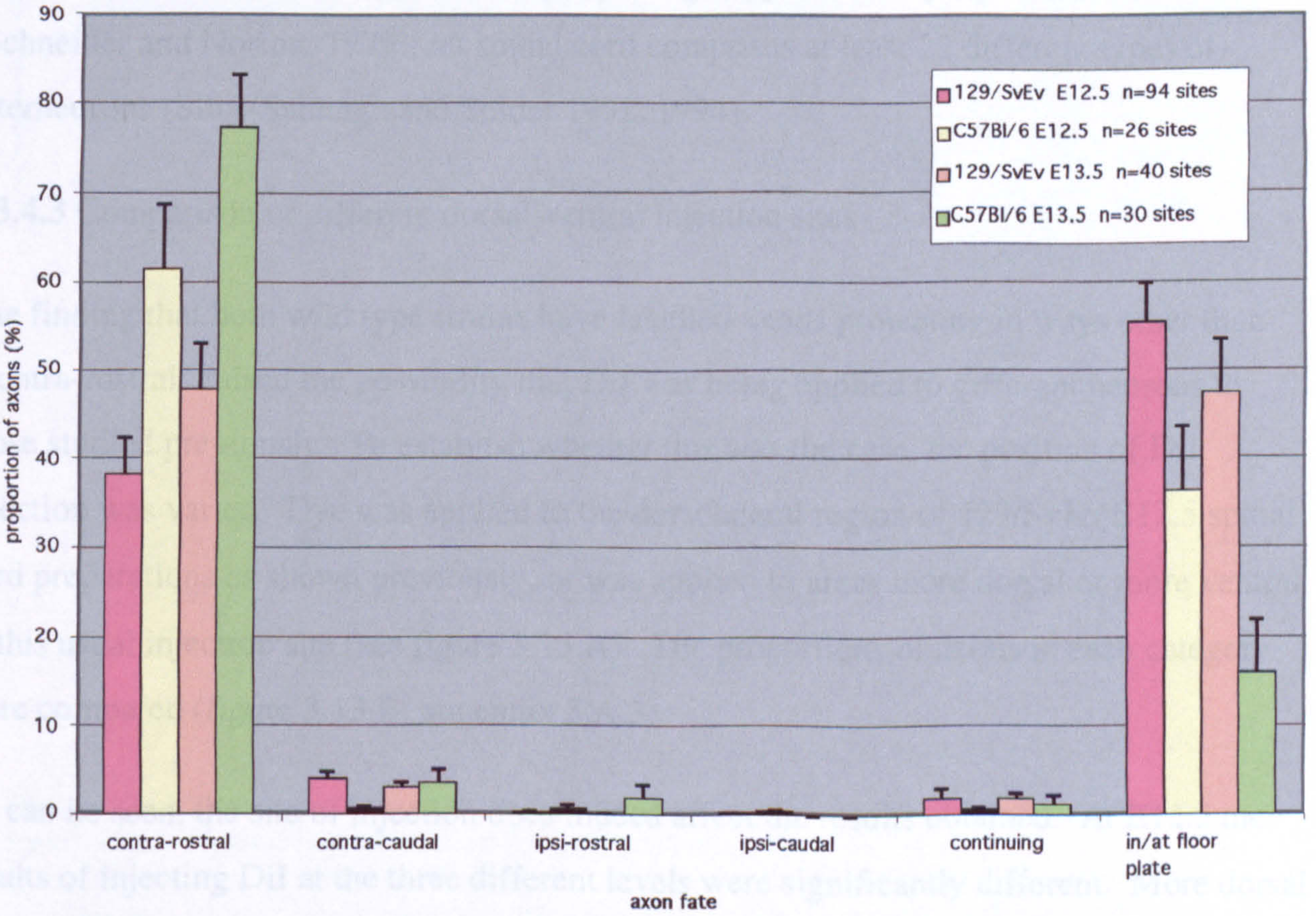

Figure 3.12 Comparison of the mean proportions of axons within each category in of 129/SvEv and C57Bl/6 mouse embryos. Bars show standard errors.

notion that many of the axons that have their growth cones within the floor plate at earlier ages subsequently make a contra-rostral turn.

Despite such similarities, the E12.5 and E13.5 embryos of the two strains do differ significantly. At both ages the C57Bl/6 embryos have significantly greater proportions of axons that have made a contra-rostral turn ($p= 0.0119$ and $p= 0.000767$ respectively), and correspondingly fewer projections within the floor plate ($p= 0.0506$ at E12.5 and $p=0.000546$ at E13.5). This is suggestive of an inherent difference in the timing of floor plate exit and turning by dorsal commissural axons of the two wild-type strains (see discussion).

Older spinal cords were not analysed as these begin to contain too many different populations of neurons for our injection technique to be sufficiently specific. For example, additional neurons "confound analysis" of chick dorsal spinal commissural projections from stage 27 onwards (Stoeckli and Landmesser, 1995), a stage estimated to be approximately equivalent to mouse E12.5 (using Hamburger and Hamilton, 1951, and Schneider and Norton, 1979). Similarly, by an age approximately equivalent to E13 mouse (Schneider and Norton, 1979); rat spinal cord comprises at least 22 different types of interneurons (Silos-Santiago and Snider 1992, 1994).

3.3.4.3 Comparison of different dorsal-ventral injection sites

The finding that both wild type strains have labelled axons projecting in ways other than "contra-rostral" raised the possibility that DiI was being applied to different neurons to those studied previously. To establish whether this was the case, the position of DiI injection was varied. Dye was applied to the dorsolateral region of 129/SvEv E12.5 spinal cord preparations as shown previously, or was applied to areas more dorsal or more ventral to this usual injection site (see figure 3.13 A). The proportions of axons in each category were compared (figure 3.13 B; appendix 3.A.3).

As can be seen, the site of injection does indeed affect the results obtained. At E12.5 the results of injecting DiI at the three different levels were significantly different. More dorsal injections of dye labelled a greater proportion of axons in or at the floor plate, and smaller

A

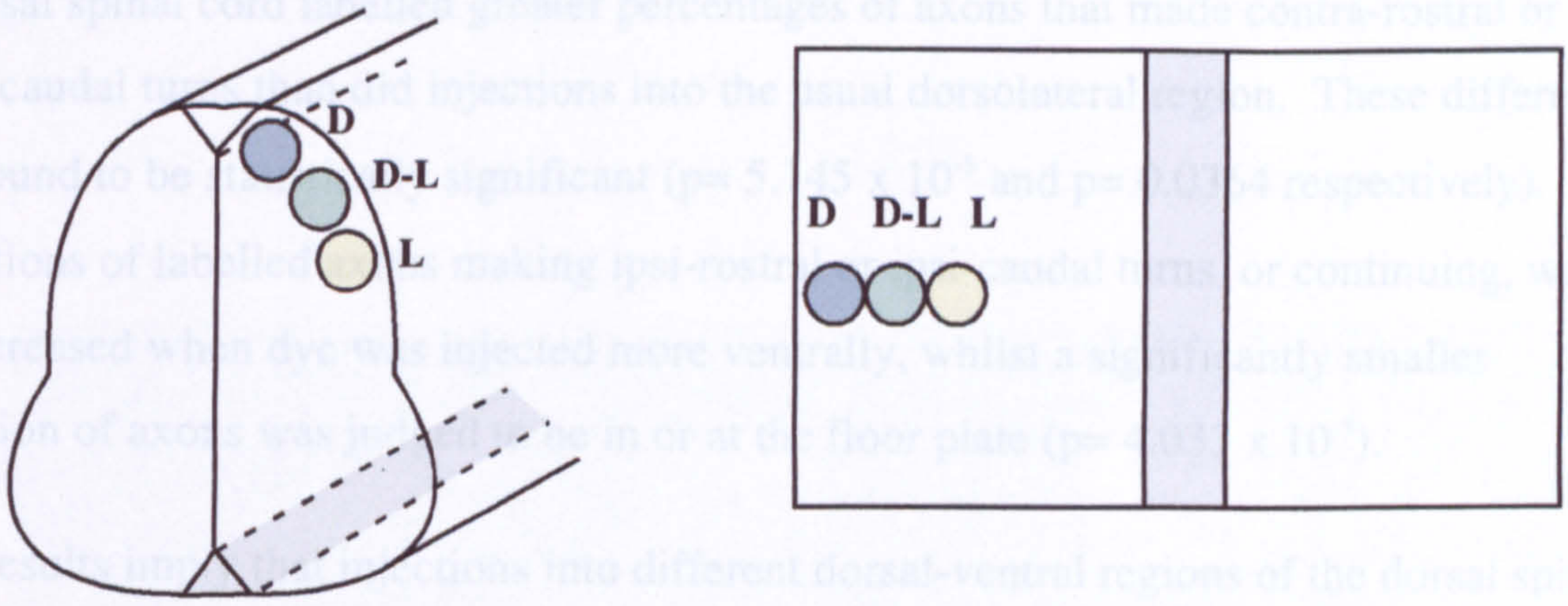

B

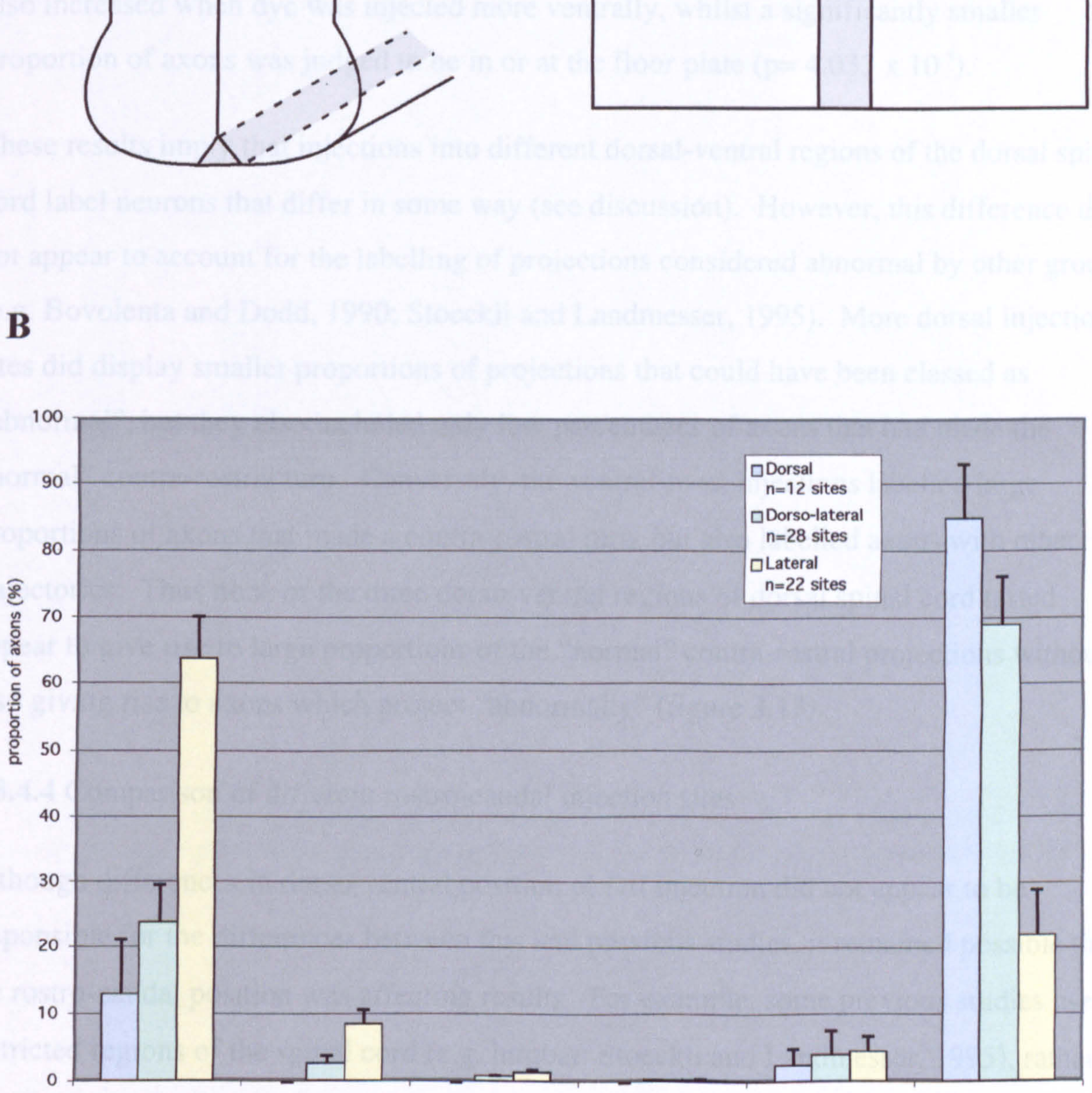

Figure 3.13 Mean proportions of axons within each category when DiI was applied to more dorsal or more lateral regions of the dorsal spinal cord.
A: The different dorso-ventral positions to which DiI was injected. Sites are shown as they would have appeared on transversely sectioned spinal cord (left) and as they were actually applied to open book preparations. D: dorsal; D-L: dorso-lateral; L: lateral.
B: Mean proportions of axons within each category for the three different dorso-ventral injection sites.

proportions of axons in all other categories. Injections of dye into more ventral regions of the dorsal spinal cord labelled greater percentages of axons that made contra-rostral or contra-caudal turns than did injections into the usual dorsolateral region. These differences were found to be statistically significant ($p= 5.145 \times 10^{-5}$ and $p= 0.0364$ respectively). Proportions of labelled axons making ipsi-rostral or ipsi-caudal turns, or continuing, were also increased when dye was injected more ventrally, whilst a significantly smaller proportion of axons was judged to be in or at the floor plate ($p= 4.033 \times 10^{-5}$).

These results imply that injections into different dorsal-ventral regions of the dorsal spinal cord label neurons that differ in some way (see discussion). However, this difference does not appear to account for the labelling of projections considered abnormal by other groups (e.g. Bovolenta and Dodd, 1990; Stoeckli and Landmesser, 1995). More dorsal injection sites did display smaller proportions of projections that could have been classed as "abnormal", but they also included only low percentages of axons that had made the "normal" contra-rostral turn. Conversely, the ventral-most injections labelled large proportions of axons that made a contra-rostral turn, but also labelled axons with other trajectories. Thus none of the three dorso-ventral regions of dorsal spinal cord tested appear to give rise to large proportions of the "normal" contra-rostral projections without also giving rise to axons which project "abnormally" (figure 3.13).

3.3.4.4 Comparison of different rostro-caudal injection sites

Although differences in dorso-ventral position of DiI injection did not appear to be responsible for the differences between this and previous studies, it remained possible that the rostro-caudal position was affecting results. For example, some previous studies used restricted regions of the spinal cord (e.g. lumbar: Stoeckli and Landmesser, 1995), rather than injecting dye along its entire length. The possibility that certain regions do in fact have only contra-rostral projections was investigated by comparing cervical and lumbar sites. Mean proportions of axons from the three most rostral injection sites of each embryo (providing that these sites were not so rostral as to be of hindbrain character) were compared with the three most caudal sites. Figure 3.14 presents the mean proportions of axons within each category when E12.5 129/SvEv spinal preparations were analysed.

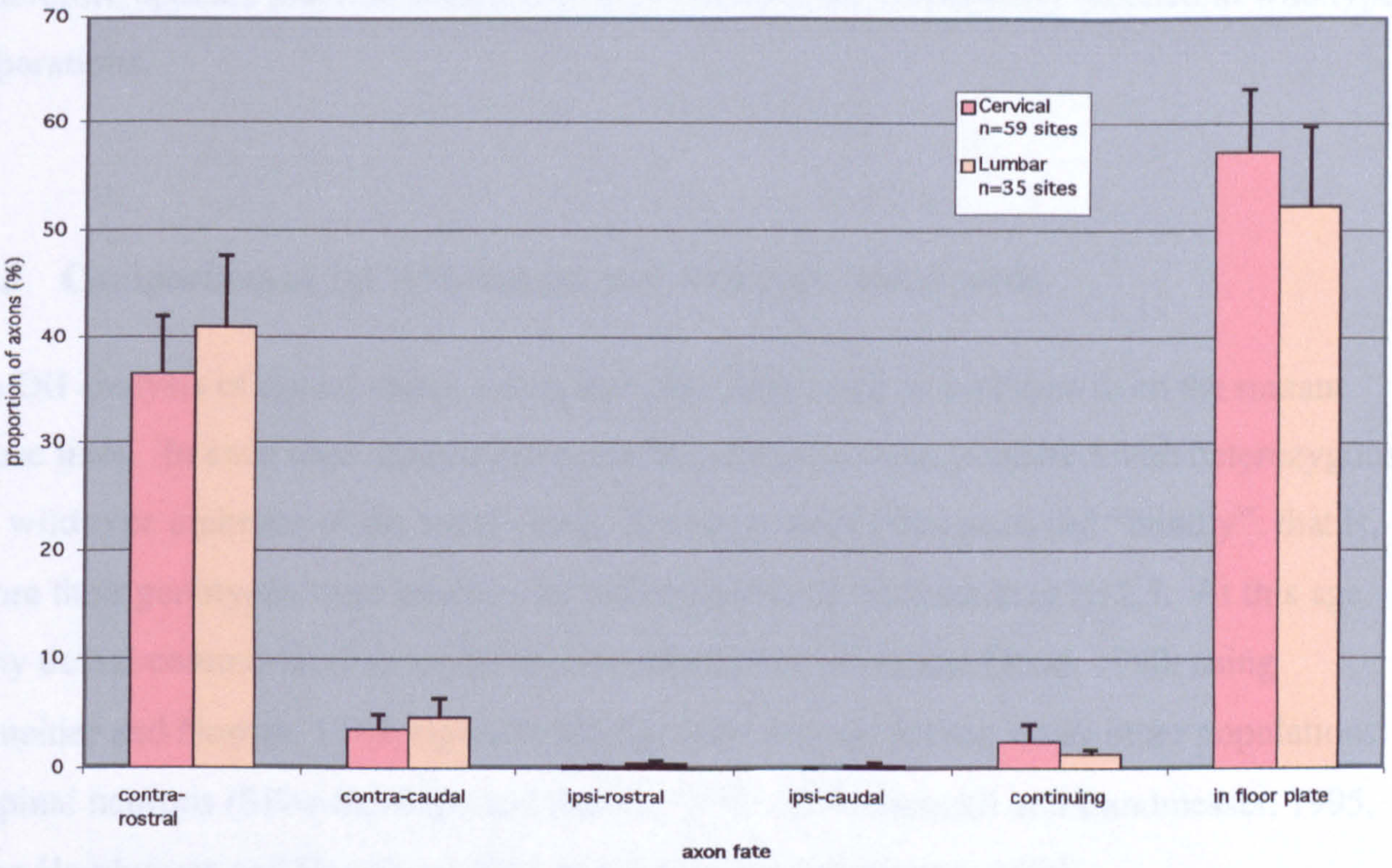

Figure 3.14 Mean proportions of axons within each category when DiI was applied to either cervical or lumbar E12.5 mouse spinal cord. Embryos were of the 129/SvEv background. Bars show standard errors.

Cervical and lumbar injections both labelled contra-caudal and continuing projections, at percentages that did not differ significantly (appendix 3.4). This indicates that the labelling of contra-caudal and continuing projections is not simply an effect of injecting DiI at all rostro-caudal levels, rather than just in lumbar regions.

It therefore appears that non-contra-rostral projections are consistently labelled in wild type preparations.

3.3.5 Comparison of IgCAM mutant and wild type spinal cords

The DiI analysis of dorsal spinal axons was also performed on embryos from the mutant mouse lines. In each case, homozygous mutant embryos were compared with heterozygous and wild type embryos of the same strain. Embryos were often analysed "blindly": that is, before their genotypes were known. Initial comparisons were made at E12.5. At this age many dorsal commissural axons have decussated (Bovolenta and Dodd, 1990, using Schneider and Norton, 1979; figure 3.12), but there are not yet too many other populations of spinal neurons (Silos-Santiago and Snider, 1992, 1994; Stoeckli and Landmesser, 1995, using Hamburger and Hamilton, 1951 and Schneider and Norton, 1979).

3.3.5.1 *TAG-1* mutant embryos

Figure 3.15 summarises the results of injecting DiI into dorsal spinal cord preparations from E12.5 TAG^{A} embryos of a 129/SvEv strain background. As can be seen, embryos of all three genotypes (wild type, heterozygote and homozygote for the mutation) had the majority of their labelled axons within either the "contra-rostral" or "in/at floor plate" categories. Although homozygous embryos had a smaller proportion of contra-rostral axons, and a correspondingly greater proportion of axons in or at the floor plate, these differences were not statistically significant (see appendix 3.A.5). There were no significant differences between the proportions of wild type, heterozygote and homozygote axons within any of the other categories. This included the ipsi-rostral category, which might have been expected to include up to 50% of axons, on the basis of experiments

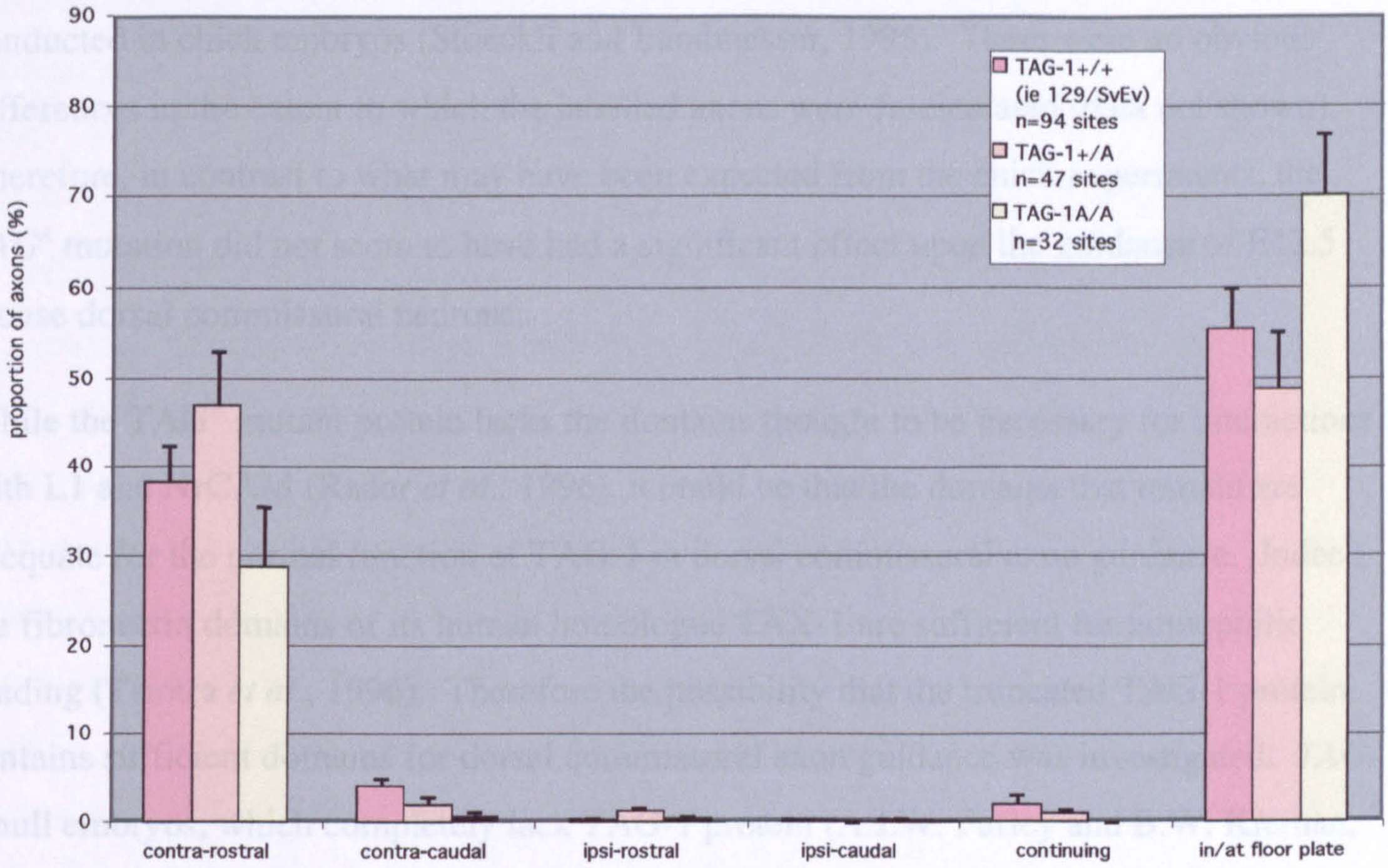

Figure 3.15 Mean proportions of axons within each category in E12.5 *TAG*^{A} (129/SvEv) embryos. Bars show standard errors.

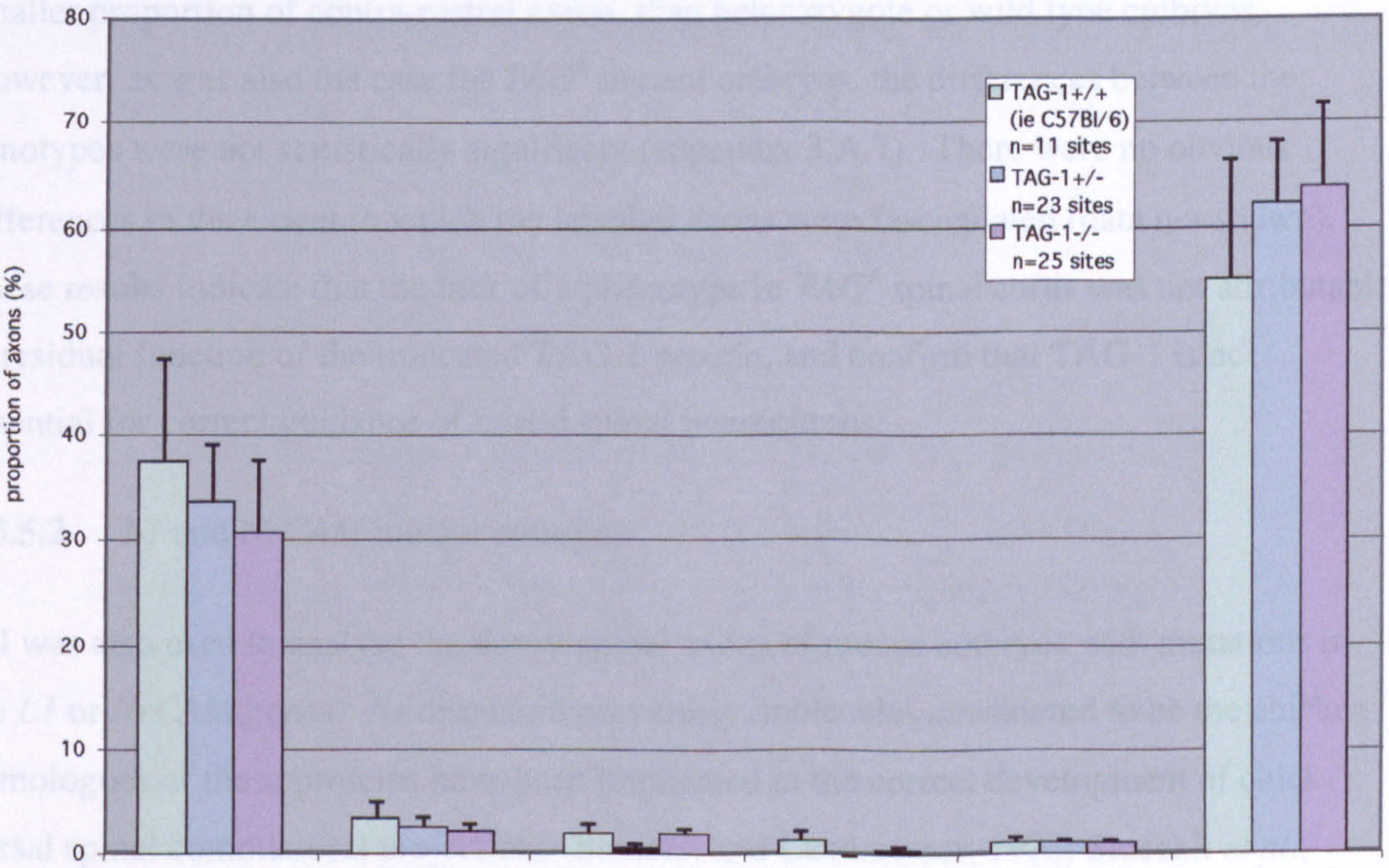

Figure 3.16 Mean proportions of axons within each category in E12.5 *TAG-1* null (C57Bl/6) embryos Bars show standard errors.

conducted in chick embryos (Stoeckli and Landmesser, 1995). There were no obvious differences in the extent to which the labelled axons were fasciculated (data not shown). Therefore, in contrast to what may have been expected from the chick experiments, the *TAG*^{A} mutation did not seem to have had a significant effect upon the guidance of E12.5 mouse dorsal commissural neurons.

While the TAG^{A} mutant protein lacks the domains thought to be necessary for interactions with L1 and NrCAM (Rader *et al.*, 1996), it could be that the domains that remain are adequate for the normal function of TAG-1 in dorsal commissural axon guidance. Indeed, the fibronectin domains of its human homologue TAX-1 are sufficient for homophilic binding (Tsiotra *et al.*, 1996). Therefore the possibility that the truncated TAG-1 protein contains sufficient domains for dorsal commissural axon guidance was investigated. *TAG-1* null embryos, which completely lack TAG-1 protein (A.J.W. Furley and B.W. Kiernan, personal communications) were compared with wild type embryos of the same C57Bl/6 genetic background. As before, the majority of axons had either made a contra-rostral turn, or appeared to be in or at the floor plate (figure 3.16). The homozygote *TAG-1* null embryos had a larger proportion of axons in or at the floor plate, and a correspondingly smaller proportion of contra-rostral axons, than heterozygote or wild type embryos. However, as was also the case for *TAG*^{A} mutant embryos, the differences between the genotypes were not statistically significant (appendix 3.A.7). There were no obvious differences in the extent to which the labelled axons were fasciculated (data not shown). These results indicate that the lack of a phenotype in *TAG*^{A} spinal cords was not attributable to residual function of the truncated TAG-1 protein, and confirm that TAG-1 is not essential for correct guidance of dorsal spinal interneurons.

3.3.5.2 *L1* and *NrCAM* mutant embryos

DiI was also used to analyse the dorsal spinal axons of mouse embryos with mutations in the *L1* or *NrCAM* genes. As discussed previously, molecules considered to be the chicken homologues of these proteins have been implicated in the correct development of chick dorsal spinal commissural projections (Stoeckli and Landmesser, 1995; Stoeckli *et al.*, 1997; Lustig *et al.*, 1999; Fitzli *et al.*, 2000).

NgCAM, thought to be the chick equivalent of L1, appears to be important for the fasciculation rather than the guidance of dorsal spinal axons (Stoeckli and Landmesser, 1995). However, there are notable differences between this protein and L1 (see discussion and review in Sonderegger and Rathjen, 1992). In contrast to NgCAM, which is expressed by dorsal spinal commissural axons both before and after decussation, the restricted expression of L1 is suggestive of a role in regulating decussation (Bovolenta and Dodd, 1990). Indeed, L1 has been implicated in at least two other rodent decussation events. As is the case in humans with *L1* mutations (Wong *et al.*, 1995), *L1* mutant mice can display agenesis of the corticospinal tract (Cohen *et al.*, 1997; Dahme *et al.*, 1997) and/or corpus callosum (Demyanenko *et al*, 1999), depending upon genetic background. Therefore it is conceivable that L1 is also involved in the guidance of rodent dorsal spinal axons at the midline. Immunofluorescent labelling of the dorsal spinal commissural neurons of *L1* mutant mice did not reveal any gross defects in guidance at the floor plate (Cohen *et al.*, 1997; figure 3.7), but unilateral injections of DiI were necessary to establish whether there were in fact subtle guidance errors.

Figure 3.17 illustrates the proportions of axons following each trajectory in E12.5 *L1* mutant spinal cord preparations (with a 129/SvEv genetic background; see methods for explanation of the crosses used). All three genotypic groups showed a similar distribution: most of the labelled axons had either made a contra-rostral turn, or seemed to have had their growth cones in/at the floor plate at the time of fixation. Hemizygous male embryos were those with the greatest proportions of their dorsal spinal projections making a contra-rostral turn, and with the smallest proportion in or at the floor plate. However, the differences between the hemizygous, heterozygous and wild type embryos were not statistically significant (appendix 3.A.8). There were no obvious differences in the extent to which the labelled axons were fasciculated (data not shown). These results indicate that the *L1* mutation does not affect the development of dorsal spinal projections.

NrCAM has also been implicated in the guidance of chick dorsal spinal commissural axons (Stoeckli and Landmesser, 1995; Stoeckli *et al.*, 1997), and is expressed by decussating axons and the floor plate in rodents (Lustig *et al.*, 1999). Therefore the role of NrCAM in guidance of the rodent axons was investigated using *NrCAM* mutant spinal preparations.

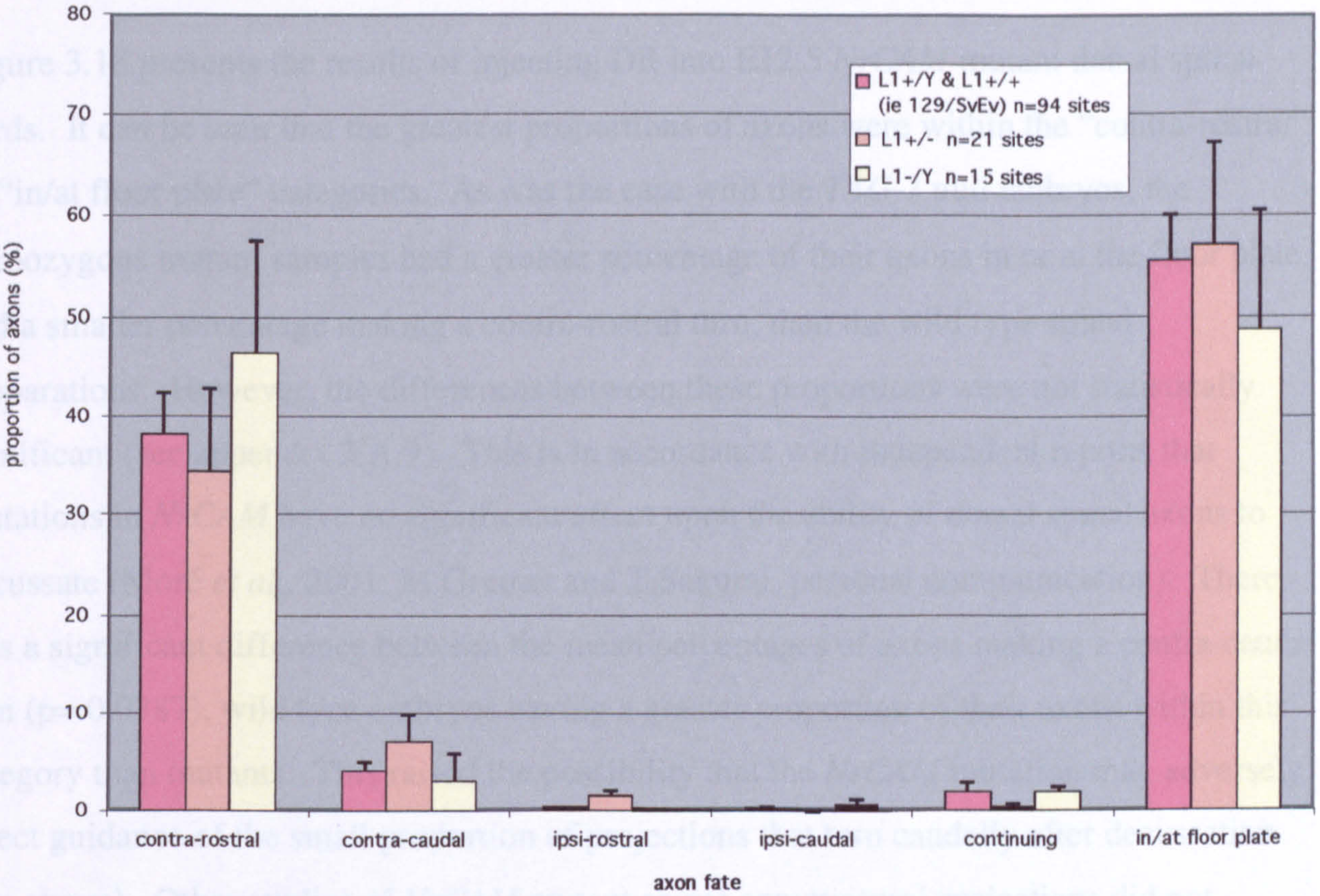

Figure 3.17 Mean proportions of axons within each category in E12.5 *L1* (129/SvEv) mutant embryos. Bars show standard errors.

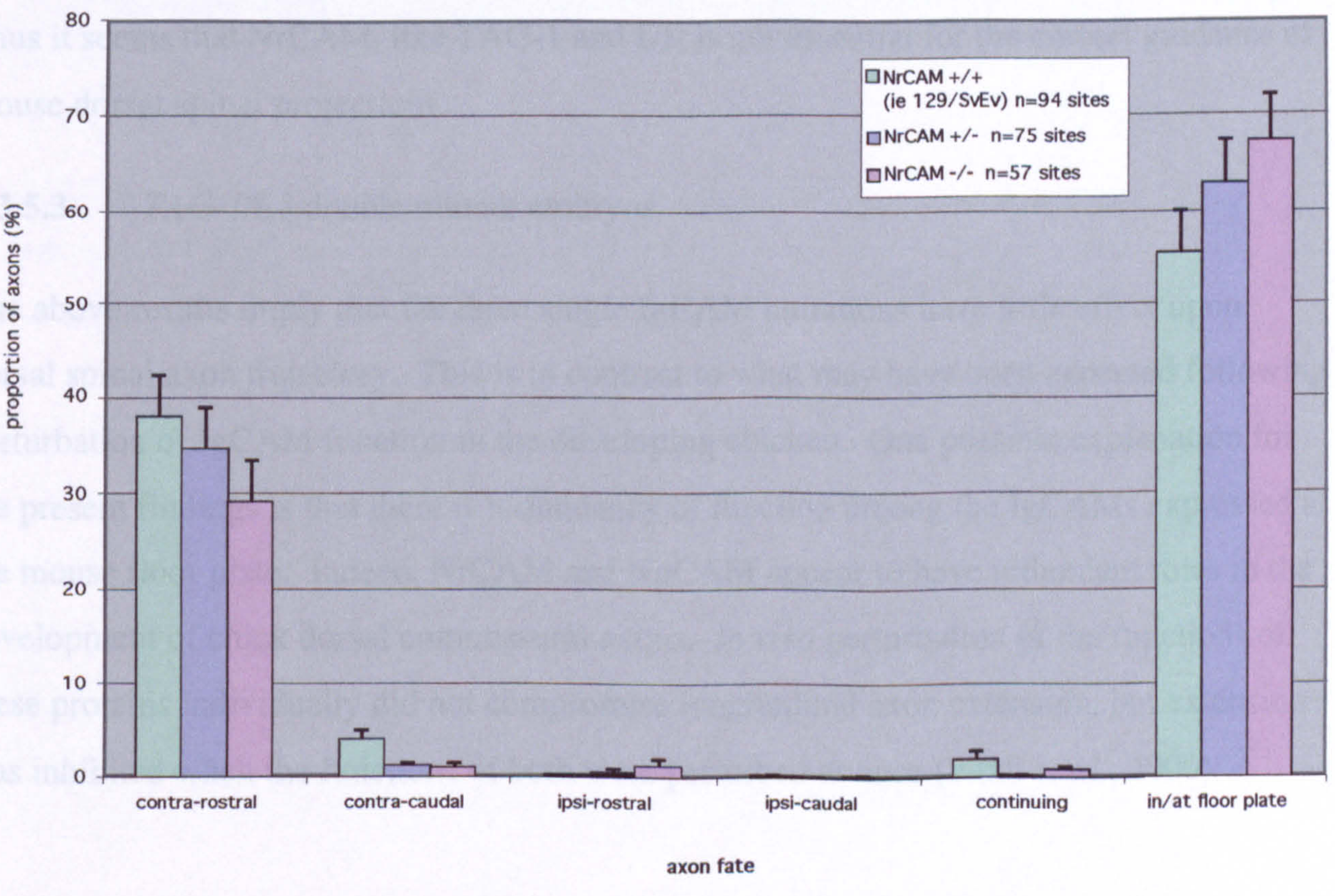

Figure 3.18 Mean proportions of axons within each category in E12.5 *NrCAM* (129/SvEv)mutant embryos. Bars show standard errors.

Figure 3.18 presents the results of injecting DiI into E12.5 *NrCAM* mutant dorsal spinal cords. It can be seen that the greatest proportions of axons were within the "contra-rostral" or "in/at floor plate" categories. As was the case with the *TAG-1* null embryos, the homozygous mutant samples had a greater percentage of their axons in or at the floor plate, and a smaller percentage making a contra-rostral turn, than the wild type spinal preparations. However, the differences between these proportions were not statistically significant (see appendix 3.A.9). This is in accordance with independent reports that mutations in *NrCAM* have no significant effect upon the ability of dorsal spinal axons to decussate (Moré *et al.*, 2001; M.Grumet and T.Sakurai, personal communication). There was a significant difference between the mean percentages of axons making a contra-caudal turn ($p= 0.0387$), wild type embryos having a greater proportion of their axons within this category than mutants. This raised the possibility that the *NrCAM* mutation may adversely affect guidance of the small proportion of projections that turn caudally after decussation (see above). Other studies of *NrCAM* mutant spinal commissural projections did not classify projections in a way that would have revealed such a difference (Moré *et al.*, 2001; M.Grumet and T.Sakurai, personal communication). Aside from this observation, the present results indicate that the *NrCAM* mutation does not perturb the guidance of dorsal spinal commissural axons. Fasciculation of the axons also seemed to have been unaffected. Thus it seems that NrCAM, like TAG-1 and L1, is not essential for the correct guidance of mouse dorsal spinal projections.

3.3.5.3 *TAG-1/L1* double mutant embryos

The above results imply that the three single IgCAM mutations have little effect upon dorsal spinal axon trajectory. This is in contrast to what may have been expected following perturbation of IgCAM function in the developing chicken. One possible explanation for the present findings is that there is redundancy of function among the IgCAMs expressed at the mouse floor plate. Indeed, NrCAM and NgCAM appear to have redundant roles in the development of chick dorsal commissural axons. *In vivo* perturbation of the functions of these proteins individually did not compromise longitudinal axon extension, but extension was inhibited when the functions of both were perturbed at once (Fitzli *et al.*, 2000).

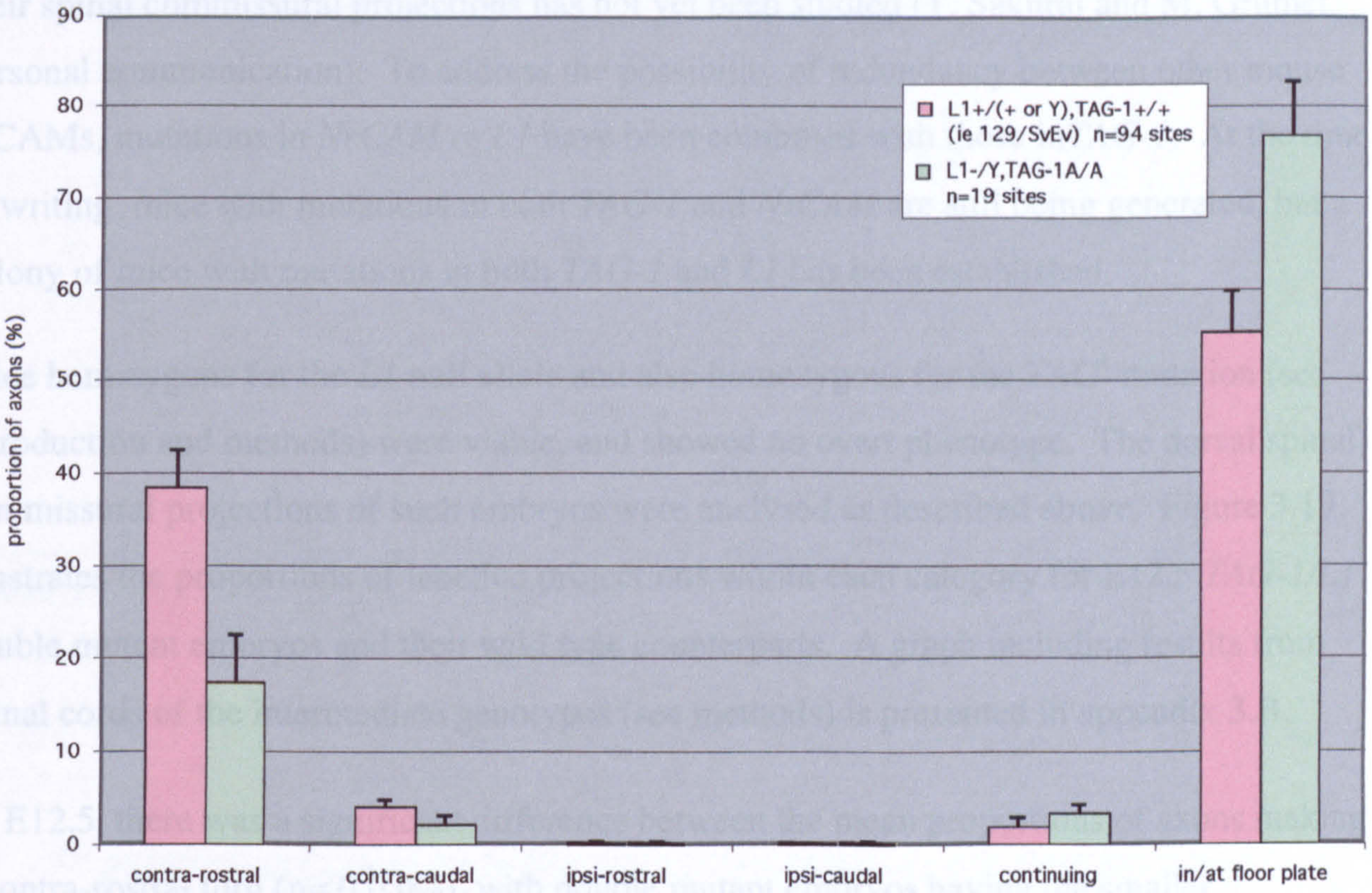

Figure 3.19 Mean proportions of axons within each category in E12.5 embryos with mutations in both *L1* and *TAG-1*. Bars show standard errors.

Therefore these IgCAMs appear to have redundant functions in the chicken spinal cord. Such a relationship between L1/NgCAM and NrCAM has previously been suggested to account for the lack of spinal commissural axon defects in *L1* mutant mouse embryos (Fitzli *et al.*, 2000). *L1/NrCAM* double mutant mice show cerebellar dysgenesis and die within a few weeks of birth (Sakurai *et al.*, 2001), although the embryonic development of their spinal commissural projections has not yet been studied (T. Sakurai and M. Grumet, personal communication). To address the possibility of redundancy between other mouse IgCAMs, mutations in *NrCAM* or *L1* have been combined with those in*TAG-1*. At the time of writing, mice with mutations in both *TAG-1* and *NrCAM* are still being generated, but a colony of mice with mutations in both *TAG-1* and *L1* has been established.

Mice hemizygous for the *L1* null allele and also homozygous for the TAG^{A} mutation (see introduction and methods) were viable, and showed no overt phenotype. The dorsal spinal commissural projections of such embryos were analysed as described above. Figure 3.19 illustrates the proportions of labelled projections within each category for E12.5 *TAG-1/L1* double mutant embryos and their wild type counterparts. A graph including results from spinal cords of the intermediate genotypes (see methods) is presented in appendix 3.B.

At E12.5, there was a significant difference between the mean proportions of axons making a contra-rostral turn ($p= 0.0384$), with double mutant embryos having the smaller proportion. The double mutant embryos had a correspondingly larger proportion of axons in or at the floor plate, although this difference was not technically significant ($p= 0.0501$). There were no statistically significant differences between the double mutant and wild type embryos in the other four categories of projection (see appendix 3.A.10).

The smaller percentage of axons making a contra-rostral turn, and the greater percentage of axons in or at the floor plate, might reflect a delay in the development of the dorsal spinal projections of double mutant embryos. Such an effect could reflect hindrance of double mutant axon growth at the floor plate, or could be a symptom of a delay at an earlier stage of development. For example, the double mutation could theoretically affect initial axon production, although such an explanation seems somewhat unlikely, as L1 is not strongly expressed by rodent commissural neurons until decussation (figure 3.4; Dodd *et al.*, 1988).

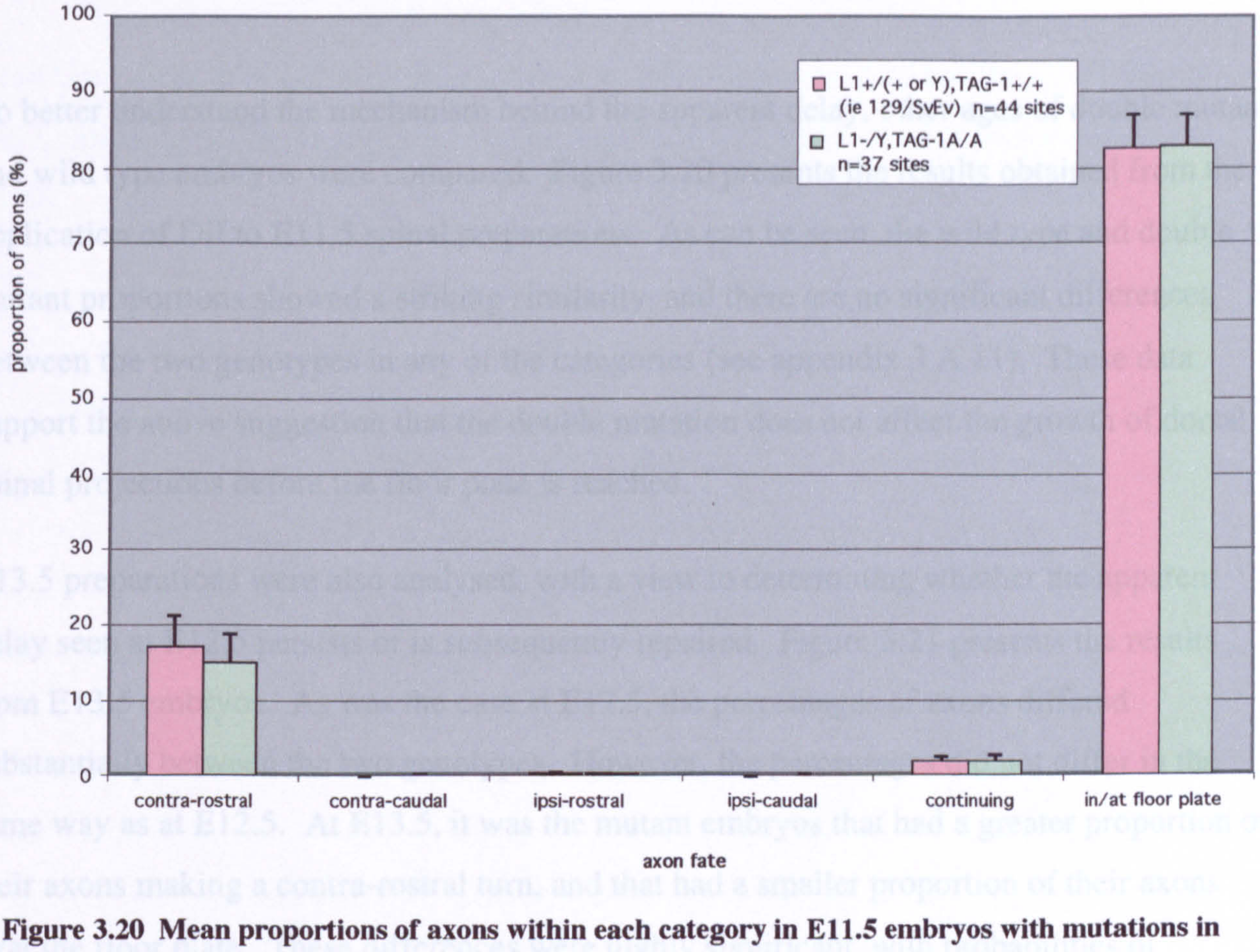

Figure 3.20 Mean proportions of axons within each category in E11.5 embryos with mutations in both *L1* and *TAG-1*. Bars show standard errors.

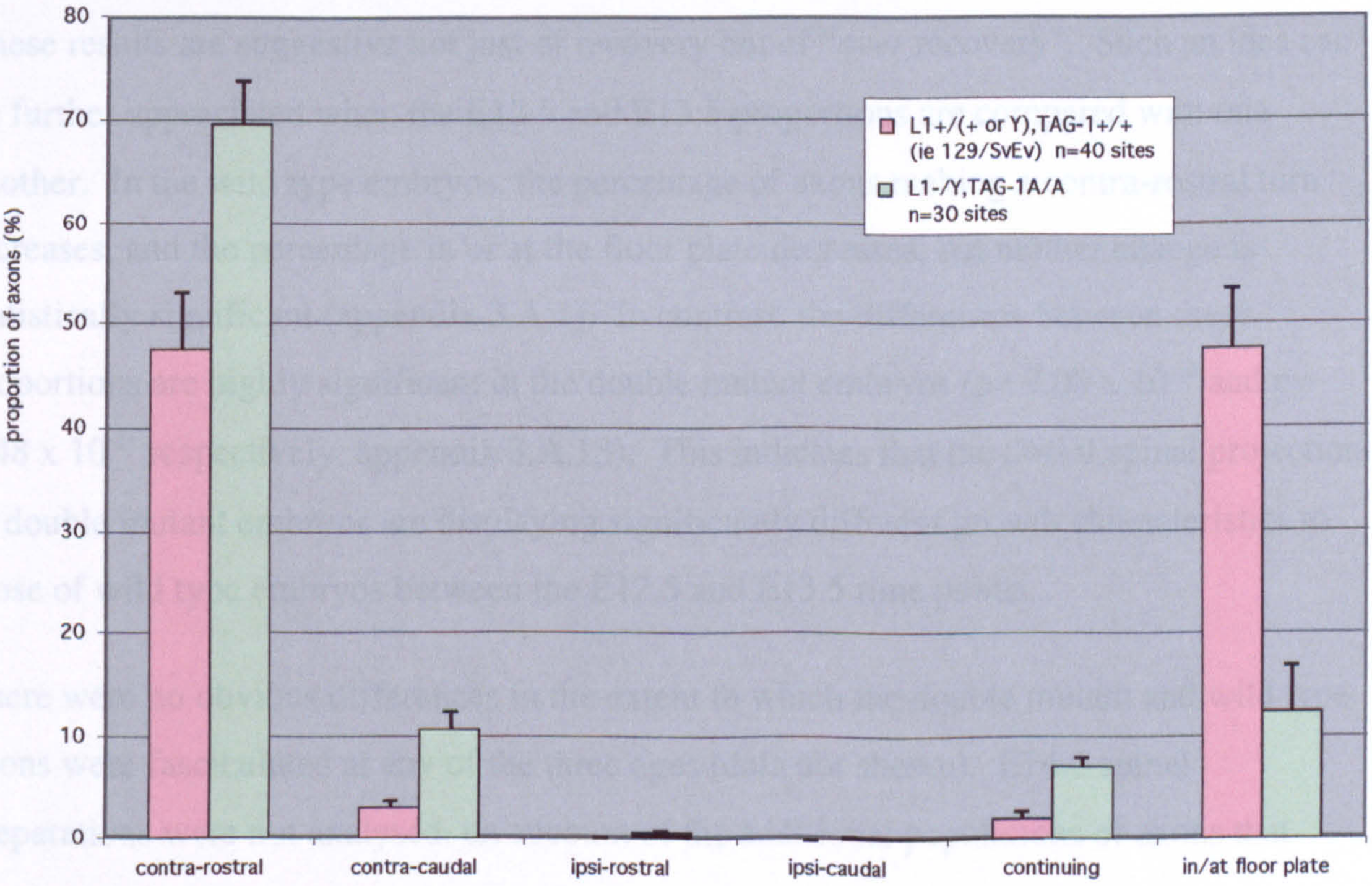

Figure 3.21 Mean proportions of axons within each category in E13.5 embryos with mutations in both *L1* and *TAG-1*. Bars show standard errors.

To better understand the mechanism behind the apparent delay, other ages of double mutant and wild type embryos were compared. Figure 3.20 presents the results obtained from the application of DiI to E11.5 spinal preparations. As can be seen, the wild type and double mutant proportions showed a striking similarity, and there are no significant differences between the two genotypes in any of the categories (see appendix 3.A.11). These data support the above suggestion that the double mutation does not affect the growth of dorsal spinal projections before the floor plate is reached.

E13.5 preparations were also analysed, with a view to determining whether the apparent delay seen at E12.5 persists or is subsequently repaired. Figure 3.21 presents the results from E13.5 embryos. As was the case at E12.5, the percentages of axons differed substantially between the two genotypes. However, the percentages did not differ in the same way as at E12.5. At E13.5, it was the mutant embryos that had a greater proportion of their axons making a contra-rostral turn, and that had a smaller proportion of their axons in/at the floor plate. These differences were highly significant, with probabilities of 0.00451 and 4.41×10^{-5} respectively (see appendix 3.A.12). The mutant embryos also had greater proportions of axons making a contra-caudal turn, making an ipsi-rostral turn, or continuing laterally ($p= 0.000468$, $p= 0.0384$ and $p= 0.000228$ respectively).

These results are suggestive not just of recovery but of "*over* recovery". Such an idea can be further appreciated when the E12.5 and E13.5 proportions are compared with one another. In the wild type embryos, the percentage of axons making a contra-rostral turn increases, and the percentage in or at the floor plate decreases, but neither change is statistically significant (appendix 3.A.1). In contrast, the differences between these proportions are highly significant in the double mutant embryos ($p= 7.08 \times 10^{-10}$ and $p= 4.48 \times 10^{-11}$ respectively; appendix 3.A.13). This indicates that the dorsal spinal projections of double mutant embryos are displaying significantly different growth characteristics to those of wild type embryos between the E12.5 and E13.5 time points.

There were no obvious differences in the extent to which the double mutant and wild type axons were fasciculated at any of the three ages (data not shown). E14.5 spinal preparations were not analysed, on account of the additional populations of axons that

would be labelled by DiI injections at this age (Silos-Santiago and Snider, 1992; Stoeckli and Landmesser, 1995, using Hamburger and Hamilton, 1951 and Schneider and Norton, 1979).

3.4 Discussion

In all cases, the majority of labelled projections were judged to be either projecting "contra-rostrally", or in or at the floor plate. The relative frequencies with which these axon fates were observed did not differ significantly between any of the E12.5 single IgCAM mutant embryos and their wild type counterparts. All other classes of projection accounted for relatively small proportions of those labelled. However, such "abnormal" projections were labelled consistently, and could not be attributed to experimental factors such as embryo age, mouse background strain, or the site at which DiI was injected. With the exception of the "contra-caudal" axons of *NrCAM* mutant embryos, these projections were observed at similar frequencies in single mutant and wild type embryos. This shows that the three single IgCAM mutations do not affect the guidance of mouse dorsal commissural axons (Stoeckli and Landmesser, 1995; Stoeckli *et al.*, 1997). However, development of the axons appeared to be compromised in embryos mutant for both *TAG-1* and *L1*, and it is possible that the TAG-1 and L1 proteins have some functional redundancy during floor plate exit.

3.4.1 Wild type embryos and the occurrence of "abnormal" projections

3.4.1.1 E12.5 mouse dorsal spinal axons do not all make a "contra-rostral" turn.

The antibody labelling and reporter gene approaches both demonstrated that the axons of wild type dorsal spinal neurons decussate in the ventral commissure. This is in accordance with previous studies which have implied that, if allowed to develop unperturbed, dorsal spinal interneurons make a contralateral and rostral turn (e.g. Bovolenta and Dodd, 1990; Stoeckli and Landmesser, 1995; Matise *et al.*, 1999).

However, unilateral application of DiI to wild type dorsolateral spinal cord also revealed the existence of axons with other trajectories. While the majority of labelled axons that made a longitudinal turn did so contralaterally and rostrally, some DiI injections labelled projections that made a rostral turn on the ipsilateral side of the floor plate. Some

projections extended caudally rather than rostrally, and some did not turn longitudinally at all (see figure 3.10). The occurrence of such non-contra-rostral projections had previously been attributed to perturbation events, such as the application of function-blocking antibodies or a gene mutation (e.g. Stoeckli and Landmesser, 1995; Matise *et al.*, 1999; Fitzli *et al.*, 2000). A number of practical steps were taken to establish whether the present labelling of such projections in wild type embryos was an artefact.

3.4.1.2 Non-contra-rostral projections in embryos of different ages

As earlier studies were conducted in species other than mouse (rat: Bovolenta and Dodd, 1990; chicken: Stoeckli and Landmesser, 1995), it was possible that the embryos used were not at comparable stages of development. For example, it could be that previous investigations used relatively older embryos, such that there had been time for any non-contra-rostral projections to be eliminated. It appears that initial analyses of rat dorsal spinal projections were conducted at an age approximately equivalent to mouse E11 (Bovolenta and Dodd, 1990, using Schneider and Norton, 1979), but that the chick projections were studied at an age equivalent to at least E13 (Holley, 1982; Stoeckli and Landmesser, 1995, using Hamburger and Hamilton, 1951 and Schneider and Norton, 1979). In order to determine whether the mouse non-contra-rostral projections were subsequently eliminated, spinal cord preparations from E12.5 129/SvEv embryos were compared with those from E11.5 and E13.5 embryos (as discussed previously, increasing complexity makes it impractical to study projections in older spinal cords: Stoeckli and Landmesser, 1995). The proportions of axons projecting contra-rostrally and contra-caudally both increased significantly between E11.5 and E12.5, while the proportion of axons judged to be in or at the floor plate showed a significant decrease. This raised the possibility that axons that had been in or at the floor plate at E11.5 had left the midline and extended longitudinally by E12.5. However, the proportions of ipsi-rostral, ipsi-caudal and continuing projections did not change significantly during this period, and none of the proportions showed a significant difference when E12.5 embryos were compared with those of E13.5. This implies that non-contra-rostral axons are not selectively eliminated between E12.5 and ages estimated to be comparable to those examined in the chick.

3.4.1.3 Non-contra-rostral projections in wild type embryos of a different strain

There are numerous cases in which the phenotype caused by a particular mutation varies with mouse strain (Gerlai, 1996). For example, mice with a mutation in the *emx-1* gene showed a reduction in the size, or an absence, of the corpus callosum if they were of a predominantly 129/Sv strain, but showed no callosal defects if they were of a C57Bl/6 genetic background (Guo *et al.*, 2000). *L1* mutant mice have also been shown to have corpus callosum deficiencies in mice of one 129Sv sub-strain (Demyanenko *et al.*, 1999) but not those of another (Cohen *et al.*, 1998). A different mutation in the *L1* gene causes hydrocephalus in mice of a C57Bl/6 strain background, but not in those of a 129/SvEv background (Dhame *et al.*, 1997). Therefore it was conceivable that the non-contra-rostral projections described here were peculiar to the mice of the 129/SvEv genetic background. To investigate this possibility, the results from 129/SvEv embryos were compared with those from the wild type C57Bl/6 embryos, which had been analysed as controls for the *TAG-1* null mutation. At both E12.5 and E13.5, the C57Bl/6 embryos also had axons within the contra-caudal, ipsi-rostral, ipsi-caudal, continuing and in/at floor plate categories. This suggests that projection of dorsal spinal axons in directions other than contra-rostral is not unique to embryos of the 129/SvEv strain. The proportions of axons within the contra-rostral, ipsi-rostral, ipsi-caudal and continuing groups did not differ significantly between the strains at either age. However, C57/Bl6 embryos had a significantly greater proportion of their dorsal spinal axons within the contra-*rostr*al category, and a greater proportion in or at the floor plate, at both E12.5 and E13.5 (appendix 3.A.2). As embryos get older, the proportion of axons making a contra-rostral turn tends to increase, and that of axons within the floor plate tends to decrease (see figures 3.11 and 3.12). Therefore it could be that development of the dorsal spinal commissural axons of mid-gestation C57/Bl6 embryos is more advanced than that of 129Sv embryos of the same age.

As seen with the 129/SvEv results, those from C57Bl/6 embryos indicate that the observed non-contra-rostral projections persist at least until ages that are equivalent to those used for chick experiments (Stoeckli and Landmesser, 1995, using Hamburger and Hamilton, 1951 and Schneider and Norton, 1979).

3.4.1.4 Non-contra-rostral projections from differently positioned injection sites

The possibility that different neurons were being labelled to those studied previously was investigated by varying the site of DiI injection. Significant differences were found between the projections labelled when DiI was applied to more dorsal, or to more ventral, areas of the dorsal spinal cord. Axons of more dorsal origin were most commonly in or at the floor plate. Axons labelled by more ventral injections were significantly more likely to have made a contra-rostral turn, but also significantly more likely to have made a contra-caudal turn. Thus no particular dorso-ventral region of mouse dorsal spinal cord appeared to be a source of purely contra-rostral projections, and variations in the site of injection do not appear to account for the differences between the current and previous results.

Nevertheless, the differences between projections from different dorso-ventral levels are still of interest. The injections could be labelling neurons of distinct populations, neurons of a single population that comprises neurons of different ages, or of a combination of the two. The idea that neurons at different locations have matured to different extents is supported by a comparison of figures 3.11 and 3.13: progressively more ventral injection sites yield results that are reminiscent of those from progressively older embryos. At E12.5 the D1A and D1B sub-populations of D1 interneuron, which appear to mature at different times, do in fact occupy different dorsal-ventral positions (Lee *et al.*, 1998; figures 3.2, 3.22). D1B interneurons begin their ventral-ward migration away from the common D1 pool before the D1As, and at E12.5 they are found in more ventral regions of the dorsal spinal cord (Lee *et al.*, 1998; figure 3.2, 3.22). The axons of D1B interneurons would therefore be expected to reach the floor plate, and possibly also extend beyond it, before those of D1A interneurons. Thus the greater proportion of axons that made a contralateral turn when DiI was injected more ventrally could conceivably be attributed to D1B neurons (figure 3.22). It should be noted that the more ventral injections are likely to have also labelled axons with dorsally located cell bodies, as these would incorporate DiI along their axon shafts. Therefore the "advanced" development of more ventrally originating axons may be even more pronounced than it appears in figure 3.13.

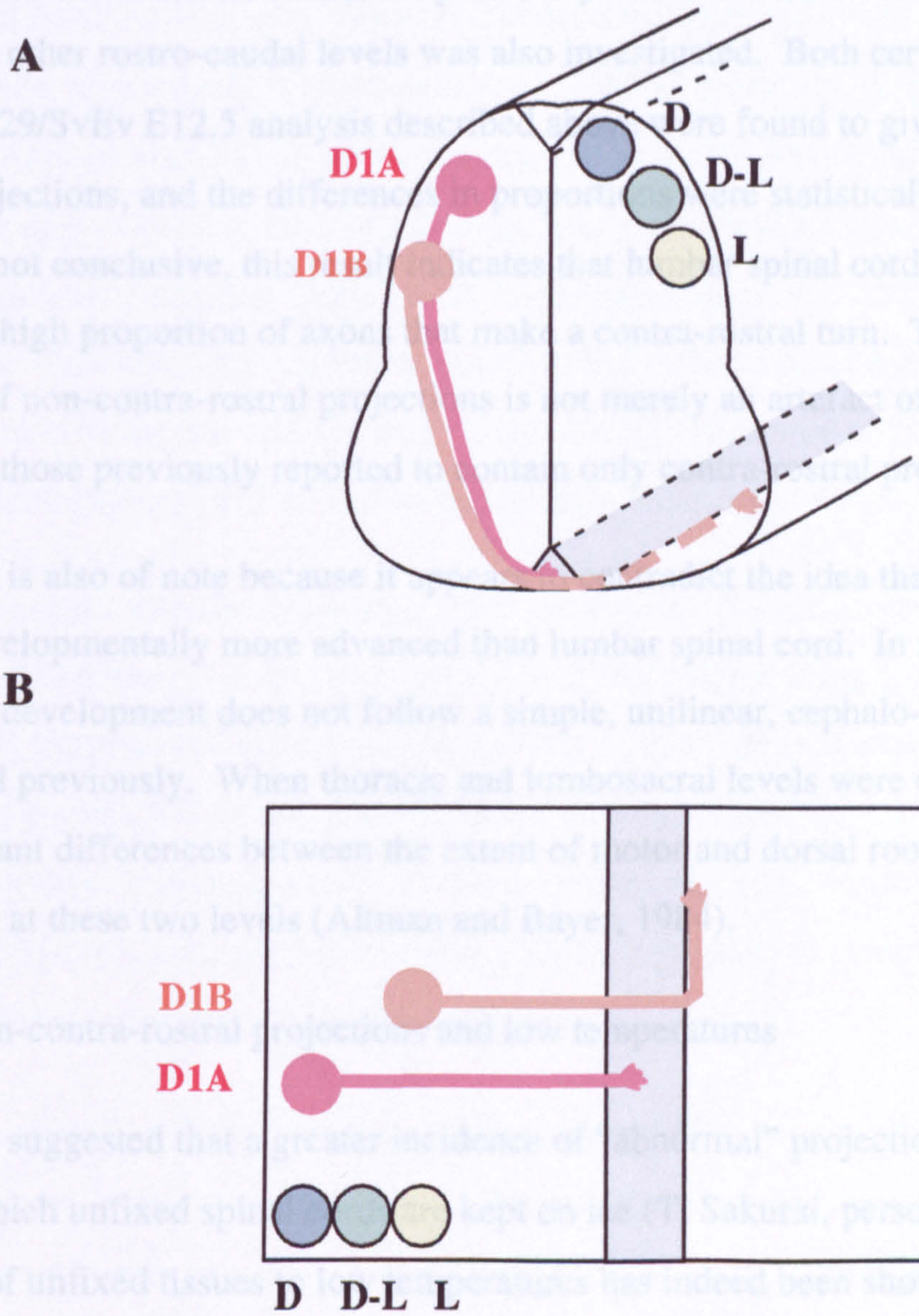

Figure 3.22 Schematic representation of how different dorso-ventral injection sites relate to the positions of D1 interneurons. The positions of D1A and D1B interneurons are shown as determined by the expression of LH2A and LH2B respectively (Lee *et al.*, 1998), in E12.5 spinal cord that has been cut transversely (A) or prepared as an open-book (B). The different injection sites used to generate the results presented in figure 3.13 are also shown, demonstrating a possible explanation for why the lateral (L) sites labelled greater proportions of axons that had made a contra-rostral turn, while dorsal (D) sites labelled greater proportions of axons that were still in or at the floor plate. D-L: dorso-lateral.

As experiments to perturb chick IgCAM function had focussed upon lumbar spinal cord (Stoeckli and Landmesser, 1995), the possibility that non-contra-rostral projections are specific to other rostro-caudal levels was also investigated. Both cervical and lumbar sites from the 129/SvEv E12.5 analysis described above were found to give rise to non-contra-rostral projections, and the differences in proportions were statistically insignificant. Although not conclusive, this result indicates that lumbar spinal cord does not have an especially high proportion of axons that make a contra-rostral turn. Thus the present labelling of non-contra-rostral projections is not merely an artefact of injecting regions other than those previously reported to contain only contra-rostral projections.

This result is also of note because it appears to contradict the idea that the cervical spinal cord is developmentally more advanced than lumbar spinal cord. In fact, the possibility that spinal development does not follow a simple, unilinear, cephalo-caudal gradient has been raised previously. When thoracic and lumbosacral levels were compared, there were no significant differences between the extent of motor and dorsal root ganglion neuron production at these two levels (Altman and Bayer, 1984).

3.4.1.5 Non-contra-rostral projections and low temperatures

It has been suggested that a greater incidence of "abnormal" projections is related to the time for which unfixed spinal cords are kept on ice (T. Sakurai, personal communication). Exposure of unfixed tissues to low temperatures has indeed been shown to cause changes in *Drosophila* axon trajectory, and has lead to at least one inaccurate description of a mutant phenotype (Grenningloh *et al.*, 1994; Lin *et al.*, 1994). However, no differences between proportions of axons within each category were observed when spinal cords were incubated on ice for various lengths of time (data not shown).

3.4.1.6 Previous reports of non-contra-rostral projections

A closer inspection of older studies revealed that such "abnormal" trajectories have in fact been observed in wild type and control animals. For example, the neurons labelled by dorsal injections are thought to correspond to a population previously termed "dorsolateral border cells" (Oppenheim *et al.*, 1988; Stoeckli and Landmesser, 1995), and these were

originally described as "*primarily* ascending commissural" neurons. Whilst on the one hand these projections are said to be "almost exclusively ascending", the proportions of dorsolateral border axons which ascend and descend were estimated to be in the region of 80% and 20% respectively (Oppenheim *et al.*, 1988). Similarly, it appeared that "at least some of the axons also had an ipsilateral branch", and that ipsilateral projections could account for approximately 20% of all projections from these neurons (Oppenheim *et al.*, 1988). Cajal also described single chick dorsal spinal interneurons that contributed to both ipsilateral and contralateral ventral funiculi, and referred to commissural axons that bifurcated to both ascend and descend (Cajal, 1909). Therefore some axons originating in the chick dorsal spinal cord do follow trajectories other than "contra-rostral".

Such projections have also been reported in mammals. For example, in rat embryos, "five axons out of hundreds" turned ipsilaterally, and "rostrally turning axons sometimes had short caudal protrusions" (Bovolenta and Dodd, 1990). Many dorsal commissural axons of neonatal rat spinal cord extend caudally instead of, or as well as, rostrally (Eide *et al.*, 1999). A study of mature cat mid-lumbar interneurons reported that one in five dorsal commissural axons descended (Bras *et al.*, 1989), a proportion comparable with that observed in the embryonic chick (Oppenheim *et al.*, 1988).

Non-contra-rostral projections have also been observed in wild type mice, although these have not always been commented upon. DiI injections have labelled axons of dorsal spinal origin that continue to extend into more lateral regions after decussation (Imondi *et al.*, 2000, figure 3H therein; T. Sakurai, personal communication), or which appear to turn ipsilaterally (Burstyn-Cohen *et al.*, 1999, figure 5 C). One study seemed to report that almost 5% of wild type commissural axons make a caudal rather than rostral turn (Matise *et al.*, 1999, table 1 therein). Another study classified injection sites as "perfect", "mildly defective" or "severely defective" according to the numbers of axons that did not display a contra-rostral trajectory. This approach saw approximately 3% of wild type injection sites classified as severely defective, and a further 30% assigned to the mildly defective category (Zou *et al.*, 2000, figure 7).

When such results are also considered, the finding that wild type dorsolateral spinal neurons do not all project contra-rostrally is perhaps not as surprising as it first appeared.

3.4.2 Single IgCAM mutant embryos

In order to test whether IgCAMs are as important for rodent dorsal spinal axon guidance as they appear to be for that of chick, DiI was applied to the dorsal spinal cords of E12.5 *TAG-1*, *L1* or *NrCAM* mutant embryos. There were no significant differences between the percentages of axons within each category when wild type embryos were compared with those homozygous for mutant *TAG-1*. This was true of mice homozygous for either the TAG^A allele on a 129/SvEv genetic background, or the *TAG-1* null allele on a C57Bl/6 background. Embryos homozygous for the TAG^A mutation on a C57Bl/6 genetic background were found to be similarly unaffected, both during the present study (data not shown) and during a brief investigation by another group (E. Stoeckli, personal communication). The results from *TAG-1* null embryos suggest that the absence of a phenotype in TAG^A mutants is not specifically attributable to the presence of truncated TAG-1 protein. There were no significant differences between the nature of the projections labelled in *L1* hemizygous mutant embryos and their wild type counterparts. *NrCAM* homozygous mutant spinal cords were also largely indistinguishable from their wild type counterparts. However, the percentage of axons making a contra-caudal turn differed significantly, *NrCAM* mutants having a slightly smaller proportion their axons in this category (appendix 3.A.9). The contra-caudal category was under-represented in both homozygous and heterozygous embryos, raising the possibility that any reduction in NrCAM expression is sufficient to affect the decision of whether to turn rostrally or caudally. Although no such result has been reported previously, the absence of other significant defects is in accordance with other recent studies of *NrCAM* mutant mouse embryos (Moré *et al.*, 2001; T. Sakurai and M. Grumet, personal communication).

3.4.2.1 Why are there no major defects?

The results presented above demonstrate that the TAG-1, L1 and NrCAM proteins are not essential for the correct guidance of mouse dorsal commissural axons at the floor plate. There are a number of possible explanations for these findings. The first is that TAG-1, L1 and/or NrCAM might not be involved in the guidance of mouse dorsal spinal axons. This is in contrast to the reports that axonin-1, NgCAM and NrCAM are important for the correct development of chick dorsal commissural axons (Stoeckli and Landmesser, 1995; Stoeckli *et al.*, 1997; Fitzli *et al.*, 2000). The apparent lack of defects in the single mutant mouse embryos may reflect inherent differences between the guidance mechanisms of different species. Different patterns of IgCAM expression suggest that chickens and rodents might indeed have distinct guidance mechanisms. For example, axonin-1 is strongly expressed on the surface of chick dorsal commissural axons both before and after decussation (Shiga and Oppenheim, 1991; Stoeckli and Landmesser, 1995). Yet TAG-1 is lost from the surface of rodent axons once the floor plate has been crossed (Dodd *et al*, 1988; Wolfer *et al*, 1994; Zou *et al.*, 2000; figure 3.4). Similarly, NgCAM is strongly expressed on the surface of chick dorsal commissural axons both before and after decussation (Shiga and Oppenheim, 1991; Stoeckli and Landmesser, 1995), but L1 is expressed on the surface of the rodent axons only once the floor plate has been reached (Dodd *et al.*, 1988). Therefore it is conceivable that these molecules function in different ways in birds and mammals. Such mechanistic differences have been described for other aspects of development, such as mouse and chicken FGF8 having distinct roles in determination of left-right asymmetry (Meyers and Martin, 1999).

It is still possible that TAG-1, L1 and/or NrCAM are necessary for correct development of mouse dorsal commissural axons. It could be that the present investigation failed to detect subtle effects. For example, mechanical rather than manual application of DiI might have allowed smaller and more precise injections, and so meant that sub-populations of axons could be studied more specifically. Sectioning of spinal cords might have revealed defects not apparent in open book preparations, such as the reduced axon fasciculation seen in the chicken experiments (Stoeckli and Landmesser, 1995). IgCAM mutant embryos might not have been analysed at sufficiently late ages in the present study. Single null mutant

embryos were only taken at E12.5, yet, as shown above, the proportion of axons making a contra-rostral turn continues to increase beyond this age (see figures 3.11 and 3.12). Therefore it is conceivable that TAG-1, L1 and/or NrCAM are specifically involved in the guidance of axons that reach the floor plate *after* E12.5. However, E13.5 TAG^{A} homozygous embryos were found not to differ significantly from wild type littermates (appendix 3.A.6), and an independent analysis of *NrCAM* null embryos reported that their dorsal spinal axons were unaffected at E11.5, E12.5 or E13.5 (Moré *et al.*, 2001).

TAG-1, L1 and/or NrCAM could be essential for the correct guidance of mouse dorsal spinal projections at E12.5, providing that the mice are not of the 129/SvEv or C57Bl/6 strains. As already mentioned, mutations can cause different phenotypes according to which genetic backgrounds are used, as different mouse strains carry alternative alleles for certain loci, and some strain specific alleles may modify the effects of a mutation. For example, mice with a mutation in the gene encoding Neuropilin-1 survive for different lengths of time depending upon which genetic background they have (Kitsukawa *et al.*, 1997). The Eph receptor B2 has been reported to cause defects in the vestibular system when present on a CD1 background, but not to have an effect when on either of the 129/SvEv or C57Bl/6 strain backgrounds (Cowan *et al.*, 2000). Effects of the *L1* mutation upon other commissural axons are known to be background dependent, with failure of corpus callosum decussation being evident in mice of the129/SvJae sub-strain but not in those of a 129/SvEv background (Cohen *et al.*, 1997; Demyanenko *et al.*, 1999). It is therefore possible that the effects of the *TAG-1, L1* and/or *NrCAM* mutations are ameliorated by alleles that are peculiar to 129/SvEv or C57Bl/6 mice. This could be tested by analysing embryos which have the mutations on other genetic backgrounds, although to back-cross a mutation onto a new background takes many generations, and cannot entirely eliminate flanking genes from the original strain (Gerlai, 1996; Lathe, 1996).

It may be that TAG-1, L1 and/or NrCAM are not necessary for guidance of the dorsal commissural axons of mouse *or* chicken embryos. It is possible that the results obtained from chicks do not simply reflect inhibition of the target IgCAM. Antibodies that prevent an interaction with one protein do not necessarily prevent, and can sometimes even promote, interactions with others (Neugebauer and Reichardt, 1991; Stoeckli *et al.*, 1991;

Buchstaller *et al.*, 1996). Certain function-blocking antibodies have been shown to stimulate cell-signalling events (Schuch *et al.*, 1989). At least two IgCAMs (F3 and L1) are known to be capable of interacting with, and activating, their binding partners when applied in a soluble form (Durbec *et al.*, 1992; Rougon *et al.*, 1994; Doherty *et al.*, 1995; Sugawa *et al.*, 1997). Such findings raise the possibility that the reported perturbations of chick commissural axon guidance (Stoeckli and Landmesser, 1995; Stoeckli et *al.*, 1997; Fitzli et *al.*, 2000) might not simply reflect blockage of IgCAM function.

3.4.2.2 The possibility of redundancy between IgCAMs.

It is important to note that the finding that TAG-1, L1 and NrCAM are not *essential* for correct dorsal commissural axon guidance does not mean that they have no function in this system. It might be that when a mouse embryo lacks one of these proteins, other molecule(s) can fulfil its roles. There are several examples of such "redundancy". In *Drosophila*, there are four neural receptor protein tyrosine phosphatases (RPTPs), and more than one of them must be mutated for a phenotype to be observed (Sun *et al.*, 2000). There could be redundancy between ephrin B ligands in the rodent floor plate (see chapter 4). In the chicken, NgCAM and NrCAM appear to have redundant roles in promoting the longitudinal extension of dorsal spinal commissural axons (Fitzli *et al.*, 2000).

The possibility that TAG-1, L1 and NrCAM are redundant with one another is being investigated by analysis of mice with multiple IgCAM mutations. As already mentioned, mice homozygous for both *L1* and *NrCAM* mutations display dysgenesis of the cerebellum and die within three weeks of birth (Sakurai *et al.*, 2001). At the time of writing, crosses are underway to enable the *TAG-1 -NrCAM* double mutant mice to be studied on a pure genetic background. As will be discussed below, embryos with mutations in both *TAG-1* and *L1* seem to have defects in the guidance of dorsal spinal axons at the floor plate, suggesting that there is indeed some functional redundancy between these two proteins.

TAG-1, L1 and NrCAM could alternatively, or additionally, have redundancy with other factors. As discussed in chapter 1, there are many neural IgCAMs, and some of these are also expressed by developing dorsal spinal interneurons. For example, Neurofascin shares 47% and 33% amino acid sequence homology with NgCAM and NrCAM respectively

(Holm *et al.*, 1996), and its expression overlaps with those of these two molecules in the developing chicken spinal cord. Neurofascin is present on the commissural and post-decussation portions of commissural axons (Rathjen *et al.*, 1987 b; Shiga and Oppenheim. 1991), in a pattern reminiscent of that of rodent L1 (Dodd *et al.*, 1988; Tran and Phelps, 2000). Neurofascin does indeed seem to compensate for NrCAM in the cerebella of *NrCAM* mutant mice (Sakurai *et al.*, 2001). F11, the chicken homologue of F3, is expressed by dorsal spinal commissural axons only after decussation (Shiga and Oppenheim, 1991), raising the possibility that, although most closely related to TAG-1 (51% amino-acid sequence homology, Holm *et al.*, 1996), F3 may be redundant with L1. Determining the expression patterns of the Neurofascin and F3 proteins in the developing mouse spinal cord would indicate whether their redundancy with L1 is in fact a possibility.

Another candidate for redundancy with NgCAM/L1 is NCAM. This molecule is expressed by commissural axons (Dodd *et al.*, 1988), and its homologue FasII has been implicated in the proper fasciculation of longitudinal axon tracts in *Drosophila* (Lin *et al.*, 1994). Studies of NCAM deficient mice (e.g. Cremer *et al.*, 1994, 1997) do not seem to have addressed the issue of dorsal commissural axon development. DM-GRASP (also known as SC1 and BEN, and as neurolin in fish) is strongly expressed by both mouse and human floor plate cells during commissural axon development (Karagogeos *et al.*, 1997; Fraboulet *et al.*, 2000). In chick, the decussating portions of the commissural axons themselves have also been reported to express DM-GRASP (El-Deeb *et al.*, 1992). DM-GRASP is capable of interacting homophilically (Tanaka *et al.*, 1991), and also heterophilcally with NgCAM (Debernardo and Chang, 1996). It would be interesting to examine embryos homozygous mutant for both *DM-GRASP* and *NrCAM*.

3.4.2.3 TAG-1, L1 and NrCAM and other axon guidance mechanisms

The functions of TAG-1, L1 and/or NrCAM could also overlap with the other molecular events that have been reported to regulate floor plate entry (summarised in figures 3.3 and 3.23). For example, rat dorsal commissural axons seem to be insensitive to the floor plate inhibitory factors Semaphorin (Sema) 3B and Slit-2 at the time of midline entry, but to become responsive to these factors after decussation (Zou *et al.*, 2000). It could be that

TAG-1 and NrCAM ensure that sensitivity is acquired only after floor plate entry. The *Drosophila* receptor for Slit proteins, the IgSF molecule Roundabout (Kidd *et al.*, 1999), is specifically down-regulated on commissural growth cones before their decussation (Kidd *et al.*, 1998 a). Roundabout, which is also known as Robo, has thus been referred to as a "gatekeeper" protein, because its surface expression determines whether the floor plate can be entered (Kidd *et al*, 1998 a). The vertebrate homologues of Slit and Robo are expressed by the floor plate and decussating axons respectively (Kidd *et al.*, 1998 a; Brose *et al.*, 1999), although it is not yet clear whether surface expression of vertebrate Robo receptors alters at the midline. In *Drosophila*, axonal expression of Robo is reduced in response to the midline protein Commissureless, or Comm (Kidd *et al.*, 1998 b). However, a vertebrate version of this protein has not yet been identified. If vertebrate Robo proteins are down-regulated at the vertebrate floor plate, it could be that interactions involving axonin-1 and floor plate NrCAM have a similar role to that performed by Comm (Chien, 1998). Labelling of IgCAM mutant mouse spinal cord with anti-Robo antibodies could indicate whether axonin-1/TAG-1-NrCAM interactions participate in the regulation of levels of Robo protein. If a rodent equivalent of Comm is discovered, it will be interesting to establish whether mice mutant for both this and TAG-1 and/or NrCAM have increased proportions of ipsilateral axons.

TAG-1-NrCAM interactions could equally have gatekeeper functions with regards to other floor plate inhibitory factors (figures 3.3 and 3.23). For example, pre-commissural axons are insensitive to Sema 3B, despite expressing the Sema 3B receptor component Neuropilin-2 (Zou *et al.*, 2000). It could be that a TAG-1-NrCAM binding event changes the ability of decussating axons to respond to Sema 3B. There are at least two other situations in which an IgSF member seems to affect the responses of axons to semaphorins. In *Drosophila*, the IgSF protein Off-Track seems to be involved in the ability of the Plexin A receptor to mediate responses to Sema 1a (Winberg *et al.*, 2001). In mice, L1 alters the sensitivity of corticospinal axons to Sema 3A, apparently via its interaction with the Sema 3A receptor Neuropilin-1 (Castellani *et al.*, 2000; He, 2000). The mechanism could involve changes in the ability of Neuropilin-1 to relieve the other part of the Sema 3A

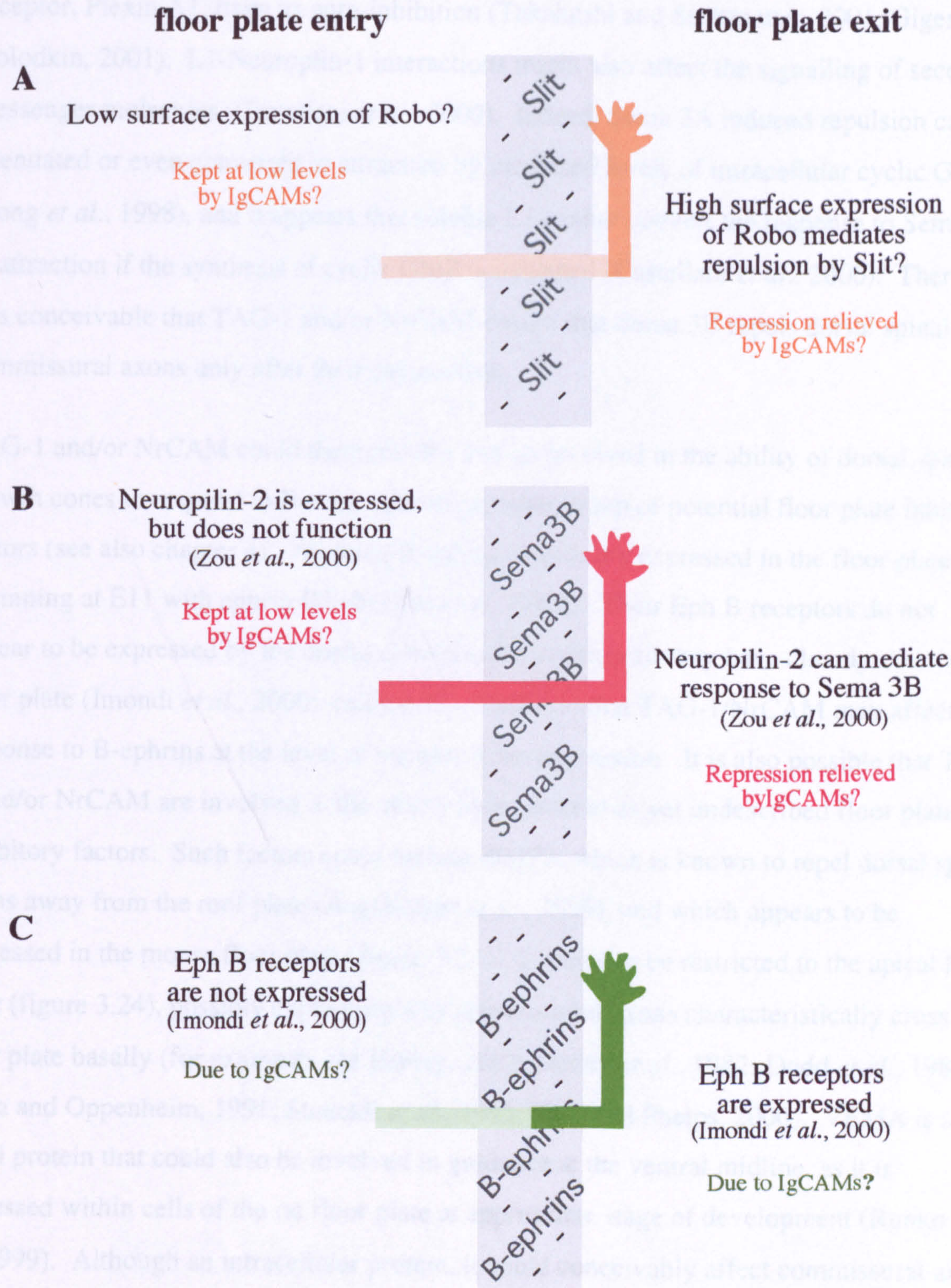

Figure 3.23 Summary of mechanisms of floor plate entry and/or exit that might involve TAG-1, L1 and/or NrCAM. A: Expression of IgCAMs in the floor plate area could theoretically maintain Robo expression at low levels to allow entry, or increase surface expression of Robo to allow exit . Note that this model is highly speculative. *Drosophil*a commissural alter their surface expression of Robo as illustrated (Kidd *et al.*, 1999 a and b), and it is known that mammalian dorsal commissural axons express Robo proteins (Kidd *et al.*, 1998 a; Brose et al., 1999; Yuan *et al.*, 2001), and acquire sensitivity to slit-2 only once the floor plate has been crossed (Zou *et al.*, 2000). However, it is not clear whether surface expression of mammalian Robo receptors changes at the floor plate, so it might not be levels of this that determine slit-sensitivity. B: Interactions between TAG-1 and NrCAM might repress neuropilin-2 function to allow floor plate entry; interactions involving the newly-expressed L1 might relieve such repression, so that Sema 3B can cause floor plate exit. C: IgCAMs might affect the expression of Eph B receptors, or affect the ability of these receptors to function. IgCAMs could also/alternatively alter the ability of commissural axons to respond to as yet uncharacterised factors.

receptor, Plexin A1, from its auto-inhibition (Takahashi and Strittmatter, 2001: Giger and Kolodkin, 2001). L1-Neuroplin-1 interactions might also affect the signalling of second messenger molecules (Castellani *et al.*, 2000). Indeed, Sema 3A induced repulsion can be attenuated or even converted to attraction by increased levels of intracellular cyclic GMP (Song *et al.*, 1998), and it appears that soluble L1 cannot convert the response to Sema 3A to attraction if the synthesis of cyclic GMP is inhibited (Castellani *et al.*, 2000). Therefore it is conceivable that TAG-1 and/or NrCAM ensure that Sema 3B repels dorsal spinal commissural axons only after their decussation.

TAG-1 and/or NrCAM could theoretically also be involved in the ability of dorsal spinal growth cones to respond to B-class ephrins, another group of potential floor plate inhibitory factors (see also chapter 4). All three B-ephrin ligands are expressed in the floor plate, beginning at E11 with ephrin B3 (Imondi *et al.*, 2000). Their Eph B receptors do not appear to be expressed by the dorsal commissural axons until they have already entered the floor plate (Imondi *et al.*, 2000), raising the possibility that TAG-1/NrCAM may affect the response to B-ephrins at the level of receptor gene expression. It is also possible that TAG-1 and/or NrCAM are involved in the ability to respond to as yet undescribed floor plate inhibitory factors. Such factors could include BMP7, which is known to repel dorsal spinal axons away from the roof plate (Augsburger *et al.*, 1999), and which appears to be expressed in the mouse floor plate (figure 3.24). It seems to be restricted to the apical floor plate (figure 3.24), possibly explaining why commissural axons characteristically cross the floor plate basally (for examples see Holley, 1982; Holley *et al.*, 1982; Dodd *et al.*, 1988; Shiga and Oppenheim, 1991; Stoeckli *et al.*, 1995; Tran and Phelps, 2000). VEMA is a novel protein that could also be involved in guidance at the ventral midline, as it is expressed within cells of the rat floor plate at appropriate stage of development (Runko *et al.*, 1999). Although an intracellular protein, it could conceivably affect commissural axons following a physical transfer to them, as has been demonstrated for the Comm protein in *Drosophila* (Tear *et al.*, 1996) and for ß-galactosidase in mice (Campbell and Peterson, 1993).

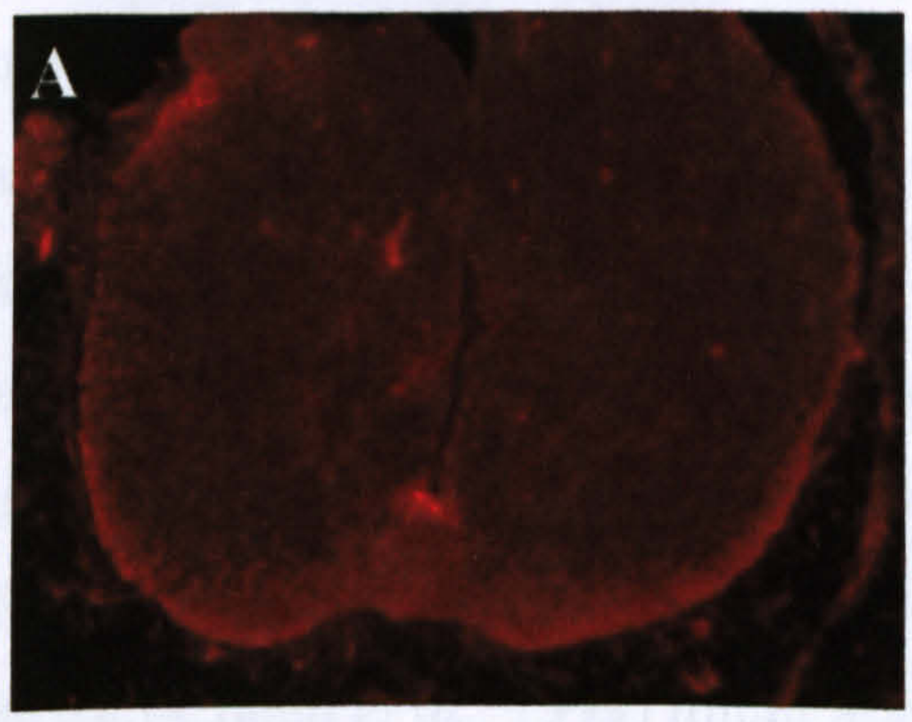

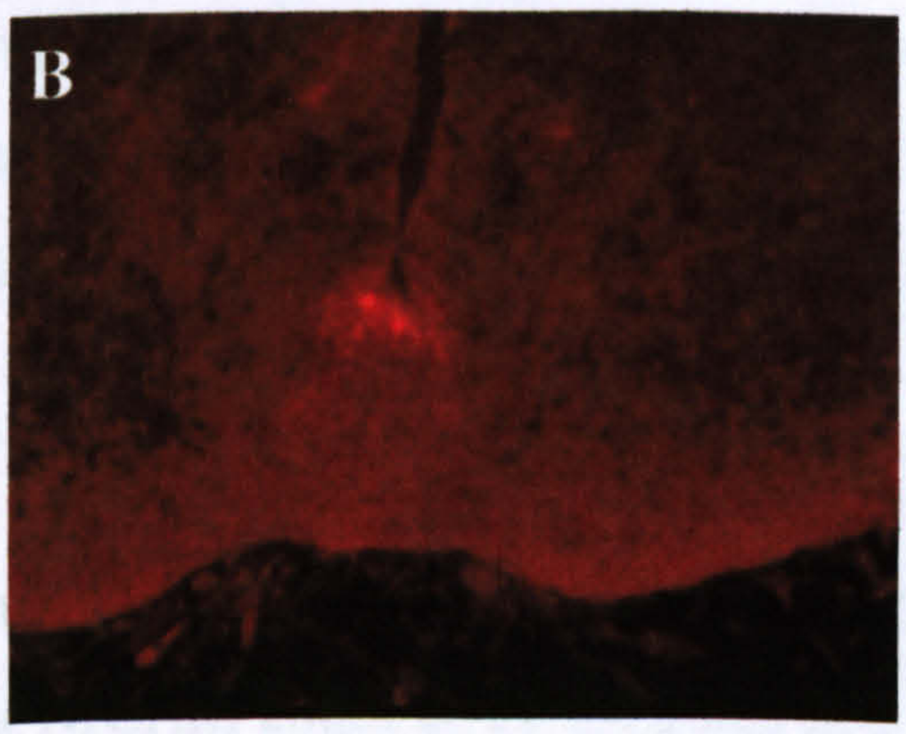

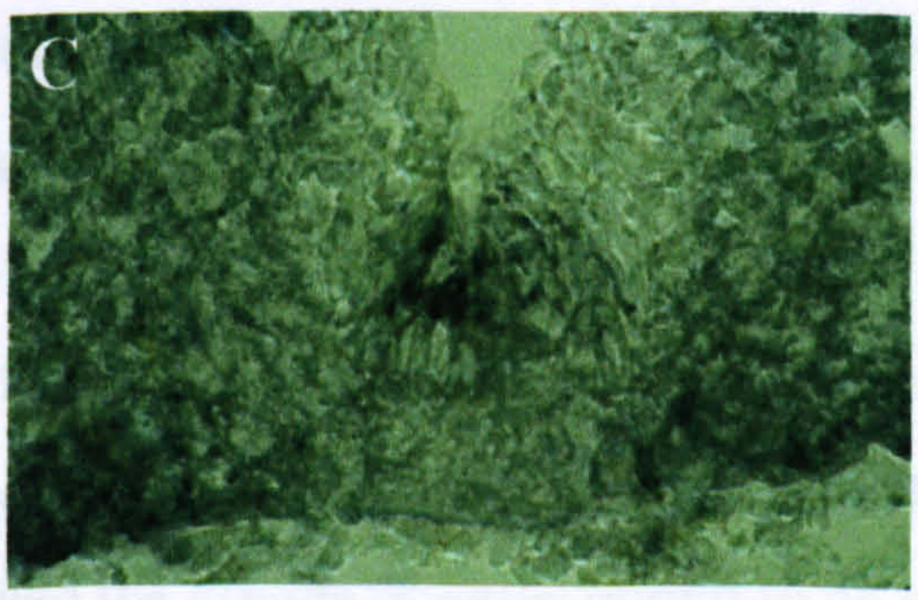

Figure 3.24 BMP7 appears to be expressed by the E12.5 cervical floor plate. A and B: two different magnifications of a transverse section of E12.5 mouse floor plate that had been labelled with the R.3331 antibody to BMP7 and a fluorescent secondary antibody. C: the floor plate of an adjacent section that had been labelled with R.3331 and a horse-radish peroxidaxe conjugated secondary antibody, to show that the labelling in B is not a non-specific artefact .

Whether TAG-1 and/or NrCAM alter axonal sensitivity to Slit proteins, semaphorin 3B, B ephrins, or as yet undiscovered midline inhibitory factors, this study demonstrates that they are not individually essential for floor plate entry. As suggested, the decision to enter floor plate appears to depend upon a balance of positive and negative cues (Stoeckli and Landmesser, 1995; Stoeckli *et al.*, 1997). When either *TAG-1* or *NrCAM* is mutated, other positive activities remain, and these might even be up-regulated to compensate. For example, dorsal spinal axons were still attracted to Netrin-1 when the functions of axonin-1, NgCAM and NrCAM were perturbed (Stoeckli *et al.*, 1997). A second floor plate attractant, F-Spondin (Burstyn-Cohen *et al.*, 1999) might also guide the mutant dorsal commissural axons into the floor plate. Such positive cues, and other mechanisms to ensure that negative factors are ignored, could mean that the absence of TAG-1, L1 or NrCAM is not sufficiently great a loss for the balance to be tipped in favour of inhibitors.

3.4.2.4 Investigating the possibility of redundancy

The possibility that other molecules and/or mechanisms promote floor plate entry in the absence of TAG-1, L1 or NrCAM could be investigated in a number of ways. As demonstrated, double mutant mice can be generated. The possibility that other factors are up-regulated to compensate for the lack of the IgCAMs could be tested by antibody labelling of sections from mutant and wild type embryos. However, as is evident in figures 3.6 and 3.7, it can be difficult to judge whether a protein is expressed more strongly or not. A third approach is that of explant culture. *In vitro* culture of chick dorsal spinal cord with floor plate explants showed the effects of perturbation to be more pronounced than *in vivo* (Stoeckli and Landmesser, 1995; Stoeckli *et al.*, 1997; summarised in figure 3.5), possibly reflecting the absence of other factors that normally influence floor plate entry. Similarly, L1 hemizygous mutant dorsal root ganglion axons fail to respond to ventral spinal cord explants *in vitro* (Castellani *et al.*, 2000), despite showing no obvious guidance defects *in vivo* (figures 3.7 and 5.11, appendix 5.D). Therefore it is possible that subtle effects of the *TAG-1, L1* and/or *NrCAM* mutations might also be more apparent *in vitro* than *in vivo.* If this proved to be the case, the *in vitro* culture system could be used to investigate how the IgCAMs act. For example, if mutant axons were found to be unable to enter floor plate

explants, antibodies could be used to block the function of candidate midline inhibitory cues. If such an antibody restored the ability of mutant axons to enter floor plate tissue, its target might be a negative factor that the IgCAMs normally negate. If the culture of mutant mouse dorsal spinal cord with floor plate revealed no defects in floor plate entry, function-blocking antibodies could be used to identify factors with which the IgCAMs are redundant. The use of specifically transfected cells rather than floor plate would allow the responses to single midline factors to be tested individually (e.g. Kennedy *et al.*, 1994; Shirasaki *et al.*, 1996; Castellani *et al.*, 2000; Zou *et al.*, 2000).

Attempts were made to set up an *in vitro* assay for dorsal commissural axon growth. Initially dorsal spinal explants were grown with floor plate tissue on a substrate of laminin, as this "two-dimensional" culturing allows the entry of axons into the floor plate to be carefully recorded (e.g. Stoeckli *et al.*, 1997; see figure 3.25). However, the explants responded poorly, and the floor plate was seldom reached by axons of any genotype. This did not appear to be due to the laminin substrate causing the axons to find netrin-1 repulsive, as has been described for *Xenopus* retinal axons (Höpker *et al.*, 1999), as neither additional Netrin-1 (as in Shirasaki *et al.*, 1996), nor greatly reduced laminin concentrations, afforded better results. This was not unexpected, as it is recognised that mouse embryonic dorsal spinal cord is more difficult to culture *in vitro* than that of either rat or chicken (M. Tessier-Lavigne and E. Stoeckli, personal communications). Axon outgrowth was more robust when explants were co-cultured in a "three-dimensional" collagen gel matrix (figure 3.25; Lumsden and Davies, 1983; Placzek *et al.*, 1993). Such a system has previously been used to test the responses of mouse dorsal spinal axons to potential midline guidance cues (e.g. Tessier-Lavigne *et al.*, 1988; Placzek *et al.*, 1990 a, b; Zou *et al.*, 2000; Castellani *et al.*, 2000). For example, such assays demonstrated that the ability to respond to Sema 3A is dependent upon axonal L1 (Castellani *et al.*, 2000), and that pre- and post- decussation commissural axons have different sensitivities to floor plate factors (Zou *et al.*, 2000). Dorsal spinal commissural axons, as defined by expression of TAG-1 protein, or ß-galactosidase, were produced from dorsal spinal explants in collagen (data not shown), but difficulties in obtaining mutant and wild type embryos of the same age meant that responses of axons of different genotypes were not compared.

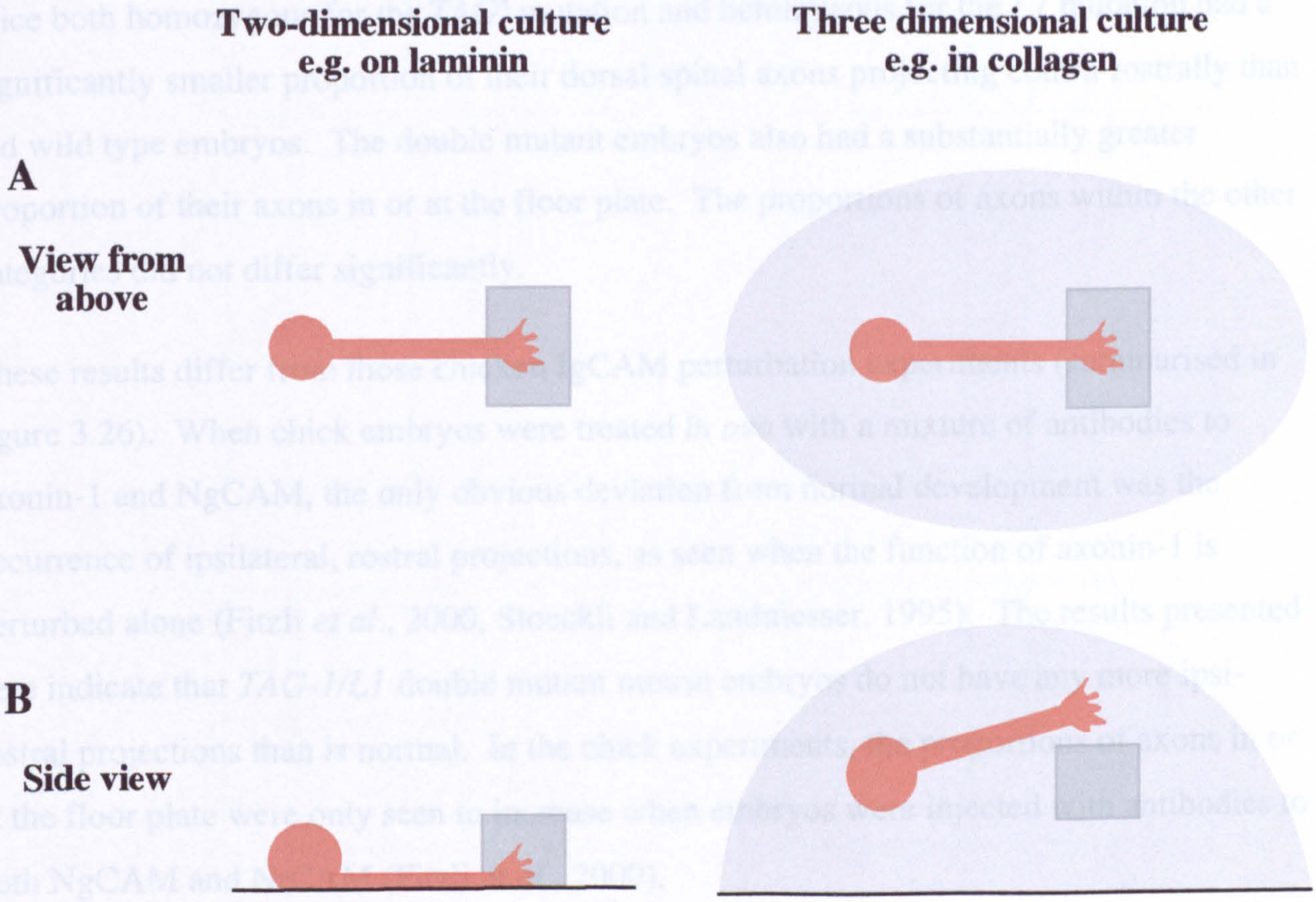

Figure 3.25 Schematic representation of one of the practical differences between "two-dimensional" and "three-dimensional" explant culture. Axons seeming to enter floor plate when viewed from above (A) may actually be at a different level within a collagen gel (B, right).

3.4.3 Double mutant embryos

In contrast to the results from single mutant embryos, the development of dorsal spinal projections appeared to be abnormal when both *L1* and *TAG-1* were mutated. At E12.5, the mice both homozygous for the TAG^{A} mutation and hemizygous for the *L1* mutation had a significantly smaller proportion of their dorsal spinal axons projecting contra-rostrally than did wild type embryos. The double mutant embryos also had a substantially greater proportion of their axons in or at the floor plate. The proportions of axons within the other categories did not differ significantly.

These results differ from those chicken IgCAM perturbation experiments (summarised in figure 3.26). When chick embryos were treated *in ovo* with a mixture of antibodies to axonin-1 and NgCAM, the only obvious deviation from normal development was the occurrence of ipsilateral, rostral projections, as seen when the function of axonin-1 is perturbed alone (Fitzli *et al.*, 2000, Stoeckli and Landmesser, 1995). The results presented here indicate that *TAG-1/L1* double mutant mouse embryos do not have any more ipsi-rostral projections than is normal. In the chick experiments, the proportions of axons in or at the floor plate were only seen to increase when embryos were injected with antibodies to both NgCAM and NrCAM (Fitzli *et al.*, 2000).

There are a number of potential explanations for such differences. As discussed above, the mouse may have additional mechanisms to allow dorsal spinal axons to enter the floor plate; conversely, the chick may have more mechanisms than the mouse for ensuring that axons leave the floor plate. Another reason for the differences between these results might be that NgCAM and L1 are not equivalent proteins. As discussed by Sonderegger and Rathjen (1992), L1 and NgCAM have many structural similarities, such as their numbers of immunoglobulin-like and fibronectin type III domains, their apparent proteolytic cleavage, and the presence of a cytoplasmic site for phosphorylation (Sonderegger and Rathjen, 1992; Burgoon *et al.*, 1995). However, the two amino acid sequences share only the same level of homology as do non-homologous members of the L1-like sub family (Holm *et al.*, 1996), and more recent analysis of structural features likens NgCAM more to NrCAM than L1 (Hortsch, 2000). As already mentioned, the expression of the molecules by

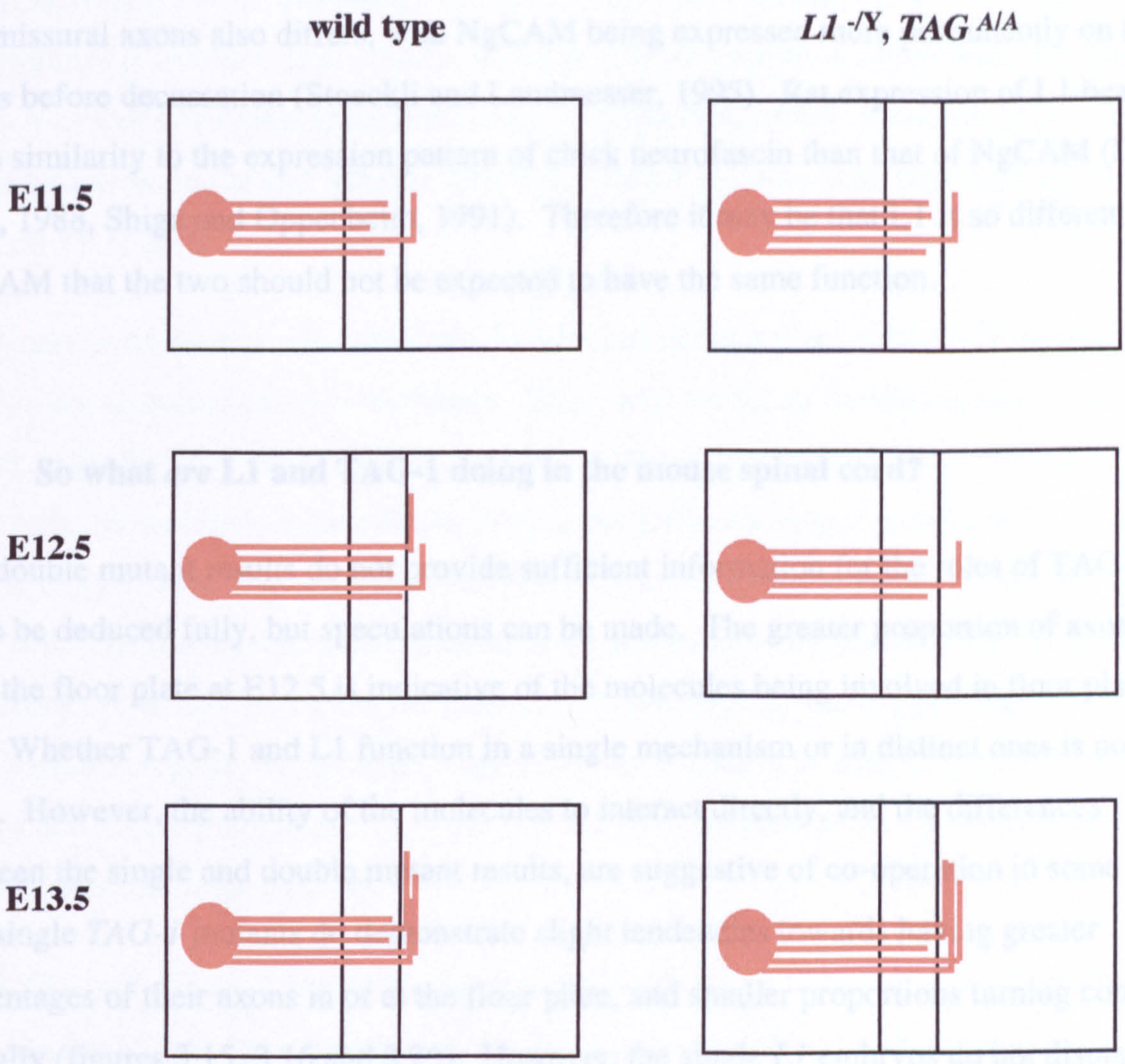

Figure 3.26 Summary of the results of injecting *TAG-1-L1* double mutant embryos (A), and how these compare to the results of chick experiments (B). At E11.5, there were no significant differences between mouse embryos of the two genotypes. At E12.5, the double mutant has a smaller proportion of axons turning contra-rostrally. By E13.5, the double mutant has the greater proportion of axons making a contra-rostral turn. In contrast, perturbation of both of the molecules thought to be equivalent to TAG-1 and L1 in chicken embryos resulted in failure of floor plate entry (Fitzli *et al.*, 2000).

commissural axons also differs, with NgCAM being expressed more prominently on the axons before decussation (Stoeckli and Landmesser, 1995). Rat expression of L1 bears more similarity to the expression pattern of chick neurofascin than that of NgCAM (Dodd et al., 1988, Shiga and Oppenheim, 1991). Therefore it may be that L1 is so different to NgCAM that the two should not be expected to have the same function.

3.4.4 So what *are* L1 and TAG-1 doing in the mouse spinal cord?

The double mutant results do not provide sufficient information for the roles of TAG-1 and L1 to be deduced fully, but speculations can be made. The greater proportion of axons in or at the floor plate at E12.5 is indicative of the molecules being involved in floor plate exit. Whether TAG-1 and L1 function in a single mechanism or in distinct ones is not clear. However, the ability of the molecules to interact directly, and the differences between the single and double mutant results, are suggestive of co-operation in some way. The single *TAG-1* mutants do demonstrate slight tendencies towards having greater percentages of their axons in or at the floor plate, and smaller proportions turning contra-rostrally (figures 3.15, 3.16 and 3.26). However, the single *L1* embryos do not display such tendencies, and if anything seem to have a greater proportion of their axons turning contra-rostrally (figure 3.17). This implies that the significantly greater proportion of axons in or at the floor plate in E12.5 *TAG-1/L1* double mutant embryo is not merely an effect of the addition of two independent, less than significant results.

TAG-1 and L1 are known to interact heterophilically in *cis* – that is, within the same cell membrane (Felsenfeld *et al.*, 1994; Stoeckli *et al.*, 1996; Rader *et al.*1996; Buchstaller *et al.*, 1996; Malhorta *et al.*, 1998). L1 and TAG-1 are co-expressed on the portions of commissural axons that are within the floor plate (Dodd *et al.*, 1988; Tran and Phelps, 2000), so it could be that they interact in *cis* in this region. If this is the case, the resulting complex might act as a receptor for floor plate inhibitory cues, or interact with such receptors. For instance, an L1-TAG-1 heterodimer could theoretically interact with the receptors for Slit-2 and/or Sema 3E, so causing decussating axons to become sensitive these

cues (Zou *et al.*, 2000). Indeed, L1 is known to interact with the semaphorin receptor Neuropilin-1 (Castellani *et al.*, 2000), although it is Neuropilin-2, rather than Neuropilin-1, that is expressed by dorsal spinal interneurons (Chen *et al.*, 1997; Kolodkin *et al.*, 1997). It would be interesting to test whether *TAG-1/L1* double mutant axons were repelled by Slit-2 or Sema 3E *in vitro*.

The presence of more axons within the double mutant floor plate at E12.5 is suggestive of a delay in dorsal spinal axon development. This could reflect an "unwillingness" of double mutant axons to leave the floor plate, or it could be symptomatic of an earlier delay. In order to better understand the roles of TAG-1 and L1 in the mouse spinal cord, E11.5 and E13.5 embryos were also analysed (the results are summarised in figure 3.26). The finding that the double mutant and wild type results are almost indistinguishable at E11.5 implies that axons are unaffected before the floor plate is reached. It remains possible that the double mutation perturbs an earlier stage of the development of a population of axons that arrives at the floor plate after E11.5, but the lack of expression of L1 by pre-commissural axons makes this seem unlikely.

At E13.5, the *TAG-1/L1* double mutant embryos were found to be significantly different from their wild type counterparts. At this age, the double mutant spinal preparations had a significantly greater proportion of axons that had made a contra-rostral turn, and a significantly smaller percentage in or at the floor plate. The proportions of projections within the "contra-caudal" and "continuing" categories were also significantly greater than those of wild type embryos.

One possible explanation for the apparent increase in non-floor-plate projections could be that there is an unusually large decrease in the proportions of axons within the "in/at floor plate" category. Thus the proportions of contra-rostral, contra-caudal and continuing axons may have increased relatively rather than absolutely. This could occur if stalled axons were selectively killed off in the double mutant embryos. Embryos with a mutation in *Sema 3A* have been shown to have their inappropriate axonal projections selectively eliminated before birth (White and Behar, 2000). It could be that some of the *TAG-1/L1* double mutant dorsal spinal axons are unable to respond to trophic factors from the midline (Wang

and Tessier-Lavigne, 1999) or adjacent glia (Booth *et al.*, 2000), such that they cannot survive beyond E12.5. It would be interesting to compare the extent of cell death within wild type and double mutant spinal cords between E12.5 and E13.5, for example using TdT-mediated dUTP-biotin nick-end labelling (TUNEL) analysis (Gavrieli *et al.*, 1993).

Alternatively, the apparent "over-recovery" could reflect an up-regulation of factors in an attempt to compensate for the absence of TAG-1 and L1. For example, if TAG-1- L1 interactions normally allow axons to respond to a floor plate inhibitory cue, it might be that the activity of another midline repulsive factor (see above) is increased, to force the axons to continue. As discussed previously, antibody labelling could be used to check for the up-regulation of factors.

3.5 Conclusions

1. **The axons of dorsal spinal interneurons do not all make a "contra-rostral" turn.**
   It has been shown that some wild type axons of dorsal spinal origin have trajectories other than that of decussating and turning rostrally.

2. **The axons of mouse dorsal spinal interneurons are guided normally in the absence of full-length TAG-1, L1 or NrCAM proteins.**
   In contrast to what may have been expected from chick experiments, single mutations in *TAG-1*, *L1* or *NrCAM* do not have significant effects upon mouse dorsal spinal axon guidance.

3. **The axons of mouse dorsal spinal interneurons are not guided normally when both *TAG-1* and *L1* are mutated.**
   Double mutant axons seem to have an impaired ability to leave the floor plate at E12.5. However, double mutant axons are more likely to have left the floor plate by E13.5 than are those of wild type embryos.

3.6 Appendices

Appendix 3.A: Statistical analyses of the differences between dorsal spinal projections labelled under various circumstances.

In each case, the differences between distributions were assessed using an "analysis of variance" test (ANOVA) in "Microsoft Excel: mac 2001", as suggested by Dytham, 1999.

This test affords the same results as a two-tailed *t*-test when two groups are compared, but as it tests whether the variance within groups is the same as the variance between groups, it is also suitable for comparisons of more than two groups. In the summary tables, "count" denotes the number of sites for each group; "sum" is the total of the percentages of axons within the category; "average" is the mean percentage per site, and "variance" is the extent to which the individual percentages varied form their mean. The ANOVA table summarises intermediate stages of the calculations used to obtain the F-statistic: "df" denotes degrees of freedom; "SS" the sum of squares, "MS" the mean square (SS/df), and the "F"-statistic is the ratio of the two MS values. The "P-value" is the probability on the F-value being obtained by chance- i.e. the probability that the variances between and within groups would differ as they do if there was no a significant difference. Where the P-value is below 0.05, the chance of the result occurring if the groups were the same is so low that the groups are concluded to be significantly different.

3.A.1: Comparison of 129/SvEv embryos of different ages.

3.A.2: Comparison of 129/SvEv and C57Bl/6 embryos at E12.5 and E13.5.

3.A.3: Comparison of the projections labelled when DiI was injected at different dorso-ventral positions.

3.A.4: Comparison of the projections labelled when DiI was injected at different rostro-caudal levels.

3.A.5: Comparison of embryos wild type, heterozygous or homozygous for the *TAG*^{A} (truncation) mutation.

3.A.6: Comparison of embryos wild type or homozygous for the *TAG*^{A} (truncation) mutation at E13.5.

3.A.7: Comparison of embryos wild type, heterozygous or homozygous for the *TAG-1* null mutation.

3.A.8: Comparison of embryos wild type, heterozygous or hemizygous for the *L1* null mutation.

3.A.9: Comparison of embryos wild type, heterozygous or homozygous for the *NrCAM* null mutation.

3.A.10: Comparison of TAG^{A} */L1* double mutant embryos with those wild type for both genes: E12.5.

3.A.11: Comparison of TAG^{A} */L1* double mutant embryos with those wild type for both genes: E11.5.

3.A.12: Comparison of TAG^{A} */L1* double mutant embryos with those wild type for both genes: E12.5.

3.A.13: Comparison of TAG^{A} */L1* double mutant embryos at different ages.

Appendix 3.B: Mean proportions of axons within each category in E12.5 *L1*/TAG^{A} double mutant embryos: all genotypic combinations.

Appendix 3.A.1

Comparison of 129Sv embryos of different ages

For data, see figure 3.11

Axons making a contra-rostral turn

SUMMARY

Groups	*Count*	*Sum*	*Average*	*Variance*
E11.5	44	754.2	17.1409091	812.171311
E12.5	94	3585.5	38.143617	1758.00872
E13.5	40	1901.6	47.54	1285.85682

ANOVA

Source of Variation	*df*	*SS*	*MS*	*F*	*P-value*
Between Groups	2	21251.9591	10625.9796	7.4810794	0.00076288
Within Groups	175	248566.594	1420.38053		
Total	177	269818.553			

I.e. there is a significant difference between the proportions at the three ages.

Comparison of E11.5 and E12.5 results only:

ANOVA

Source of Variation	*df*	*SS*	*MS*	*F*	*P-value*
Between Groups	1	13220.6263	13220.6263	9.06169586	0.00311209
Within Groups	136	198418.178	1458.95719		
Total	137	211638.804			

I.e. there is a significant difference in the proportion of axons which make a contra-rostral turn between E11.5 and E12.5.

Comparison of E12.5 and E13.5 results only:

ANOVA

Source of Variation	*df*	*SS*	*MS*	*F*	*P-value*
Between Groups	1	2477.44753	2477.44753	1.53069713	0.21820429
Within Groups	132	213643.227	1618.5093		
Total	133	216120.675			

I.e. there is no significant change in the proportion of axons which make a contra-rostral turn between E12.5 and E13.5.

Axons in/at the floor plate

SUMMARY

Groups	*Count*	*Sum*	*Average*	*Variance*
E11.5	43	3553.6	82.6418605	847.272968
E12.5	94	5207	55.393617	2064.4348
E13.5	40	1900.1	47.5025	1472.74384

ANOVA

Source of Variation	*df*	*SS*	*MS*	*F*	*P-value*
Between Groups	2	30276.8207	15138.4104	9.24191439	0.00015328
Within Groups	174	285014.911	1638.01673		
Total	176	315291.731			

ie there is a significant difference between the proportions at the three ages.

Comparison of E11.5 and E12.5 results only:

ANOVA

Source of Variation	*df*	*SS*	*MS*	*F*	*P-value*
Between Groups	1	21905.4795	21905.4795	12.9944064	0.00043841
Within Groups	135	227577.901	1685.76223		
Total	136	249483.38			

I.e. there is a significant difference between the proportion of axons within the floor plate between E11.5 and E12.5.

Comparison of E12.5 and E13.5 results only:

ANOVA

Source of Variation	*df*	*SS*	*MS*	*F*	*P-value*
Between Groups	1	1747.26998	1747.26998	0.92466884	0.33801025
Within Groups	132	249429.446	1889.61701		
Total	133	251176.716			

I.e. there is no significant change in the proportion of axons within the floor plate between E12.5 and E13.5.

Appendix 3.A.1 continued

Axons making a contra-caudal turn

SUMMARY

Groups	*Count*	*Sum*	*Average*	*Variance*
E11.5	44	0	0	0
E12.5	94	369.5	3.93085106	126.229038
E13.5	40	119.6	2.99	26.8609231

ANOVA

Source of Variation	*df*	*SS*	*MS*	*F*	*P-value*
Between Groups	2	466.127569	233.063785	3.18968923	0.04359003
Within Groups	175	12786.8765	73.0678659		
Total	177	13253.0041			

I.e. there is a significant difference between the proportions at the three ages.

Comparison of E11.5 and E12.5 results only:

ANOVA

Source of Variation	*df*	*SS*	*MS*	*F*	*P-value*
Between Groups	1	463.09983	463.09983	5.36501956	0.02203962
Within Groups	136	11739.3005	86.3183863		
Total	137	12202.4004			

I.e. there is a significant differnce in the proportion of axons which make a contra-caudal turn between E11.5 and E12.5.

Comparison of E12.5 and E13.5 results only:

ANOVA

Source of Variation	*df*	*SS*	*MS*	*F*	*P-value*
Between Groups	1	24.8384681	24.8384681	0.25640959	0.61344233
Within Groups	132	12786.8765	96.8702768		
Total	133	12811.715			

I.e. there is no significant change in the proportion of axons which make a contra-caudal turn between E12.5 and E13.5.

Axons making an ipsi-rostral turn

SUMMARY

Groups	*Count*	*Sum*	*Average*	*Variance*
E11.5	44	15.4	0.35	1.88162791
E12.5	94	32.5	0.34574468	2.38723976
E13.5	40	3.1	0.0775	0.11717308

ANOVA

Source of Variation	*df*	*SS*	*MS*	*F*	*P-value*
Between Groups	2	2.25459258	1.12729629	0.64156524	0.52770142
Within Groups	175	307.493048	1.75710313		
Total	177	309.74764			

I.e. there is no significant difference between the proportions at the three ages.

Axons making an ipsi-caudal turn

SUMMARY

Groups	*Count*	*Sum*	*Average*	*Variance*
E11.5	44	0	0	0
E12.5	94	21	0.22340426	1.14310226
E13.5	40	0	0	0

ANOVA

Source of Variation	*df*	*SS*	*MS*	*F*	*P-value*
Between Groups	2	2.21396127	1.10698064	1.82225873	0.16471425
Within Groups	175	106.308511	0.6074772		
Total	177	108.522472			

I.e. there is no significant difference between the proportions at the three ages.

Axons continuing to extend laterally

SUMMARY

Groups	*Count*	*Sum*	*Average*	*Variance*
E11.5	44	78.9	1.79318182	31.6969292
E12.5	94	184.5	1.96276596	112.705588
E13.5	40	76.8	1.92	24.6924103

ANOVA

Source of Variation	*df*	*SS*	*MS*	*F*	*P-value*
Between Groups	2	0.86589269	0.43294635	0.00591568	0.99410198
Within Groups	175	12807.5916	73.1862379		
Total	177	12808.4575			

I.e. there is no significant difference between the proportions at the three ages.

Appendix 3.A.2

Comparison of 129/SvEv and C57Bl/6 embryos at E12.5

For data, see figure 3.12

Axons making a contra-rostral turn

SUMMARY

Groups	*Count*	*Sum*	*Average*	*Variance*
129Sv	26	1596.4	61.4	1432.096
C57Bl/6	94	3585.5	38.143617	1758.00872

ANOVA

Source of Variation	*df*	*SS*	*MS*	*F*	*P-value*
Between Groups	1	11015.5021	11015.5021	6.5220644	0.0119284
Within Groups	118	199297.211	1688.95942		
Total	119	210312.713			

ie the proportions of axons are significantly different

Axons making an ipsi-caudal turn

SUMMARY

Groups	*Count*	*Sum*	*Average*	*Variance*
129Sv	26	10	0.38461538	1.8461538
C57Bl/6	94	21	0.22340426	1.1431023

ANOVA

Source of Variation	*df*	*SS*	*MS*	*F*	*P-value*
Between Groups	1	0.52930987	0.52930987	0.4096655	0.5233802
Within Groups	118	152.462357	1.29205387		
Total	119	152.991667			

ie the proportions of axons are not significantly different

Axons making a contra-caudal turn

SUMMARY

Groups	*Count*	*Sum*	*Average*	*Variance*
129Sv	26	17.5	0.67307692	3.77884615
C57Bl/6	94	369.5	3.93085106	126.229038

ANOVA

Source of Variation	*df*	*SS*	*MS*	*F*	*P-value*
Between Groups	1	216.153314	216.153314	2.15536447	0.1447333
Within Groups	118	11833.7717	100.286201		
Total	119	12049.925			

ie the proportions of axons are not significantly different

Axons continuing to extend laterally

SUMMARY

Groups	*Count*	*Sum*	*Average*	*Variance*
129Sv	26	16	0.61538462	4.6461538
C57Bl/6	94	184.5	1.96276596	112.70559

ANOVA

Source of Variation	*df*	*SS*	*MS*	*F*	*P-value*
Between Groups	1	36.9743897	36.9743897	0.4116882	0.5223583
Within Groups	118	10597.7735	89.8116401		
Total	119	10634.7479			

ie the proportions of axons are not significantly different

Axons making an ipsi-rostral turn

SUMMARY

Groups	*Count*	*Sum*	*Average*	*Variance*
129Sv	26	17.5	0.67307692	4.77884615
C57Bl/6	94	32.5	0.34574468	2.38723976

ANOVA

Source of Variation	*df*	*SS*	*MS*	*F*	*P-value*
Between Groups	1	2.18221495	2.18221495	0.75406468	0.3869551
Within Groups	118	341.484452	2.89393603		
Total	119	343.666667			

ie the proportions of axons are not significantly different

Axons in/at the floor plate

SUMMARY

Groups	*Count*	*Sum*	*Average*	*Variance*
129Sv	26	940.6	36.1769231	1419.4338
C57Bl/6	94	5207	55.393617	2064.4348

ANOVA

Source of Variation	*df*	*SS*	*MS*	*F*	*P-value*
Between Groups	1	7521.02968	7521.02968	3.90139	0.0505809
Within Groups	118	227478.282	1927.78205		
Total	119	234999.312			

ie the proportions of axons are not significantly different

Appendix 3.A.2 continued

Comparison of 129/SvEv and C57Bl/6 embryos at E13.5

For data, see figure 3.12

Axons making a contra-rostral turn

SUMMARY

Groups	*Count*	*Sum*	*Average*	*Variance*
129Sv	40	1901.6	47.54	1285.85682
C57Bl/6	30	2314.2	77.14	1107.77697

ANOVA

Source of Variation	*df*	*SS*	*MS*	*F*	*P-value*
Between Groups	1	15019.8857	15019.8857	12.4140418	0.0007668
Within Groups	68	82273.948	1209.911		
Total	69	97293.8337			

ie the proportions of axons are significantly different

Axons making a contra-caudal turn

SUMMARY

Groups	*Count*	*Sum*	*Average*	*Variance*
129Sv	40	119.6	2.99	26.8609231
C57Bl/6	30	110	3.66666667	80.9195402

ANOVA

Source of Variation	*df*	*SS*	*MS*	*F*	*P-value*
Between Groups	1	7.84933333	7.84933333	0.15725295	0.6929401
Within Groups	68	3394.24267	49.9153333		
Total	69	3402.092			

ie the proportions of axons are not significantly different

Axons making an ipsi-rostral turn

SUMMARY

Groups	*Count*	*Sum*	*Average*	*Variance*
129Sv	40	3.1	0.0775	0.11717308
C57Bl/6	30	60	2	83.7931034

ANOVA

Source of Variation	*df*	*SS*	*MS*	*F*	*P-value*
Between Groups	1	63.3601071	63.3601071	1.76971199	0.1878621
Within Groups	68	2434.56975	35.8024963		
Total	69	2497.92986			

ie the proportions of axons are not significantly different

Axons making an ipsi-caudal turn

No injection sites of either strain had any labelled axons which made a contra-caudal turn

Axons continuing to extend laterally

SUMMARY

Groups	*Count*	*Sum*	*Average*	*Variance*
129Sv	40	76.8	1.92	24.69241
C57Bl/6	30	38.3	1.27666667	37.413575

ANOVA

Source of Variation	*df*	*SS*	*MS*	*F*	*P-value*
Between Groups	1	7.09504762	7.09504762	0.235578	0.6289785
Within Groups	68	2047.99767	30.1176127		
Total	69	2055.09271			

ie the proportions of axons are not significantly different

Axons in/at the floor plate

SUMMARY

Groups	*Count*	*Sum*	*Average*	*Variance*
129Sv	40	1900.1	47.5025	1472.7438
C57Bl/6	30	477.5	15.9166667	1064.4421

ANOVA

Source of Variation	*df*	*SS*	*MS*	*F*	*P-value*
Between Groups	1	17102.8263	17102.8263	13.17005	0.000546
Within Groups	68	88305.8314	1298.61517		
Total	69	105408.658			

ie the proportions of axons are significantly different

Appendix 3.A.3

Comparison of the projections labelled when DiI was injected at different dorso-ventral positions For data, see figure 3.1.3

Axons making a contra-rostral turn

SUMMARY

Groups	*Count*	*Sum*	*Average*	*Variance*
Dorsal	12	155	12.9166667	874.810606
Dorso-lateral	28	662.3	23.6535714	1043.44554
Lateral	22	1400.6	63.6636364	937.87671

ANOVA

Source of Variation	*df*	*SS*	*MS*	*F*	*P-value*
Between Groups	2	27495.1262	13747.5631	14.1083158	9.82776E-06
Within Groups	59	57491.3572	974.429783		
Total	61	84986.4834			

ie the proportions of axons are significantly different

Comparison of dorsal and dorso-lateral sites only:

ANOVA

Source of Variation	*df*	*SS*	*MS*	*F*	*P-value*
Between Groups	1	968.36144	968.36144	0.97358945	0.330027909
Within Groups	38	37795.9463	994.630166		
Total	39	38764.3078			

ie the proportions of axons are not significantly different

Comparison of dorso-lateral and lateral sites only:

ANOVA

Source of Variation	*df*	*SS*	*MS*	*F*	*P-value*
Between Groups	1	19721.9212	19721.9212	19.7761241	5.14537E-05
Within Groups	48	47868.4406	997.259178		
Total	49	67590.3618			

ie the proportions of axons are significantly different

Axons making a contra-caudal turn

SUMMARY

Groups	*Count*	*Sum*	*Average*	*Variance*
Dorsal	12	0	0	0
Dorso-lateral	28	72	2.57142857	60.2724868
Lateral	22	183.6	8.34545455	125.182597

ANOVA

Source of Variation	*df*	*SS*	*MS*	*F*	*P-value*
Between Groups	2	663.636699	331.818349	4.59971826	0.013919
Within Groups	59	4256.19169	72.1388422		
Total	61	4919.82839			

ie the proportions of axons are significantly different

Comparison of dorsal and dorso-lateral sites only:

ANOVA

Source of Variation	*df*	*SS*	*MS*	*F*	*P-value*
Between Groups	1	55.5428571	55.5428571	1.29696704	0.261897
Within Groups	38	1627.35714	42.825188		
Total	39	1682.9			

ie the proportions of axons are not significantly different

Comparison of dorso-lateral and lateral sites only:

ANOVA

Source of Variation	*df*	*SS*	*MS*	*F*	*P-value*
Between Groups	1	410.741112	410.741112	4.63220992	0.036435
Within Groups	48	4256.19169	88.6706602		
Total	49	4666.9328			

ie the proportions of axons are significantly different

Appendix 3.A.3 continued

Axons in/at the floor plate

SUMMARY

Groups	*Count*	*Sum*	*Average*	*Variance*
Dorsal	12	1015	84.5833333	879.356061
Dorso-lateral	28	1930.5	68.9464286	1522.19443
Lateral	22	481.5	21.8863636	1094.23647

ANOVA

Source of Variation	*df*	*SS*	*MS*	*F*	*P-value*
Between Groups	2	40066.7865	20033.3932	16.0264686	2.76034E-06
Within Groups	59	73751.1322	1250.01919		
Total	61	113817.919			

ie the proportions of axons are significantly different

Comparison of dorsal and dorso-lateral sites only:

ANOVA

Source of Variation	*df*	*SS*	*MS*	*F*	*P-value*
Between Groups	1	2053.90744	2053.90744	1.53722971	0.222632764
Within Groups	38	50772.1663	1336.10964		
Total	39	52826.0738			

ie the proportions of axons are not significantly different

Comparison of dorso-lateral and lateral sites only:

ANOVA

Source of Variation	*df*	*SS*	*MS*	*F*	*P-value*
Between Groups	1	27284.4844	27284.4844	20.4383852	4.03261E-05
Within Groups	48	64078.2156	1334.96282		
Total	49	91362.7			

ie the proportions of axons are significantly different

Axons making an ipsi-rostral turn

SUMMARY

Groups	*Count*	*Sum*	*Average*	*Variance*
Dorsal	12	0	0	0
Dorso-lateral	28	18.6	0.66428571	4.68978836
Lateral	22	29	1.31818182	8.06060606

ANOVA

Source of Variation	*df*	*SS*	*MS*	*F*	*P-value*
Between Groups	2	14.0384709	7.01923544	1.39959132	0.254767
Within Groups	59	295.897013	5.01520361		
Total	61	309.935484			

ie the proportions of axons are not significantly different

Axons making an ipsi-caudal turn

SUMMARY

Groups	*Count*	*Sum*	*Average*	*Variance*
Dorsal	12	0	0	0
Dorso-lateral	28	4.8	0.17142857	0.39693122
Lateral	22	6	0.27272727	1.16017316

ANOVA

Source of Variation	*df*	*SS*	*MS*	*F*	*P-value*
Between Groups	2	0.57793046	0.28896523	0.48599116	0.617528
Within Groups	59	35.0807792	0.59458948		
Total	61	35.6587097			

ie the proportions of axons are not significantly different

Axons continuing to extend laterally

SUMMARY

Groups	*Count*	*Sum*	*Average*	*Variance*
Dorsal	12	30	2.5	75
Dorso-lateral	28	112	4	356.240741
Lateral	22	99.3	4.51363636	109.080281

ANOVA

Source of Variation	*df*	*SS*	*MS*	*F*	*P-value*
Between Groups	2	32.0800587	16.0400293	0.07431663	0.928464
Within Groups	59	12734.1859	215.833659		
Total	61	12766.266			

ie the proportions of axons are not significantly different

Appendix 3.A.4

Comparison of the projections labelled when DiI was injected at different rostro-caudal levels For data, see figure 3.14

Axons making a contra-rostral turn

SUMMARY

Groups	*Count*	*Sum*	*Average*	*Variance*
cervical	59	2154	36.5084746	1841.74562
lumbar	35	1431.5	40.9	1654.40882

ANOVA

Source of Variation	*df*	*SS*	*MS*	*F*	*P-value*
Between Groups	1	423.665408	423.665408	0.23901971	0.6260785
Within Groups	92	163071.146	1772.51245		
Total	93	163494.811			

ie the proportions of axons are not significantly different

Axons making an ipsi-caudal turn

SUMMARY

Groups	*Count*	*Sum*	*Average*	*Variance*
cervical	59	5	0.08474576	0.42372881
lumbar	35	16	0.45714286	2.31428571

ANOVA

Source of Variation	*df*	*SS*	*MS*	*F*	*P-value*
Between Groups	1	3.04652517	3.04652517	2.71426425	0.1028663
Within Groups	92	103.261985	1.12241289		
Total	93	106.308511			

ie the proportions of axons are not significantly different

Axons making a contra-caudal turn

SUMMARY

Groups	*Count*	*Sum*	*Average*	*Variance*
cervical	59	208.5	3.53389831	126.421245
lumbar	35	161	4.6	128.879412

ANOVA

Source of Variation	*df*	*SS*	*MS*	*F*	*P-value*
Between Groups	1	24.9683285	24.9683285	0.19609195	0.6589334
Within Groups	92	11714.3322	127.329698		
Total	93	11739.3005			

ie the proportions of axons are not significantly different

Axons continuing to extend laterally

SUMMARY

Groups	*Count*	*Sum*	*Average*	*Variance*
cervical	59	141.5	2.39830508	172.11879
lumbar	35	43	1.22857143	13.7844538

ANOVA

Source of Variation	*df*	*SS*	*MS*	*F*	*P-value*
Between Groups	1	30.0584218	30.0584218	0.26458964	0.6082179
Within Groups	92	10451.5613	113.603927		
Total	93	10481.6197			

ie the proportions of axons are not significantly different

Axons making an ipsi-rostral turn

SUMMARY

Groups	*Count*	*Sum*	*Average*	*Variance*
cervical	59	10	0.16949153	1.69491525
lumbar	35	22.5	0.64285714	3.49369748

ANOVA

Source of Variation	*df*	*SS*	*MS*	*F*	*P-value*
Between Groups	1	4.92249884	4.92249884	2.08608516	0.1520437
Within Groups	92	217.090799	2.3596826		
Total	93	222.013298			

ie the proportions of axons are not significantly different

Axons in/at the floor plate

SUMMARY

Groups	*Count*	*Sum*	*Average*	*Variance*
cervical	59	3381	57.3050847	2093.52601
lumbar	35	1826	52.1714286	2058.49916

ANOVA

Source of Variation	*df*	*SS*	*MS*	*F*	*P-value*
Between Groups	1	578.956267	578.956267	0.27826659	0.5991095
Within Groups	92	191413.48	2080.5813		
Total	93	191992.436			

ie the proportions of axons are not significantly different

Appendix 3.A.5

Comparison of embryos wild type, heterozygous or homozygous for the *TAGA* (truncation) mutation at E12.5 For data, see figure 3.15

Axons making a contra-rostral turn

SUMMARY

Groups	*Count*	*Sum*	*Average*	*Variance*
Wildtype	94	3585.5	38.143617	1758.00872
Heterozygote	47	2208.5	46.9893617	1711.97358
Homozygote	32	919.7	28.740625	1475.18894

ANOVA

Source of Variation	*df*	*SS*	*MS*	*F*	*P-value*
Between Groups	2	6430.68719	3215.3436	1.89810106	0.1530151
Within Groups	170	287976.453	1693.97914		
Total	172	294407.14			

ie the proportions of axons are not significantly different

Axons making a contra-caudal turn

SUMMARY

Groups	*Count*	*Sum*	*Average*	*Variance*
Wildtype	94	369.5	3.93085106	126.229038
Heterozygote	47	91.4	1.94468085	36.1068733
Homozygote	32	20.7	0.646875	9.08063508

ANOVA

Source of Variation	*df*	*SS*	*MS*	*F*	*P-value*
Between Groups	2	302.898292	151.449146	1.88180738	0.1554736
Within Groups	170	13681.7164	80.4806846		
Total	172	13984.6147			

ie the proportions of axons are not significantly different

Axons making an ipsi-rostral turn

SUMMARY

Groups	*Count*	*Sum*	*Average*	*Variance*
Wildtype	94	32.5	0.34574468	2.38723976
Heterozygote	47	55.6	1.18297872	15.5401388
Homozygote	32	12.5	0.390625	3.26990927

ANOVA

Source of Variation	*df*	*SS*	*MS*	*F*	*P-value*
Between Groups	2	23.3939409	11.6969704	1.91527019	0.1504671
Within Groups	170	1038.22687	6.10721687		
Total	172	1061.62081			

ie the proportions of axons are not significantly different

Axons making an ipsi-caudal turn

SUMMARY

Groups	*Count*	*Sum*	*Average*	*Variance*
Wildtype	94	21	0.22340426	1.14310226
Heterozygote	47	2.1	0.04468085	0.0460037
Homozygote	32	7.5	0.234375	1.7578125

ANOVA

Source of Variation	*df*	*SS*	*MS*	*F*	*P-value*
Between Groups	2	1.1306461	0.56532305	0.58990158	0.5555126
Within Groups	170	162.916868	0.95833452		
Total	172	164.047514			

ie the proportions of axons are not significantly different

Axons continuing to extend laterally

SUMMARY

Groups	*Count*	*Sum*	*Average*	*Variance*
Wildtype	94	184.5	1.96276596	112.705588
Heterozygote	47	49	1.04255319	5.23380204
Homozygote	32	0	0	0

ANOVA

Source of Variation	*df*	*SS*	*MS*	*F*	*P-value*
Between Groups	2	98.0579111	49.0289555	0.77733923	0.461254
Within Groups	170	10722.3746	63.0727916		
Total	172	10820.4325			

ie the proportions of axons are not significantly different

Axons in/at the floor plate

SUMMARY

Groups	*Count*	*Sum*	*Average*	*Variance*
Wildtype	94	5207	55.393617	2064.4348
Heterozygote	47	2293.6	48.8	1942.6487
Homozygote	32	2239.6	69.9875	1539.18435

ANOVA

Source of Variation	*df*	*SS*	*MS*	*F*	*P-value*
Between Groups	2	8716.09831	4358.04915	2.25140738	0.1083805
Within Groups	170	329068.991	1935.69995		
Total	172	337785.089			

ie the proportions of axons are not significantly different

Appendix 3.A.6

Comparison of embryos wild type or homozygous for the *TAGA* (truncation) mutation at E13.5

Axons making a contra-rostral turn

SUMMARY

Groups	*Count*	*Sum*	*Average*	*Variance*
TAG-1A/A	67	3552.5	53.0223881	1418.72813
wild type	40	1901.6	47.54	1285.85682

ANOVA

Source of Variation	*df*	*SS*	*MS*	*F*	*P-value*
Between Groups	1	752.818984	752.818984	0.54975334	0.4600736
Within Groups	105	143784.472	1369.37593		
Total	106	144537.291			

ie the proportions of axons are not significantly different

axons making an ipsi-caudal turn

SUMMARY

Groups	*Count*	*Sum*	*Average*	*Variance*
TAG-1A/A	67	24.7	0.36865672	2.87824514
wild type	40	0	0	0

ANOVA

Source of Variation	*df*	*SS*	*MS*	*F*	*P-value*
Between Groups	1	3.40404519	3.40404519	1.8815376	0.17308343
Within Groups	105	189.964179	1.80918266		
Total	106	193.368224			

ie the proportions of axons are not significantly different

axons making a contra-caudal turn

SUMMARY

Groups	*Count*	*Sum*	*Average*	*Variance*
TAG-1A/A	67	332.6	4.9641791	61.5577883
wild type	40	119.6	2.99	26.8609231

ANOVA

Source of Variation	*df*	*SS*	*MS*	*F*	*P-value*
Between Groups	1	97.6166991	97.6166991	2.0056695	0.1596719
Within Groups	105	5110.39003	48.6703812		
Total	106	5208.00673			

ie the proportions of axons are not significantly different

axons continuing to extend laterally

SUMMARY

Groups	*Count*	*Sum*	*Average*	*Variance*
TAG-1A/A	67	178.1	2.65820896	21.1797422
wild type	40	76.8	1.92	24.6924103

ANOVA

Source of Variation	*df*	*SS*	*MS*	*F*	*P-value*
Between Groups	1	13.6492766	13.6492766	0.60705413	0.43765165
Within Groups	105	2360.86699	22.4844475		
Total	106	2374.51626			

ie the proportions of axons are not significantly different

axons making an ipsi-rostral turn

SUMMARY

Groups	*Count*	*Sum*	*Average*	*Variance*
TAG-1A/A	67	40.2	0.6	5.23090909
wild type	40	3.1	0.0775	0.11717308

ANOVA

Source of Variation	*df*	*SS*	*MS*	*F*	*P-value*
Between Groups	1	6.83791355	6.83791355	2.05248974	0.1549281
Within Groups	105	349.80975	3.33152143		
Total	106	356.647664			

ie the proportions of axons are not significantly different

axons in/at the floor plate

SUMMARY

Groups	*Count*	*Sum*	*Average*	*Variance*
TAG-1A/A	67	2574.2	38.4208955	1699.11895
wild type	40	1900.1	47.5025	1472.74384

ANOVA

Source of Variation	*df*	*SS*	*MS*	*F*	*P-value*
Between Groups	1	2065.74249	2065.74249	1.2790684	0.26064891
Within Groups	105	169578.86	1615.03677		
Total	106	171644.603			

ie the proportions of axons are not significantly different

Appendix 3.A.7

Comparison of embryos wild type, heterozygous or homozygous for the *TAG-1* null mutation For data, see figure 3.16

Axons making a contra-rostral turn

SUMMARY

Groups	*Count*	*Sum*	*Average*	*Variance*
Wildtype	11	410.9	37.3545455	1112.92673
Heterozygote	23	837.6	36.4173913	1459.90514
Homozygote	25	769.6	30.784	1156.6389

ANOVA

Source of Variation	*df*	*SS*	*MS*	*F*	*P-value*
Between Groups	2	514.274558	257.137279	0.2027939	0.81704342
Within Groups	56	71006.5139	1267.97346		
Total	58	71520.7885			

ie the proportions of axons are not significantly different

Axons making an ipsi-caudal turn

SUMMARY

Groups	*Count*	*Sum*	*Average*	*Variance*
Wildtype	11	14.8	1.34545455	9.47272727
Heterozygote	23	1.9	0.0826087	0.15695652
Homozygote	25	11.6	0.464	4.04906667

ANOVA

Source of Variation	*df*	*SS*	*MS*	*F*	*P-value*
Between Groups	2	11.877677	5.93883851	1.70238792	0.19154315
Within Groups	56	195.357916	3.48853422		
Total	58	207.235593			

ie the proportions of axons are not significantly different

Axons making a contra-caudal turn

SUMMARY

Groups	*Count*	*Sum*	*Average*	*Variance*
Wildtype	11	38.1	3.46363636	29.6165455
Heterozygote	23	15.7	0.6826087	2.00513834
Homozygote	25	51.4	2.056	20.7184

ANOVA

Source of Variation	*df*	*SS*	*MS*	*F*	*P-value*
Between Groups	2	60.7829528	30.3914764	2.03209772	0.14061322
Within Groups	56	837.520098	14.955716		
Total	58	898.303051			

ie the proportions of axons are not significantly different

Axons continuing to extend laterally

SUMMARY

Groups	*Count*	*Sum*	*Average*	*Variance*
Wildtype	11	10.8	0.98181818	4.34163636
Heterozygote	23	14.2	0.6173913	4.37150198
Homozygote	25	26.4	1.056	6.30923333

ANOVA

Source of Variation	*df*	*SS*	*MS*	*F*	*P-value*
Between Groups	2	2.47000983	1.23500492	0.23765519	0.78926568
Within Groups	56	291.011007	5.19662513		
Total	58	293.481017			

ie the proportions of axons are not significantly different

Axons making an ipsi-rostral turn

SUMMARY

Groups	*Count*	*Sum*	*Average*	*Variance*
Wildtype	11	19.8	1.8	17.142
Heterozygote	23	9.2	0.4	3.68
Homozygote	25	46.3	1.852	13.6517667

ANOVA

Source of Variation	*df*	*SS*	*MS*	*F*	*P-value*
Between Groups	2	28.9643797	14.4821898	1.3982264	0.2555249
Within Groups	56	580.0224	10.3575429		
Total	58	608.98678			

ie the proportions of axons are not significantly different

Axons in/at the floor plate

SUMMARY

Groups	*Count*	*Sum*	*Average*	*Variance*
Wildtype	11	606	55.0909091	1406.65491
Heterozygote	23	1421.5	61.8043478	1532.79043
Homozygote	25	1594.7	63.788	1580.07693

ANOVA

Source of Variation	*df*	*SS*	*MS*	*F*	*P-value*
Between Groups	2	584.172232	292.086116	0.19083962	0.8268002
Within Groups	56	85709.7851	1530.53188		
Total	58	86293.9573			

ie the proportions of axons are not significantly different

Appendix 3.A.8
Comparison of embryos wild type, heterozygous or hemizygous for the *L1* null mutation For data, see figure 3.17

Axons making a contra-rostral turn

SUMMARY

Groups	*Count*	*Sum*	*Average*	*Variance*
Wild-type (+/+ or +/Y)	94	5207	55.393617	2064.4348
Heterozygote (+/-)	21	1196.5	56.9761905	2201.0119
L1 hemizygote (-/Y)	15	731	48.7333333	2110.78095

ANOVA

Source of Variation	*df*	*SS*	*MS*	*F*	*P-value*
Between Groups	2	683.794324	341.897162	0.16350486	0.84934084
Within Groups	127	265563.608	2091.05203		
Total	129	266247.402			

ie the proportions of axons are not significantly different

Axons making an ipsi-caudal turn

SUMMARY

Groups	*Count*	*Sum*	*Average*	*Variance*
Wild-type (+/+ or +/Y)	94	21	0.22340426	1.14310226
Heterozygote (+/-)	21	0	0	0
L1 hemizygote (-/Y)	15	10	0.66666667	4.38095238

ANOVA

Source of Variation	*df*	*SS*	*MS*	*F*	*P-value*
Between Groups	2	3.96584834	1.98292417	1.50219876	0.22656903
Within Groups	127	167.641844	1.32001452		
Total	129	171.607692			

ie the proportions of axons are not significantly different

Axons making a contra-caudal turn

SUMMARY

Groups	*Count*	*Sum*	*Average*	*Variance*
Wild-type (+/+ or +/Y)	94	369.5	3.93085106	126.229038
Heterozygote (+/-)	21	146	6.95238095	176.147619
L1 hemizygote (-/Y)	15	45	3	135

ANOVA

Source of Variation	*df*	*SS*	*MS*	*F*	*P-value*
Between Groups	2	185.879779	92.9398897	0.68815252	0.50436732
Within Groups	127	17152.2529	135.05711		
Total	129	17338.1327			

ie the proportions of axons are not significantly different

Axons continuing to extend laterally

SUMMARY

Groups	*Count*	*Sum*	*Average*	*Variance*
Wild-type (+/+ or +/Y)	94	184.5	1.96276596	112.705588
Heterozygote (+/-)	21	10	0.47619048	1.63690476
L1 hemizygote (-/Y)	15	27	1.8	9.31428571

ANOVA

Source of Variation	*df*	*SS*	*MS*	*F*	*P-value*
Between Groups	2	38.0903008	19.0451504	0.22722303	0.79706627
Within Groups	127	10644.7578	83.8169904		
Total	129	10682.8481			

ie the proportions of axons are not significantly different

Axons making an ipsi-rostral turn

SUMMARY

Groups	*Count*	*Sum*	*Average*	*Variance*
Wild-type (+/+ or +/Y)	94	32.5	0.34574468	2.38723976
Heterozygote (+/-)	21	29.5	1.4047619	10.9404762
L1 hemizygote (-/Y)	15	2	0.13333333	0.26666667

ANOVA

Source of Variation	*df*	*SS*	*MS*	*F*	*P-value*
Between Groups	2	21.4361527	10.7180763	3.0619207	0.05026786
Within Groups	127	444.556155	3.50044217		
Total	129	465.992308			

ie the proportions of axons are not significantly different

Axons in/at the floor plate

SUMMARY

Groups	*Count*	*Sum*	*Average*	*Variance*
Wild-type (+/+ or +/Y)	94	5207	55.393617	2064.4348
Heterozygote (+/-)	21	1196.5	56.9761905	2201.0119
L1 hemizygote (-/Y)	15	731	48.7333333	2110.78095

ANOVA

Source of Variation	*df*	*SS*	*MS*	*F*	*P-value*
Between Groups	2	683.794324	341.897162	0.16350486	0.84934084
Within Groups	127	265563.608	2091.05203		
Total	129	266247.402			

ie the proportions of axons are not significantly different

Appendix 3.A.9

Comparison of embryos wild type, heterozygous or homozygous for the *NrCAM* null mutation **For data, see figure 3.18**

Axons making a contra-rostral turn

SUMMARY

Groups	*Count*	*Sum*	*Average*	*Variance*
Wildtype	94	3585.5	38.143617	1758.00872
Heterozygote	75	2607.1	34.7613333	1469.7397
Homozygote	57	1663.7	29.1877193	1147.50431

ANOVA

Source of Variation	*df*	*SS*	*MS*	*F*	*P-value*
Between Groups	2	2846.05987	1423.02993	0.94300382	0.39100362
Within Groups	223	336515.79	1509.03942		
Total	225	339361.85			

ie the proportions of axons are not significantly different

Axons making a contra-caudal turn

SUMMARY

Groups	*Count*	*Sum*	*Average*	*Variance*
Wildtype	94	369.5	3.93085106	126.229038
Heterozygote	75	99.5	1.32666667	14.7263063
Homozygote	57	62.6	1.09824561	13.9055326

ANOVA

Source of Variation	*df*	*SS*	*MS*	*F*	*P-value*
Between Groups	2	402.766871	201.383435	3.30021369	0.03868451
Within Groups	223	13607.757	61.0213319		
Total	225	14010.5239			

ie the proportions of axons are significantly different

Axons making an ipsi-rostral turn

SUMMARY

Groups	*Count*	*Sum*	*Average*	*Variance*
Wildtype	94	32.5	0.34574468	2.38723976
Heterozygote	75	54	0.72	7.71783784
Homozygote	57	77.5	1.35964912	34.1763784

ANOVA

Source of Variation	*df*	*SS*	*MS*	*F*	*P-value*
Between Groups	2	36.4806596	18.2403298	1.50261462	0.22479199
Within Groups	223	2707.01049	12.1390605		
Total	225	2743.49115			

ie the proportions of axons are not significantly different

Axons making an ipsi-caudal turn

SUMMARY

Groups	*Count*	*Sum*	*Average*	*Variance*
Wildtype	94	21	0.22340426	1.14310226
Heterozygote	75	6	0.08	0.34486486
Homozygote	57	12	0.21052632	0.91917293

ANOVA

Source of Variation	*df*	*SS*	*MS*	*F*	*P-value*
Between Groups	2	0.96771666	0.48385833	0.58864765	0.55593758
Within Groups	223	183.302195	0.82198294		
Total	225	184.269912			

ie the proportions of axons are not significantly different

Axons continuing to extend laterally

SUMMARY

Groups	*Count*	*Sum*	*Average*	*Variance*
Wildtype	94	184.5	1.96276596	112.705588
Heterozygote	75	19.1	0.25466667	0.95872793
Homozygote	57	49.2	0.86315789	5.93701128

ANOVA

Source of Variation	*df*	*SS*	*MS*	*F*	*P-value*
Between Groups	2	126.683768	63.3418839	1.29767483	0.27522082
Within Groups	223	10885.0382	48.8118304		
Total	225	11011.7219			

ie the proportions of axons are not significantly different

Axons in/at the floor plate

SUMMARY

Groups	*Count*	*Sum*	*Average*	*Variance*
Wildtype	94	5207	55.393617	2064.4348
Heterozygote	75	4714.3	62.8573333	1622.12329
Homozygote	57	3836	67.2982456	1378.44268

ANOVA

Source of Variation	*df*	*SS*	*MS*	*F*	*P-value*
Between Groups	2	5470.71589	2735.35795	1.56718858	0.21091989
Within Groups	223	389222.349	1745.3917		
Total	225	394693.065			

ie the proportions of axons are not significantly different

Appendix 3.A.10

Comparison of TAGA/L1 double mutant embryos with those wild type for both genes: E12.5 For data, see figure 3.19

Axons making a contra-rostral turn

SUMMARY

Groups	*Count*	*Sum*	*Average*	*Variance*
L1-/Y TAG-1A/A	19	329.5	17.3421053	524.771462
wild type	94	3585.5	38.143617	1758.00872

ANOVA

Source of Variation	*df*	*SS*	*MS*	*F*	*P-value*
Between Groups	1	6839.00322	6839.00322	4.38953565	0.0384347
Within Groups	111	172940.697	1558.0243		
Total	112	179779.701			

ie the proportions of axons are significantly different

axons making a contra-caudal turn

SUMMARY

Groups	*Count*	*Sum*	*Average*	*Variance*
L1-/Y TAG-1A/A	19	42.5	2.23684211	17.9824561
wild type	94	369.5	3.93085106	126.229038

ANOVA

Source of Variation	*df*	*SS*	*MS*	*F*	*P-value*
Between Groups	1	45.3559655	45.3559655	0.41735211	0.51959464
Within Groups	111	12062.9847	108.675538		
Total	112	12108.3407			

ie the proportions of axons are not significantly different

axons making an ipsi-rostral turn

SUMMARY

Groups	*Count*	*Sum*	*Average*	*Variance*
L1-/Y TAG-1A/A	19	5.9	0.31052632	1.03877193
wild type	94	32.5	0.34574468	2.38723976

ANOVA

Source of Variation	*df*	*SS*	*MS*	*F*	*P-value*
Between Groups	1	0.01960385	0.01960385	0.00903999	0.92442361
Within Groups	111	240.711193	2.1685693		
Total	112	240.730796			

ie the proportions of axons are not significantly different

axons making an ipsi-caudal turn

SUMMARY

Groups	*Count*	*Sum*	*Average*	*Variance*
L1-/Y TAG-1A/A	19	4	0.21052632	0.84210526
wild type	94	21	0.22340426	1.14310226

ANOVA

Source of Variation	*df*	*SS*	*MS*	*F*	*P-value*
Between Groups	1	0.00262117	0.00262117	0.00239531	0.96105351
Within Groups	111	121.466405	1.09429194		
Total	112	121.469027			

ie the proportions of axons are not significantly different

axons continuing to extend laterally

SUMMARY

Groups	*Count*	*Sum*	*Average*	*Variance*
L1-/Y TAG-1A/A	19	61.8	3.25263158	27.4448538
wild type	94	184.5	1.96276596	112.705588

ANOVA

Source of Variation	*df*	*SS*	*MS*	*F*	*P-value*
Between Groups	1	26.2961366	26.2961366	0.26594118	0.6070932
Within Groups	111	10975.627	98.879523		
Total	112	11001.9232			

ie the proportions of axons are not significantly different

axons in/at the floor plate

SUMMARY

Groups	*Count*	*Sum*	*Average*	*Variance*
L1-/Y TAG-1A/A	19	1459.3	76.8052632	725.932749
wild type	94	5207	55.393617	2064.4348

ANOVA

Source of Variation	*df*	*SS*	*MS*	*F*	*P-value*
Between Groups	1	7246.08002	7246.08002	3.92235404	0.05012209
Within Groups	111	205059.226	1847.38041		
Total	112	212305.306			

ie the proportions of axons are not significantly different

Appendix 3.A.11

Comparison of TAGA/L1 double mutant embryos with those wild type for both genes: E11.5 For data, see figure 3.20

Axons making a contra-rostral turn

SUMMARY

Groups	*Count*	*Sum*	*Average*	*Variance*
L1-/Y TAG-1A/A	37	556.1	15.0297297	624.73548
wild type	44	754.2	17.1409091	812.171311

ANOVA

Source of Variation	*df*	*SS*	*MS*	*F*	*P-value*
Between Groups	1	89.5817712	89.5817712	0.12326226	0.72645747
Within Groups	79	57413.8437	726.757515		
Total	80	57503.4254			

ie the proportions of axons are not significantly different

axons making an ipsi-caudal turn

SUMMARY

Groups	*Count*	*Sum*	*Average*	*Variance*
L1-/Y TAG-1A/A	37	2.7	0.07297297	0.19702703
wild type	44	0	0	0

ANOVA

Source of Variation	*df*	*SS*	*MS*	*F*	*P-value*
Between Groups	1	0.10702703	0.10702703	1.1920439	0.27823623
Within Groups	79	7.09297297	0.08978447		
Total	80	7.2			

ie the proportions of axons are not significantly different

axons making a contra-caudal turn

SUMMARY

Groups	*Count*	*Sum*	*Average*	*Variance*
L1-/Y TAG-1A/A	37	2.9	0.07837838	0.2272973
wild type	44	0	0	0

ANOVA

Source of Variation	*df*	*SS*	*MS*	*F*	*P-value*
Between Groups	1	0.12347014	0.12347014	1.1920439	0.27823623
Within Groups	79	8.1827027	0.10357852		
Total	80	8.30617284			

ie the proportions of axons are not significantly different

axons continuing to extend laterally

SUMMARY

Groups	*Count*	*Sum*	*Average*	*Variance*
L1-/Y TAG-1A/A	37	66	1.78378378	38.1402853
wild type	44	78.9	1.79318182	31.6969292

ANOVA

Source of Variation	*df*	*SS*	*MS*	*F*	*P-value*
Between Groups	1	0.00177518	0.00177518	5.13E-05	0.99430573
Within Groups	79	2736.01822	34.6331421		
Total	80	2736.02			

ie the proportions of axons are not significantly different

axons making an ipsi-rostral turn

SUMMARY

Groups	*Count*	*Sum*	*Average*	*Variance*
L1-/Y TAG-1A/A	37	5	0.13513514	0.67567568
wild type	44	15.4	0.35	1.88162791

ANOVA

Source of Variation	*df*	*SS*	*MS*	*F*	*P-value*
Between Groups	1	0.9278979	0.9278979	0.69657818	0.40645267
Within Groups	79	105.234324	1.33208005		
Total	80	106.162222			

ie the proportions of axons are not significantly different

axons in/at the floor plate

SUMMARY

Groups	*Count*	*Sum*	*Average*	*Variance*
L1-/Y TAG-1A/A	37	3068	82.9189189	666.57991
wild type	43	3553.6	82.6418605	847.272968

ANOVA

Source of Variation	*df*	*SS*	*MS*	*F*	*P-value*
Between Groups	1	1.52659208	1.52659208	0.00199848	0.9644572
Within Groups	78	59582.3414	763.876172		
Total	79	59583.868			

ie the proportions of axons are not significantly different

Appendix 3.A.12

Comparison of *TAG/L1* double mutant embryos with those wild type for both genes: E13.5 For data, see figure 3.21

Axons making a contra-rostral turn

SUMMARY

Groups	*Count*	*Sum*	*Average*	*Variance*
L1-/Y TAG-1D/D	30	2088.7	69.6233333	542.60392
wild type	40	1901.6	47.54	1285.85682

ANOVA

Source of Variation	*df*	*SS*	*MS*	*F*	*P-value*
Between Groups	1	8360.11905	8360.11905	8.62863066	0.00451391
Within Groups	68	65883.9297	968.881319		
Total	69	74244.0487			

ie the proportions of axons are significantly different

axons making an ipsi-caudal turn

SUMMARY

Groups	*Count*	*Sum*	*Average*	*Variance*
L1-/Y TAG-1D/D	30	4.8	0.16	0.27213793
wild type	40	0	0	0

ANOVA

Source of Variation	*df*	*SS*	*MS*	*F*	*P-value*
Between Groups	1	0.43885714	0.43885714	3.78133372	0.05596483
Within Groups	68	7.892	0.11605882		
Total	69	8.33085714			

ie the proportions of axons are not significantly different

axons making a contra-caudal turn

SUMMARY

Groups	*Count*	*Sum*	*Average*	*Variance*
L1-/Y TAG-1D/D	30	313.8	10.46	129.844552
wild type	40	119.6	2.99	26.8609231

ANOVA

Source of Variation	*df*	*SS*	*MS*	*F*	*P-value*
Between Groups	1	956.586857	956.586857	13.514853	0.00046828
Within Groups	68	4813.068	70.7804118		
Total	69	5769.65486			

ie the proportions of axons are significantly different

axons continuing to extend laterally

SUMMARY

Groups	*Count*	*Sum*	*Average*	*Variance*
L1-/Y TAG-1D/D	30	210.5	7.01666667	35.6724713
wild type	40	76.8	1.92	24.6924103

ANOVA

Source of Variation	*df*	*SS*	*MS*	*F*	*P-value*
Between Groups	1	445.303048	445.303048	15.1592097	0.00022783
Within Groups	68	1997.50567	29.3750833		
Total	69	2442.80871			

ie the proportions of axons are significantly different

axons making an ipsi-rostral turn

SUMMARY

Groups	*Count*	*Sum*	*Average*	*Variance*
L1-/Y TAG-1D/D	30	17	0.56666667	1.99954023
wild type	40	3.1	0.0775	0.11717308

ANOVA

Source of Variation	*df*	*SS*	*MS*	*F*	*P-value*
Between Groups	1	4.1020119	4.1020119	4.45896399	0.03839602
Within Groups	68	62.5564167	0.9199473		
Total	69	66.6584286			

ie the proportions of axons are significantly different

axons in/at the floor plate

SUMMARY

Groups	*Count*	*Sum*	*Average*	*Variance*
L1-/Y TAG-1D/D	30	368.7	12.29	633.26369
wild type	40	1900.1	47.5025	1472.74384

ANOVA

Source of Variation	*df*	*SS*	*MS*	*F*	*P-value*
Between Groups	1	21255.7741	21255.7741	19.0680877	4.41E-05
Within Groups	68	75801.6568	1114.73025		
Total	69	97057.4309			

ie the proportions of axons are significantly different

Appendix 3.A.13
Comaprison of *TAG-1/L1* double mutant embryos at different ages

Axons making a contra-rostral turn

SUMMARY

Groups	*Count*	*Sum*	*Average*	*Variance*
E11.5	37	556.1	15.0297297	624.73548
E12.5	19	329.5	17.3421053	524.771462
E13.5	30	2088.7	69.6233333	542.60392

ANOVA

Source of Variation	*df*	*SS*	*MS*	*F*	*P-value*
Between Groups	2	56628.6931	28314.3465	49.2972146	7.7444E-15
Within Groups	83	47671.8773	574.359967		
Total	85	104300.57			

ie the proportions of axons are significantly different

E11.5 vs E12.5

ANOVA

Source of Variation	*SS*	*df*	*MS*	*F*	*P-value*
Between Groups	67.1249583	1	67.1249583	0.11349908	0.737501
Within Groups	31936.3636	54	591.414141		
Total	32003.4886	55			

ie the proportions of axons are not significantly different

E12.5 vs E13.5

ANOVA

Source of Variation	*SS*	*df*	*MS*	*F*	*P-value*
Between Groups	31795.8425	1	31795.8425	59.3455724	7.0774E-10
Within Groups	25181.4	47	535.774468		
Total	56977.2424	48			

ie the proportions of axons are significantly different

axons making an ipsi-rostral turn

SUMMARY

Groups	*Count*	*Sum*	*Average*	*Variance*
E11.5	37	5	0.13513514	0.67567568
E12.5	19	5.9	0.31052632	1.03877193
E13.5	30	17	0.56666667	1.99954023

ANOVA

Source of Variation	*df*	*SS*	*MS*	*F*	*P-value*
Between Groups	2	3.0898352	1.5449176	1.26947407	0.2863774
Within Groups	83	101.008886	1.21697453		
Total	85	104.098721			

ie the proportions of axons are not significantly different

axons continuing to extend laterally

SUMMARY

Groups	*Count*	*Sum*	*Average*	*Variance*
E11.5	37	66	1.78378378	38.1402853
E12.5	19	61.8	3.25263158	27.4448538
E13.5	30	210.5	7.01666667	35.6724713

ANOVA

Source of Variation	*df*	*SS*	*MS*	*F*	*P-value*
Between Groups	2	464.972904	232.486452	6.65034676	0.0020947
Within Groups	83	2901.55931	34.9585458		
Total	85	3366.53221			

ie the proportions of axons are significantly different

E11.5 vs E12.5

ANOVA

Source of Variation	*SS*	*df*	*MS*	*F*	*P-value*
Between Groups	27.0845042	1	27.0845042	0.78335194	0.3800421
Within Groups	1867.05764	54	34.5751415		
Total	1894.14214	55			

ie the proportions of axons are not significantly different

E12.5 vs E13.5

ANOVA

Source of Variation	*SS*	*df*	*MS*	*F*	*P-value*
Between Groups	164.810965	1	164.810965	5.06775896	0.0290908
Within Groups	1528.50904	47	32.5214688		
Total	1693.32	48			

ie the proportions of axons are significantly different

axons making a contra-caudal turn

SUMMARY

Groups	*Count*	*Sum*	*Average*	*Variance*
E11.5	37	2.9	0.07837838	0.2272973
E12.5	19	42.5	2.23684211	17.9824561
E13.5	30	313.8	10.46	129.844552

ANOVA

Source of Variation	*df*	*SS*	*MS*	*F*	*P-value*
Between Groups	2	1877.35458	938.677288	19.0147401	1.5913E-07
Within Groups	83	4097.35891	49.36577		
Total	85	5974.71349			

ie the proportions of axons are significantly different

E11.5 vs E12.5

ANOVA

Source of Variation	*SS*	*df*	*MS*	*F*	*P-value*
Between Groups	58.4866582	1	58.4866582	9.51670509	0.00320745
Within Groups	331.866913	54	6.14568358		
Total	390.353571	55			

ie the proportions of axons are significantly different

E12.5 vs E13.5

ANOVA

Source of Variation	*SS*	*df*	*MS*	*F*	*P-value*
Between Groups	786.603789	1	786.603789	9.04103326	0.00422892
Within Groups	4089.17621	47	87.0037492		
Total	4875.78	48			

ie the proportions of axons are significantly different

axons making an ipsi-caudal turn

SUMMARY

Groups	*Count*	*Sum*	*Average*	*Variance*
E11.5	37	2.7	0.07297297	0.19702703
E12.5	19	4	0.21052632	0.84210526
E13.5	30	4.8	0.16	0.27213793

ANOVA

Source of Variation	*df*	*SS*	*MS*	*F*	*P-value*
Between Groups	2	0.26934159	0.1346708	0.37082325	0.6913035
Within Groups	83	30.1428677	0.36316708		
Total	85	30.4122093			

ie the proportions of axons are not significantly different

axons in/at the floor plate

SUMMARY

Groups	*Count*	*Sum*	*Average*	*Variance*
E11.5	37	3068	82.9189189	666.57991
E12.5	19	1459.3	76.8052632	725.932749
E13.5	30	368.7	12.29	633.26369

ANOVA

Source of Variation	*df*	*SS*	*MS*	*F*	*P-value*
Between Groups	2	92278.0682	46139.0341	69.0899579	2.162E-18
Within Groups	83	55428.3132	667.811003		
Total	85	147706.381			

ie the proportions of axons are significantly different

E11.5 vs E12.5

ANOVA

Source of Variation	*SS*	*df*	*MS*	*F*	*P-value*
Between Groups	469.212162	1	469.212162	0.68361982	0.41198167
Within Groups	37063.6662	54	686.364189		
Total	37532.8784	55			

ie the proportions of axons are not significantly different

E12.5 vs E13.5

ANOVA

Source of Variation	*SS*	*df*	*MS*	*F*	*P-value*
Between Groups	48417.6517	1	48417.6517	72.3997973	4.481E-11
Within Groups	31431.4365	47	668.753968		
Total	79849.0882	48			

ie the proportions of axons are significantly different

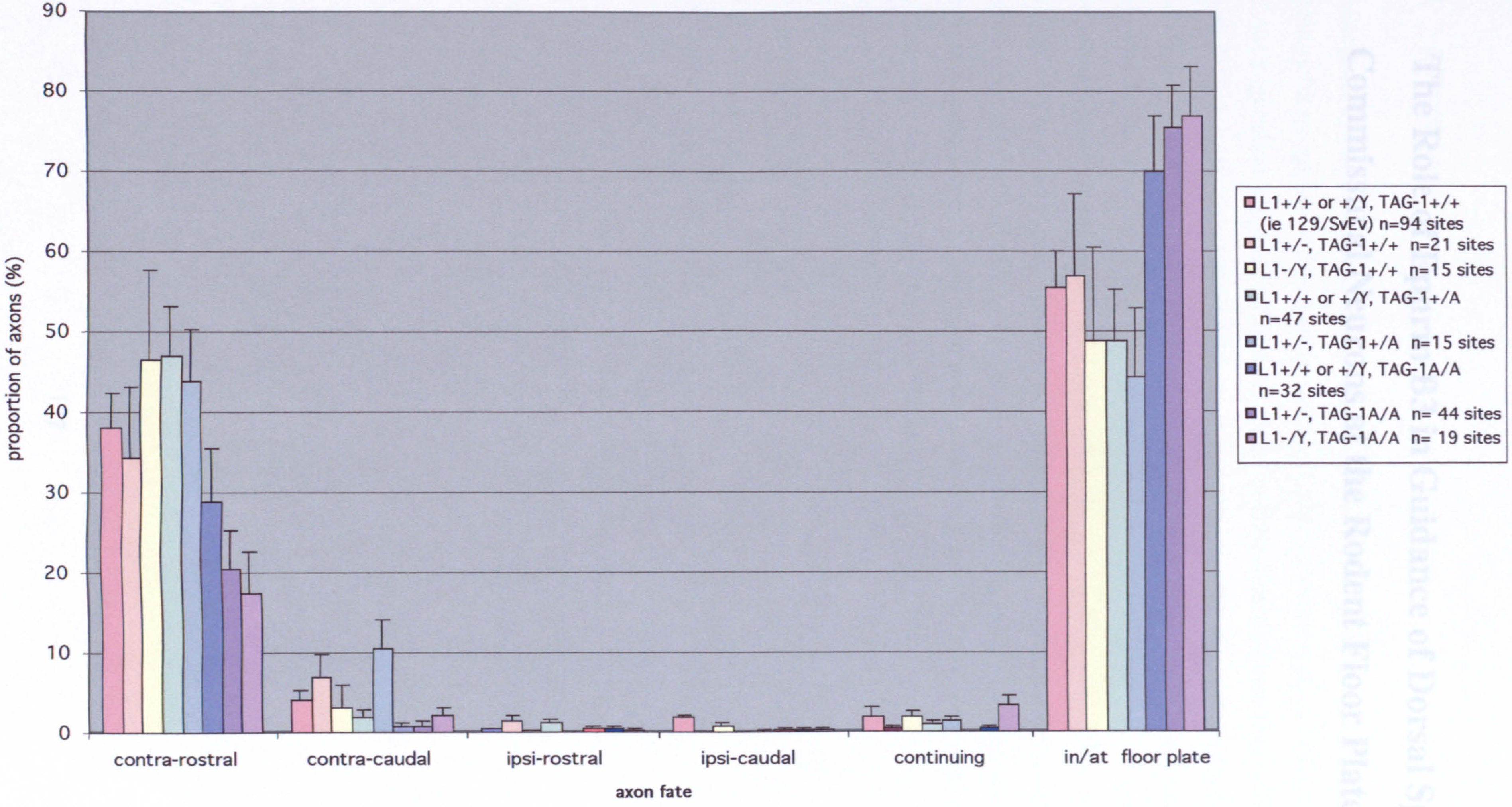

Appendix 3.B Mean proportions of axons within each category in E12.5 *L1/ TAG*^{A} double mutant embryos
Bars show standard errors. For details of the crosses used to generate these embryos, see methods.

4 The Role of Ephrin B3 in Guidance of Dorsal Spinal Commissural Neurons at the Rodent Floor Plate

4.1 Abstract

As discussed in the previous chapter, it is thought that the floor plate is inherently inhibitory for the growth of dorsal spinal axons, and that molecules such as TAG-1 and NrCAM might allow commissural axons to ignore midline negative cues. One molecule that could contribute to a midline inhibitory activity is ephrin B3. DiI was used to label the dorsal spinal projections of mouse embryos homozygous for a mutation in the *ephrin B3* gene. At E12.5, homozygotes had a greater proportion of their axons in or at the floor plate, and a smaller proportion turning contra-rostrally, than heterozygotes. This implies that ephrin B3 normally forces axons to extend out of the floor plate and into the contra-lateral spinal cord. At E13.5, the dorsal spinal projections of homozygotes are statistically indistinguishable from those of heterozygotes, indicating that the lack of ephrin B3 is overcome once the floor plate begins to express ephrins B1 and B2.

4.2 Introduction

Eph receptors are cell surface tyrosine kinases, so named after the erythropoietin-producing hepatocellular carcinoma cell line, from which the first family member was isolated. There are now known to be at least fourteen vertebrate Eph receptors, classified as either EphA or EphB receptors according to their sequence homology and which class of ligands they prefer to bind (figure 4.1). The ligands, referred to as ephrins (for "Eph receptor interacting"), are either attached to the cell membrane by a glycosylphosphatidyl-inositol (GPI) anchor (A-ephrins) or by a trans-membrane domain (B-ephrins) (Drescher, 1997; Eph Nomenclature Committee, 1997; Holland *et al.*, 1998). Figure 4.1 summarises the different classes of ephrins and Eph receptors, demonstrates ligand-receptor interactions, and includes names by which each protein has previously been known (using Gale *et al.*, 1996b; Drescher, 1997; Eph Nomenclature Committee, 1997). Despite this classification, it should be noted that at least one Eph A receptor is able to interact with ligands of the B ephrin class (Gale *et al.*, 1996b), and that ephrins can also act as *receptors* for the Eph proteins. For example, treatment of B-ephrin expressing cells with soluble, aggregated EphB2 leads to phosphorylation of the B-ephrins (Holland *et al.*, 1996; Brückner *et al.*, 1997), and soluble Eph B extracellular domains can cause collapse of retinal axon growth cones (Birgbauer *et al.*, 2001). Mutations in EphB2 have non-cell autonomous effects (Henkemeyer *et al.*, 1996), and at least one B-ephrin can interact with adaptor proteins that might mediate cell autonomous effects upon signalling complexes and the cytoskeleton (Brückner *et al.*, 1999; Cowan and Henkemeyer, 2001). Thus Eph/ephrin signalling is in fact thought to be bi-directional (Brückner and Klein, 1998; Holland *et al.*, 1998).

Eph receptors and their ligands have been implicated in a number of aspects of development (reviewed by Flanagan and Vanderhaeghen, 1998; Frisén *et al.*, 1999; Holder and Klein, 1999; O'Leary and Wilkinson, 1999). Ephrin B2 appears to have a role in the formation of arteries and veins, and possibly also in establishing differences between these vessel types (Wang *et al.*, 1998). Eph B2 and Eph B3 seem to mediate fusion of the palatal shelves during craniofacial development (Orioli *et al.*, 1996). EphB2 may also be involved

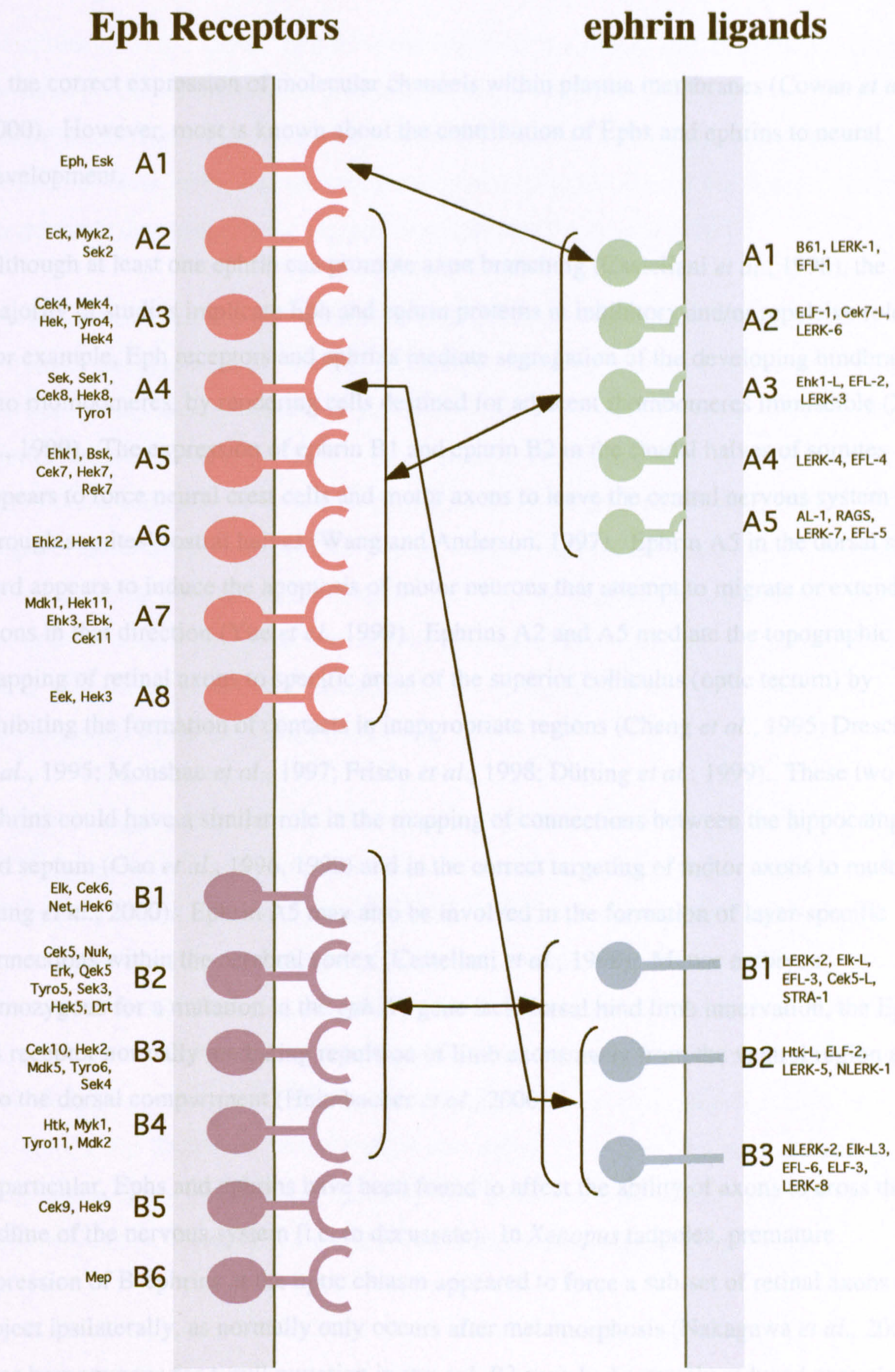

Figure 4.1 Eph receptors, ephrin ligands and their interactions. Ligands of the ephrin A subclass are attached to the cell membrane by a GPI anchor; ligands of the B subclass have trans-membrane domains. The Eph receptors are classified as either A or B on the basis of extracellular domain sequence and the subclass of ephrin ligand with which they preferentially interact. Arrows indicate the interactions between proteins or between members of the bracketed groups of proteins (using Gale *et al.*, 1996 b; Drescher, 1997). Names by which the proteins have previously been known are also given (Eph Nomenclature Committee, 1997).

in the correct expression of molecular channels within plasma membranes (Cowan *et al.*, 2000). However, most is known about the contribution of Ephs and ephrins to neural development.

Although at least one ephrin can promote axon branching (Castellani *et al.*, 1998), the majority of studies implicate Eph and ephrin proteins in inhibitory and/or repulsive roles. For example, Eph receptors and ephrins mediate segregation of the developing hindbrain into rhombomeres, by rendering cells destined for adjacent rhombomeres immiscible (Xu *et al.*, 1999). The expression of ephrin B1 and ephrin B2 in the caudal halves of somites appears to force neural crest cells and motor axons to leave the central nervous system only through somites' rostral halves (Wang and Anderson, 1997). Ephrin A5 in the dorsal spinal cord appears to induce the apoptosis of motor neurons that attempt to migrate or extend axons in that direction (Yue *et al.*, 1999). Ephrins A2 and A5 mediate the topographic mapping of retinal axons to specific areas of the superior colliculus (optic tectum) by inhibiting the formation of contacts in inappropriate regions (Cheng *et al.*, 1995; Drescher *et al.*, 1995; Monshau *et al.*, 1997; Frisén *et al.*, 1998; Dütting *et al.*, 1999). These two ephrins could have a similar role in the mapping of connections between the hippocampus and septum (Gao *et al.*, 1996, 1999) and in the correct targeting of motor axons to muscles (Feng *et al.*, 2000). Ephrin A5 may also be involved in the formation of layer-specific connections within the cerebral cortex (Castellani *et al.*, 1998). Mouse embryos homozygous for a mutation in the *eph A4* gene lack dorsal hind limb innervation, the Eph A4 receptor normally mediating repulsion of limb axons away from the ventral region and into the dorsal compartment (Helmbacher *et al.*, 2000).

In particular, Ephs and ephrins have been found to affect the ability of axons to cross the midline of the nervous system (i.e. to decussate). In *Xenopus* tadpoles, premature expression of B-ephrins at the optic chiasm appeared to force a sub-set of retinal axons to project ipsilaterally, as normally only occurs after metamorphosis (Nakagawa *et al.*, 2000). Mice homozygous for a null mutation in the *eph B2* gene had a greatly reduced posterior part to their anterior commissure, a tract that links the two cerebral hemispheres

(Henkemeyer *et al.*, 1996). Eph B3 is thought to have a similar role in development of the posterior portion of the anterior commissure, as the failure of axons to decussate was exacerbated in mice with mutations in both *eph B3* and *eph B2* (Orioli *et al.*, 1996). The products of these genes also seemed to co-operate in decussation of the corpus callosum, another tract that connects the cerebral hemispheres (Orioli *et al.*, 1996).

Eph B2 mutant mice also showed a temporary inability of inner ear efferent axons to decussate: axons entered the midline, but seemed reluctant to leave it (Cowan *et al.*, 2000). Eph A8 appears to be necessary for the decussation of a tract that connects the superior and inferior colliculi (Park *et al.*, 1997). In the absence of Eph A4, some corticospinal tract (CST) axons aberrantly re-decussate (Dottori *et al.*, 1998; Kullander *et al.*, 2001 a; Leighton *et al.*, 2001 ; Coonan *et al.*, 2001). It seems that corticospinal Eph A4 is a receptor for an inhibitory activity within the spinal cord midline (Kullander *et al.*, 2001 a), and that ephrin B3 is at least part of such an activity (Kullander *et al.*, 2001 a, b; Yokoyama *et al.*, 2001). The effects of *eph* and *ephrin* mutations upon mouse brain commissures are summarised in figure 4.2, after Frisén *et al.*, 1999.

It has been suggested that ephrin B3 also guides spinal commissural axons. Ephrin B3 mRNA is expressed by the ventral midline of the mid-gestation spinal cord (Gale *et al.*, 1996 a; Bergemann *et al.*, 1998; Imondi *et al.*, 2000), at the time when the first dorsal spinal commissural axons complete their decussation and extend out of the floor plate (Wentworth, 1984). Dorsal spinal neurons have been reported to express Eph B1 mRNA, and post-midline commissural axons express surface molecules to which ephrin B3 can bind. Dorsal spinal axons are also repelled by ephrin B3 *in vitro* (Imondi *et al.*, 2000). Therefore it was decided to investigate whether ephrin B3 is involved in the guidance of mouse dorsal spinal commissural axons *in vivo*, and DiI was used to compare the dorsal spinal projections of embryos that either did or did not have ephrin B3 protein.

corpus callosum

axons fail to decussate in *EphB3* mutant mice.
failure is more pronounced in
EphB2/EphB3 double mutants
(EphB2 and EphB3 appear to be expressed in the midline; cortical axons express their ligands)

midbrain commissure

axons fail to decussate in e*phA8* mutant mice
(EphA8 is expressed by the axons; presumably ephrins in surrounding tissue means that the axons can only extend across the midline)

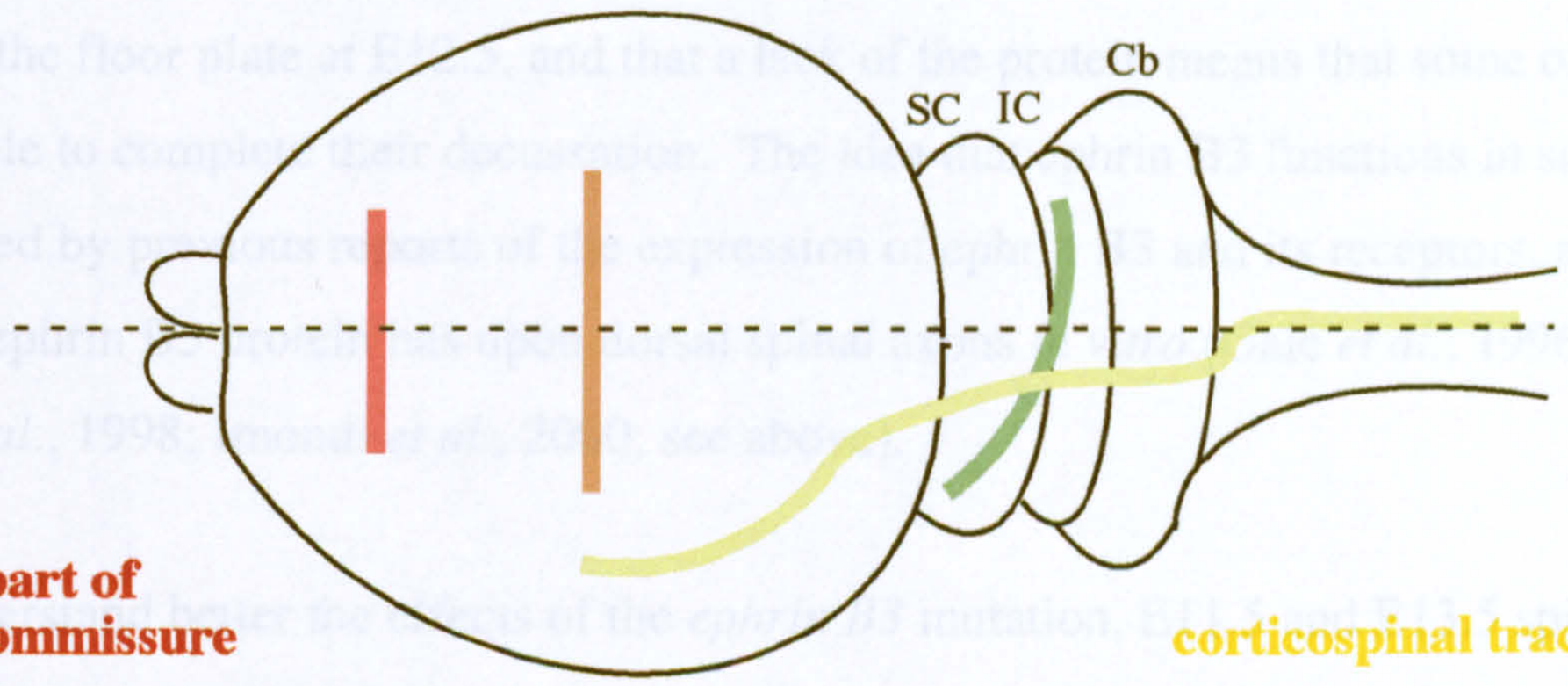

posterior part of anterior commissure

axons fail to decussate in *ephA4*
and *ephB2* mutant mice.
failure is more pronounced
in *ephB2/ephB3* double mutants
(axons express ephrin B1; EphB2 and EphA4 in surrounding tissue means that the axons can only extend across the midline)

corticospinal tract

axons can re-decussate in *EphA4*
and *ephrin B3* mutant mice
(axons express EphA4; ephrin B3 is in the midline).

Figure 4.2 Summary of the effects of *eph/ephrin* mutations upon decussating axons of the mouse brain Using Frisen *et al.*, 1999 and references mentioned in the text. SC- superior colliculus; IC- inferior colliculus; Cb- cerebellum. In addition, mice homozygous for a mutation in *Eph B2* have a temporary defect in the decussation of their inner ear efferent axons, However, these axons form a normal commissure by E14. (Cowan *et al.*, 2000). In *Xenopus*, premature expression of B-ephrins in the optic chiasm can force retinal axons that normally decussate to extend ipsilaterally (Nakagawa *et al*, 2000).

4.3 Results and Discussion

As presented in figure 4.3, E12.5 embryos homozygous for the *ephrin B3* mutation had on average a smaller proportion of their axons making a contra-rostral turn than did heterozygotes. Homozygous embryos also had a correspondingly larger proportion of their dorsal spinal projections in or at the floor plate. Both of these differences were statistically significant ($p= 0.0128$ and $p= 0.00570$ respectively). There were no other significant differences between the labelled spinal projections of the two groups of embryos. This result suggests that ephrin B3 might normally cause spinal commissural axons to be expelled from the floor plate at E12.5, and that a lack of the protein means that some of the axons are unable to complete their decussation. The idea that ephrin B3 functions in such a way is supported by previous reports of the expression of ephrin B3 and its receptors, and the effect that ephrin B3 protein has upon dorsal spinal axons *in vitro* (Gale *et al.*, 1996 a; Bergemann *et al.*, 1998; Imondi *et al.*, 2000; see above).

In order to understand better the effects of the *ephrin B3* mutation, E11.5 and E13.5 spinal cords were also analysed. The differences between heterozygous and homozygous E11.5 *ephrin B3* mutant embryos were slight (figure 4.4) and statistically insignificant (see appendix 4.A.2). Thus the pre-commissural development of dorsal spinal commissural axons did not appear to have been affected by the *ephrin B3* mutation. At E13.5, the dorsal spinal projections of homozygote and heterozygote embryos were also statistically indistinguishable (see figure 4.5 and appendix 4.A.3). This is suggestive of there being a repair of the mutant phenotype between E12.5 and E13.5. Such a recovery may reflect the onset of expression of other repulsive factors by the floor plate. Indeed, the floor plate begins to express ephrin B2 at around E12, and its expression of ephrin B1 begins at E13 (Imondi *et al.*, 2000; summarised in figure 4.6). Purified versions of either protein can bind to, and induce the collapse of, dorsal commissural axons *in vitro* (Imondi *et al.*, 2000). Therefore it is conceivable that the subsequent floor plate expression of ephrins B1 and B2 provides sufficient repulsion for stalled commissural axons to proceed (figure 4.7). Such a redundancy between Ephs and ephrins has already been proposed to explain the recovery of

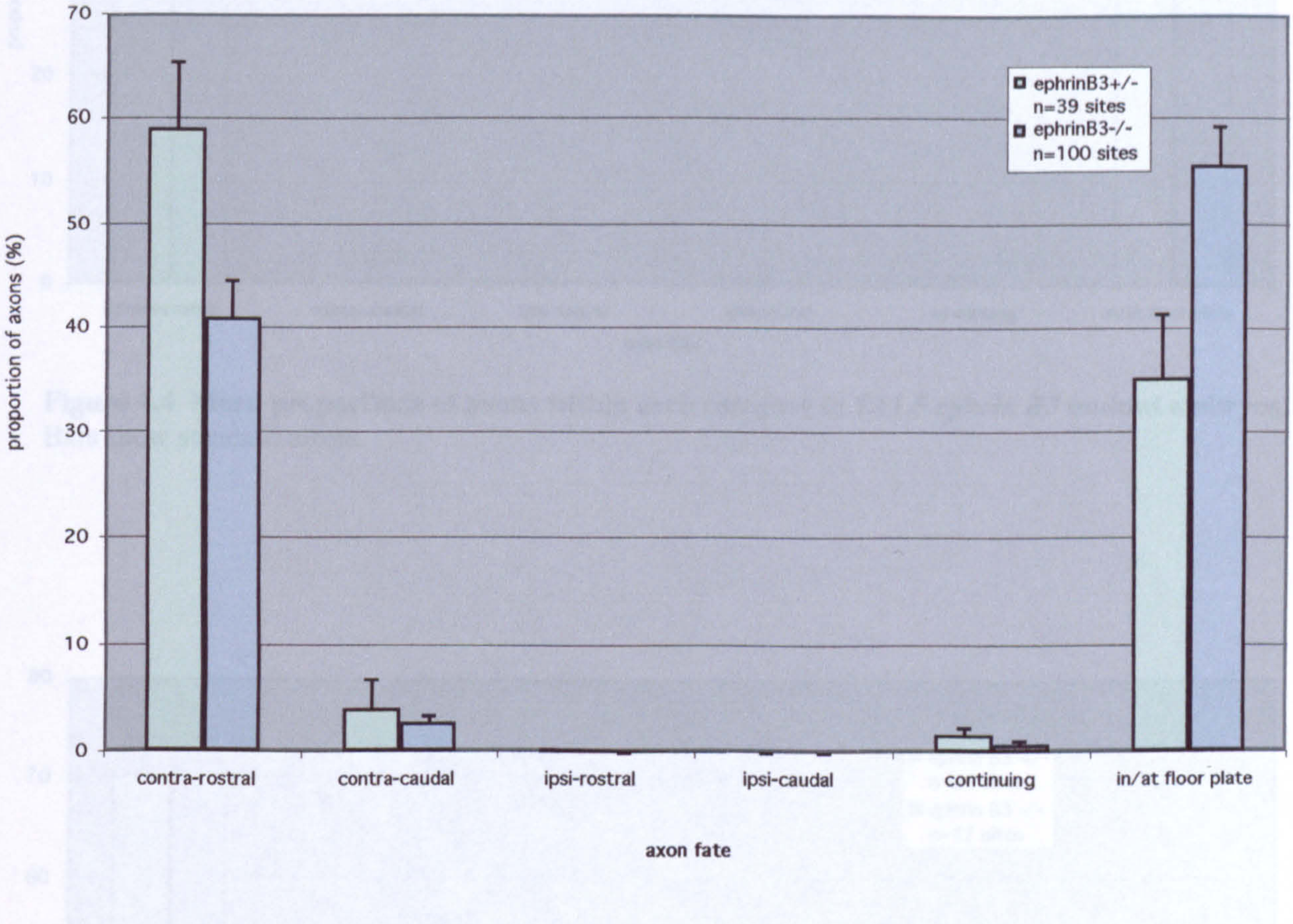

Figure 4.3 Mean proportions of axons within each category in E12.5 e*phrin B3* mutant embryos. Bars show standard errors.

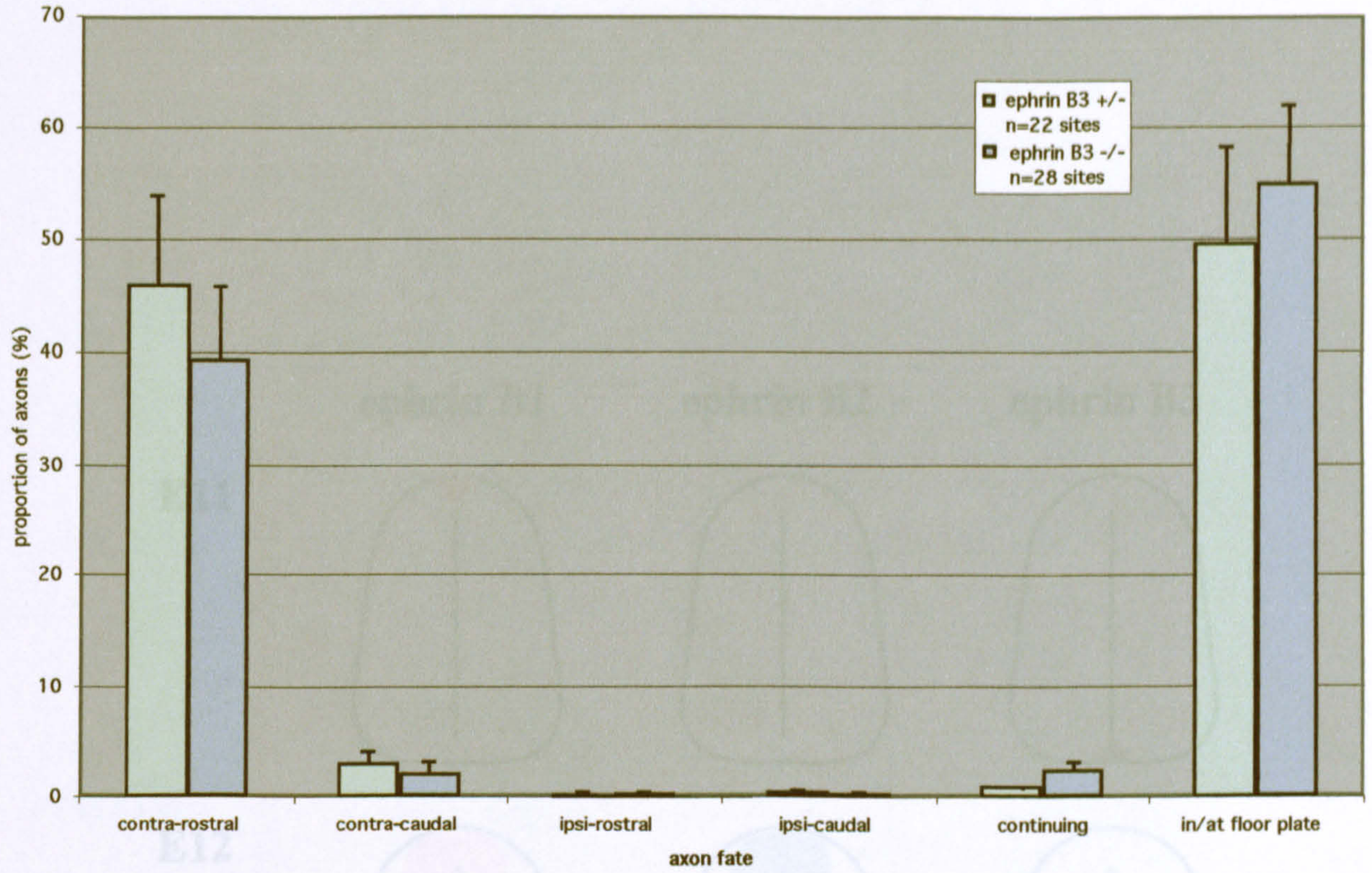

Figure 4.4 Mean proportions of axons within each category in E11.5 e*phrin B3* mutant embryos.
Bars show standard errors.

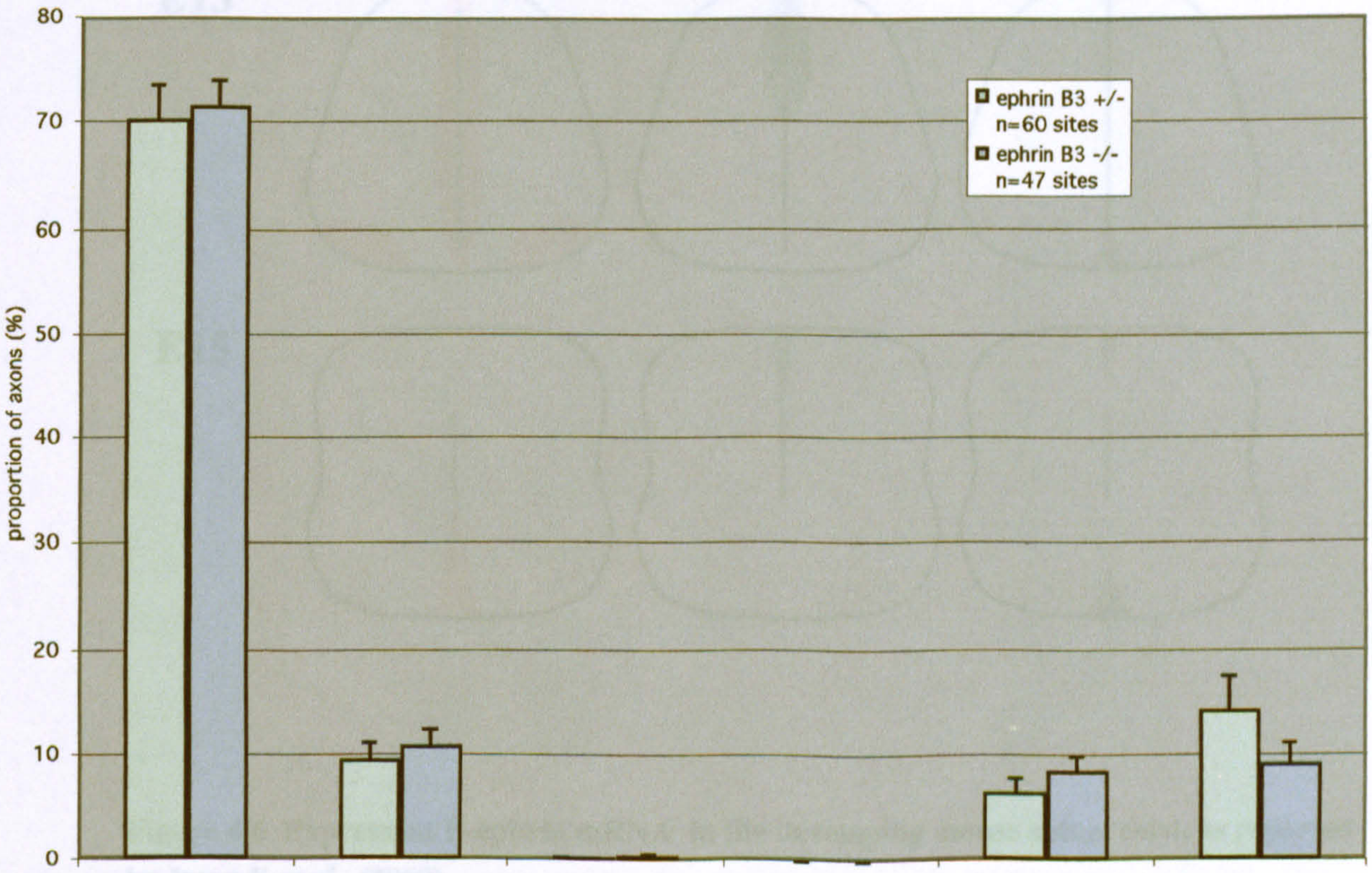

Figure 4.5 Mean proportions of axons within each category in E13.5 e*phrin B3* mutant embryos.
Bars show standard errors.

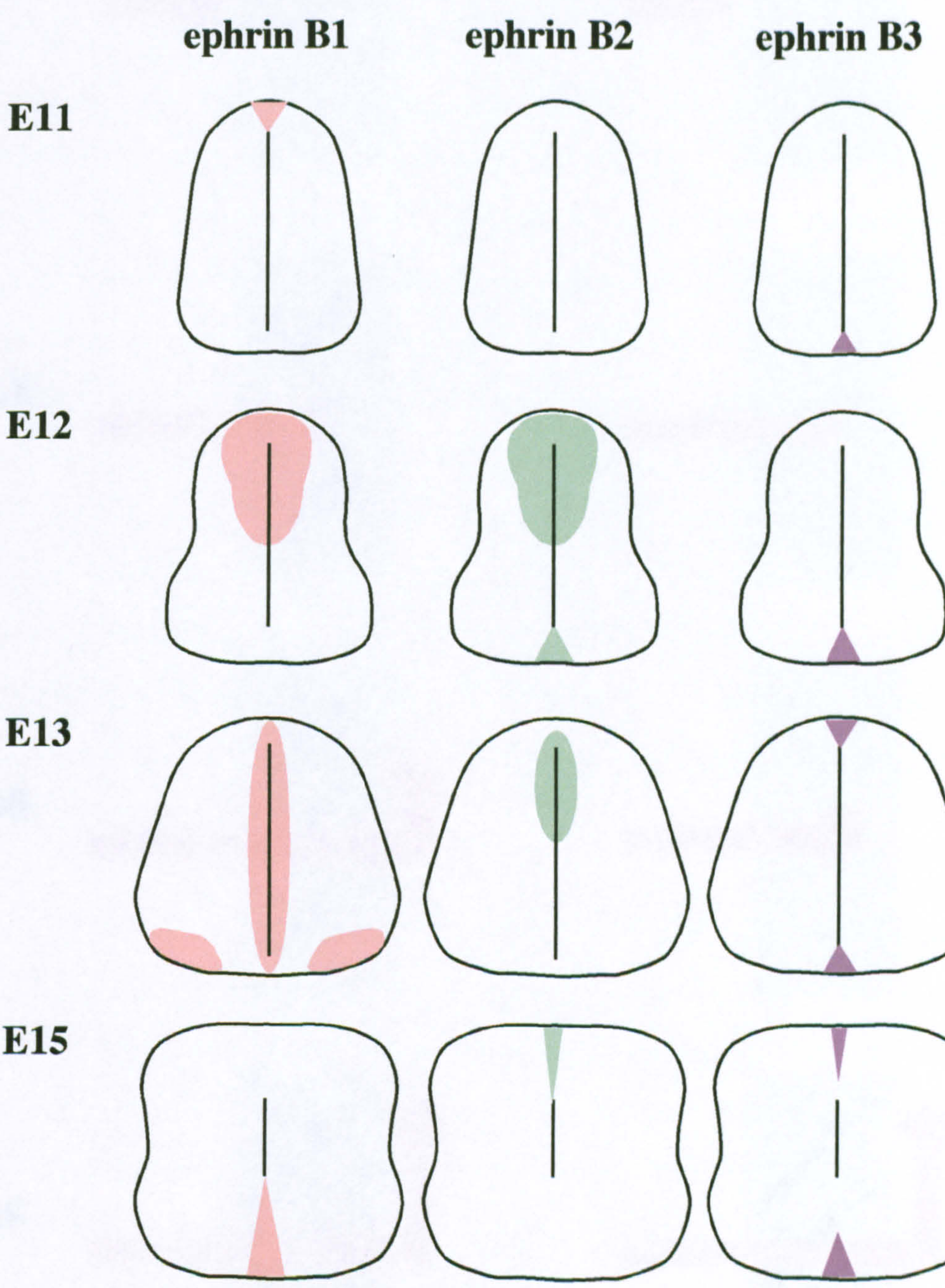

Figure 4.6 Expression B-ephrin mRNA in the developing mouse spinal cord, as reported by Imondi *et al.*, (2000).

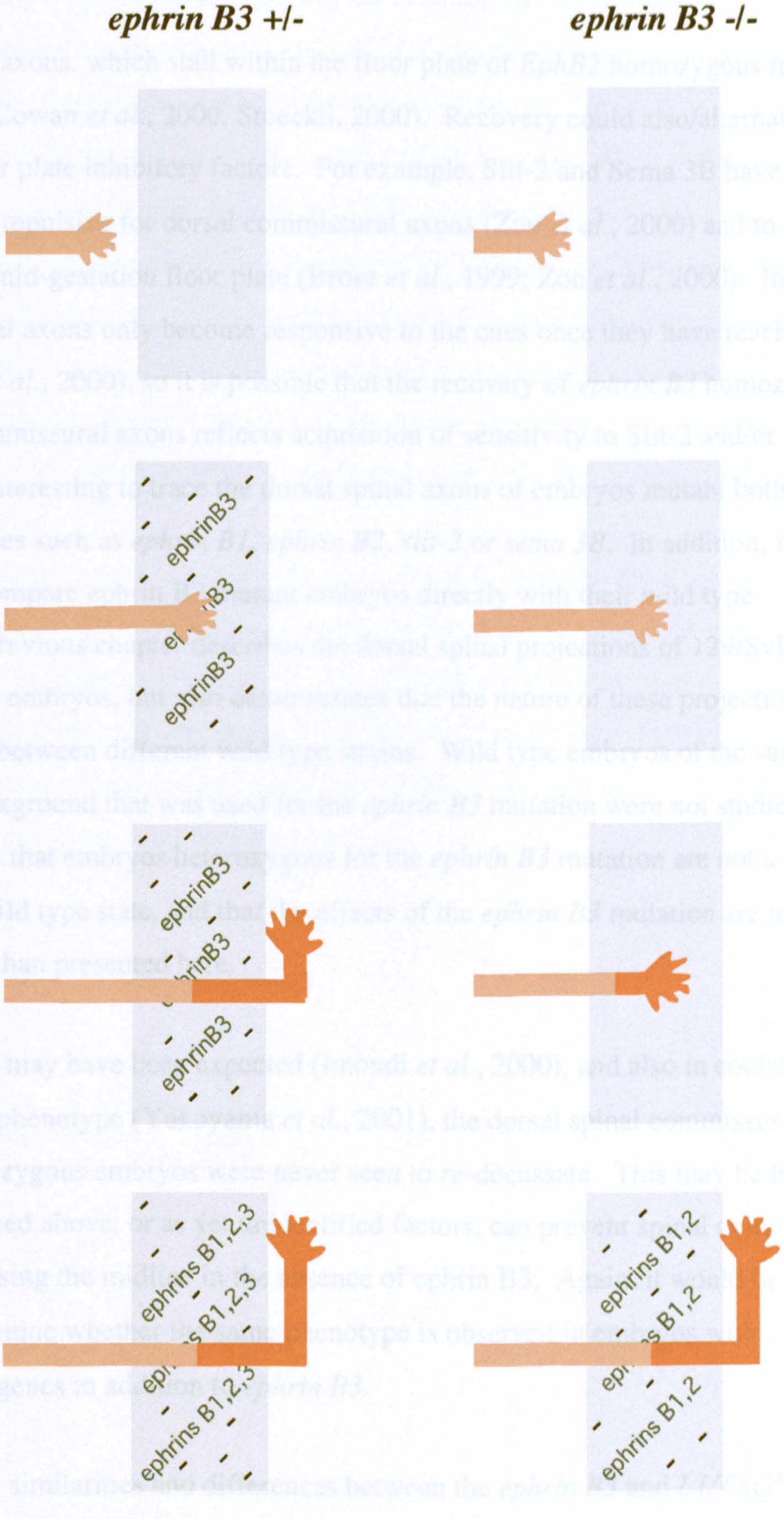

Figure 4.7 Schematic representation of what may be happening at the floor plate of *ephrin B3* heterozygous and homozygous mutant embryos. Axons are shown crossing the floor plate as in open book preparations. At E10.5, most axons have yet to reach the floor plate. At E11.5, axons have entered the floor plate. The heterozygote floor plate begins to express ephrin B3, but this does not have an effect upon axon trajectory as no Eph B receptors are expressed at the axon surface. At E12.5, the EphB1 receptor is expressed (dark orange). Axons are repelled out of the floor plate by ephrin B3 in heterozygous embryos, but there is as yet no ephrin ligand for the receptor in the homozygote floor plate. By E13.5, the *ephrin B3* mutant floor plate is also repulsive, as other B-ephrins are expressed. These provide sufficient repulsion to force the commissural axons to extend out of the midline. Using Imondi *et al*., 2000.

inner ear efferent axons, which stall within the floor plate of *EphB2* homozygous mutant mouse embryos (Cowan *et al.*, 2000, Stoeckli, 2000). Recovery could also/alternatively involve other floor plate inhibitory factors. For example, Slit-2 and Sema 3B have also been shown to be repulsive for dorsal commissural axons (Zou *et al.*, 2000) and to be expressed by the mid-gestation floor plate (Brose *et al.*, 1999; Zou *et al.*, 2000). In both cases, commissural axons only become responsive to the cues once they have reached the floor plate (Zou *et al.*, 2000), so it is possible that the recovery of *ephrin B3* homozygous mutant dorsal commissural axons reflects acquisition of sensitivity to Slit-2 and/or Sema 3B. It would be interesting to trace the dorsal spinal axons of embryos mutant both for *ephrin B3* and genes such as *ephrin B1*, *ephrin B2*, *slit-2* or *sema 3B*. In addition, it would be of interest to compare ephrin B3 mutant embryos directly with their wild type littermates. The previous chapter describes the dorsal spinal projections of 129/SvEv and C57Bl/6 wild type embryos, but also demonstrates that the nature of these projections can vary significantly between different wild type strains. Wild type embryos of the same mixed genetic background that was used for the *ephrin B3* mutation were not studied. Thus it remains possible that embryos heterozygous for the *ephrin B3* mutation are not a true reflection of the wild type state, and that the effects of the *ephrin B3* mutation are in fact more pronounced than presented here.

In contrast to what may have been expected (Imondi *et al.*, 2000), and also in contrast to the corticospinal tract phenotype (Yokoyama *et al.*, 2001), the dorsal spinal commissural axons of *ephrin B3* homozygous embryos were never seen to *re*-decussate. This may be because the factors mentioned above, or as yet unidentified factors, can prevent spinal commissural axons from re-crossing the midline in the absence of ephrin B3. Again, it would be interesting to determine whether the same phenotype is observed in embryos with mutations in other genes in addition to *ephrin B3*.

There were notable similarities and differences between the *ephrin B3* and *L1/TAG*^{A} double mutant embryos. In both cases, mutant spinal preparations showed a stall of axons at E12.5, implicating the molecules in the process of floor plate exit. At E13.5, *ephrin B3*

homozygous mutant dorsal spinal axons were indistinguishable from those of heterozygotes, whereas a large proportion of *L1/TAG*^{A} double mutant dorsal spinal axons were still in or at the floor plate. It is thus theoretically possible that L1/TAG-1 and ephrin B3 form part of a single mechanism: that L1 and TAG-1 normally allow axons to respond to ephrin B3 at E12.5, and to other factors at E13.5. Indeed, there is evidence that L1 can interact with at least one known receptor for ephrin B3, L1 seeming to be phosphorylated by EphB2 *in vitro* (Zisch *et al.*, 1997). Further experiments would be needed to determine whether L1 and TAG-1 are in fact involved in the ability to respond to ephrin B3. For example, *in vitro* culture of wild type or *L1/TAG*^{A} double mutant axons with ephrin B3-expressing cells would reveal the effect of the double mutation with respect to this ephrin.

In summary, the results presented show that ephrin B3 is involved in the development of vertebrate dorsal spinal commissural projections. At E12.5, it seems that extension of the axons is delayed in or at the floor plate of *ephrin B3* homozygous mutant embryos. This possibly reflects the absence of an inhibitory factor that normally forces the axons to continue. There seems to be a complete recovery of this phenotype by E13.5, when the floor plate begins to express other B-ephrin ligands.

4.4 Conclusions

1. **At E12.5, ephrin B3 is involved in the ability of mouse dorsal spinal commissural axons to extend out of the floor plate and into the contra-lateral spinal cord.**

2. **At E13.5, other factors can cause dorsal commissural axons to extend out of the floor plate.**

4.5 Appendices

Appendix 4.A: Statistical analyses of the differences between *ephrin B3* heterozygous and homozygous mutant embryos.

4.A.1: Comparison of E12.5 embryos heterozygous or homozygous for the *ephrin B3* mutation

4.A.2: Comparison of E11.5 embryos heterozygous or homozygous for the *ephrin B3* mutation

4.A.3: Comparison of E13.5 embryos heterozygous or homozygous for the *ephrin B3* mutation

Appendix 4.A.1

Comparison of E12.5 embryos heterozygous or homozygous for the *ephrin B3* mutation For data see figure 4.3.

Axons making a contra-rostral turn

SUMMARY

Groups	*Count*	*Sum*	*Average*	*Variance*
EphrinB3+/-	39	2301.6	59.0153846	1577.60028
EphrinB3-/-	100	4094.1	40.941	1386.73719

ANOVA

Source of Variation	*df*	*SS*	*MS*	*F*	*P-value*
Between Groups	1	9165.936539	9165.93654	6.36666038	0.01277092
Within Groups	137	197235.7927	1439.67732		
Total	138	206401.7292			

ie the proportions of axons making are significantly different

Axons making a contra-caudal turn

SUMMARY

Groups	*Count*	*Sum*	*Average*	*Variance*
EphrinB3+/-	39	162.1	4.15641026	272.344103
EphrinB3-/-	100	282.8	2.828	44.4737535

ANOVA

Source of Variation	*df*	*SS*	*MS*	*F*	*P-value*
Between Groups	1	49.51243062	49.5124306	0.45981652	0.49885343
Within Groups	137	14751.9775	107.678668		
Total	138	14801.48993			

ie the proportions of axons are not significantly different

Axons making an ipsi-rostral turn

SUMMARY

Groups	*Count*	*Sum*	*Average*	*Variance*
EphrinB3+/-	39	5	0.12820513	0.64102564
EphrinB3-/-	100	0	0	0

ANOVA

Source of Variation	*df*	*SS*	*MS*	*F*	*P-value*
Between Groups	1	0.461169526	0.46116953	2.5937145	0.10959013
Within Groups	137	24.35897436	0.17780273		
Total	138	24.82014388			

ie the proportions of axons are not significantly different

Axons making an ipsi-caudal turn

No labelled axons in E12.5 embryos of either *ephrin B3* genotype made an ipsi-rostral turn.

Axons continuing to extend laterally

SUMMARY

Groups	*Count*	*Sum*	*Average*	*Variance*
EphrinB3+/-	39	61.4	1.57435897	22.1045884
EphrinB3-/-	100	81.9	0.819	5.82135253

ANOVA

Source of Variation	*df*	*SS*	*MS*	*F*	*P-value*
Between Groups	1	16.0087194	16.0087194	1.54855097	0.2154742
Within Groups	137	1416.28826	10.3378705		
Total	138	1432.29698			

ie the proportions of axons are not significantly different

Axons in/at the floor plate

SUMMARY

Groups	*Count*	*Sum*	*Average*	*Variance*
Ephrin83+/-	39	1370.1	35.1307692	1532.53534
Ephrin83-/-	100	5546.6	55.466	1446.98752

ANOVA

Source of Variation	*df*	*SS*	*MS*	*F*	*P-value*
Between Groups	1	11602.4049	11602.4049	7.88894933	0.00570133
Within Groups	137	201488.107	1470.71611		
Total	138	213090.512			

ie the proportions of axons are significantly different

Appendix 4.A.2

Comparison of E11.5 embryos heterozygous or homozygous for the *ephrin B3* mutation For data see figure 4.4.

Axons making a contra-rostral turn

SUMMARY

Groups	*Count*	*Sum*	*Average*	*Variance*
EphrinB3+/-	22	1005.5	45.7045455	1526.79188
EphrinB3-/-	28	1105.6	39.4857143	1166.65905

ANOVA

Source of Variation	*df*	*SS*	*MS*	*F*	*P-value*
Between Groups	1	476.461969	476.461969	0.35980652	0.551435
Within Groups	48	63562.4238	1324.21716		
Total	49	64038.8858			

ie the proportions of axons are not significantly different

Axons making an ipsi-caudal turn

SUMMARY

Groups	*Count*	*Sum*	*Average*	*Variance*
EphrinB3+/-	22	10.7	0.48636364	1.73170996
EphrinB3-/-	28	8.8	0.31428571	1.33238095

ANOVA

Source of Variation	*df*	*SS*	*MS*	*F*	*P-value*
Between Groups	1	0.36480519	0.36480519	0.24205975	0.6249651
Within Groups	48	72.3401948	1.50708739		
Total	49	72.705			

ie the proportions of axons are not significantly different

Axons making a contra-caudal turn

SUMMARY

Groups	*Count*	*Sum*	*Average*	*Variance*
EphrinB3+/-	22	67.3	3.05909091	32.3396753
EphrinB3-/-	28	62.5	2.23214286	30.7007804

ANOVA

Source of Variation	*df*	*SS*	*MS*	*F*	*P-value*
Between Groups	1	8.42494675	8.42494675	0.26815842	0.6069484
Within Groups	48	1508.05425	31.4177969		
Total	49	1516.4792			

ie the proportions of axons are not significantly different

Axons continuing to extend laterally

SUMMARY

Groups	*Count*	*Sum*	*Average*	*Variance*
EphrinB3+/-	22	22.8	1.03636364	6.23194805
EphrinB3-/-	28	72	2.57142857	17.2628571

ANOVA

Source of Variation	*df*	*SS*	*MS*	*F*	*P-value*
Between Groups	1	29.0311481	29.0311481	2.33428758	0.1331164
Within Groups	48	596.968052	12.4368344		
Total	49	625.9992			

ie the proportions of axons are not significantly different

Axons making an ipsi-rostral turn

SUMMARY

Groups	*Count*	*Sum*	*Average*	*Variance*
EphrinB3+/-	22	5.9	0.26818182	1.58227273
EphrinB3-/-	28	10.3	0.36785714	1.05559524

ANOVA

Source of Variation	*df*	*SS*	*MS*	*F*	*P-value*
Between Groups	1	0.1224013	0.1224013	0.09517863	0.759029
Within Groups	48	61.7287987	1.28601664		
Total	49	61.8512			

ie the proportions of axons are not significantly different

Axons in/at the floor plate

SUMMARY

Groups	*Count*	*Sum*	*Average*	*Variance*
EphrinB3+/-	22	1087.9	49.45	1768.73976
EphrinB3-/-	28	1540.9	55.0321429	1359.44522

ANOVA

Source of Variation	*df*	*SS*	*MS*	*F*	*P-value*
Between Groups	1	383.895129	383.895129	0.24952372	0.6196927
Within Groups	48	73848.5561	1538.51158		
Total	49	74232.4512			

ie the proportions of axons are not significantly different

Appendix 4.A.3

Comparison of E13.5 embryos heterozygous or homozygous for the *ephrin B3* mutation For data see figure 4.5.

Axons making a contra-rostral turn

SUMMARY

Groups	*Count*	*Sum*	*Average*	*Variance*
EphrinB3+/-	60	4240.8	70.68	577.814847
EphrinB3-/-	47	3362.5	71.5425532	325.918585

ANOVA

Source of Variation	*df*	*SS*	*MS*	*F*	*P-value*
Between Groups	1	19.6081718	19.6081718	0.04194618	0.8381189
Within Groups	105	49083.3309	467.460294		
Total	106	49102.9391			

ie the proportions of axons are not significantly different

Axons making an ipsi-caudal turn

SUMMARY

Groups	*Count*	*Sum*	*Average*	*Variance*
EphrinB3+/-	60	0	0	0
EphrinB3-/-	47	0.9	0.01914894	0.01723404

ANOVA

Source of Variation	*df*	*SS*	*MS*	*F*	*P-value*
Between Groups	1	0.00966395	0.00966395	1.27996749	0.26048243
Within Groups	105	0.79276596	0.00755015		
Total	106	0.80242991			

ie the proportions of axons are not significantly different

Axons making a contra-caudal turn

SUMMARY

Groups	*Count*	*Sum*	*Average*	*Variance*
EphrinB3+/-	60	519.9	8.665	156.550788
EphrinB3-/-	47	504.3	10.7297872	134.377354

ANOVA

Source of Variation	*df*	*SS*	*MS*	*F*	*P-value*
Between Groups	1	112.36109	112.36109	0.76521115	0.38369914
Within Groups	105	15417.8548	146.836712		
Total	106	15530.2159			

ie the proportions of axons are not significantly different

Axons continuing to extend laterally

SUMMARY

Groups	*Count*	*Sum*	*Average*	*Variance*
EphrinB3+/-	60	415.3	6.92166667	115.862404
EphrinB3-/-	47	400.5	8.5212766	102.485624

ANOVA

Source of Variation	*df*	*SS*	*MS*	*F*	*P-value*
Between Groups	1	67.4362657	67.4362657	0.61304525	0.43540591
Within Groups	105	11550.2206	110.002101		
Total	106	11617.6568			

ie the proportions of axons are not significantly different

Axons making an ipsi-rostral turn

SUMMARY

Groups	*Count*	*Sum*	*Average*	*Variance*
EphrinB3+/-	60	23.8	0.39666667	1.95863277
EphrinB3-/-	47	23.3	0.49574468	2.07693802

ANOVA

Source of Variation	*df*	*SS*	*MS*	*F*	*P-value*
Between Groups	1	0.25871399	0.25871399	0.12868387	0.72052085
Within Groups	105	211.098482	2.01046174		
Total	106	211.357196			

ie the proportions of axons are not significantly different

Axons in/at the floor plate

SUMMARY

Groups	*Count*	*Sum*	*Average*	*Variance*
EphrinB3+/-	59	808.4	13.7016949	572.540859
EphrinB3-/-	47	428.6	9.11914894	190.842886

ANOVA

Source of Variation	*df*	*SS*	*MS*	*F*	*P-value*
Between Groups	1	549.3608	549.3608	1.36077095	0.24607189
Within Groups	104	41986.1426	403.71291		
Total	105	42535.5034			

ie the proportions of axons are not significantly different

5 Further Analysis of the Developing Nervous System in *TAG-1* Mutant Mice

Please note that throughout this chapter, the term "*TAG-1* null mutant" refers to mice or embryos carrying either one (heterozygotes) or two (homozygotes) copies of the TAG-1 allele (shown in figure 1.7).

5.1 Abstract

The *TAG-1* null allele includes a *tau-lacZ* reporter construct, which is positioned downstream of *TAG-1* gene regulatory sequences. The distribution of ß-galactosidase activity in *TAG-1* null embryos was found to be very similar to that previously described for TAG-1 immunoreactivity. Thus the *TAG-1* null allele is a useful tool for studying structures that normally express TAG-1. Most of these structures appeared to develop normally in *TAG-1* null homozygotes. These included the facial (VIIth cranial) and limb nerves, even though TAG-1 has previously been implicated in their development. However, it seemed that the *TAG-1* null mutation did have an adverse effect upon development of the habenulointerpeduncular tract and hypoglossal (XIIth cranial) nerve.

The *TAG-1* null allele was also used to study the effects of other mutations upon structures that normally express TAG-1. Preliminary results suggest that TAG-1-expressing structures were largely unaffected by either the *L1* single mutation or the *L1/TAG*^{A} double mutation.

5.2 Introduction

Previous studies have indicated that TAG-1 is not only expressed by developing spinal neurons. Yamamoto *et al.* (1986) described expression of an antigen now known to be TAG-1 in many regions of the mouse nervous system between E10 and birth. They reported immunoreactivity within the cranial nerves, developing cerebellum, mesencephalon, optic and olfactory nerves, habenulointerpeduncular tract (HIPT; also known as the *fasciculus retroflexus*), anterior commissure and cerebral cortices. Wolfer *et al.* (1994) recorded TAG-1-like immunoreactivity within many of the same structures between E10 and E17, and between P0 and P15. In addition the latter study reported expression by the embryonic dorsal root ganglia, sympathetic nervous system and rhombencephalon. Yoshihara *et al.* (1995) described in detail the expression of TAG-1 mRNA by several regions of the adult rat brain. It is thus conceivable that TAG-1 might be involved in the development of neurons other than those of the dorsal spinal cord.

TAG-1 has been suggested to have roles in the development of other neurons. Those of the facial (VIIth cranial) nerve specifically express TAG-1 during a period of caudal migration (Garel *et al.*, 2000). Mutations in the genes encoding the *ebf-1* or *krox-20* transcription factors cause premature cessation of both this migration and facial nerve neuron TAG-1 expression (Garel *et al.*, 2000; Cordes, 2001). The chicken homologue of TAG-1, axonin-1, seems to mediate the repulsion of chicken dorsal root ganglion (DRG) axons by the notochord (Masuda et al., 2000). Axonin-1 has also been suggested to mediate the fasciculation of sensory axons along motor axons in the developing chick hind limb (Xue and Honig, 1999). This appears to be necessary if sensory axons are to reach their target muscles (Landmesser and Honig, 1986; Honig *et al.*, 1998). In addition, antibodies that perturb the function of the related molecule NgCAM seem to cause incorrect sorting of axons into nerves in chick hind-limb plexus regions (Honig and Rutishauser, 1996). Another region in which TAG-1 might function is the postnatal cerebellum. Cerebellar granule cells express the protein particularly strongly (Furley *et al.*, 1990; Wolfer *et al.*, 1994; Yoshihara *et al.*, 1995; Wolfer *et al.*, 1998), at stages when much cerebellar

development occurs (Altman and Bayer, 1997), and when few other structures maintain strong expression of TAG-1 (Yoshihara *et al.*, 1995).

Thus it is conceivable that TAG-1 could influence development of the facial nerve, limb nerves, cerebellum, and/ or the many other regions of the nervous system that express the protein. It was therefore decided to conduct a general survey of the roles of TAG-1 in neural development. Its expression was determined using a reporter gene, and expressing structures were examined for gross anatomical defects in its absence.

As the *TAG-1* null mutation was produced by partial replacement of the gene by a *tau-lacZ* construct, *TAG-1* null mutant mice should express a tau-ß-galactosidase protein in all cells that would normally express TAG-1 (Callahan and Thomas, 1994; Mombaerts *et al.*, 1996; A.J.W. Furley, personal communication). ß-galactosidase activity can be detected by treatment with X-gal, which is converted to a blue stain in all cells that contain the enzyme. As tau is a protein that is transported throughout axons, the tau-ß-galactosidase fusion proteins is similarly transported, and treatment with X-gal allows axons to be traced (Callahan and Thomas, 1994; Mombaerts *et al.*, 1996). In this way, structures that would normally have expressed TAG-1 could be stained and compared in animals that had either one or two copies of the mutant *TAG-1* allele. This allowed animals that did have wild type TAG-1 protein to be compared with those that did not.

Whole embryos were examined from the age of E10.5, when TAG-1 protein is first expressed at appreciable levels (Yamamoto *et al.*, 1986), to the age of E13.5, after which time the embryonic epidermis prevents effective staining of whole embryos (Whiting *et al.*, 1991). At later stages, isolated brains were stained for ß-galactosidase activity. Brains were taken from mice aged E16.5, P2 and P15, as these ages represent late embryonic, neonatal and more advanced post-natal development respectively. These are also ages for which TAG-1 immunoreactivity has been described previously (Wolfer *et al.*, 1994), allowing the reliability of ß-galactosidase reporter protein expression to be verified. At all of the ages studied, heterozygote *TAG-1* null embryos /brains were compared with those of

homozygotes, in order to determine whether the absence of TAG-1 protein had affected neural development.

The *TAG-1* null allele was also used to study TAG-1 expressing structures in other mutant embryos. The effects of the *L1* mutation were investigated by comparing otherwise wild type *TAG-1* null heterozygous embryos with those that were also hemizygous for the *L1* mutation. In addition, *TAG-1* null heterozygous "control" embryos were compared with those hemizygous for the *L1* mutation and also homozygous for *TAG-1* mutations, in order to investigate the effects of simultaneous absences of both full-length TAG-1 and L1 proteins.

5.3 Results

5.3.1 Embryonic development of *TAG-1* null mutant mice

5.3.1.1 E10.5 embryos

E10.5 embryos, the youngest studied here, showed staining of the nervous system at all levels from the rhombencephalon caudally (figure 5.1; see table 5.1 for summary, and appendix 5.A for an alphabetical list of the abbreviations used). Spinal staining was restricted to the ventral horn and ventral roots. This is in accordance with previous work (Yamamoto *et al.*, 1986; Dodd *et al.* 1988; Vaughn *et al.*, 1992; Wolfer *et al.*, 1994). The most rostral spinal cord also had staining in the dorsal horn and dorsal root ganglia, both of which normally begin to express TAG-1 between E10 and E11 (Yamamoto *et al.*, 1986; Vaughn *et al.*, 1992; Wolfer *el al.*, 1994). Within the rhombencephalon, the facial and hypoglossal nerve nuclei were stained. Short projections of these nerves were often also labelled, as was the trigeminal (Vth cranial nerve) ganglion (figure 5.1). Again, these are structures that have been reported to express TAG-1 from between E10 and E11 (Wolfer *et al.*, 1994). The oculomotor nerve did not appear to be labelled in embryos of this age, which is in contrast to one report of TAG-1 protein expression (Wolfer *et al.*, 1994), but in agreement with another (Yamamoto *et al.*, 1986).

The staining of homozygous embryos was usually stronger than that of heterozygotes. This was expected, as homozygotes possess two copies of the *tau-lacZ* gene, and so express more of the tau-ß-galactosidase protein. The stained structures did not appear to differ between heterozygous (n=8) and homozygous (n=28) embryos at this age (figure5.1). The lesser extension of hypoglossal nerve rootlets of the homozygous embryo shown in figure 5.1 can be attributed to normal differences in the extent to which littermates had developed (Kaufman, 1992; data not shown).

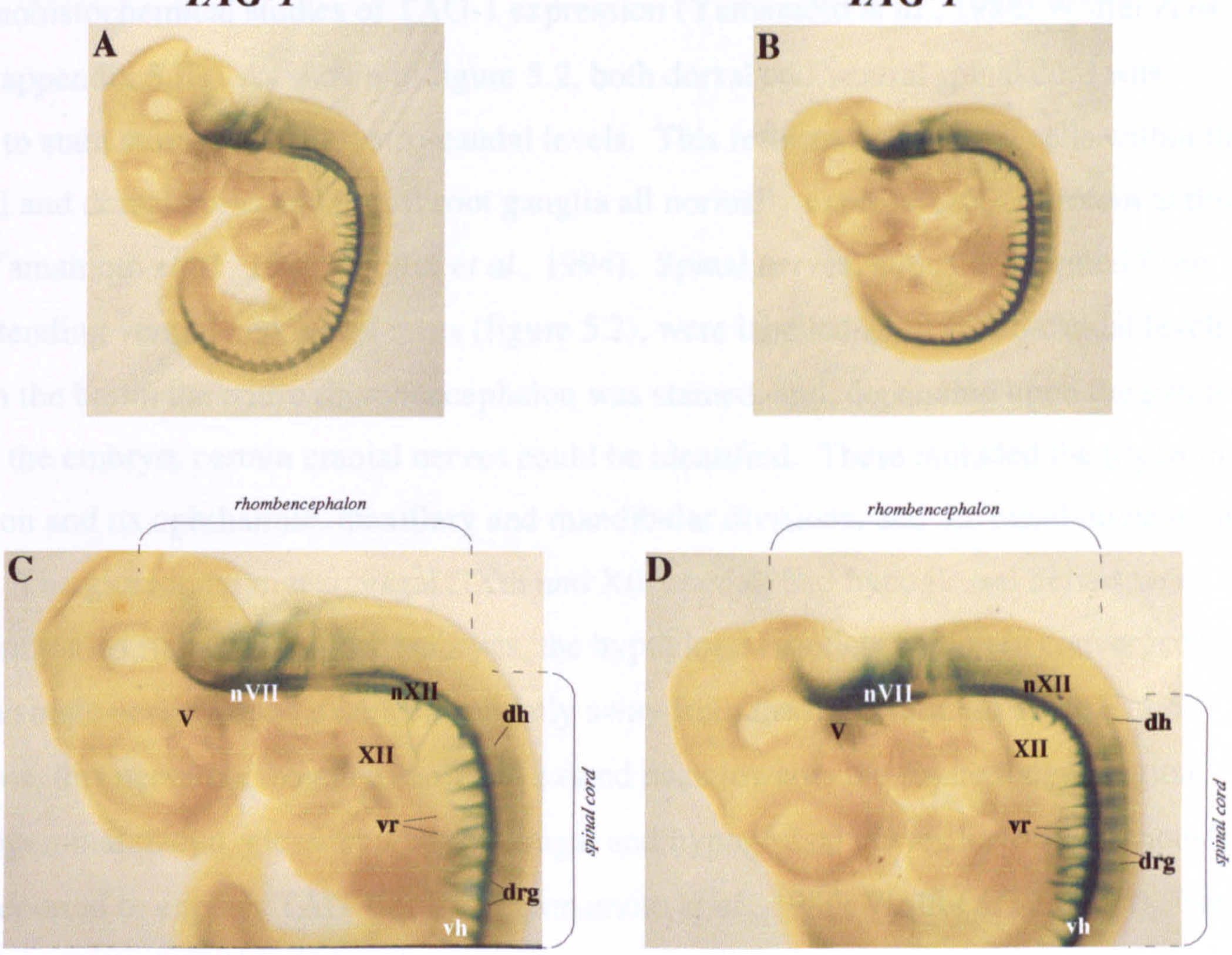

Figure 5.1 Expression of the tau-ß-galactosidase protein in E10.5 mouse embryos with the *TAG-1* null mutant allele. Areas of ß-galactosidase activity are labelled as indicated in table 5.1 and appendix 5.A. Embryos with two copies of the mutant allele have more of the enzyme and so stain more strongly, but otherwise homozygous embryos were indistinguishable from heterozygotes.

5.3.1.2 E11.5 embryos

At E11.5, staining was more extensive than at E10.5, in accordance with immunohistochemical studies of TAG-1 expression (Yamamoto *et al.*, 1986; Wolfer *et al.*, 1994; appendix 5.B). As shown in figure 5.2, both dorsal and ventral spinal cord was found to stain strongly, at all rostro-caudal levels. This reflects the fact that cells within the ventral and dorsal horns and dorsal root ganglia all normally express TAG-1 protein at this age (Yamamoto *et al.*, 1986; Wolfer *et al.*, 1994). Spinal nerves, which are formed from the extending ventral and dorsal roots (figure 5.2), were labelled at all rostro-caudal levels. Within the brain, the entire rhombencephalon was stained, and, depending upon the precise age of the embryo, certain cranial nerves could be identified. These included the trigeminal ganglion and its ophthalmic, maxillary and mandibular divisions, and the facial nucleus and nerve. The glossopharyngeal, vagal (IXth and Xth cranial) and hypoglossal nerves were frequently also stained. In older embryos, the hypoglossal rootlets had often converged to form a single nerve, which extended caudally away from the hindbrain. In some E11.5 embryos, this nerve had begun to turn and extend back towards the future tongue region. The trigeminal, facial, glossopharyngeal, vagal and hypoglossal nerves have all previously been reported to express TAG-1 at E11 (Yamamoto *et al.*, 1986; Wolfer *et al.*, 1994). The only apparent discrepancy between the present staining and a previous immunohistochemical study (Yamamoto *et al.*, 1986) is that the trochlear (IVth cranial) nerve did not appear to be labelled. This may be because the E11.5 nerve was too immature to contain sufficient ß-galactosidase for it to be visible at low magnification. The accessory (XIth cranial) nerve, which has been reported to express TAG-1 at this age (Wolfer *et al.*, 1994), was not identified. This is presumably because it could not be distinguished from the strongly stained hindbrain and vagus, along which it extends (e.g. appendices 5.B and 5.D).

The more developmentally advanced embryos within E11.5 litters also had staining within the ventral mesencephalon, or tegmentum. This area included the oculomotor (IIIrd cranial) nerve and interpeduncular nuclei. The oculomotor nerve was commonly seen

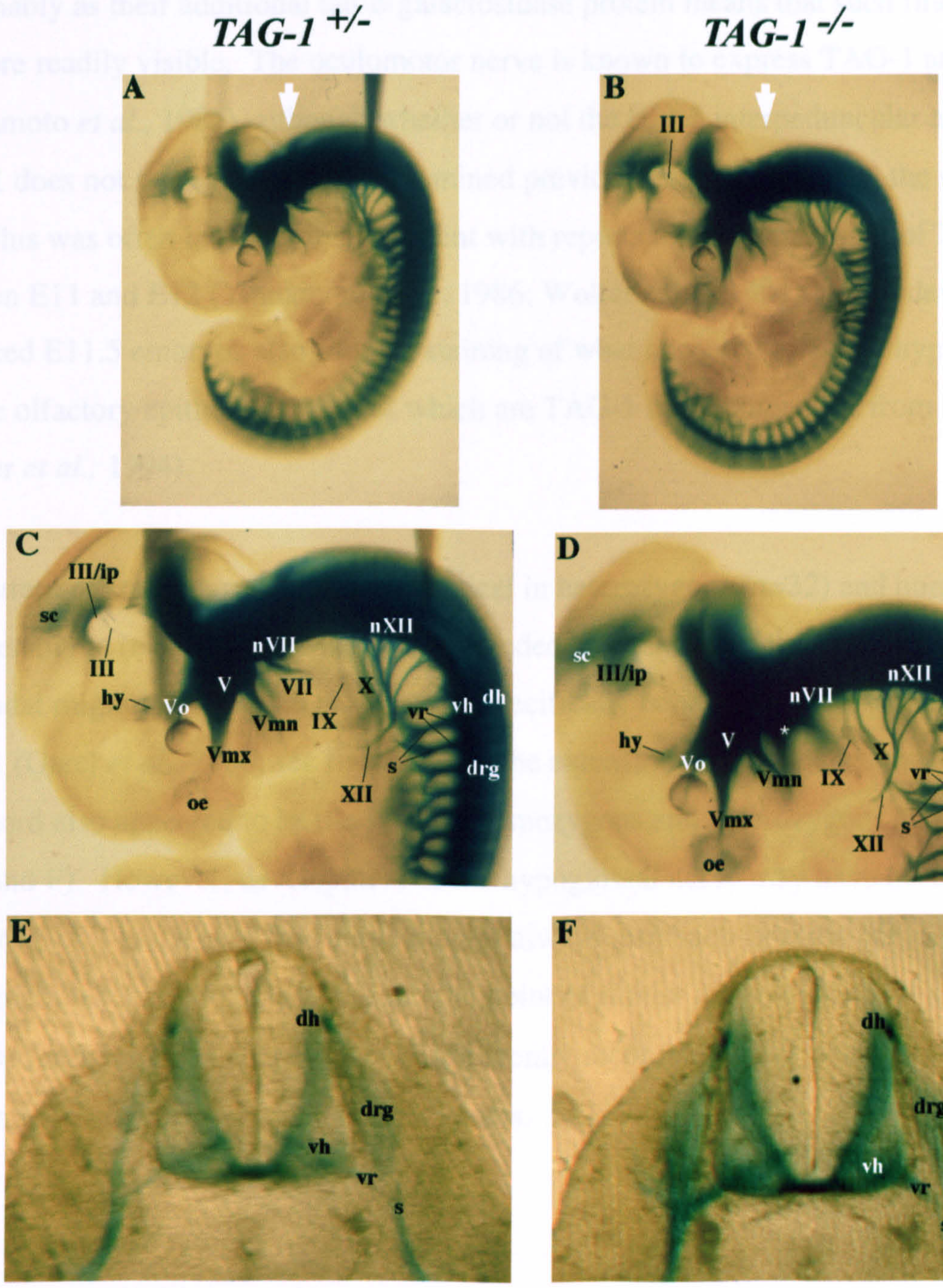

Figure 5.2 Expression of the tau-ß-galactosidase protein in E11.5 mouse embryos with the *TAG-1* null mutant allele. Areas of ß-galactosidase activity are labelled as indicated in table 5.1 and appendix 5.A. A and B: whole embryos; C and D: head and neck regions; E and F: transverse sections through the spinal cord. Note that the transparency of the embryos means that it is often possible to see structures on both sides of the body at once. For example, the homozygote embryo in D did have a facial nerve, but in this was obscured by the contralateral trigeminal ganglion (asterisk). White arrows indicate the direction from which the photographs of figure 5.3 were taken.

extending towards the eye. This nerve was most often labelled in homozygote embryos, presumably as their additional tau-ß-galactosidase protein means that such fine structures are more readily visible. The oculomotor nerve is known to express TAG-1 at this age (Yamamoto *et al.*, 1986), although whether or not the E11.5 interpeduncular area expresses TAG-1 does not seem to have been examined previously. More dorsally, the superior colliculus was often labelled, in agreement with reports that its expression of TAG-1 begins between E11 and E12 (Yamamoto *et al.*, 1986; Wolfer *et al.*, 1994). More developmentally advanced E11.5 embryos also showed staining of what appeared to be the hypothalamus and the olfactory epithelium, both of which are TAG-1 immunoreactive from E11 onwards (Wolfer *et al.*, 1994).

The pattern of staining was virtually identical in heterozygous (n=32) and homozygous E11.5 embryos (n=32; figure 5.2). This included the staining of the facial nerve nucleus, the caudal migration of which is known to specifically coincide with its expression of TAG-1 (Garel *et al.*, 2000; see figure 5.3). The extension of DRG axons away from the notochord also appeared to be the same in homozygous and heterozygous embryos (figure 5.2 E and F). However, development of the hypoglossal nerve may have been affected by the *TAG-1* null mutation. This nerve did not always turn back towards the tongue region, and sometimes failed to extend beyond the point of rootlet convergence. As will be discussed more fully in chapter 6, such apparently incomplete development was seen more frequently in homozygotes than heterozygotes.

5.3.1.3 E12.5 embryos

As shown in figure 5.4, the pattern of staining at E12.5 was similar to that at E11.5. Spinal nerves were seen to have extended further, and staining of both ventral and dorsal rami, and their branches, was evident in transverse section (figure 5.4 E and F, and appendix 5.C). Identifiable branches included medial and lateral branches of dorsal rami, and the sympathetic white *rami communicantes*, lateral cutaneous branches, muscular branches,

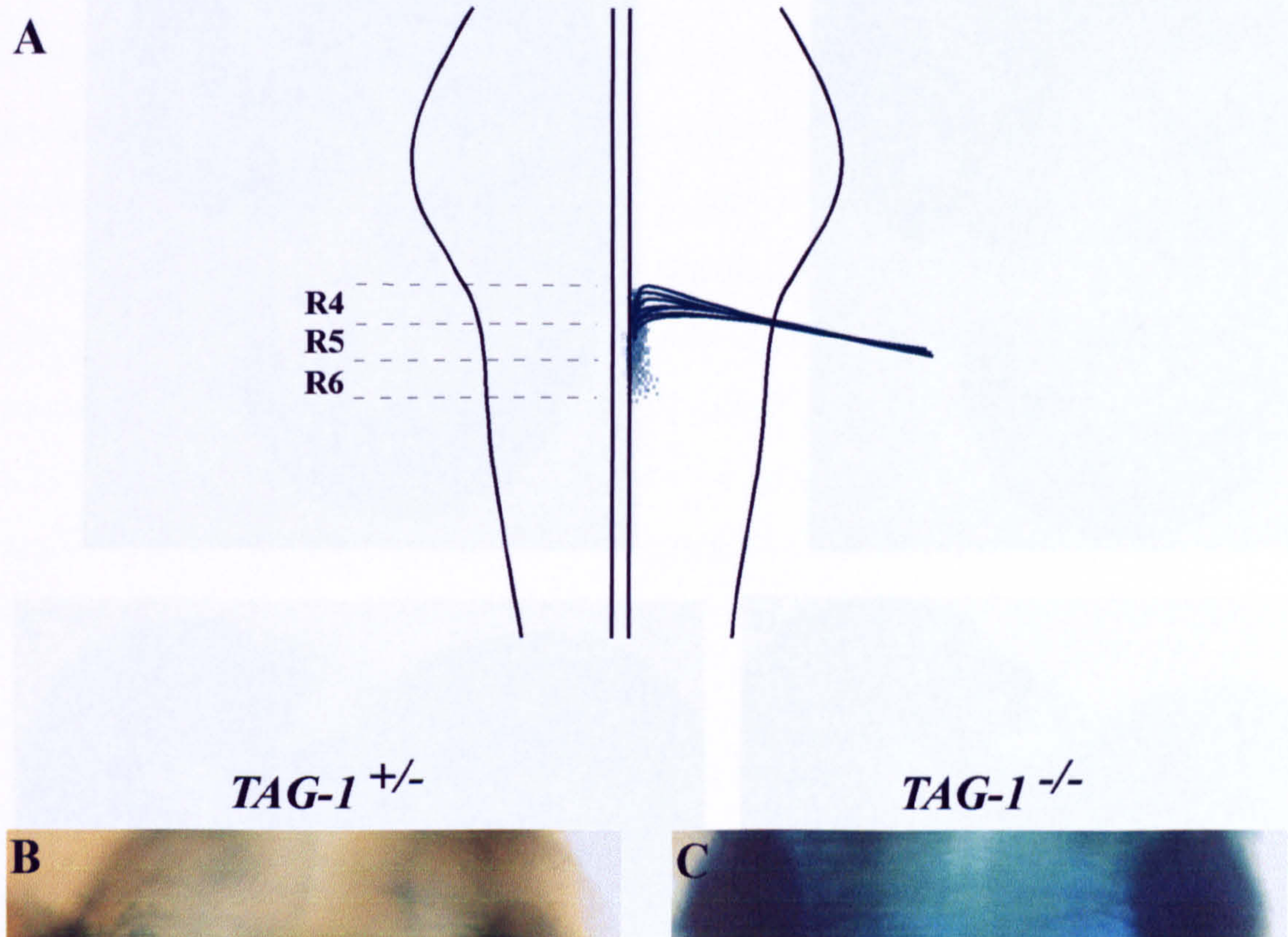

Figure 5.3 Comparison of the facial nerve nucleus of E11.5 mouse embryos either heterozygous or homozygous for the *TAG-1* null mutation. E11.5 mouse embryo hind-brains are shown as viewed from above, as illustrated in figure 5.2. A: the nature of the mouse facial nerve nucleus at E11.5 (after Garel *et al.*, 2000). Facial nerve neurons originate in rhombomere 4 (R4) and send axons out of the central nervous system at this level, but they then migrate caudally. TAG-1 is expressed by the cells as they migrate through rhombomere 5 (R5) and into rhombomere 6 (R6), but is subsequently down-regulated. In mice mutant for *Krox-20* or *Ebf1*, both the migration and expression of TAG-1 are perturbed (Garel *et al.*, 2000). However, the migration appears to occur normally in the absence of TAG-1 (compare B and C).

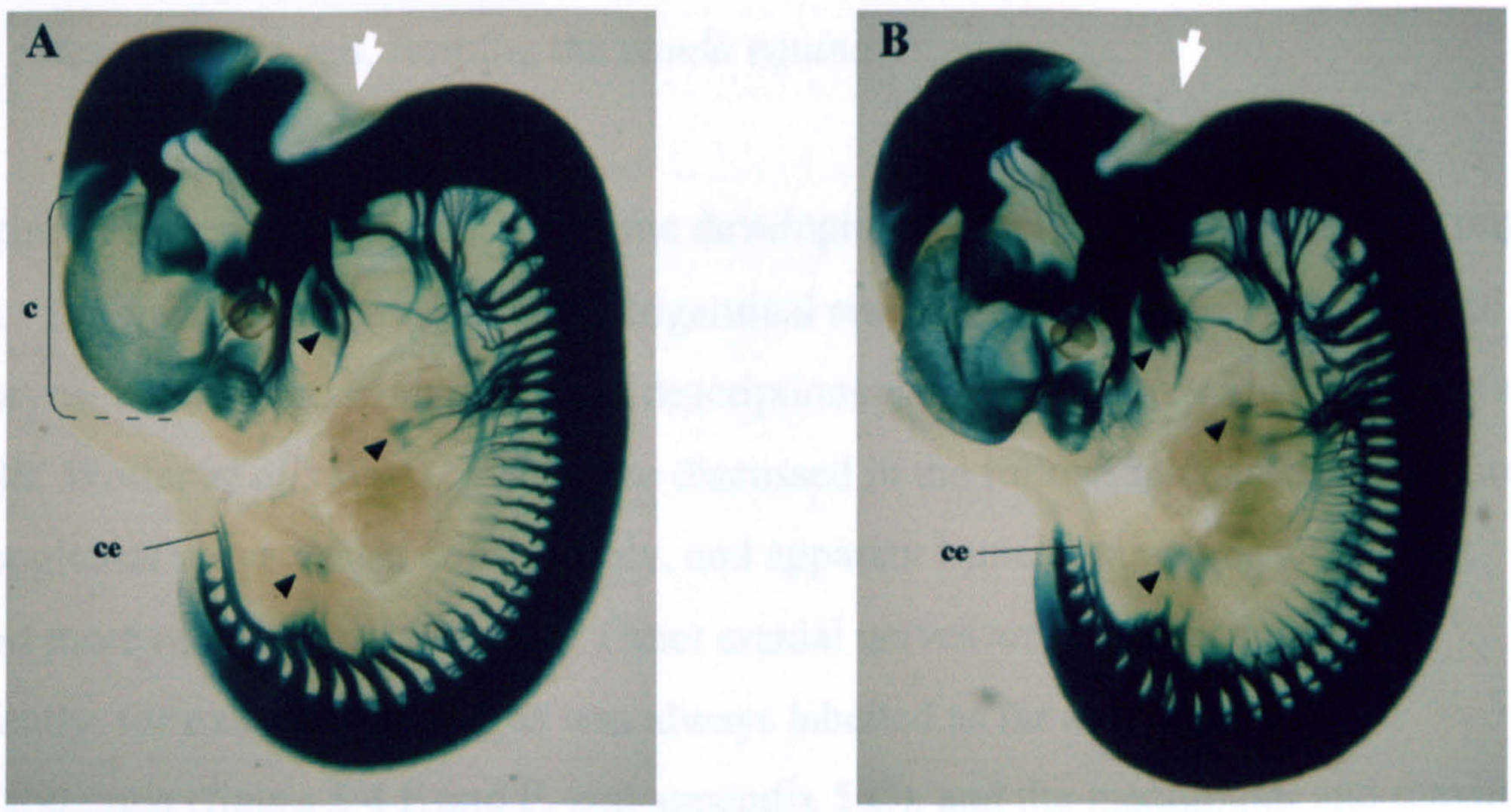

Figure 5.4 Expression of tau-ß-galactosidase protein in E12.5 mouse embryos with the *TAG-1* null mutation. A-B: whole embryos; C-D: head and neck regions; E-F: transverse sections through E12.5 embryos at the thoracic level. In each case, heterozygous embryos are on the left, homozygous embryos on the right. For abbreviations, see table 5.1 or appendix 5.A. White arrows in A and B indicate the direction from which the photographs of figure 5.5 were taken. Arrowheads in A and B point to regions of non-neuronal expression within the developing mandible and limbs. Note that the clearing procedure (see methods) means that staining on both sides of the embryo can be seen at once. Transverse sections from other rostro-caudal levels are shown in appendix 5.C.

and intercostal/subcostal branches of ventral rami. In addition, spinal nerves were often seen to extend into the tail, forming the *cauda equina.*

The entire rhombencephalon, including the developing cerebellum and pons, was strongly stained. The hypoglossal, vagal, facial, trigeminal and oculomotor nerves were stained in all embryos, as expected from published descriptions of TAG-1 expression (Yamamoto *et al.*, 1986; Wolfer *et al.*, 1994). As will be discussed in the following chapter, the nature of the hypoglossal nerve varied considerably, and apparent truncation and/or misrouting occurred more often in homozygotes. Other cranial nerves were stained relatively consistently: for example, the vagus was always labelled as far as the lower thorax/abdomen (figure 5.4 E and F, and appendix 5.C), and the mandibular and maxillary branches of the trigeminal nerve were seen to extend into their respective target areas.

Within the midbrain, the tegmentum, including oculomotor and interpeduncular nuclei, contained ß-galactosidase activity. The oculomotor nerve was still stained, and the trochlear nerve was usually also labelled, presumably as it began to accumulate sufficient ß-galactosidase. The superior colliculus was stained in all cases. The inferior colliculus was usually also labelled, although this region seemed to contain less staining than the superior colliculus (figure 5.4 C and D). This observation is in accordance with reports that the superior colliculus is more TAG-1 immunoreactive than the inferior colliculus at this age (Wolfer *et al.*, 1994). A band of staining connecting the mesencephalon and diencephalon might correspond to the mammilothalamic tract, which has been reported to express TAG-1 protein at E12 (Wolfer *et al.*, 1994). Dorsal to this were radially projecting axons that could constitute the *stria medullaris*, a tract that covers the surface of the thalamus and which is known to begin to express TAG-1 between E12 and E13 (Wolfer *et al.*, 1994). In accordance with reported TAG-1 expression, the lateral hypothalamus was stained (Wolfer *et al.*, 1994). So too was an area just below it, which may correspond to part of the forming pituitary gland (figure 5.4 C and D).

Punctate staining was observed across the cerebral cortices, in agreement with reports that cortical TAG-1 expression begins at E12 to E13 (Wolfer *et al.*, 1994). The olfactory epithelium was still labelled, again in accordance with previous findings (Wolfer *et al.*, 1994). In addition, staining was observed within the mandibular process (arrowed in figure 5.4 A and B). This staining could not be attributed to the mandibular division of the trigeminal nerve, and may have been in Meckel's cartilage or a developing salivary gland. Similar mesenchymal staining was seen within the limbs (arrowed in figure 5.4 A and B), and again this could correspond to cartilage. Neither limb nor mandibular mesenchyme has previously been reported to express TAG-1.

There were no obvious differences between whole homozygous (n=22) and heterozygous (n=65) embryos at E12.5 (figure 5.4). This was also the case when transverse sections were compared (figure 5.4 E and F; appendix 5.C). The extension of DRG axons away from the notochord (figure 5.4 E and F), and the migration of the facial nerve nucleus (figure 5.5), both appeared to be unaffected by the *TAG-1* null mutation. The possible disruption of hypoglossal nerve development will be discussed in chapter 6.

5.3.1.4 E13.5 embryos

At E13.5, most of the nervous system appeared to express tau-ß-galactosidase (figure 5.6). As would be predicted from descriptions of TAG-1 expression (Yamamoto *et al.*, 1986; Wolfer *et al.*, 1994), the dorsal spinal cord stained strongly. So too did the dorsal root ganglia, making it difficult to determine whether the ventral spinal cord was also still labelled in the whole embryos. Spinal nerves, including both dorsal and ventral rami, were still strongly stained, and the *cauda equina* could be identified in all embryos. At limb levels, segmental nerves could be seen to have formed plexuses, and stained nerves had begun to extend from these into the limbs (figure 5.6 E and F).

The rhombencephalon was still stained. In caudal regions, which correspond to the medulla oblongata, the intensity of stain appeared to be lower than at E12.5. However, the

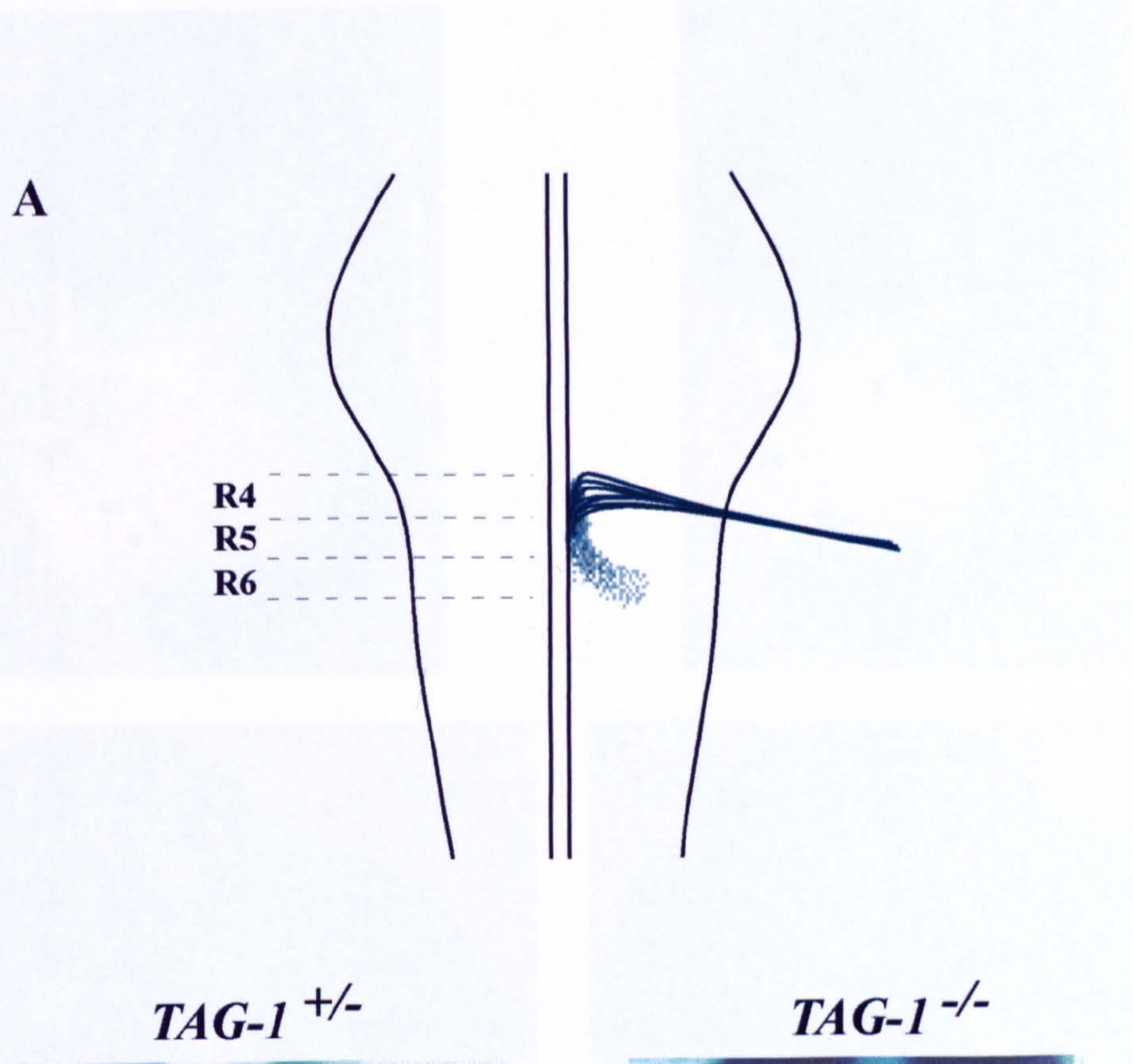

Figure 5.5 Comparison of the facial nerve nucleus of E12.5 mouse embryos either heterozygous or homozygous for the *TAG-1* null mutation. E12.5 mouse embryo hind-brains are shown as viewed from above, as indicated in figure 5.4.
A: The mouse facial nerve nucleus at E12.5, (after Garel *et al.*, 2000). Once in rhombomere 6 (R6), the facial nerve cell bodies migrate laterally. This appears to occur normally in the absence of TAG-1 (compare B and C).

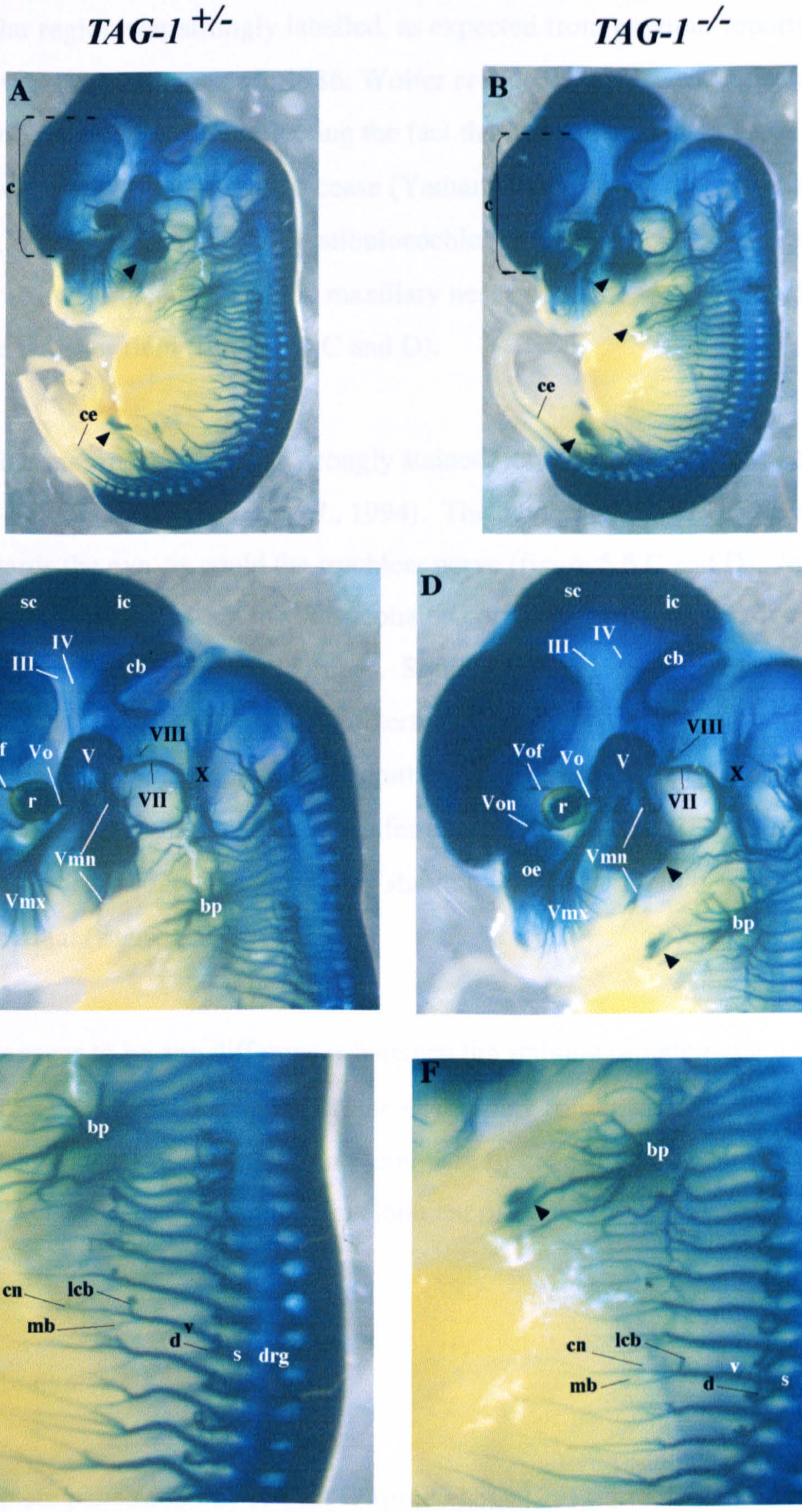

Figure 5.6 Expression of tau-ß-galactosidase protein in E13.5 mouse embryos with the TAG-1 null mutation. Heterozygous embryos are on the left, and homozygous embryos on the right, in each case. Arrowheads indicate patches of non-neuronal ß-galactosidase activity in the jaw and limbs. The patches are fainter in the heterozygous embryo as they contain less ß-galactosidase protein. For abbreviations, see table 5.1 or appendix 5.A.

future cerebellar region was strongly labelled, as expected from previous reports of TAG-1 immunoreactivity (Yamamoto *et al.*, 1986; Wolfer *et al.*, 1994). The hypoglossal nerve was not always evident, possibly reflecting the fact that the expression of TAG-1 by hypoglossal axons has been reported to cease (Yamamoto *et al.*, 1986), or at least lessen (Wolfer *et al.*, 1994) at this age. The vestibulocochlear (VIIIth cranial), facial and trigeminal nerves were labelled, and the maxillary nerve could be seen to branch profusely over the future whisker field (figure 5.6 C and D).

All of the visible mesencephalon was strongly stained, reflecting the fact that both colliculi express TAG-1 at this time (Wolfer *et al.*, 1994). The oculomotor nerve could be seen extending towards the eye, as could the trochlear nerve (figure 5.6 C and D). Structures expressing ß-galactosidase within the diencephalon could not be identified, due to intense labelling of the surrounding cerebral cortices. Similarly, the precise expression pattern of deep telencephalic structures could not be determined, as embryos were not sectioned. Staining could be seen within the olfactory epithelium and retina, as expected from their expression of TAG-1 protein at this age (Wolfer *et al.*, 1994). As at E12.5, the E13.5 limbs and mandibular process contained patches of staining that appeared to be mesenchymal rather than neuronal (figure 5.6, arrowed).

There did not appear to be any differences between the staining of heterozygote (n=9) and homozygote (n=5) embryos. In particular, the developing forelimbs had almost indistinguishable patterns of nerve staining (compare figure 5.6 E and F), making it seem unlikely that TAG-1 is essential for the development of mouse limb innervation prior to E13.5.

5.3.1.5 E16.5 brains

To allow complete penetration by X-gal (Whiting *et al.*, 1991), and to better observe the resulting staining, E16.5 brains were dissected out and stained in isolation. As can be seen

in figure 5.7, a number of different regions of the E16.5 brain contained ß-galactosidase activity.

Within the hindbrain, several cranial nerve nuclei were stained. These included what appeared to correspond to the hypoglossal, vestibular, cochlear, facial and trigeminal nerve nuclei (figure 5.7). These nuclei have all been reported to express TAG-1 mRNA in the adult rat brain (Yoshihara *et al.*, 1995). While the respective cranial nerve axons all express TAG-1 protein at around this age (Yamamoto *et al.*, 1986; Wolfer *et al.*, 1994), the expression of TAG-1 by embryonic cranial nerve nuclei has not been examined previously.

The inferior olive and superior olive /trapezoid body were also found to contain tau-ß-galactosidase at E16.5. As was the case for that of the cranial nerve nuclei, this staining could not be compared with previous reports of TAG-1 immunoreactivity. The inferior olive is known to express TAG-1 mRNA in the adult rodent brain (Yamamoto *et al.*, 1986), but its embryonic of TAG-1 expression has not been recorded; expression of TAG-1 by the superior olive does not seem to have been examined at any age. The grey nucleus of the pons was strongly stained, and it appeared that other pontine nuclei might also have been expressing tau-ß-galactosidase (figure 5.7). In addition it seems likely that part of the staining of this region included the cerebral peduncle, which is known to express TAG-1 protein at E16.5 (Wolfer *et al.*, 1994). The forming cerebellum appeared to express ß-galactosidase posteriorly and superficially, but otherwise showed very little staining, as expected from the finding that cerebellar expression of TAG-1 is relatively low at this time (Yamamoto *et al.*, 1986; Wolfer *et al.*, 1994).

The superior and inferior colliculi of the midbrain were both stained, reflecting previous reports of their TAG-1 immunoreactivity (Yamamoto *et al.*, 1986; Wolfer *et al.*, 1994). In the pre-tectal area, staining appeared to include that of the posterior commissure, which is known to express TAG-1 at E16 (Wolfer *et al.*, 1994). Ventrally, the tegmentum contained staining that is likely to correspond to the cerebral peduncle and the interpeduncular nucleus. The red nucleus could also be identified. Although these two nuclei have not

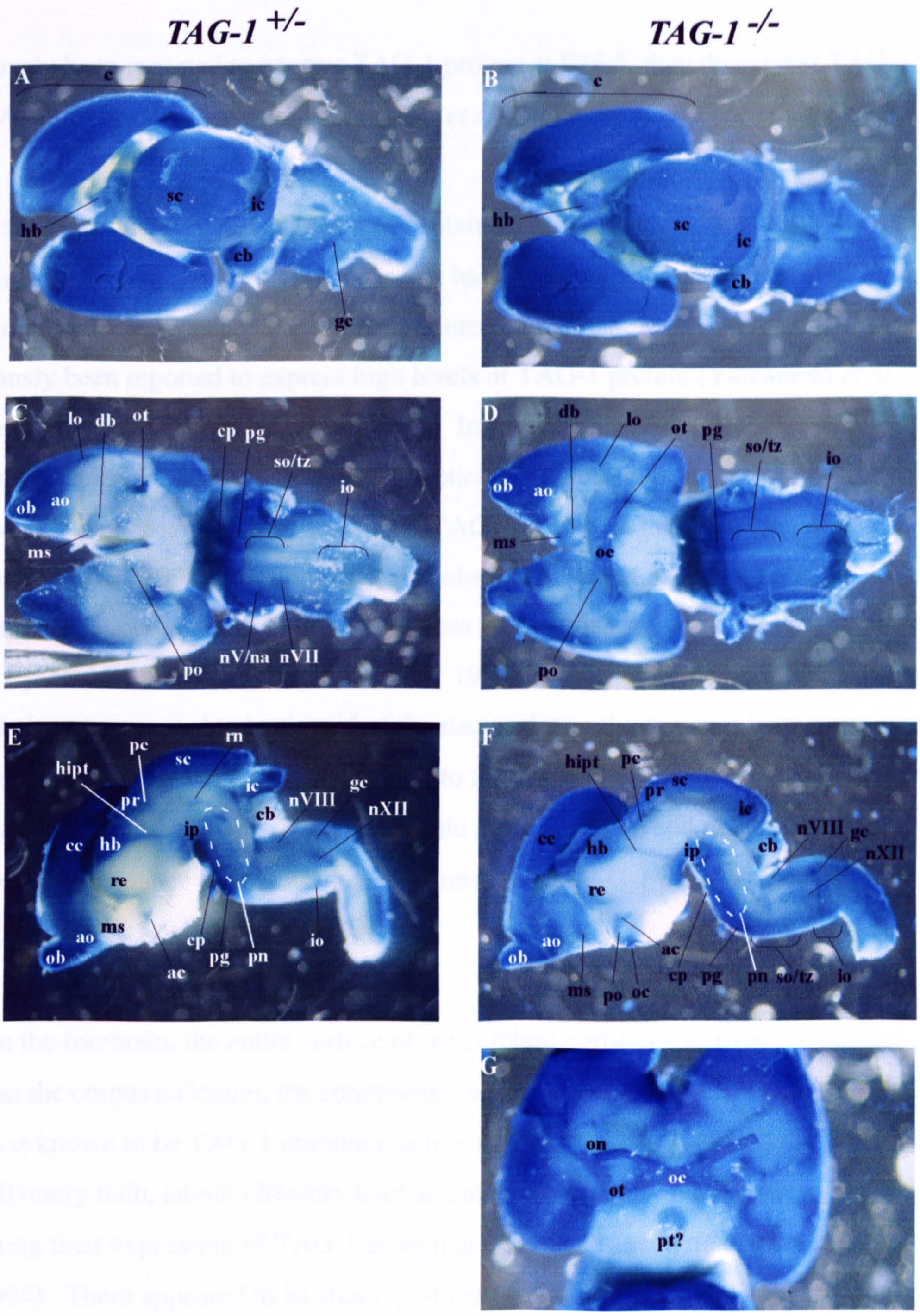

Figure 5.7 Expression of the tau-ß-galactosidase protein in the brains of E16.5 mouse embryos with the *TAG-1* mutant allele. Structures which stained for ß-galactosidase activity are labelled as indicated in table 5.1 and appendix 5.A. A-B: superior aspect. C-D: inferior aspect. E-F: view from the cut surface after sagittal bisection. G: A different TAG-1 -/- brain, illustrating staining of the intact optic nerve, chiasm and tract, and also staining that may correspond to the proximal pituitary.

previously been reported to express TAG-1 protein at E16.5, they do express TAG-1 mRNA in the adult rodent brain (Yoshihara *et al.*, 1995).

The habenular nuclei of the thalamus were stained, as was the tract that connects the habenula to the interpeduncular nucleus, the habenulointerpeduncular tract (HIPT, or *fasciculus retroflexus*). The habenular and interpeduncular nuclei and the HIPT have previously been reported to express high levels of TAG-1 protein (Yamamoto *et al.*, 1986; Wolfer *et al.*, 1994; Yoshihara *et al.*, 1995). In addition, there was staining within a structure that might either be the thalamic reticular nucleus or reuniens nucleus. Both of these nuclei have been reported to express TAG-1 mRNA in the adult rodent brain (Yoshihara *et al.*, 1995). Staining was also observed in what appeared to be the pre-optic region of the hypothalamus, although this area was not listed amongst those that expressed TAG-1 protein at E16 or E17 (Wolfer *et al.*, 1994). Posterior to the optic chiasm the hypothalamus appeared to be devoid of ß-galactosidase activity, apart from a small region that may have connected the hypothalamus to the pituitary gland before dissection. When not removed during brain dissection, the optic nerves, chiasm and tracts were strongly stained, in accordance with their intense expression of TAG-1 protein at E16.5 (figure 5.7 G; Wolfer *et al.*, 1994).

Within the forebrain, the entire surface of the cerebral cortices was strongly labelled. So too was the corpus callosum, the commissure which links the two cerebral hemispheres and which is known to be TAG-1 immunoreactive from E16 onwards (Wolfer *et al.*, 1994). The olfactory bulb, lateral olfactory tract and anterior olfactory nucleus were also stained, reflecting their expression of TAG-1 protein at this age (Yamamoto *et al.*, 1986; Wolfer *et al.*, 1994). There appeared to be staining of the medial septum and diagonal band, both of which have been reported to express TAG-1 mRNA in the adult rodent brain (Yoshihara *et al.*, 1995). Other components of the septum might also have been stained, although the extent and intensity of labelling in the septal area meant that it was difficult to identify individual structures with certainty.

There did not appear to be any gross differences between *TAG-1* null heterozygous (n=3) and homozygous (n=4) E16.5 brains. The red nucleus is evident in the heterozygote brain shown in figure 5.7 E, but not in the homozygote embryo shown in figure 5.7 F. However, this nucleus was identified in other homozygotes, and could not be identified in the two other heterozygous brains. This indicates that the apparent absence this nucleus, or of staining within it, is not related to an absence of TAG-1 protein. Staining of more E16.5 brains would be needed to confirm this.

Another structure that could have been affected by the *TAG-1* null mutation is the HIPT. This appeared to be less strongly stained in homozygous brains, which is contrary to the observation that two copies of the mutant allele lead to more intense staining. This apparent reduction in staining was common to all four of the E16.5 *TAG-1* null homozygote brains examined.

5.3.2 Post-natal neural development of *TAG-1* mutant brains

5.3.2.1 P2 brains

Figure 5.8 illustrates the pattern of ß-galactosidase activity in the brains of P2 mice that carried the *TAG-1* null mutation. Within the medulla oblongata, the superior olivary and facial nerve nuclei were identified, although no other structures could be distinguished from the general staining throughout the rhombencephalon. The grey and anterior nuclei of the pons were labelled. A report of TAG-1 immunoreactivity within the P2 cerebral peduncle (Wolfer *et al.*, 1994) makes it seem likely that this tract also contributes to the staining of the anterior pontine area. While the P2 rhombencephalon has been reported to be TAG-1 immunoreactive (Wolfer *et al.*, 1994), hindbrain nuclei have not previously been considered individually, so it was not possible to compare their expression of tau-ß-galactosidase with that of native TAG-1 protein.

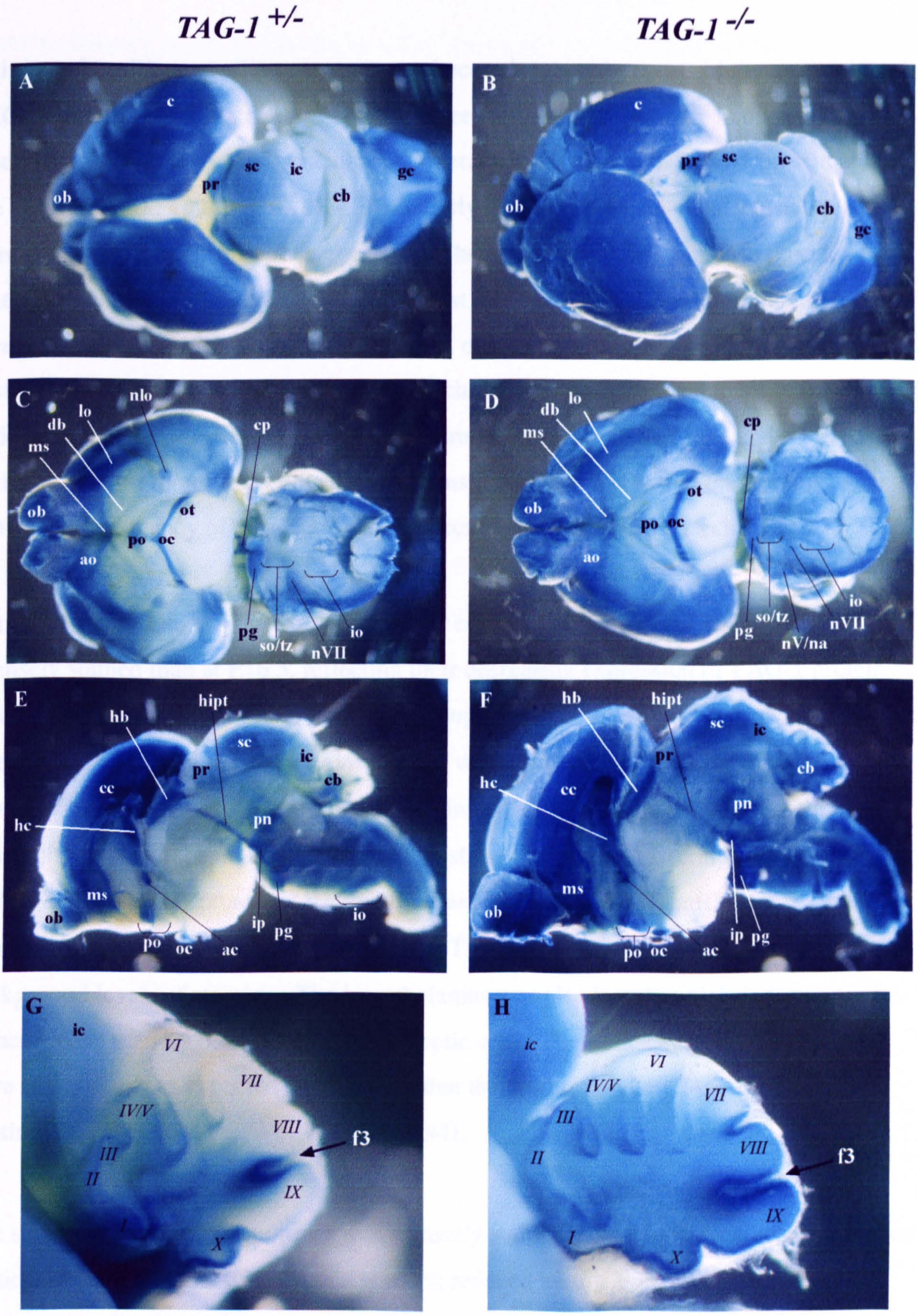

Figure 5.8 Expression of the tau-ß-galactosidase protein in the brains of P2 mice with the *TAG-1* null mutant allele. A-B: superior aspect. C-D: inferior aspect. E-F: view from the cut surface, following the "redevelopment" of sagittally bisected brains. G-H: sagittally bisected cerebella, showing the intense staining of fissure 3 (f3). Italicized Roman numerals indicate the developing cerebellar lobules. For abbreviations see table 5.1 or appendix 5.A.

Staining of the P2 cerebellum was in general accordance with reports of the expression of TAG-1 protein (Yamamoto *et al.*, 1986; Wolfer *et al.*, 1994). Labelling appeared to be predominantly in the external granule cell layer, as is the case with TAG-1 protein at this age (Wolfer *et al.*, 1994). However, particularly high levels of tau-ß-galactosidase activity were observed in the posterior cerebellum, a phenomenon that has not been reported for TAG-1 protein or mRNA at any age. The most intense labelling was around fissure 3, or *fissure secundum*, which separates lobule VIII of the central lobe from lobule IX of the posterior lobe (Altman and Bayer, 1997). Such staining was observed in all of the P2 brains examined (n=9), yet was not seen in cerebella that expressed *lacZ* under the control of the *math-1* promoter (data not shown). Thus it seems unlikely that the staining reflects a non-specific tendency of ß-galactosidase to accumulate within this fissure.

Within the midbrain, the superior and inferior colliculi were stained. They were less intensely stained than at E16.5, reflecting their decreasing expression of TAG-1 protein (Wolfer *et al.*, 1994). The pretectum was strongly stained, as was the interpeduncular area. The red nucleus may have been stained, but it was difficult to distinguish this structure from anterior pontine nuclei and low level staining throughout the tegmentum. In the diencephalon, the habenular nuclei and HIPT stained strongly, reflecting their expression of high levels of TAG-1 protein at P2, and their expression of TAG-1 mRNA in the adult (Wolfer *et al.*, 1994; Yoshihara *et al.*, 1995). The rest of the thalamus showed only background levels of staining. The hypothalamus was also largely unlabeled, its only ß-galactosidase activity being within the pre-optic area. The optic chiasm and optic tract were still stained, as expected from reports that their expression of TAG-1 protein continues until at least P6 (Wolfer *et al.*, 1994).

The surface of the cerebral cortices was intensely stained, despite the previous finding that cortical expression of TAG-1 protein is much reduced by this time (Wolfer *et al.*, 1994). The corpus callosum and anterior commissure were both stained strongly, as expected from their continued robust expression of TAG-1 protein (Wolfer *et al.*, 1994). In addition, the hippocampal commissure was stained. The olfactory bulbs were labelled, as were the

anterior olfactory nuclei and lateral olfactory tracts, all of which express TAG-1 protein at P2 (Wolfer *et al.*, 1994). Septal nuclei were stained strongly, although the diagonal band of the septum was not as prominent as at E16.5 (compare figures 5.7 C and D and 5.8 C and D).

As shown in figure 5.8, there were no major differences between the brains of P2 heterozygous and homozygous *TAG-1* null mutant mice (n=6 and n=3 respectively).

5.3.2.2 P15 brains

Figure 5.9 illustrates the expression of tau-ß-galactosidase in P15 brains. At this age, much of the hindbrain stained for ß-galactosidase activity. The inferior olivary, gracile/ cuneate, hypoglossal and pontine grey nuclei were all apparent. Although the rhombencephalon has been reported to be devoid of TAG-1 immunoreactivity at this age (Wolfer *et al.*, 1994), the adult hypoglossal nucleus and inferior olive have been reported to express TAG-1 mRNA (Yoshihara *et al.*, 1995). Other rhombencephalic nuclei could not be identified, as much of the region was stained (figure 5.9 G and H). It may be that this staining corresponded to ß-galactosidase activity within raphe nuclei that lie along the sagittal midline of the hindbrain, although such nuclei have not previously been reported to express TAG-1. Within the cerebellum, the external granular layer was particularly strongly stained, reflecting its strong expression of both TAG-1 protein and mRNA (Furley *et al.*, 1990; Wolfer *et al.*, 1994; Yoshihara *et al.*, 1995).

Within the P15 mesencephalon, it was again difficult to identify individual structures on account of substantial "background" staining. Both the superior and inferior colliculi were labelled, with the inferior colliculus appearing to be more intensely stained (figure 5.9 A and B). Expression of TAG-1 protein by these areas has previously been reported to cease soon after birth (Wolfer *et al.*, 1994), although both colliculi have been reported to express TAG-1 mRNA in the adult rodent (Yoshihara *et al.*, 1995). A region of staining deep to the

TAG-1 $^{+/-}$ *TAG-1* $^{-/-}$

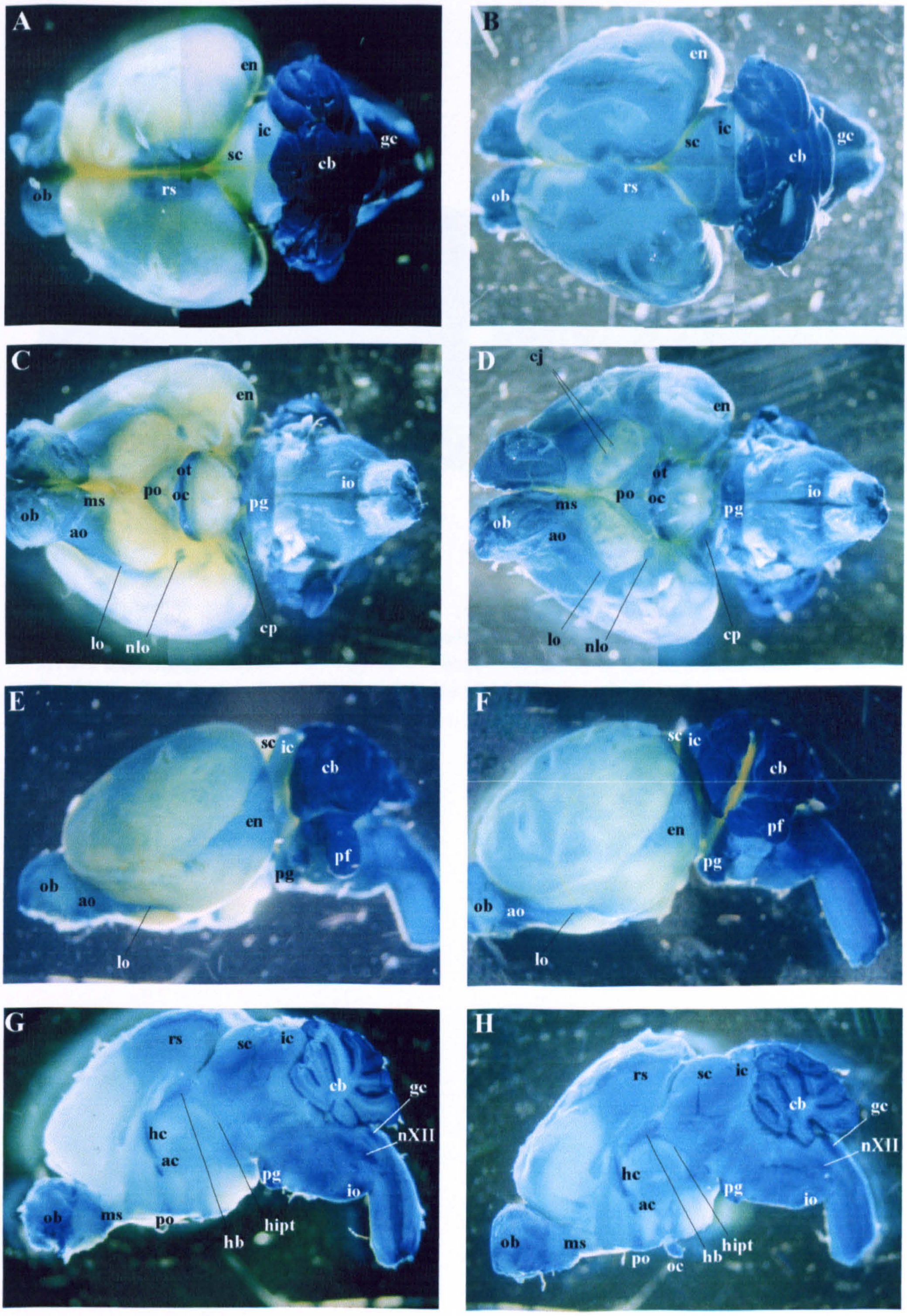

Figure 5.9 Expression of the tau-ß-galactosidase protein in the brains of P15 mice with the *TAG-1* null mutant allele. Structures which stained for ß-galactosidase activity are labelled as indicated in the summary list overleaf. A-B: superior aspect. C-D: inferior aspect. E-F: lateral aspect. G-H: medial aspect, after sagittal bisection. For abbreviations, see table 5.1 or appendix 5.A.

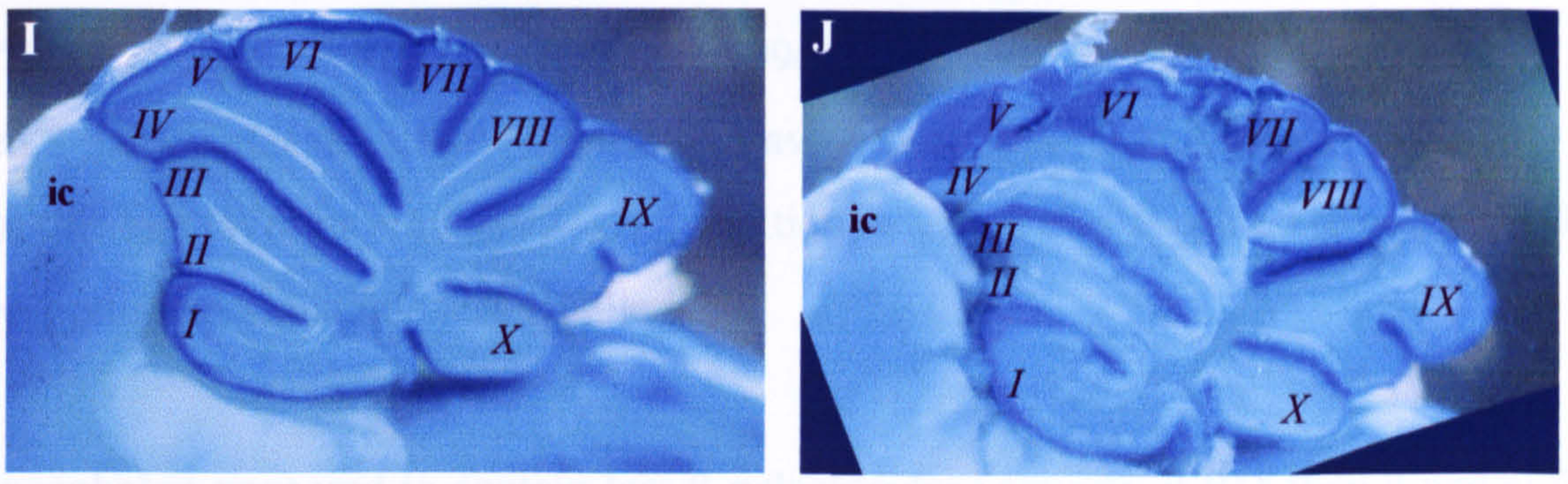

Figure 5.9 Expression of the tau-ß-galactosidase protein in the brains of P15 mice with the *TAG-1* null mutant allele. I-J: sagittally bisected cerebella; italicized Roman numerals indicate the developing lobules. For abbreviations, see table 5.1 or appendix 5.A.

tectum might correspond to peri-aqueductal (or central) grey matter, which is also known to express TAG-1 mRNA in the adult rodent brain (Yoshihara *et al.*, 1995).

The habenular nucleus and HIPT were also stained. The nucleus is known to express TAG-1 mRNA in the adult rodent (Yoshihara *et al.*, 1995), although the tract is not thought to express TAG-1 protein at P15 (Wolfer *et al.*, 1994). The optic chiasm and tract also contained ß-galactosidase activity, the former having been reported to express TAG-1 protein at this age (Wolfer *et al.*, 1994). In addition, a region that appeared to correspond to the pre-optic hypothalamus was labelled.

The telencephalon appeared to contain less ß-galactosidase activity at P15 than it had at P2. All regions of the cerebral cortex showed diffuse staining, but intense staining was restricted to the retrosplenial cortex, and what appears to be the entorhinal cortex. The retrosplenial, or posterior cingulate, cortex is known to express TAG-1 protein until P6 (Wolfer *et al.*, 1994), and to express TAG-1 mRNA in the adult rodent (Yoshihara *et al.*, 1995). However, the entorhinal cortex appears not to express TAG-1 mRNA in the adult (Yoshihara *et al.*, 1995). The anterior and hippocampal commissures could be identified, reflecting expression of TAG-1 protein, at least by the former, at P15 (Wolfer *et al.*, 1994).

The olfactory bulb, the lateral olfactory tract and its nucleus, and the anterior olfactory nucleus all contained ß-galactosidase activity, even though their surface expression of TAG-1 protein ceases before P15 (Wolfer *et al.*, 1994). Expression of TAG-1 mRNA by the adult olfactory bulb has been reported previously, although expression by the tract and nuclei were not mentioned (Yoshihara *et al.*, 1995). The olfactory tubercle has also been reported to express TAG-1 mRNA in the adult rat (Yoshihara *et al.*, 1995), and this area was indeed found to be stained, although ß-galactosidase activity appeared to be restricted to clusters of cells known as Islands of Cajella, rather than being throughout the tubercle. This was particularly evident in brains with two copies of the *tau-lacZ* reporter gene (figure 5.9 D). What appears to be the medial septum was also stained.

There were no obvious differences between the brains from *TAG-1* null heterozygous and homozygous P15 mice (n=13 and n=8 respectively; figure 5.9).

5.3.3 Use of the *TAG-1* null allele to study other mutant embryos

5.3.3.1 *L1* mutant embryos

The *TAG-1* null allele was also used to investigate effects of the *L1* null mutation upon TAG-1-expressing structures. As shown above, embryos with only one *TAG-1* null allele differed little, if at all, from wild type embryos (compare figure 5.2 with appendix 5.B). Therefore the *TAG-1* null heterozygous genotype was used as a "background", and embryos that were otherwise wild type were compared with those that were also hemizygous for the *L1* mutation.

As can be seen in figures 5.10 and 5.11, there were no obvious differences between whole-mount stained embryos at either E11.5 or E12.5. The staining of *L1* hemizygous embryos (n=9 at E11.5; n=1 at E12.5) was indistinguishable from that of embryos that carried only one copy of the *TAG-1* null allele (n=5 at E11.5; n=4 at E12.5). Spinal nerves, the brachial plexus, and the oculomotor, trigeminal, facial, glossopharyngeal, vagal and hypoglossal nerves all appeared to be developing normally in the absence of L1 protein (for a more detailed analysis of the hypoglossal nerves of these embryos, see chapter 6). Staining of the mid-brain also appeared to be unaffected by the absence of L1. These results are in agreement with those obtained by whole-mount immunohistochemistry (appendix 5.D).

5.3.3.2 *TAG-1/L1* double mutant embryos

TAG-1 null heterozygote "control" embryos were also compared with those that were both hemizygous for the *L1* mutation and that carried two mutant *TAG-1* alleles ($L1^{-/Y}$, $TAG^{-/-}$).

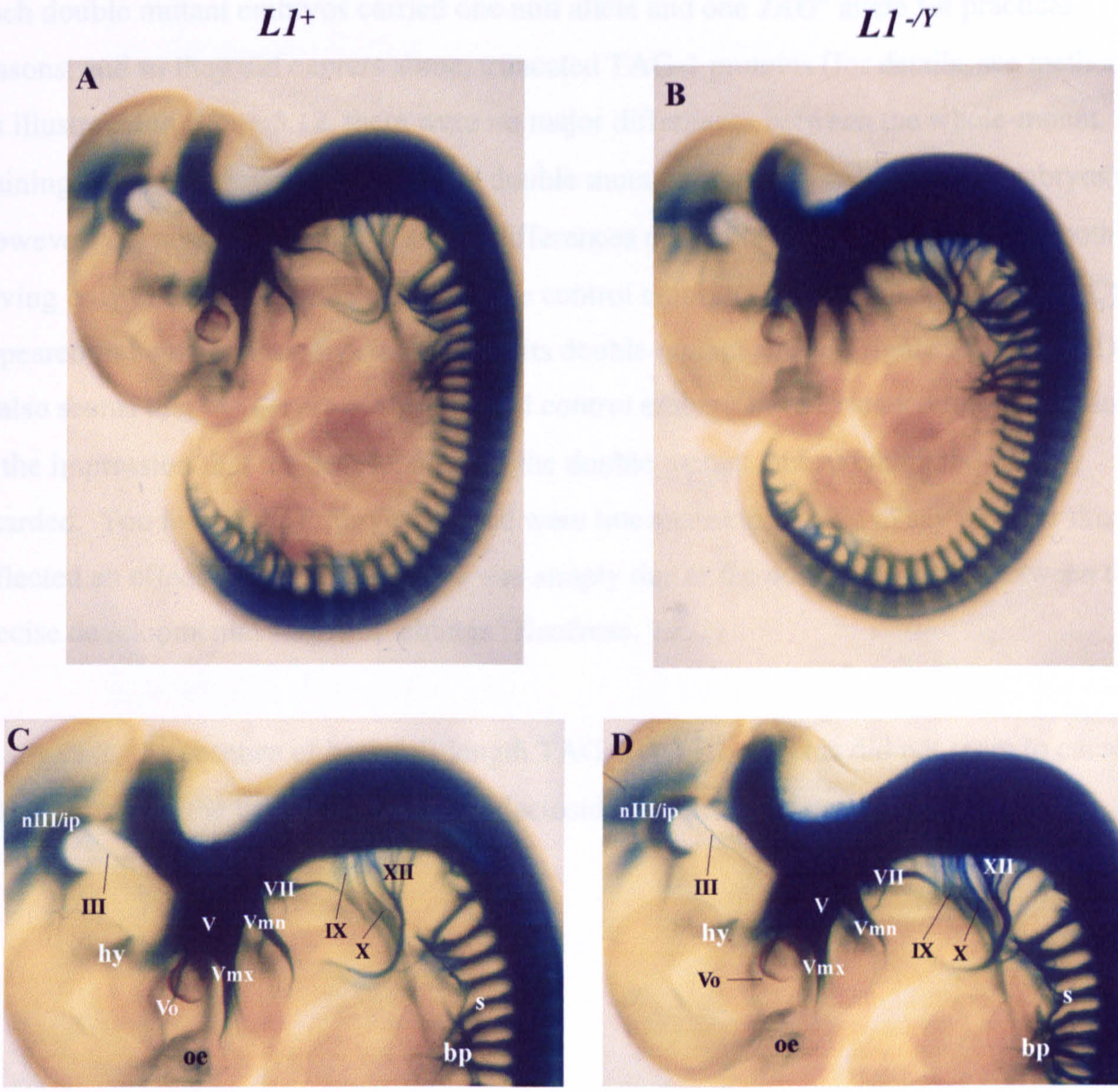

Figure 5.10 Comparison of E11.5 *L1*$^{+}$ and *L1*$^{-/Y}$ mouse embryos using the *tau-lacZ* component of the *TAG-1* null mutation. Embryos either hemizygous or wild type for the *L1* null mutation, and also heterozygous for the *TAG-1* null mutation, were stained for ß-galactosidase activity. The *L1* mutation does not obviously affect the development of TAG-1-expressing structures. A-B: whole embryos. C-D: head and neck regions. For abbreviations, see table 5.1 or appendix 5.A.

Such double mutant embryos carried one null allele and one *TAG*^{A} allele for practical reasons, and so they did express some, truncated TAG-1 proteins (for details, see methods). As illustrated in figure 5.12, there were no major differences between the whole-mount staining of such embryos at E11.5 (n=9 double mutants embryos, n=11 control embryos). However, the possibility of more subtle differences could not be ruled out. Despite both having only one *lacZ*–containing allele, the control embryo shown (figure 5.12 A and C) appeared to be more strongly stained than its double mutant sibling (figure 5.12 B and D). It also seems that the nerves of the pictured control embryo have extended further, adding to the impression that the development of the double mutant embryo might be slightly retarded. Too few of the embryos studied were littermates to be able to say whether this reflected an effect of the mutations, or was simply due to the normal variation between the precise developmental stages of siblings (Kaufman, 1992).

In any case, the absence of both full-length TAG-1 and L1 proteins did not seem to cause major defects in the development of ß-galactosidase expressing structures at E11.5.

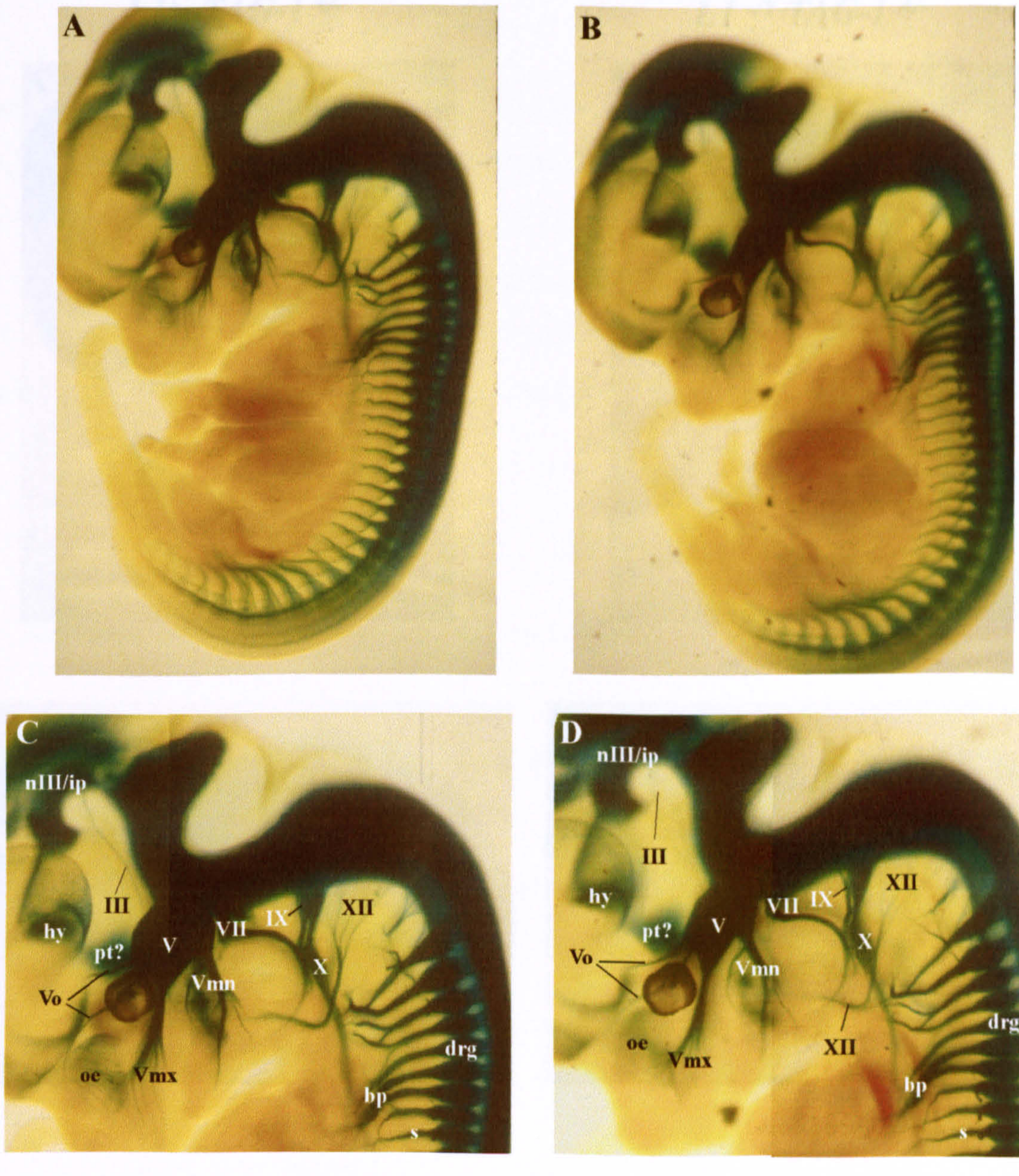

Figure 5.11 Comparison of E12.5 *L1*$^{+}$ and *L1*$^{-/Y}$ mouse embryos using the *tau-lacZ* component of the *TAG-1* null mutation. As at E11.5, there are no obvious differences between the TAG-1-expressing structures of *L1* wild type and *L1* hemizygous mutant embryos. A-B: whole embryos. C-D: head and neck regions. For abbreviations, see table 5.1 or appendix 5.A.

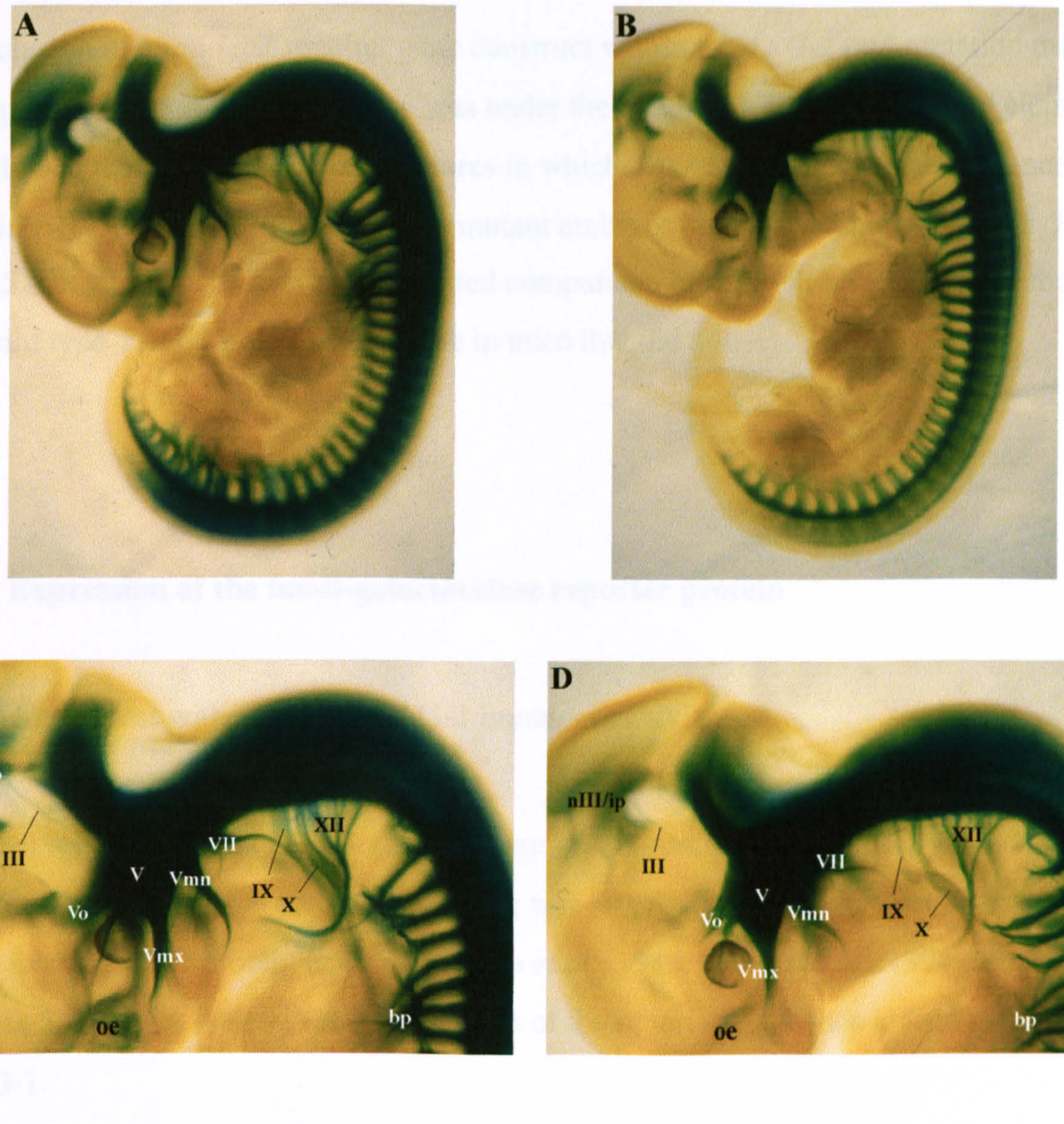

Figure 5.12 Comparison of E11.5 *L1*$^{+}$,*TAG-1* $^{+/-}$ and *L1*$^{-/Y}$, *TAG-1* $^{A/-}$ mouse embryos. Embryos carrying one copy of the *TAG-1* null allele express both wild type TAG-1 protein and tau-ß-galactosidase in structures that normally express TAG-1. Otherwise wild type embryos were compared with those that had no full length TAG-1 or L1 protein. Double embryos did not appear to differ from those heterozygous for the *TAG-1* mutation only. A-B: whole embryos. C-D: head and neck regions. For abbreviations, see table 5.1 or appendix 5.A.

5.4 Discussion

The inclusion of a *tau-lacZ* reporter gene construct within the *TAG-1* null mutation meant that expression of tau-ß-galactosidase was under the control of *TAG-1* regulatory elements. This allowed the identification of structures in which *TAG-1* regulatory gene sequences are active in E10.5, E11.5, E12.5 and E13.5 mutant embryos, and in the brains of E16.5, P2 and P15 mutant mice. It also and permitted comparison of these structures in mice that did have wild type TAG-1 protein with those in mice that did not.

5.4.1 Expression of the tau-ß-galactosidase reporter protein

5.4.1.1 Agreement with reports of TAG-1 immunoreactivity

The observed expression of tau-ß-galactosidase is summarised in table 5.1. As mentioned throughout section 5.3, the pattern of staining was largely in agreement with reports of the expression of TAG-1 protein (e.g. Yamamoto *et al.*, 1986; Wolfer *et al.*, 1994; see also appendix 5.B). This indicates that expression of the reporter gene does indeed reflect that of TAG-1.

5.4.1.2 The absence of staining in neurons previously reported to express TAG-1 protein

In general, structures previously reported to express TAG-1 protein were also found to contain ß-galactosidase activity. However, at least one TAG-1-immunoreactive structure could not be identified. The trochlear (IVth cranial) nerve was not stained for ß-galactosidase activity until E12.5, even though it has previously been reported to express TAG-1 antigens at E11 (Yamamoto *et al.*, 1986). The reason for this discrepancy is not

Table 5.1 Summary of the expression of tau-ß-galactosidase in mice with the *TAG-1* null mutation. The presence of ß-galactosidase activity within a structure is indicated by red shading, the strength of the colour reflecting the intensity of the stain. White represents a lack of expression of ß-galactosidase by a structure, or lack of the structure, at a particular age. The absence of a box signifies that the structure was either not tested, or could not be identified because of other staining in the vicinity. Abbreviations used within th chapter are given on the right, in addition to being listed alphabetically in appendix 5.A.

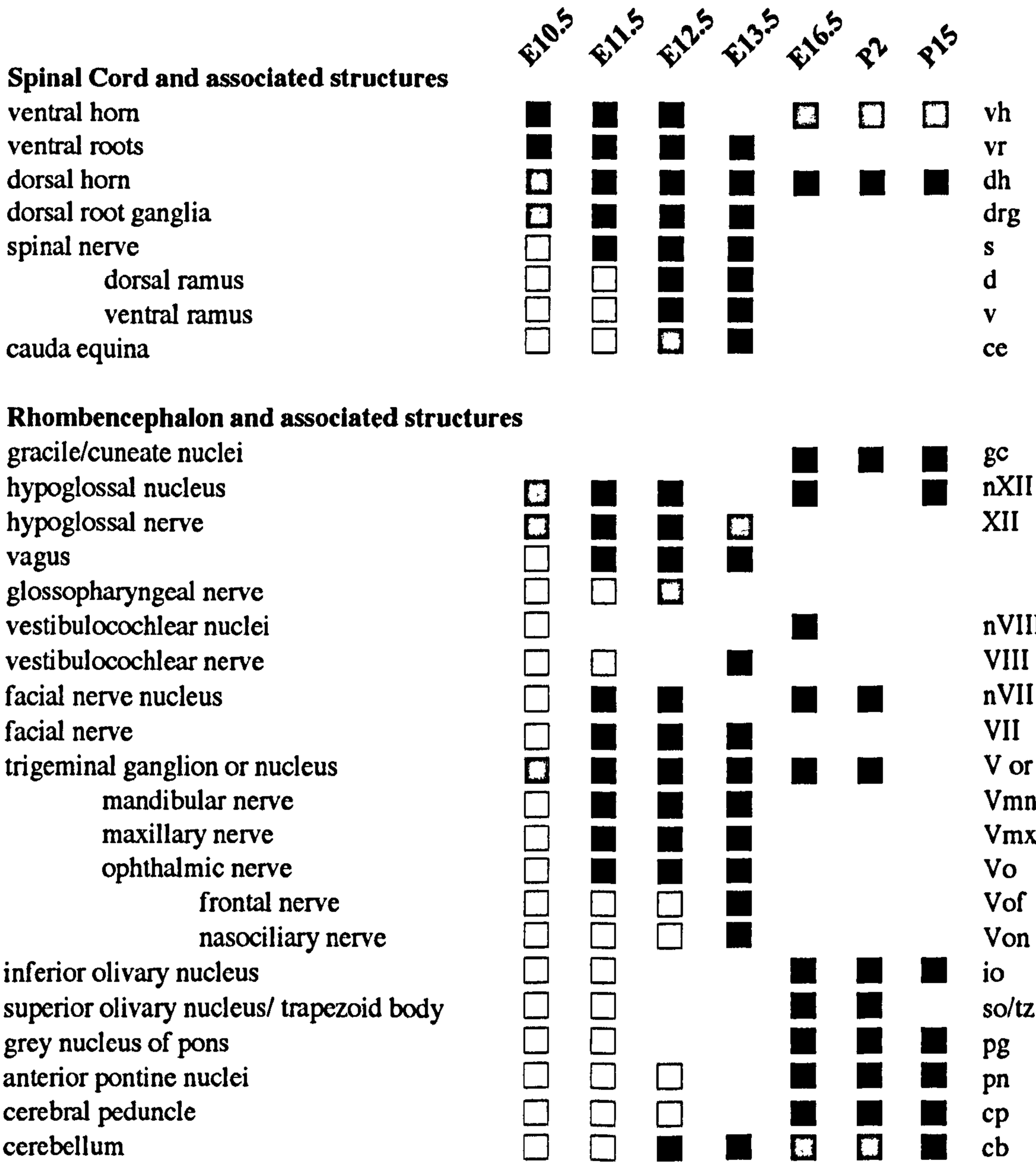

		E10.5	E11.5	E12.5	E13.5	E16.5	P2	P15	
Mesencephalon and associated structures									
tegmentum:	interpeduncular nucleus	□	▣	■	■	■	■	▣	ipn
	oculomotor nucleus	□	▣	■	■				nIII
	oculomotor nerve	□	▣	■	■				III
tectum:	superior colliculus	□	▣	■	■	■	▣	□	sc
	inferior colliculus	□	□	▣	■	■	▣	■	ic
pretectum		□	□	□	■	■	■	▣	pr
red nucleus		□				■			rn
trochlear nerve		□	□	■	▣				IV
mammilothalamic tract?		□	□	■					mt?
Diencephalon and associated structures									
habenular nucleus		□	□	□		■	■	■	hb
habenulointerpeduncular tract		□	□	□		■	■	■	hipt
reticular or reuniens nucleus		□	□	□		■	□	□	re
stria medullaris?		□	□	■					sm?
lateral hypothalamus		□	▣	■			□	□	hy
preoptic area		□	□			■	■	■	po
pituitary?		□	□	■		■	■	■	pt?
Telencephalon and associated structures									
cerebral cortex		□	□	▣	■	■	■	▣	c
corpus callosum		□	□	□		■	■	□	cc
anterior commissure		□	□	□		■	■	■	ac
posterior commissure?		□	□	□		■			pc?
hippocampal commissure		□	□	□		□	■	■	hc
olfactory epithelium		□	□	▣	■				oe
olfactory bulb		□	□			■	■	■	ob
anterior olfactory nucleus		□	□	□		■	■	■	ao
lateral olfactory tract		□	□	□		■	■	■	lo
nucleus of lateral olfactory tract		□	□	□		□	■	■	nlo
islands of Cajella		□	□	□		□	□	■	cj
medial septum		□	□	□		▣	■	▣	ms
diagonal band		□	□	□		▣	▣	□	db
entorhinal cortex		□	□	□	■	■	■	■	en
retrosplenial cortex		□	□	□	■	■	■	■	rs
retina		□	□	■	■				r
optic nerve		□	□	■	■	■			on
optic chiasm		□	□	□		■	■	■	oc
optic tract		□	□	□		■	■	■	ot

clear. It could be that the E11.5 nerve is too thin to be stained sufficiently strongly for it to be visible at low power magnification.

As far as could be determined, all other reportedly TAG-1-immunoreactive structures expressed ß-galactosidase. Structures previously reported to express TAG-1 protein could not always be identified, but this often reflected widespread, intense staining of so many neurons within an area that it was difficult to distinguish individual nuclei or tracts. This was more of a problem here than in immunohistochemical studies, as ß-galactosidase activity persists for longer than immunoreactivity (see below) and so can accumulate within an area. Other structures were not identified due to their deep location. For example, Ammon's horn of the hippocampus was found to be TAG-1 immunoreactive in coronal sections of E16 and P2 mouse brains (Wolfer *et al.*, 1994), but it lies too far from the external or mid-sagittal surfaces to have been examined during the present study. Staining of sectioned *TAG-1* null mutant brains would allow a more thorough comparison of the TAG-1 and ß-galactosidase expression patterns.

5.4.1.3 Staining of neurons not previously reported to express TAG-1 protein

In general, it seems that almost all of the structures that normally express TAG-1 protein were stained for ß-galactosidase activity. Staining was also detected in some areas not previously reported to be TAG-1-immunoreactive. For instance, the present study offers the first report of *TAG-1* gene activity within the late embryonic, and early postnatal, superior and inferior olivary nuclei. It also constitutes the first description of *TAG-1* gene activity within the developing posterior commissure, red nucleus, pretectum, neonatal septal nuclei or islands of Cajella. The present study found the superior and inferior colliculi to contain ß-galactosidase activity at P15 (figure 5.9), even though both have been reported to lose their TAG-1 immunoreactivity before either E17 (Yamamoto *et al.*, 1986) or P4 (Wolfer *et al.*, 1994), depending on which antibody was used. Similarly, the olfactory bulb, lateral olfactory tract and HIPT were found to stain for ß-galactosidase activity at P15 (figure 5.9), even though they are thought to cease to express TAG-1 protein

before this age (Wolfer *et al.*, 1994). There are a number of possible explanations for the labeling of these structures in the present, but not previous, studies.

5.4.1.3.1 Structures might express the *TAG-1* gene, but not have been examined previously

In many cases the neurons might not have actually been examined before. For example, the rhombencephalon is known to express TAG-1 protein up until around birth (Yamamoto *et al.*, 1986; Wolfer *et al.*, 1994), but its immunoreactivity had not previously been attributed to individual nuclei.

5.4.1.3.2 Structures might express the *TAG-1* gene, but not be TAG-1 immunoreactive

Stained neurons might normally express the *TAG-1* gene, but not express recognisable TAG-1 protein. The presence of TAG-1 mRNA, but an absence of immunoreactivity, has previously been demonstrated for the adult rat brain and spinal cord (Furley *et al.*, 1990). The olfactory bulb provides a more specific example: this structure ceases to be TAG-1 immunoreactive at P9 (Wolfer *et al.*, 1994), but its expression of TAG-1 mRNA persists into adulthood (Yoshihara *et al*, 1995; Wolfer *et al.*, 1998). There are several possible explanations for such differences.

It could be that the *TAG-1* gene is transcribed, but that the resulting mRNA is not translated. The mRNA might in fact be translated, but the resulting TAG-1 protein might not be recognised by antibodies. For example, it could be held within an intracellular compartment that antibodies cannot penetrate. Indeed, surface expression of the related IgCAM L1 seems to be regulated by endocytosis, with significant amounts of the protein being found within clathrin-coated vesicles (Long *et al.*, 2001). It might be that TAG-1 protein is expressed at the cell surface, but at levels too low to be detected (Furley et al., 1990), or that the protein is localised to a particular part of the cell membrane. Both axonin-1 and L1 seem to be targeted to growth cones (Vogt *et al.*, 1996; Kamiguchi and Lemmon, 1998), so it is possible that some cells bodies do express the *TAG-1* gene, but that only distant parts of the cell are normally TAG-1-immunoreactive. Alternatively, cells

might normally express an isoform of TAG-1 that is not recognised by the antibodies used. Differences in the exposure of particular epitopes have previously been suggested to explain differences between TAG-1 immunohistochemical studies (Wolfer *et al.*, 1994), and have been demonstrated for the related molecule NrCAM (Denburg *et al.*, 1995).

Another possibility is that the presence of ß-galactosidase activity reflects production of TAG-1 protein that is secreted, such that it is lost from tissue during antibody-labelling procedures. The latter is an attractive explanation, as TAG-1/axonin-1 is predominantly a secreted protein *in vivo* (Ruegg *et al*, 1989; Furley *et al.*, 1990). Indeed, dorsal spinal neurons continue to produce and secrete TAG-1 *in vitro* at stages when the protein is no longer detected at the cell surface (Dodd et al., 1988; Karagogeos *et al.*, 1991). It has been suggested that this might reflect cleavage of TAG-1 from the cell surface by endogenous phospholipase enzymes (Furley *et al.*, 1990; Karagogeos, *et al.*, 1991; Lierheimer *et al.*, 1997). Such cleavage could be physiologically important, as soluble axonin-1 can affect the guidance and fasciculation of dorsal spinal axons when applied experimentally (Stoeckli and Landmesser, 1995; Stoeckli *et al.*, 1997). There is at least one example of a secreted protein being used physiologically to control the defasciculation of axons at choice points (Fambrough and Goodman, 1996).

5.4.1.3.3 ß-galactosidase perdurance

The ß-galactosidase mRNA and protein is very stable, such that ß-galactosidase activity can persist, or "perdure", within cells. Thus reporter ß-galactosidase can be present within cells for longer than the native product of the gene sequences that drive its expression (Echelard *et al.*, 1994; Slack, 2001). Such perdurance of ß-galactosidase has been suggested to account for the staining of neural crest cells in E11.5 *wnt-1-lacZ* transgenic mice, even though the cells normally cease to express wnt-1 mRNA at E9.5 (Echelard *et al.*, 1994). Therefore perdurance could theoretically contribute to the staining of cells beyond the end of their TAG-1 immunoreactivity. However, it seems unlikely that perdurance accounts for all of this staining. The superior and inferior colliculi were found to contain ß-galactosidase activity at least eleven days after their TAG-1 immunoreactivity is thought to

cease (figure 5.9; Wolfer *et al.*, 1994), but ß-galactosidase has not been reported to persist for this long. In fact, hypoglossal nerve staining began to lessen at approximately the same time as has been reported for its TAG-1 immunoreactivity (figure 5.6; Wolfer *et al.*, 1994). This suggests that perdurance cannot explain all of the unexpectedly late staining that was observed.

5.4.1.3.4 Non-physiological activity of the *TAG-1* gene

It could be that the presence of ß-galactosidase reflects non-physiological transcription of the *TAG-1* null mutant allele. The *TAG-1* null mutation could conceivably have deleted a part of the *TAG-1* gene that normally represses its activity in certain cells. Such a deletion has been suggested to explain some of the ectopic ß-galactosidase activity in mice carrying a *GnRH* (gonadotrophin-releasing-hormone*)-lacZ* reporter transgene (Skynner *et al.*, 1999).

Chicken *NgCAM* and rat and human *L1* are known to contain sequences that can mediate repression of expression in certain cells (Kallunki *et al.*, 1995; Schoenherr *et al.*, 1996). The *L1* gene contains a neural-restrictive silencer element (NRSE), to which the neural-restrictive silencer factor (NRSF) can bind (Schoenherr *et al.*, 1996). NRSE sequences mediated suppression of NgCAM expression by non-neuronal cells *in vitro* (Kallunki *et al.*, 1995), and *L1* regulatory elements that lacked their NRSEs caused ectopic expression of *lacZ in vivo* (Kallunki *et al.*, 1997, 1998). The many regions displaying ectopic ß-galactosidase activity included limb and mandibular mesenchyme and Rathke's pouch, part of the developing pituitary gland (Kallunki *et al.*, 1997). Thus the NRSE of L1 seemed to prevent expression of L1 protein within areas that unexpectedly contained ß-galactosidase activity in the present study (see below). This raises the possibility that *TAG-1* contains an NRSE that is deleted by the *TAG-1* null mutation. Indeed, the mutation incorporates the second intron of *TAG-1*, and it is the second intron of the *L1* gene that contains its NRSE (Kallunki *et al.*, 1997). However, perturbation of the *L1* NRSE led to considerably more widespread ectopic expression than was seen here, and *TAG-1* was not among the genes identified when a DNA database was searched for NRSE -containing sequences (Schoenherr *et al.*, 1996). It could be that the *TAG-1* null mutation deleted an as yet

uncharacterised silencer element, such as that which mediates repression of TAG-1 expression by thyroid hormone (Alvarez-Dolado *et al.*, 2001).

5.4.1.4 Staining of non-neural structures

ß-galactosidase activity was also observed within the E12.5 and E13.5 mandibular process and limbs, in a pattern that has not previously been described for TAG-1 protein at any age. The possible explanations for this staining are the same as those discussed above for neuronal staining. However, the mandibular and limb staining is perhaps unlikely to reflect ß-galactosidase perdurance, as there was no appreciable staining of the jaw, limbs or cells migrating towards these regions at E10.5 or E11.5. The idea that *TAG-1* is normally transcribed in the developing jaw and limbs is supported by the observation that regulatory sequences of *TAX-1,* the human *TAG-1* gene, can also drive ß-galactosidase expression within limb mesenchyme (A.J.W. Furley, personal communication; appendix 5.E). However, the presence of TAG-1 mRNA would need to be demonstrated before the mandibular and/or limb *TAG-1* gene activity could be said to be a normal occurrence.

If these regions do indeed express TAG-1, it would be interesting to compare the expression of TAG-1-driven ß-galactosidase, and/or TAG-1 mRNA, with that of tissue specific markers. Expression of TAG-1 by developing muscles would mean that the protein is present both on extending axons and their targets (Yamamoto *et al.*, 1986; Dodd *et al.*, 1988; Furley *et al.*, 1990; Wolfer *et al.*, 1994). Such expression is known to be important for axon guidance in *Drosophila.* The presence of the IgCAM fasciclin II on both motor axons and their target muscles is involved in the formation and stabilisation of neuromuscular synapses (Schuster *et al.*, 1996; Davis *et al.*, 1997). Fasciclin III-positive motor axons selectively innervate muscles that express fasciclin III, and form synapses with muscles that express the protein ectopically (Kose *et al.*, 1997). Similarly, connectin-positive motor axons innervate muscles that express connectin, and ectopic expression of connectin causes the axons to form inappropriate synapses (Nose *et al.* 1992, 1997). Therefore, if TAG-1 is indeed expressed on the surface of developing muscle cells, it is conceivable that homophilic interactions with axonal TAG-1 are important for correct

muscle innervation. Another possibility is that the TAG-1 gene is active within developing bone. Osteogenic cells have been shown to contain the mRNA of axon guidance proteins that include Sema 3A and netrins, and it has been suggested that such molecules control the extension of axons into forming bones (Togari *et al*, 2000).

5.4.1.5 ß-galactosidase activity in the developing cerebellum

The expression of ß-galactosidase also differed slightly from that expected within the cerebellum. As shown in figure 5.8 G and H, staining of P2 cerebella was particularly intense posteriorly, around fissure 3. Such localisation has not previously been described for TAG-1 protein (Wolfer *et al.*, 1994) or mRNA (Yoshihara *et al.*, 1995) in the neonate cerebellum. However, the perdurance of ß-galactosidase means that staining does not necessarily reflect transcription at the age of sampling (Echelard *et al.*, 1994; Skynner *et al.*, 1999), and it could be that the selective elevation of *TAG-1* expression did in fact occur at an earlier stage of development. Other molecules are known to have restricted patterns of expression within the cerebellum (summarised in appendix 5.F). For example, the P1 mouse cerebellum displays Eph B receptor reactivity within the external granular layer (EGL) of lobules VII to X, while ephrin A reactivity is restricted to the EGL of lobule VII (Rogers *et al.*, 1999). The TAG-1 related protein F3 is selectively expressed within the molecular layer of posterior lobules between P1 and P2 (Virgintino *et al.*, 1999). In the adult rat brain, mRNA of the TAG-1-like molecule BIG-2 is found restricted to the Purkinje cells of lobules IX and X, and the granular cell layer of lobules I to VI (Yoshihara *et al.*, 1995). The possibility that *TAG-1* is more strongly expressed by the posterior cerebellum is interesting, as the descent of *TAG-1* mutant granule cells from the external to the internal granular layer seems to be most severely compromised in such regions (K. Ohyama and R. Yoshida, personal communication).

Whatever the reasons for the differences between ß-galactosidase activity and TAG-1 immunoreactivity, the two patterns were largely in accordance. This allowed use of the *TAG-1* null mutant allele as a marker for cells that normally express TAG-1. The lack of obvious differences between *TAG-1* null heterozygotes and wild types (as in appendices

5.B and 5.D, Yamamoto *et al.*, 1986; Wolfer *et al.*, 1994) meant that the heterozygous animals could be used as controls to study the effects of mutations upon cells that normally express TAG-1.

5.4.2 Effects of the *TAG-1* and *L1* null mutations upon structures that normally express TAG-1 protein

Embryos and brains homozygous for the *TAG-1* null mutation were compared with those that were heterozygous, in order to determine whether the absence of TAG-1 protein had affected neural development. Aside from darker staining, which reflected the presence of two copies of the *tau-lacZ* allele, homozygous E10.5, E11.5, E12.5 and E13.5 embryos, and E16.5, P2 and P15 brains, were almost indistinguishable from their heterozygous equivalents. This finding was supported by results from TAG^{A} mutant embryos and brains stained for *math-1*-driven ß-galactosidase expression (appendix 5.G, and data not shown). An absence of TAG-1 protein did not appear to have disrupted the gross development of segmental nerve projections, including those innervating the limbs. The majority of cranial nerves, and many regions of the brain proper, also appeared to be unaffected. Possible exceptions to this were the hypoglossal nerve, which will be discussed in the following chapter, and the habenulointerpeduncular tract. For a discussion of effects of the *TAG-1* null mutation upon intrinsic neurons of the spinal cord, see chapter 3.

The *TAG-1* null allele was also used to study the effects of the *L1* mutation upon TAG-1 expressing structures. At both E11.5 and E12.5, there were no obvious differences between *L1* hemizygous and control embryos. Neither were there any apparent differences between E11.5 control embryos and *L1* hemizygotes that were also carrying two *TAG-1* mutant alleles. This implies that the lack of differences between E11.5 *TAG-1* homozygous and heterozygous embryos cannot be attributed to compensation by L1, and *vice versa*.

5.4.2.1 Segmental nerves

Spinal nerves appeared to be unaffected by an absence of TAG-1 protein. This included the contribution by DRG axons, indicating that TAG-1 is not required for their guidance away from the notochord, as might have been expected (Masuda *et al.*, 2000). As shown in figures 5.4 E and F and 5.6 E and F, the segmental nerves of homozygous E12.5 and E13.5 embryos afforded the same branches as those of heterozygotes. This finding is supported by immunohistochemistry of wild type and TAG^{A} embryos (data not shown). The spinal nerves of *L1* hemizygous embryos showed no differences from those of control embryos at E11.5 or E12.5 (figures 5.10 and 5.11). The spinal nerves of *TAG-1/L1* double mutant embryos were also indistinguishable from those of control embryos at E11.5 (figure 5.12).

Extension of nerves from the brachial plexus into the forelimb also appeared to be unaffected in E13.5 *TAG-1* null homozygous embryos (figure 5.6 E and F). This was perhaps unexpected, as axonin-1 has been implicated in correct innervation of the chicken hind limb (Landmesser and Honig, 1986; Honig *et al.*, 1998; Xue and Honig, 1999), and TAG-1 might be expressed within the developing mouse limbs (see figure 5.6 and above discussion). Even if TAG-1 protein is not expressed by limb mesenchyme, it is conceivable that axonal TAG-1 is important for sensitivity to proteins that are. Axon guidance genes expressed within the developing mouse limb include *netrin-3* (Püschel, 1999; Wang *et al.*, 1999 b), *slit-2*, *slit-3* (Yuan *et al.*, 1999), *robo-1* (Yuan *et al.*, 1999; Vargesson *et al.*, 2001), *robo-2* (Vargesson *et al.*, 2001), and *sema 3A* (Wright *et al.*, 1995; Taniguchi *et al.*, 1997). Related molecules are known to be important for guidance of *Drosophila* axons into musculature (e.g. Winberg *et al.*, 1998), and mutations in Sema 3A can lead to inappropriate innervation of mouse limbs (Taniguchi *et al.*, 1997; White and Behar, 2000). The response of corticospinal axons to Sema 3A depends upon axonal expression of the IgCAM L1 (Castellani *et al.*, 2000), so it is conceivable that axonal TAG-1 can affect the sensitivity of axons to guidance factors in the limbs. Indeed, axonin-1 seems to be important in the repulsion of dorsal root ganglion axons by notochord (Masuda *et al.*, 2000). The above results imply that TAG-1 is not essential for the guidance of limb

innervation before E12.5/E13.5, but it would be interesting to compare the *TAG-1* null heterozygous and homozygous mutant limbs at later stages of development.

5.4.2.2 Cranial nerves

The oculomotor, trochlear, trigeminal, facial, vagal and hypoglossal nerves were frequently apparent in stained *TAG-1* null embryos. Other than the hypoglossal nerve, which will be discussed in the following chapter, these nerves did not seem to be affected by a lack of TAG-1 protein. The cranial nerves of *L1* single, and *L1/TAG-1* double, mutant embryos also appeared to develop normally (figures 5.10, 5.11 and 5.12, and appendix 5.D). These results contrast with those from mice homozygous for a mutation in the *neuropilin-2* gene, in which the oculomotor, trochlear, trigeminal and facial nerves are all substantially defasciculated (Chen *et al.*, 2000; Giger *et al.*, 2000).

When cranial nerve nuclei and ganglia could be distinguished from other stained structures, these also appeared to be identical in *TAG-1* null homozygotes and heterozygotes. This observation included the facial nerve nucleus, even though a failure of this nucleus to migrate caudally is concurrent with loss of TAG-1 expression in *krox-20* or *ebf-1* mutant mice (Garel *et al.*, 2000). The present result implies that TAG-1 is either not involved in migration of facial nerve neurons, or that its function is redundant with those of other molecules.

5.4.2.3 The brain

There were few, if any, major differences between the developing brains of heterozygous and homozygous *TAG-1* null mice. Although it was often difficult to identify nuclei and tracts, particularly in the more strongly stained homozygous brains, the structures that could be distinguished generally appeared to be unaffected by a lack of TAG-1 protein.

One possible exception was the habenulointerpeduncular tract (HIPT, or *fasciculus retroflexus*). At E16.5, this tract seemed to be less prominent in homozygous brains, despite the fact that homozygote brains generally showed more intense staining than those of heterozygotes. The HIPT appeared as a fainter structure in all of the E16.5 brains examined, in both halves of each bisected brain, ruling out the possibility that less prominent HIPTs were merely further away from the cut surface after uneven bisection.

There are a number of possible explanations for the fainter appearance of the homozygous HIPT (illustrated in figure 5.13). The tract could have been displaced laterally, such that more tissue lay in between it and the medial surface of the brain (figure 5.13 B). There might be fewer axons produced, or fewer axons following the correct pathway (figure 5.13 C). For example, TAG-1 could be involved in the ability to respond to Netrin-1, which seems to attract habenular axons ventrally, or in the ability to respond to Sema 3F, which seems to prevent habenular axons from straying caudally (Funato *et al.*, 2000; Giger *et al.*, 2000). The weaker staining could also reflect defasciculation (figure 5.13 D), as has been reported in mice homozygous for mutations in both *EphB2* and *EphB3* (Orioli *et al.*, 1996), and those homozygous mutant for the Sema 3F receptor Neuropilin-2 (Chen *et al.*, 2000). Axonin-1 has indeed been implicated in the fasciculation of other populations of axons (Yamamoto *et al.*, 1990; Stoeckli and Landmesser, 1995; Xue and Honig, 1999). Another possibility is that TAG-1 protein normally has a positive effect upon activity of the *TAG-1* gene in habenular neurons. Thus homozygous mutants could theoretically lack a factor that increases the activity of *TAG-1* promoter elements in the heterozygous tracts.

A preliminary comparison of the tract proved inconclusive (figure 5.13 E and F). It is possible that the tract is narrower in the homozygous *TAG-1* null mutant brain than in the wild type: this could signify that fewer HIPT axons are produced, or that some HIPT axons are incorrectly guided. However, more work would be needed to determine whether this is in fact the case. Sectioning of more E16.5 brains, and examination of these at a higher magnification, would demonstrate whether the tract is indeed affected by the lack of TAG-1. Labelling of the tract with antibodies, or the application of a tracer such as DiI to the habenula, would assist in this verification. In addition, such labelling might show whether

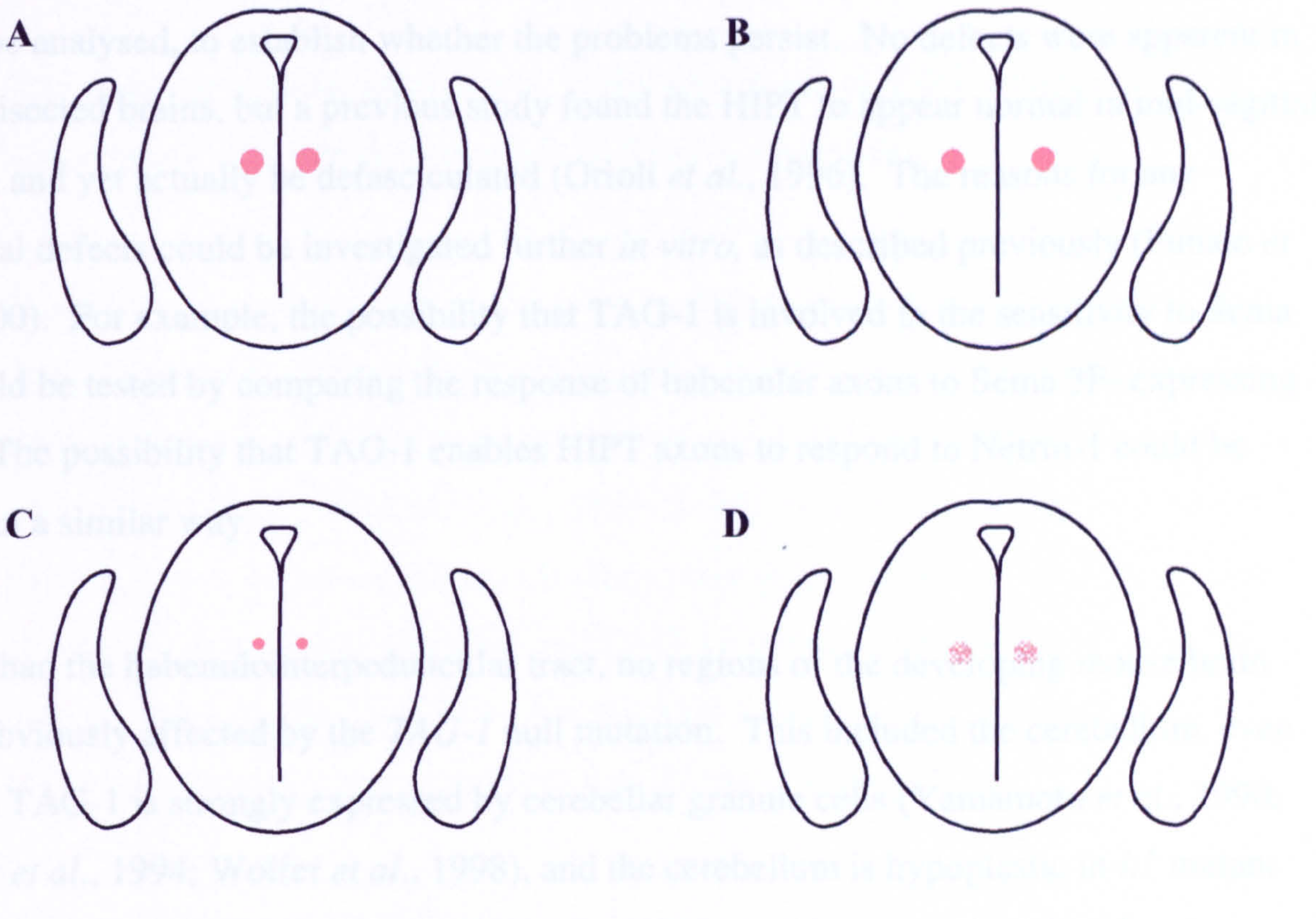

Figure 5.13 The habenulointerpeduncular tract (HIPT) in embryos homozygous for the *TAG-1* null mutation. A: illustration to show the position of the wild type HIPT (red) in coronal sections of E16.5 mouse brain. B-D: possible reasons for the tract appearing to be less intensely stained in brains from embryos homozygous for the *TAG-1* null mutation. B: the tract could lie more laterally than in wild type brains, meaning that it is further from the cut surface, such that the view of it is obscured by more tissue; C: the tract could contain fewer axons; D: the tract could be defasciculated. E-F: the HIPT is visible in unstained vibratome sections of E16.5 mouse brain. The sections show that the integrity of the tract is not severely affected by the *TAG-1* null mutation, and that the homozygous tracts are unlikely to appear fainter due to having a substantially more lateral position. The possibilities that the tract consists of fewer axons, is defasciculated, or is not affected at all, cannot be ruled out.

a proportion of HIPT axons were projecting incorrectly. If a defect was found, older brains could be analysed, to establish whether the problems persist. No defects were apparent in older bisected brains, but a previous study found the HIPT to appear normal in mid-sagittal section and yet actually be defasciculated (Orioli *et al.*, 1996). The reasons for any potential defects could be investigated further *in vitro,* as described previously (Funato *et al.*, 2000). For example, the possibility that TAG-1 is involved in the sensitivity to Sema 3F could be tested by comparing the response of habenular axons to Sema 3F- expressing cells. The possibility that TAG-1 enables HIPT axons to respond to Netrin-1 could be tested in a similar way.

Other than the habenulointerpeduncular tract, no regions of the developing mouse brain were obviously affected by the *TAG-1* null mutation. This included the cerebellum, even though TAG-1 is strongly expressed by cerebellar granule cells (Yamamoto *et al.*, 1990; Wolfer *et al.*, 1994; Wolfer *et al.*, 1998), and the cerebellum is hypoplastic in *L1* mutant mice (Fransen *et al.*, 1998). The lack of gross differences between *TAG-1* null heterozygous and homozygous cerebella was in agreement with an independent analysis of *TAG-1* null mice (Fukamauchi *et al.*, 2001), and the results from TAG^A mice (see appendix 5.G). Cerebella from mice homozygous for either *TAG-1* mutation were foliated normally (figures 5.8 G and H, 5.9 I and J, and appendix 5.G), and the widths of TAG^A homozygous mutant and wild-type cerebella were statistically identical (data not shown). However, these results do not rule out the possibility that TAG-1 is important for cerebellar development. Cerebella from mice homozygous for a *contactin/F3* mutation appear normal at a gross level, but have significant defects in their cellular organisation (Berglund *et al.*, 1999). Indeed, *TAG-1* mutant cerebella contain ectopic clusters of granule cells, which indicate that the descent of these cells from the external to internal granule cell layer is impaired (K. Ohyama and R. Yoshida, personal communication). The absence of gross defects might reflect functional redundancy of TAG-1 with other factors. The IgCAMs L1 and NrCAM have recently been shown to have redundant functions in cerebellar development (Sakurai *et al.*, 2001), so it could be that these, or other, proteins can compensate for a lack of TAG-1.

5.5 Conclusions

1. The staining pattern afforded by X-gal treatment of *TAG-1* null tissue is in accordance with previous reports of TAG-1 expression.

In addition to verifying this, the present study has raised the possibility that the *TAG-1* gene is also transcribed within cells not previously reported to be TAG-1 immunoreactive. Staining within the limbs and mandible might reflect previously undescribed *TAG-1* gene activity. Alternatively, this staining might be a result of the deletion of as yet uncharacterised repressor gene sequences. The significant agreement of the ß-galactosidase and TAG-1 expression patterns means that mice heterozygous for the *TAG-1* null mutation are a valuable tool for studying the effects of mutations upon structures that normally express *TAG-1*.

2. There are few major differences between mice that are homozygous or heterozygous for the *TAG-1* null mutation.

As will be discussed in the following chapter, the hypoglossal nerve may be affected by the absence of TAG-1 protein. The results presented above also raise the possibility that TAG-1 is involved in development of the HIPT. No other anatomical aberrations were detected, implying that TAG-1 is not essential for the gross development of many of the structures that normally express it. However, this does not mean that TAG-1 is not involved in the development of apparently unaffected structures. As in the cerebellum, *TAG-1* null mutation might affect *their* development, but in a more subtle way than would have been evident here. Alternatively TAG-1 could be functionally redundant with other factors, although the present results suggest that, at least at E11.5 and E12.5, TAG-1 is not redundant with L1.

5.6 Appendices

Appendix 5.A: Alphabetical list of abbreviations used in chapter 5.

Appendix 5.B: Expression of TAG-1 protein in a wild-type E11.5 embryo.

Appendix 5.C: Sections through E12.5 *TAG-1* null mutant embryos stained for ß-galactosidase activity

5.C.1 Sections through an E12.5 *TAG-1* null heterozygous embryo stained for ß-galactosidase activity

5.C.2 Sections through an E12.5 *TAG-1* null homozygous embryo stained for ß-galactosidase activity

Appendix 5.D: Comparison of E11.5 $L1^{+}$ and $L1^{-/Y}$ embryos by whole-mount immunohistochemistry.

Appendix 5.E: Expression of tau-ß-galactosidase under the control of *TAX-1* promoter elements.

Appendix 5.F: Expression of axon guidance molecules within restricted regions of the cerebellum.

Appendix 5.G: Comparison of brains from mice either heterozygous or homozygous for the TAG^{A} allele, using expression of the *math-1-lacZ* reporter construct.

5.G.1 E16.5

5.G.2 P2

5.G.3 P15

Appendix 5.A Alphabetical list of abbreviations used in chapter 5

Appendix 5.A Alphabetical list of abbreviations used in chapter 5

Abbreviations used in figures 5.1, 2, 4, 6, 7, 8, 9, 10, 11 and 12. These abbreviations are also listed by region on the right hand side of table 5.1.

III	oculomotor nerve
IV	trochlear nerve
V	trigeminal ganglion
Vmn	mandibular division of trigeminal nerve
Vmx	maxillary division of trigeminal nerve
Vo	ophthalmic division of trigeminal nerve
Vof	frontal nerve
Von	nasociliary nerve
VII	facial nerve
VIII	vestibulocochlear nerve
IX	glossopharyngeal nerve
X	vagus
XII	hypoglossal nerve
ac	anterior commissure
ao	anterior olfactory nucleus
bp	brachial plexus
c	cerebral cortex
cb	cerebellum
cc	corpus callosum
ce	cauda equina
cj	islands of Cajella of olfactory tubercle
cn	subcostal/ intercostal nerve
cp	cerebral peduncle
d	dorsal ramus of spinal nerve
db	diagonal band
dh	spinal dorsal horn
drg	dorsal root ganglion
egl	external granular cell layer of cerebellum
en	entorhinal cortex
gc	gracile/cuneate nuclei
ic	inferior colliculus
ip	interpeduncular nucleus
io	inferior olivary nucleus
hc	hippocampal commissure
hipt	habenulointerpeduncular tract
hn	habenular nucleus

Appendix 5.A Alphabetical list of abbreviations (continued)

hy	lateral hypothalamus
lcb	lateral cutaneous branch of ventral ramus
ld	lateral branch of dorsal ramus
lo	lateral olfactory tract
mb	muscular branch of ventral ramus
md	medial branch of dorsal ramus
ms	medial septum
mt	mammilothalamic tract
nIII	oculomotor nerve nucleus
nV/na	spinal trigeminal nucleus/nucleus ambiguus
nVII	facial nerve nucleus
nVIII	vestibular/cochlear nuclei
nXII	hypoglossal nerve nucleus
nlo	nucleus of lateral olfactory tract
ob	olfactory bulb
oe	olfactory epithelium
oc	optic chiasm
on	optic nerve
ot	optic tract
pc	posterior commissure
pf	paraflocculus of cerebellum
pg	grey nucleus of pons
pr	pretectum
pn	anterior pontine nuclei
po	preoptic area
pt	pituitary
r	retina
re	reticular nucleus or reuniens nucleus
rn	red nucleus
rs	retrosplenial cortex
s	spinal nerve
sc	superior colliculus
sm	stria medullaris
so/tz	superior olivary nucleus/trapezoid body
v	ventral ramus of spinal nerve
vh	spinal ventral horn
vr	spinal ventral roots
wr	white ramus communicante

Appendix 5.B Expression of TAG-1 protein in a wild type E11.5 mouse embryo

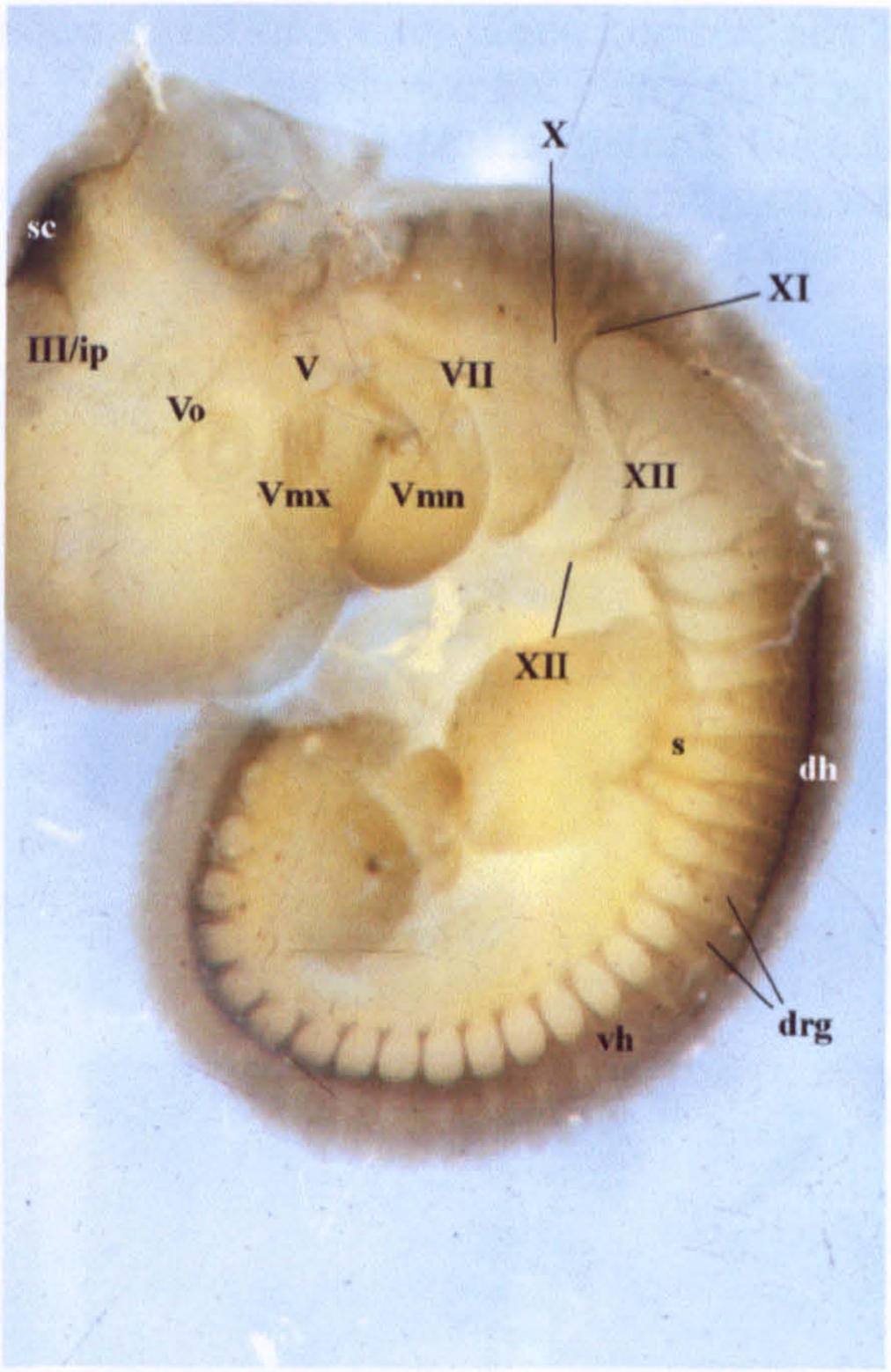

Abbreviations:

ventral horn	vh
spinal nerve	s
dorsal horn	dh
dorsal root ganglia	drg
hypoglossal nerve	XII
accessory nerve	XI
vagus	X
facial nerve	VII
trigeminal ganglion	V
mandibular division	Vmn
maxillary division	Vmx
ophthalmic division	Vo
interpeduncular nucleus	ip
oculomotor nucleus	nIII
superior colliculus	sc

Embryos were labelled using the 4D7 monoclonal antibody to TAG-1 (Dodd et al., 1988). The expression pattern is very similar to that of tau-ß-galactosidase in TAG-1 null mutant embryos at this age (figure 5.2).

Appendix 5.C.1 Sections through an E12.5 *TAG-1* null heterozygous embryo stained for ß-galactosidase activity

100μm thick vibratome sections were taken horizontally through the whole embryo shown on the left. The sections shown are every third section from the region between the white dashed lines. Dorsal is towards the top. Abbreviations are as listed in appendix 5.A, and white arrow heads indicate what appears to be mesenchymal staining.

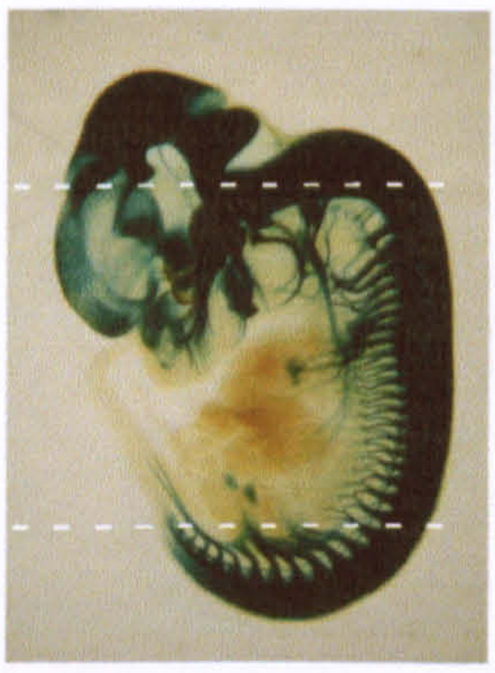

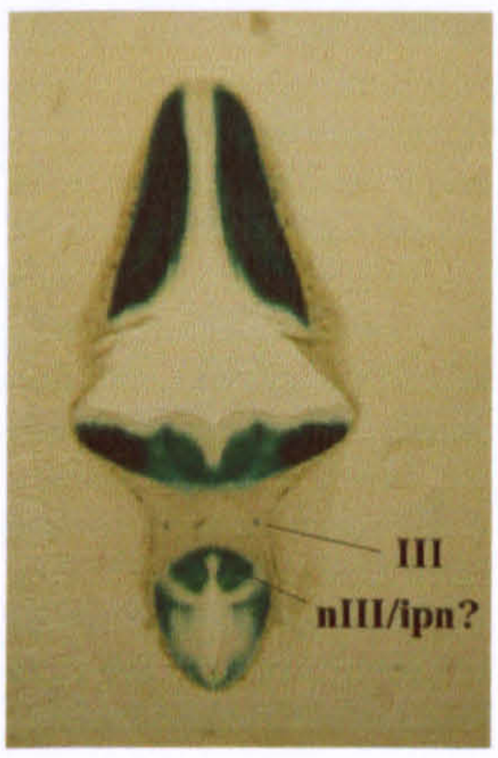

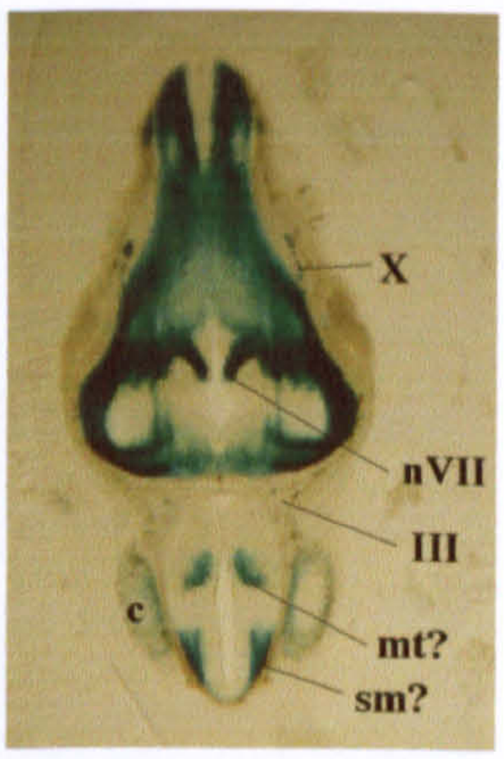

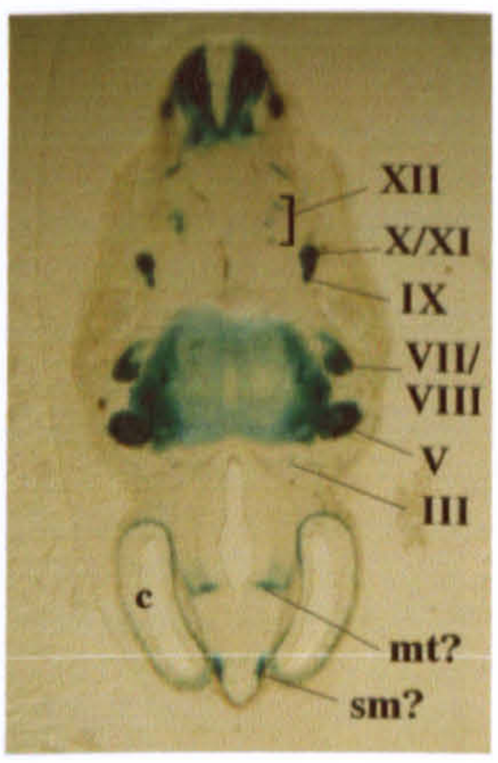

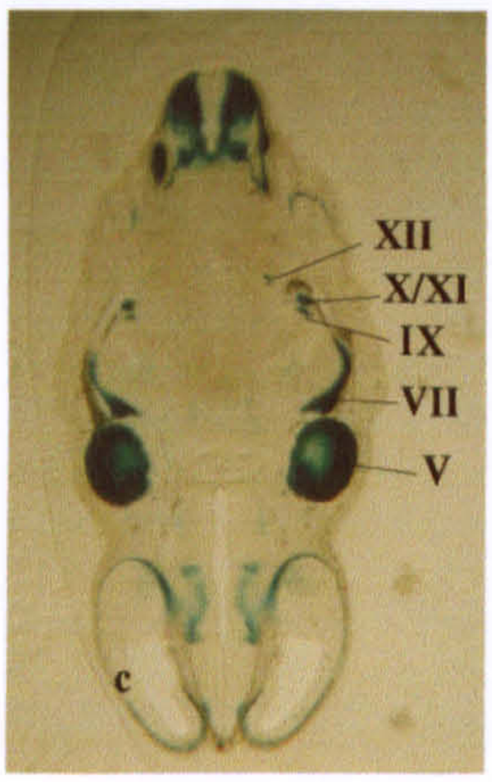

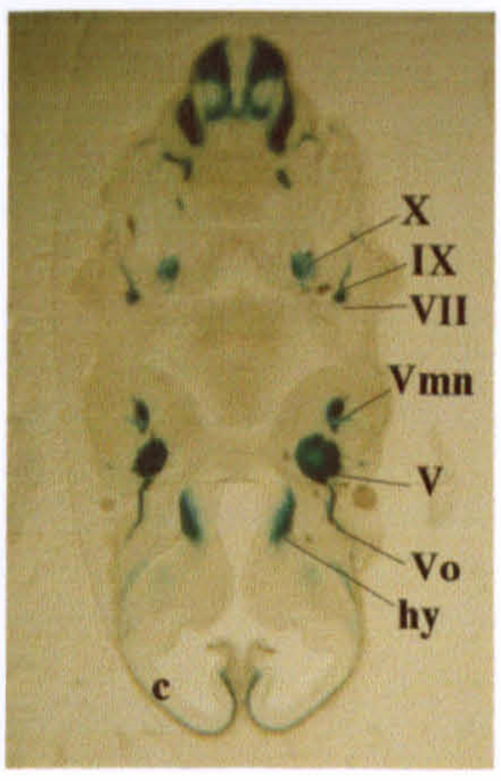

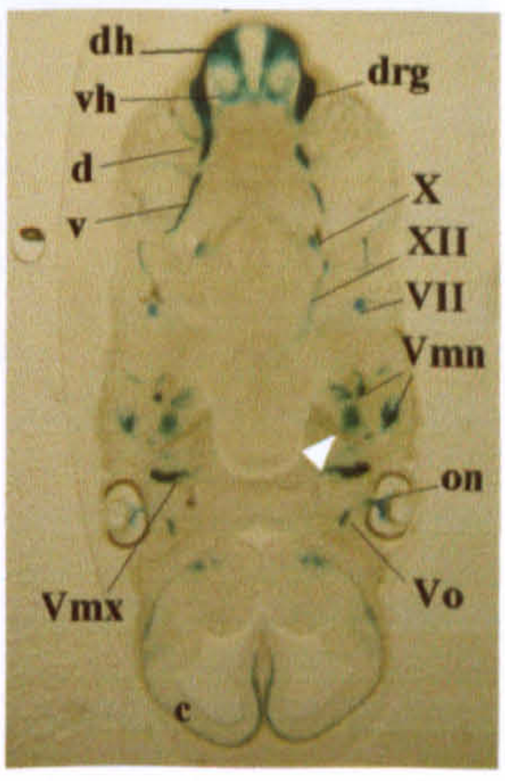

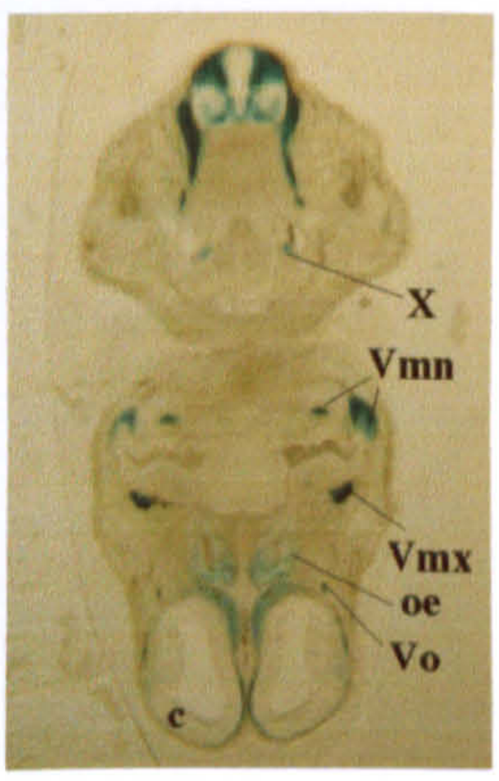

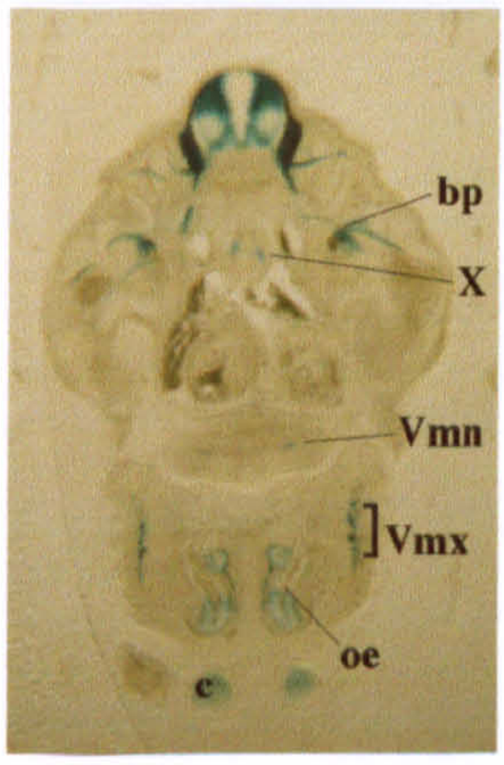

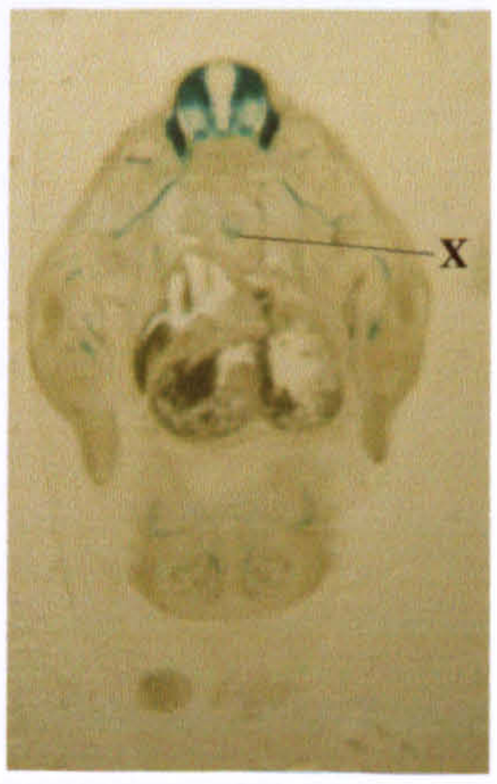

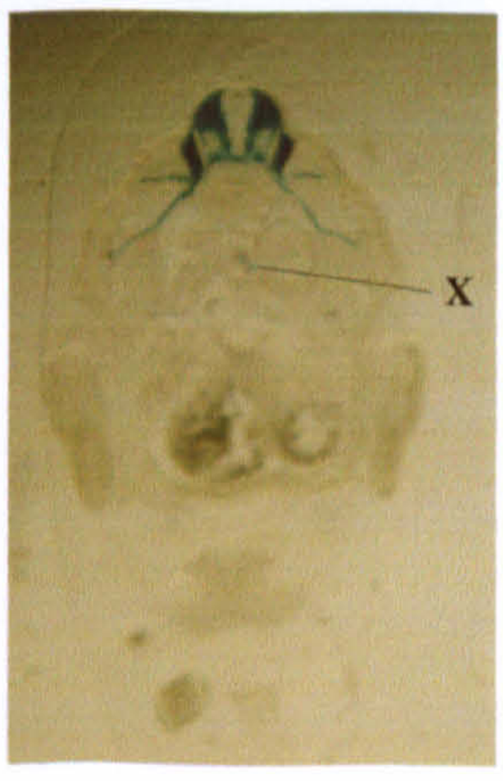

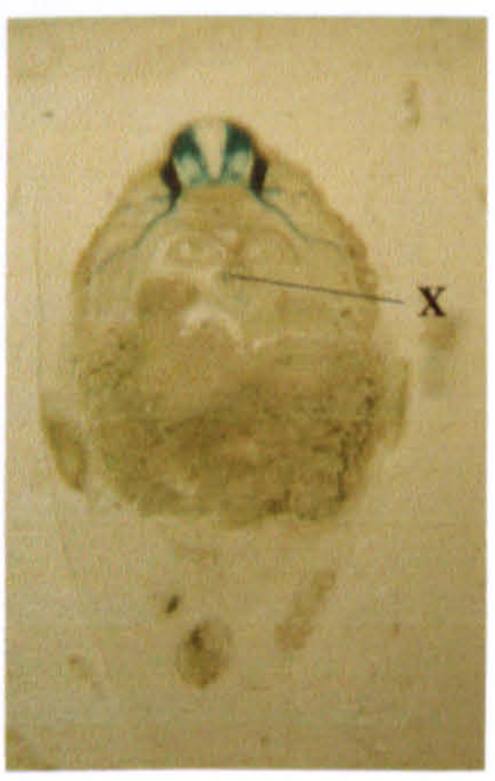

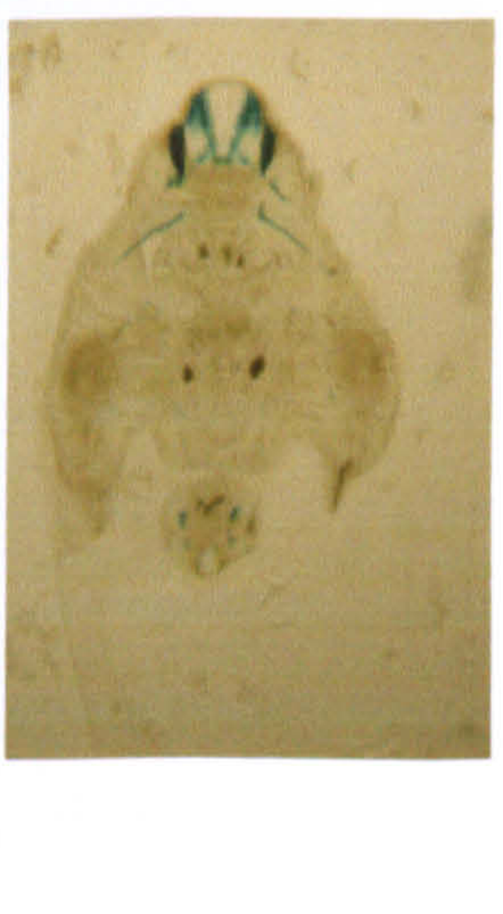

Appendix 5.C.2 Sections through an E12.5 *TAG-1* null homozygous embryo stained for ß-galactosidase activity

100μm thick vibratome sections were taken horizontally through the whole embryo shown on the left. The sections shown are every third section from the region between the white dashed lines. Dorsal is towards the top. Abbreviations are as listed in appendix 5.A, and white arrow heads indicate what appears to be mesenchymal staining.

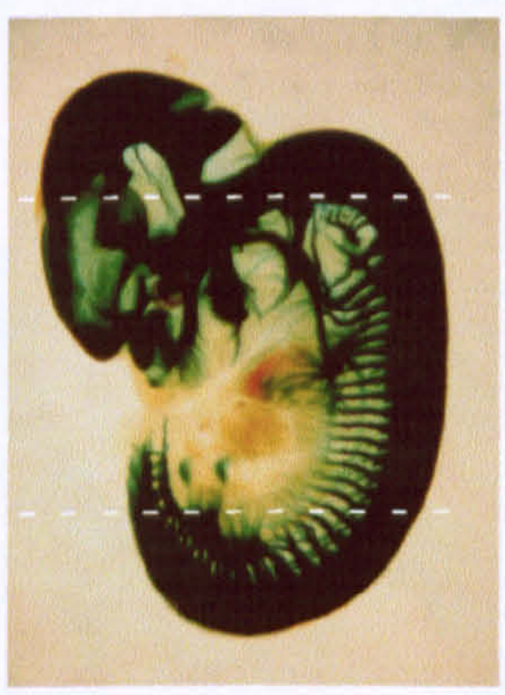

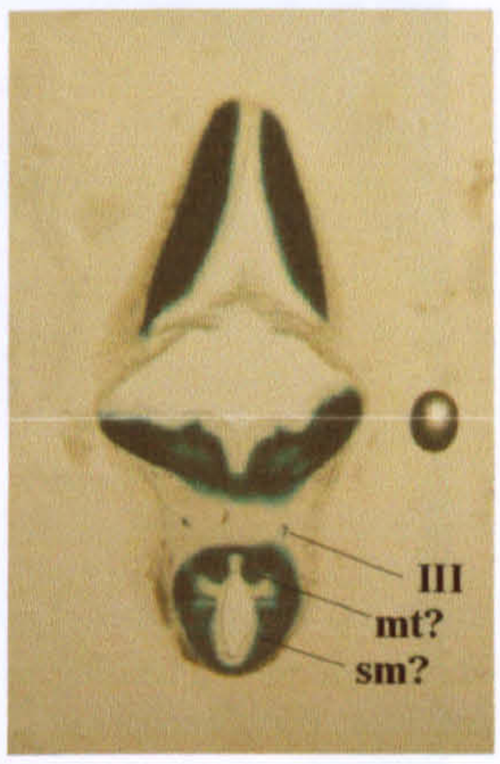

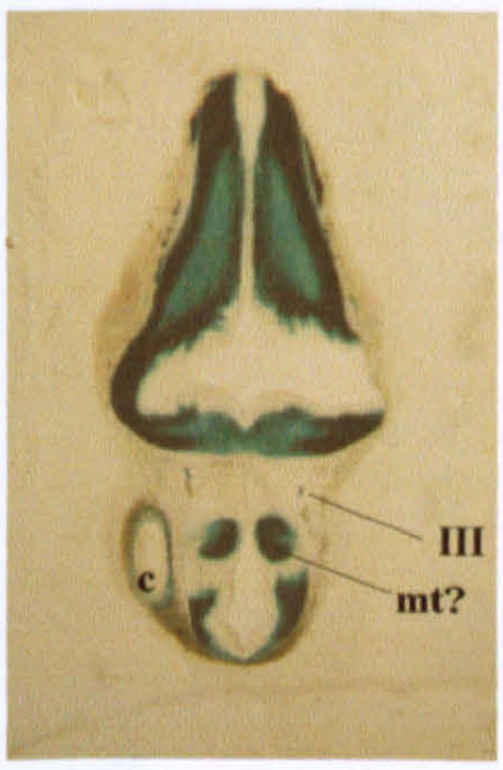

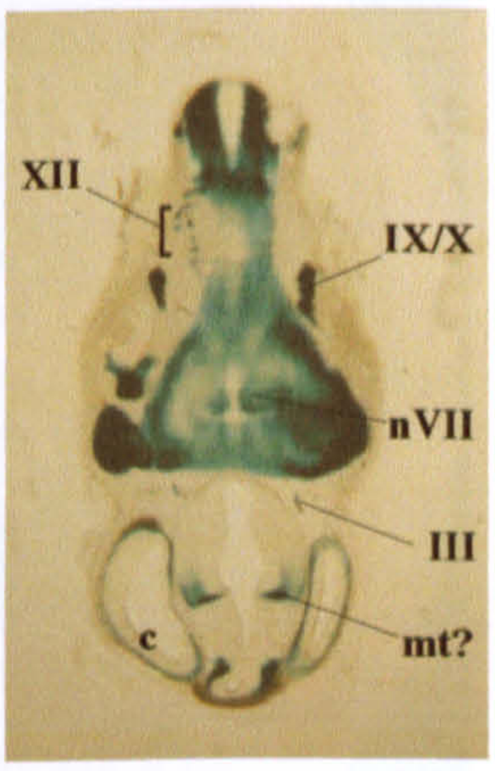

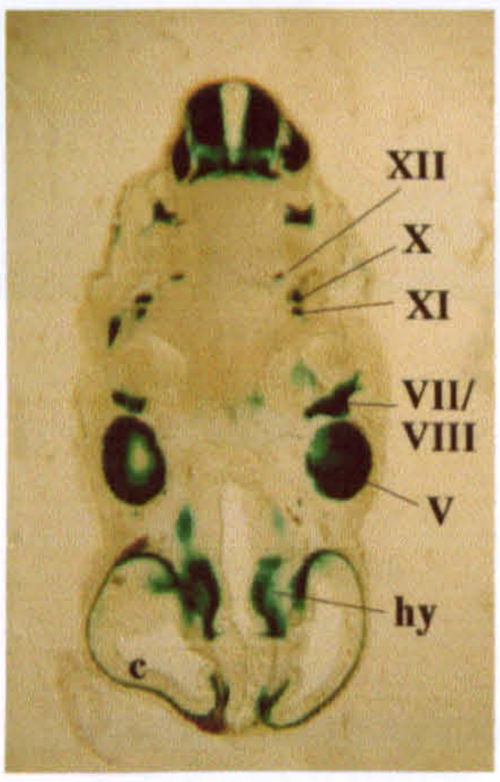

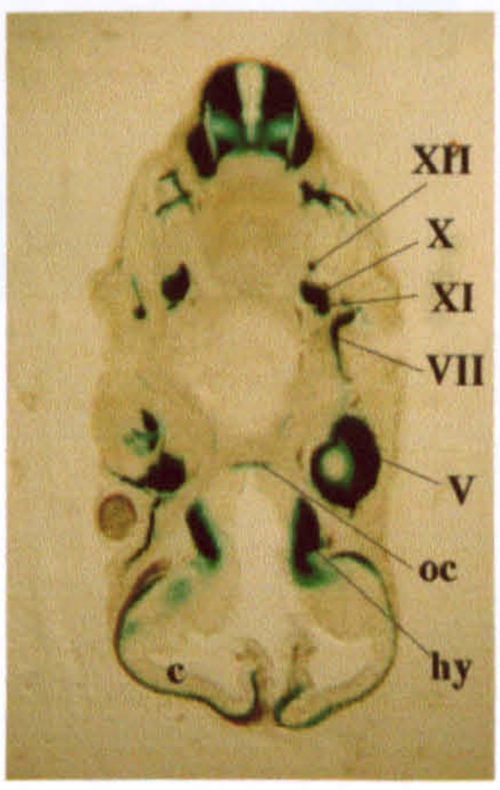

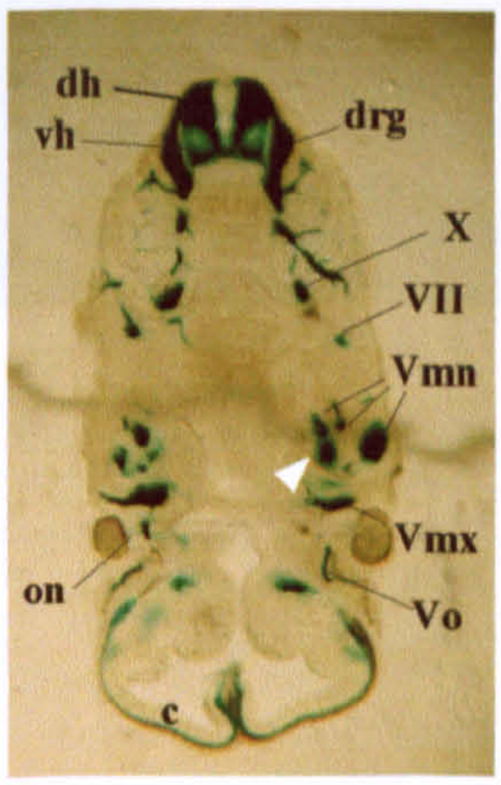

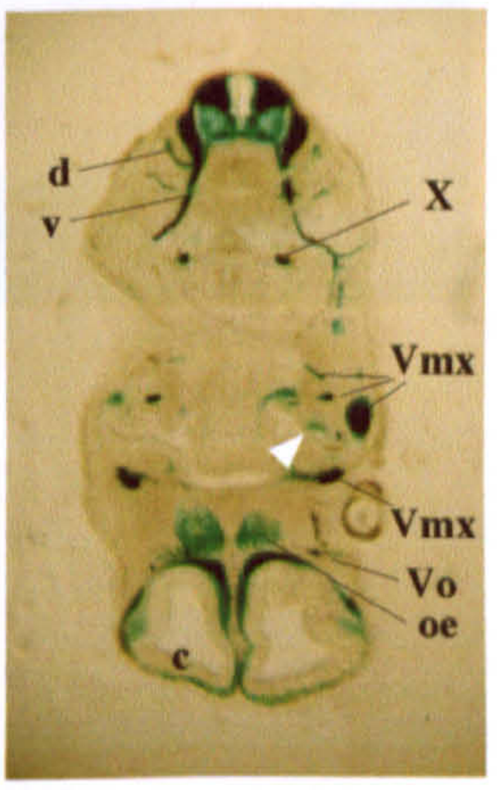

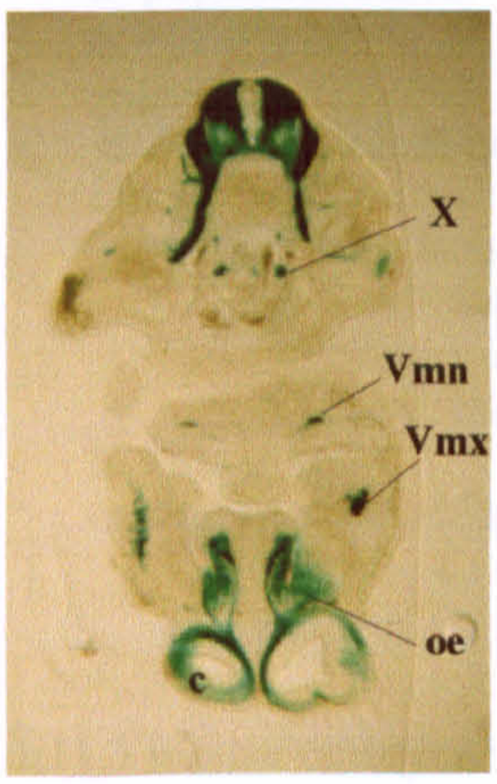

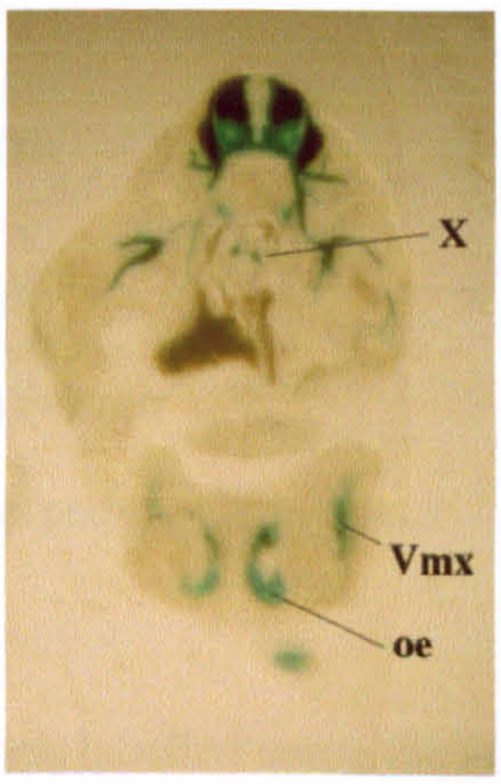

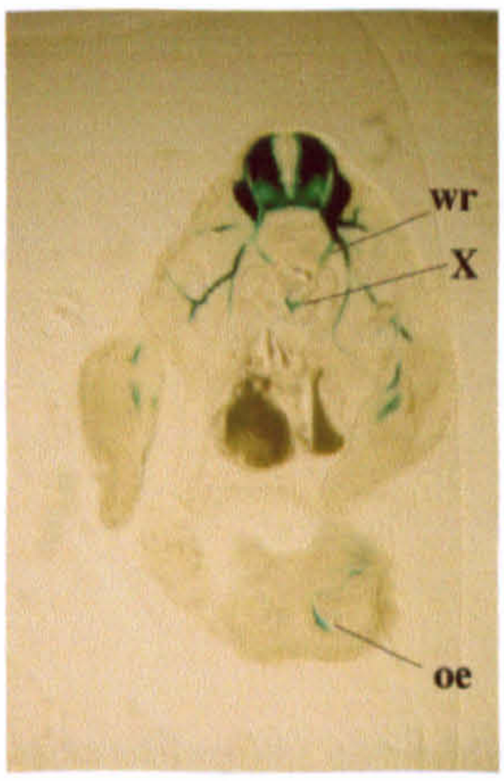

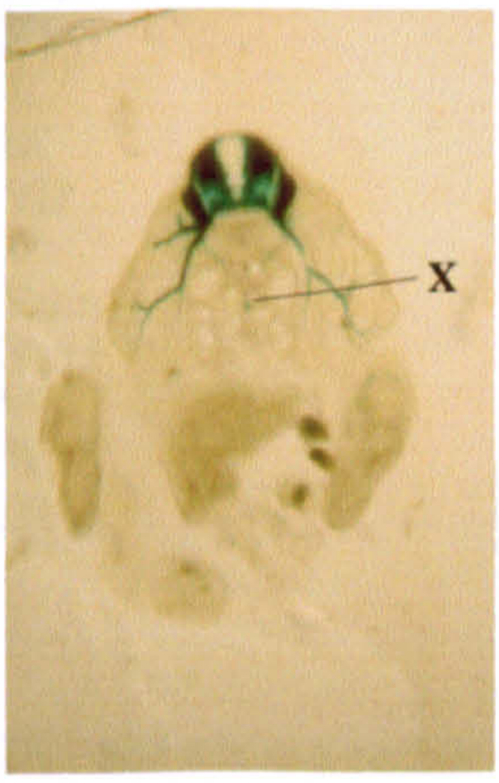

Appendix 5.D Comparison of E11.5 *L1*$^{+}$ and *L1*$^{-/Y}$ mouse embryos by whole-mount immunohistochemistry

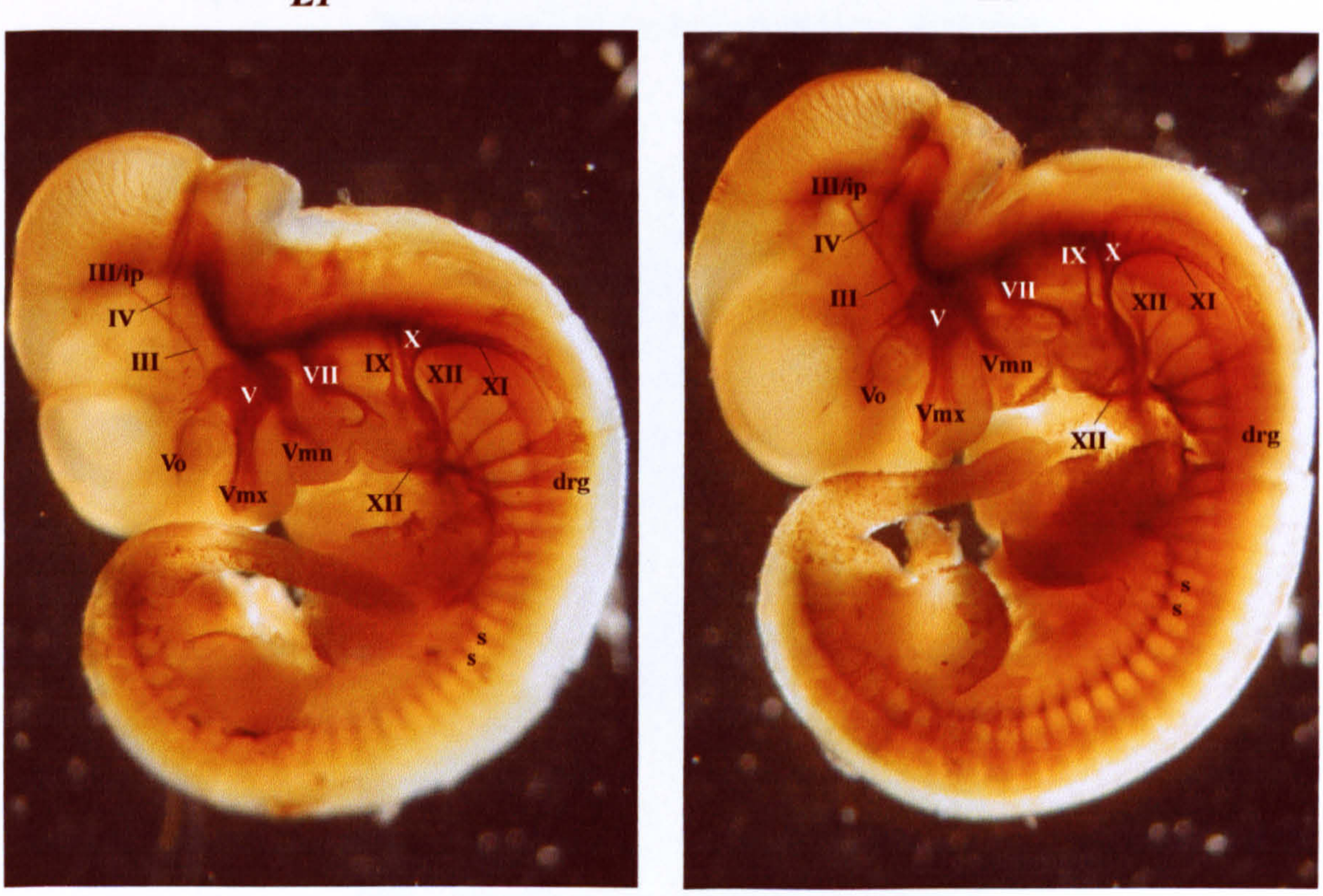

Abbreviations

spinal nerve	s
dorsal root ganglion	drg
hypoglossal nerve	XII
accessory nerve	XI
vagus	X
glossopharyngeal nerve	IX
facial nerve	VII
trigeminal ganglion	V
mandibular division	Vmn
maxillary division	Vmx
ophthalmic division	Vo
trochlear nerve	IV
oculomotor nerve/interpeduncular nucleus	III/ip

E11.5 mouse embryos were labelled using the anti-neurofilament antibody 2H3 and a horse-radish peroxidase conjugated secondary antibody. Embryos with only mutant *L1* alleles were indistinguishable from those which had only wild type versions of the *L1* gene.

Appendix 5.E Expression of tau-ß-galactosidase protein under the control of *TAX-1* promoter elements

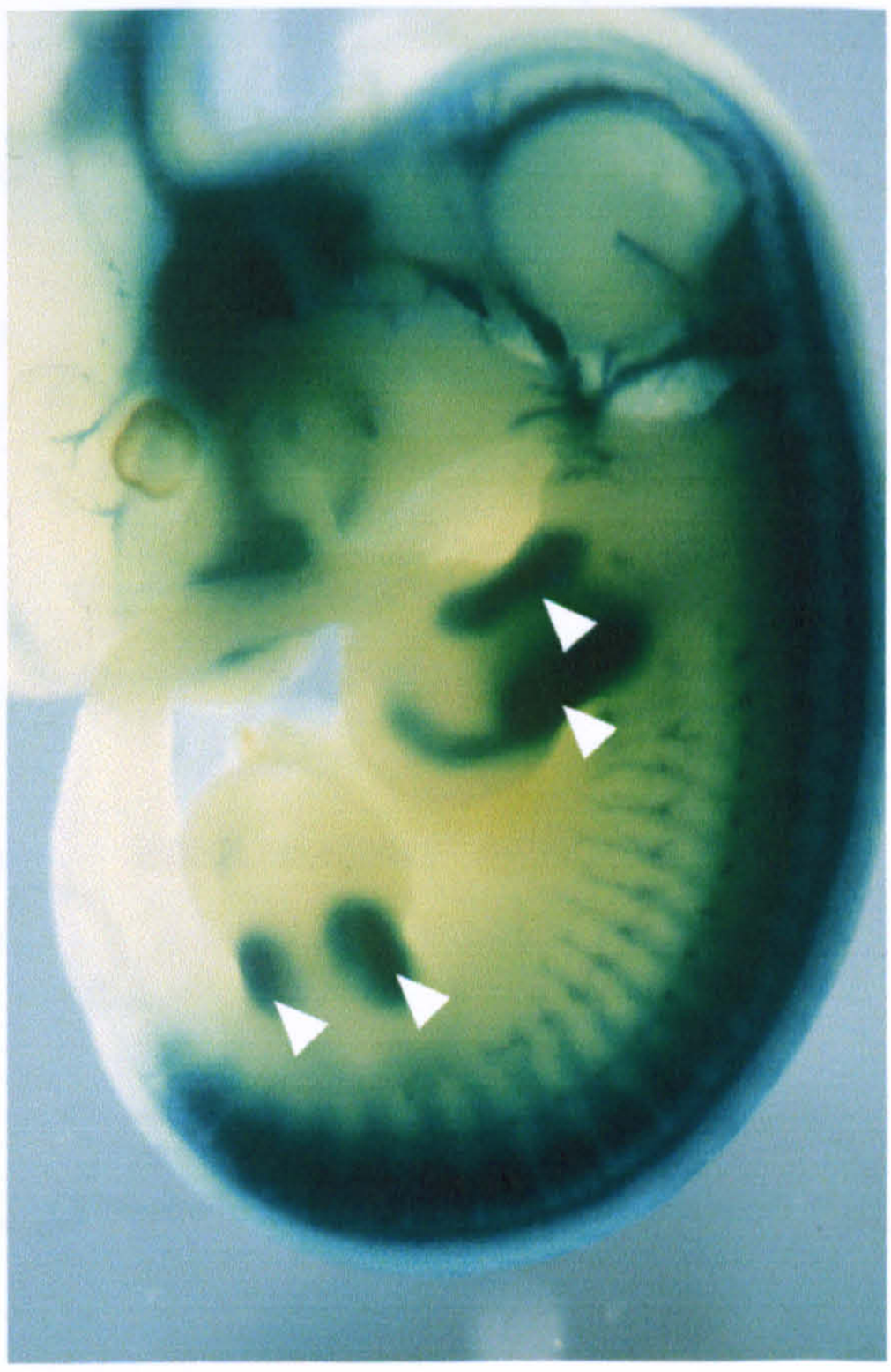

An E11.5 "TGii" embryo, expressing tau-ß-galactosidase under the control of regulatory elements of the human *TAG-1* gene, *TAX-1* (Kozlov *et al.*, 1995; courtesy of A.J.W. Furley). Staining is seen in only a subset of the neurons that usually express murine TAG-1, namely sensory neurons (as shown in figure 5.2; A.J.W. Furley, personal communication). In addition, the limbs contain large patches of ß-galactosidase activity that do not appear to be axonal (arrowheads). This staining is reminiscent of that seen in the limbs and jaw of embryos with the *TAG-1* null mutation (figures 5.4 and 5.6).

Appendix 5.F Expression of axon guidance molecules within restricted regions of the cerebellum

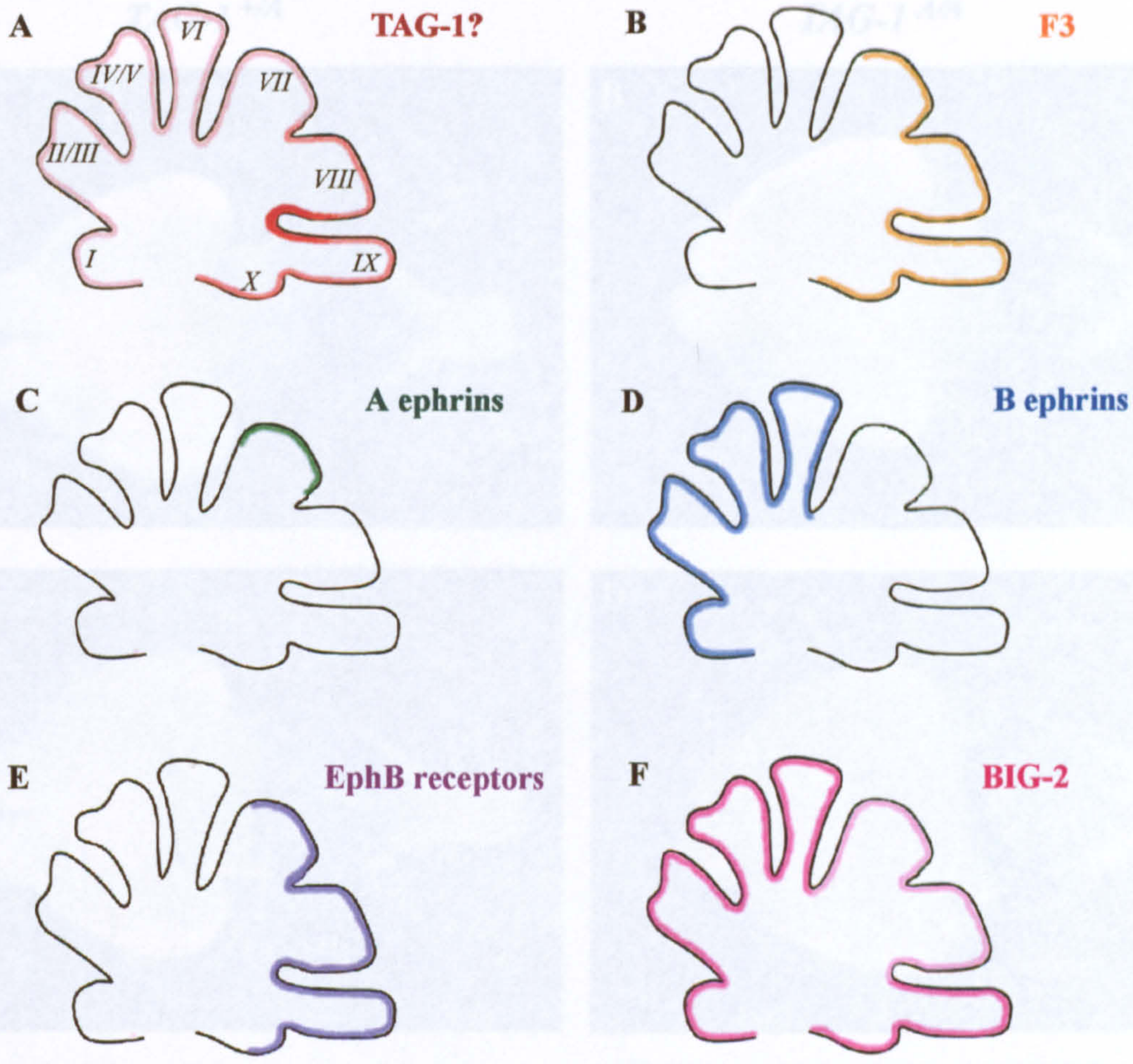

The expression patterns of selected axon guidance molecules within the rodent cerebellum. The cerebellar template is based upon the P2 cerebellum, as seen after mid-sagittal section (see figure 5.8. g and h). Roman numerals in A denote cerebellar lobules, which were identified using Altman and Bayer, 1997. Rostral is to the left in each case.

A: Possible expression of *TAG-1*. The greater expression posteriorly, particularly around fissure 3, was suggested by the presence of *TAG-1*-promoter-driven ß-galactosidase expression (figure 5.5, g and h). It was assumed that the staining was within the external granular layer (EGL), as this is the only layer of the cerebellum that expresses TAG-1 protein at this age (Wolfer *et al.*, 1994). While the above distribution of ß-galactosidase activity was observed at P2, no such expression has been reported for TAG-1. It may be that the above expression pattern occurs at a n earlier stage of development, or is an artefact of the TAG-1 null mutation.

B: Expression of F3 at P1 to P3, as determined by immunohistochemisry. Immunoreaactivity was predominantly within the molecular layer (Virgintino *et al.*, 1999).

C: Expression of ephrin-A ligands at P1, as determined by binding of a labelled EphA7 receptor. Labelling was predominantly of the EGL (Rogers *et al.*, 1999).

D: Expression of ephrin-B ligands at P1, as determined by immunohistochemistry. Expression appeared to be within the Purkinje cell layer (Rogers *et al.*, 1999).

E: Expression of EphB receptors at P1, as determined by binding of a labelled ephrin-B1 ligand. Labelling was predominantly of the EGL (Rogers *et al.*, 1999).

F: Expression of BIG-2 mRNA in the adult cerebellum, as determined by *in situ* hybridisation (Yoshihara *et al.*, 1995). The mRNA was detected at low levels throughout the granular cell layer, with particularly strong expression in anterior folia. Lobules IX and X contained strong expression within their *Purkinje* cells. TAG-1 and F3 mRNA were evenly distributed in the adult cerebellar lobules.

Appendix 5.G.2 Comparison of brains from mice either heterozygous or homozygous for the *TAG*^{A} allele, using expression of the *math-1-lacZ* reporter construct: P2

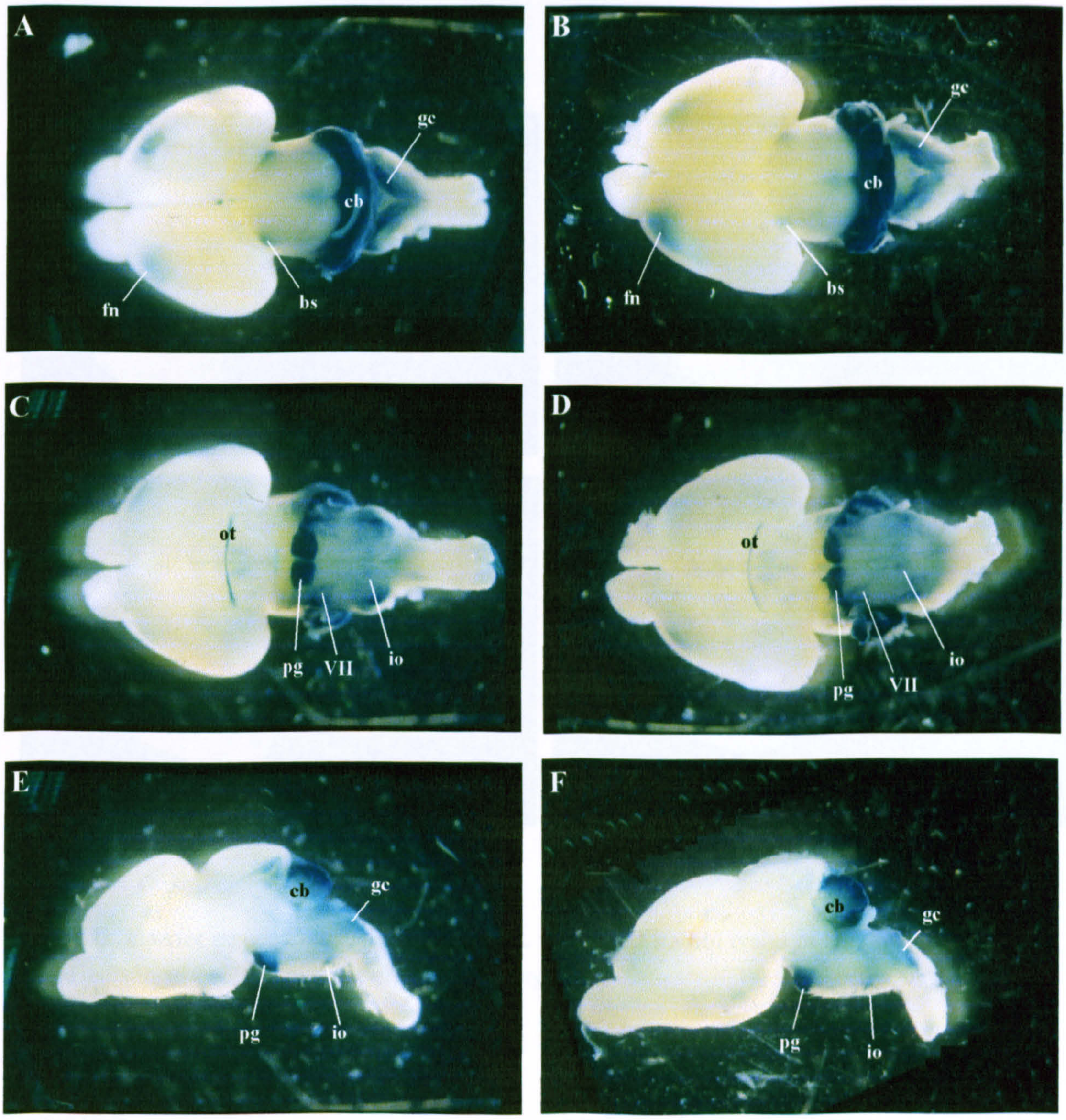

A and B: superior aspect; C and D: inferior aspect; E and F: medial aspect, after mid-sagittal bisection. The X-gal stained brains of P2 *TAG*$^{A/A}$ mice were indistinguishable from those of *TAG*$^{+/A}$ mice.

Abbreviations:

gracile/cuneate nuclei	gc	inferior olive	io
facial nerve nucleus	VII	grey nucleus of pons	pg
cerebellum	cb	optic tract	ot
brachium of superior colliculus	bs	frontal neocortex	fn

Appendix 5.G.1 Comparison of brains from mice either heterozygous or homozygous for the *TAG*^{A} allele, using expression of the *math-1-lacZ* reporter construct: E16.5

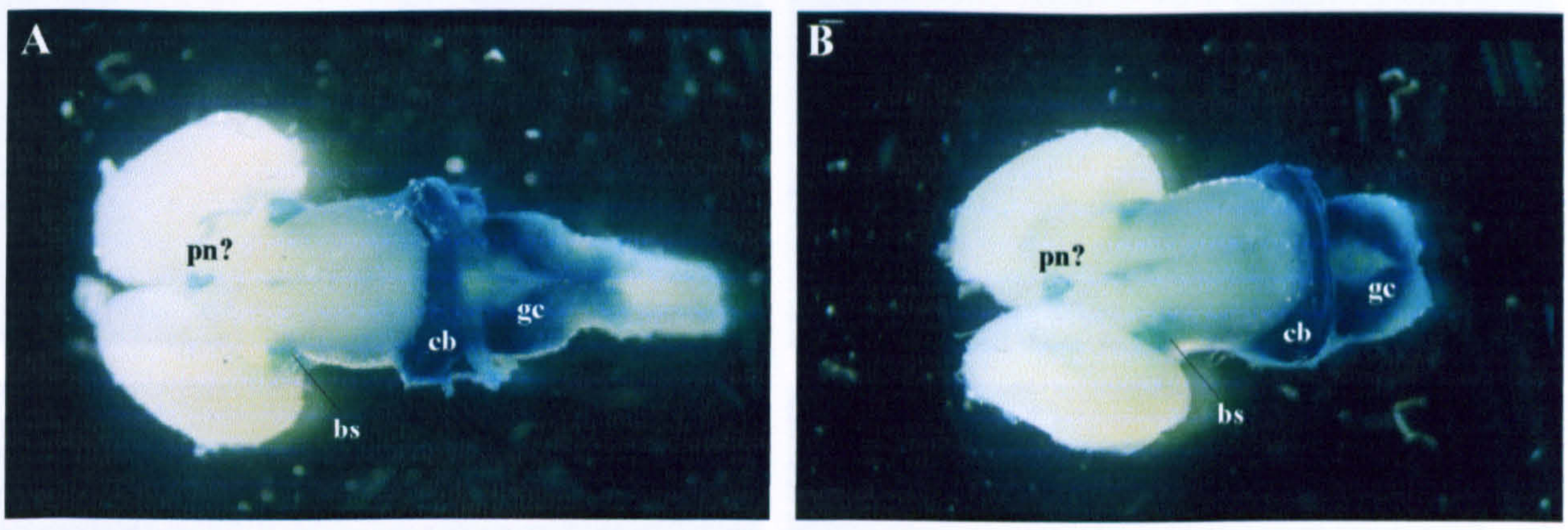

A and B: superior aspect; C and D: inferior aspect. The X-gal stained brains of E16.5 *TAG*$^{A/A}$ embryos were indistinguishable from those of *TAG*$^{+/A}$ embryos.

Abbreviations:

gracile/cuneate nuclei	gc	grey nucleus of pons	pg
cerebellum	cb	cerebral peduncle	cp
optic tract	ot	brachium of superior colliculus	bs
pineal gland?	pn?		

Appendix 5.G.3 Comparison of brains from mice either heterozygous or homozygous for the *TAG*^{A} allele, using expression of the *math-1-lacZ* reporter construct: P15

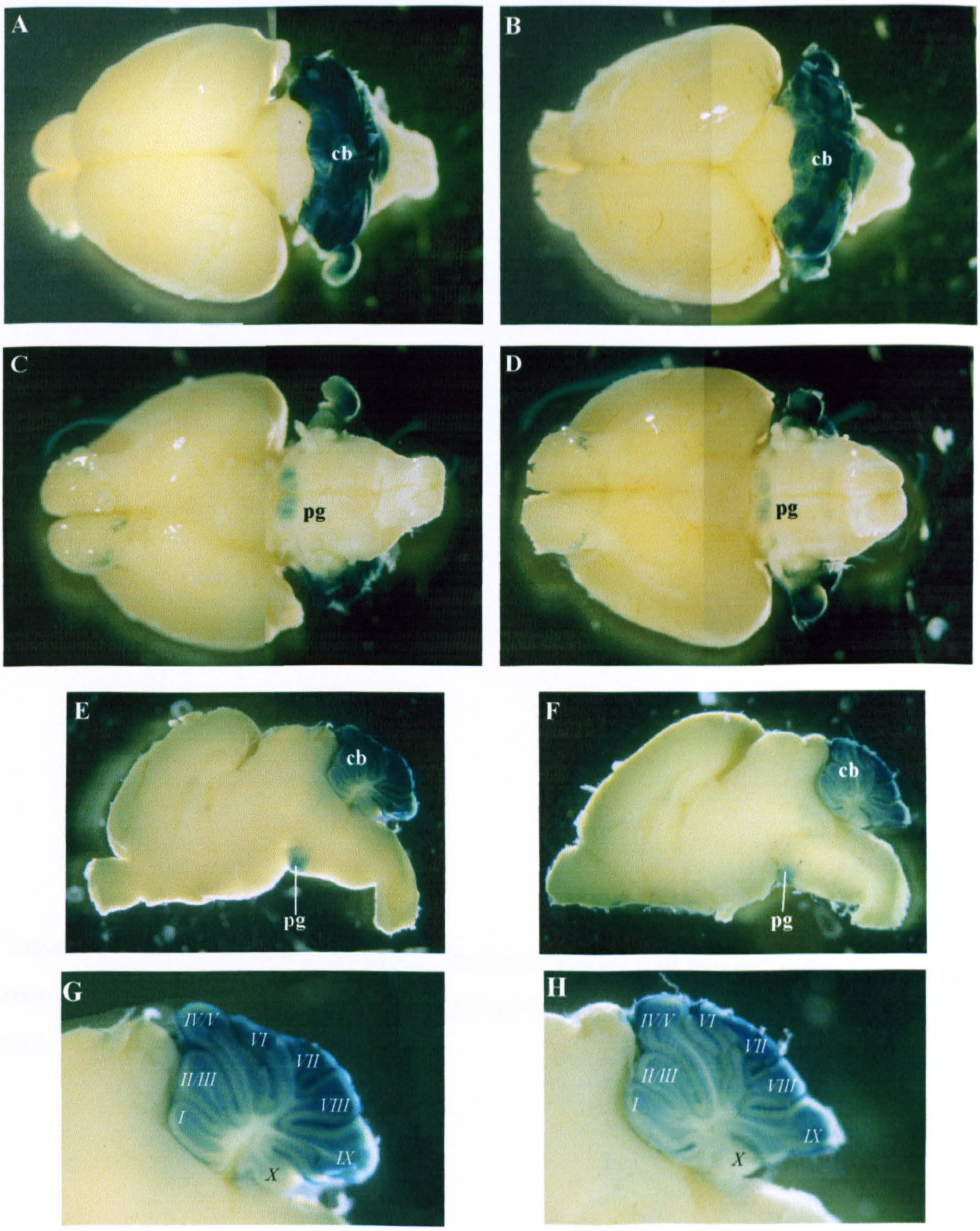

A and B: superior aspect; C and D: inferior aspect; E and F: medial aspect, after mid-sagittal bisection. G and H: medial aspect of cerebellum after mid-sagittal bisection. Roman numerals denote developing lobules. The X-gal stained brains of P15 *TAG*$^{A/A}$ mice were indistinguishable from those of *TAG*$^{+/A}$ mice.

Abbreviations:	grey nucleus of pons	pg
	cerebellum	cb

6 Effect of the *TAG-1* Null Mutation upon the Hypoglossal (XIIth Cranial) Nerve

Please note that throughout this chapter, the term "*TAG-1* null mutant" refers to mice or embryos carrying either one (heterozygotes) or two (homozygotes) copies of the TAG-1 allele (shown in figure 1.7).

6.1 Abstract

The XIIth cranial, or hypoglossal, nerve supplies motor innervation to muscles of the tongue. It expresses TAG-1 during its development (Yamamoto *et al.*, 1986; Wolfer *et al.*, 1994), and so contains ß-galactosidase activity in embryos that carry the *TAG-1* null allele. Staining of whole embryos indicated that the *TAG-1* null mutation might affect development of the hypoglossal nerve. Therefore the development of this nerve was studied in more detail. Where possible, the frequencies with which nerves showed particular phenotypes were compared statistically. There seemed to be a significant difference between the hypoglossal nerves of *TAG-1* null heterozygous and homozygous embryos at E11.5, the nerves of homozygotes being less likely to extend beyond the point of rootlet convergence. There also appeared to be a significant difference between the hypoglossal nerves of heterozygotes and homozygotes at E12.5. These results suggest that TAG-1 might indeed be involved in extension of the hypoglossal nerve.

6.2 Introduction

The XIIth cranial, or hypoglossal, nerve supplies motor innervation to all of the intrinsic, and all but one of the extrinsic, muscles of the tongue. It is therefore critical for chewing, swallowing, breathing and speech (Friedland *et al.*, 1995; Mu and Sanders, 1999). Damage of the nerve, for example due to injury or during surgery, or if it is compressed by inflammation or a tumour, results in loss of tongue function. The tongue may atrophy, and the loss of motor input to musculature can severely impair ability to swallow and speak (e.g. Morini *et al.*, 1998; Giuffrida *et al.*, 2000). A number of disorders are characterised by tongue dysfunction, including cerebral palsy, Downs syndrome and sleep apnoea (Sokoloff, 2000). In the latter case, it has been shown that direct electrical stimulation of the hypoglossal nerve can relieve symptoms (Eisele *et al.*, 1997). It is therefore conceivable that defects in innervation of the tongue by the hypoglossal nerve may underlie the tongue dysfunction seen in a number of swallowing, breathing and/or speech disorders.

Preliminary analysis of *TAG-1* null embryos stained for ß-galactosidase activity raised the possibility that guidance of the hypoglossal nerve was affected by the mutation (chapter 5). Therefore the development of this nerve was investigated in more detail. Statistical analysis suggested that the hypoglossal nerve was indeed affected by the *TAG-1* null mutation at both E11.5 and E12.5, implicating TAG-1 protein in hypoglossal nerve development.

6.3 Results

6.3.1 The hypoglossal nerve in E10.5 mouse embryos carrying the *TAG-1* null allele

At E10.5 (figure 6.1), the hypoglossal nerve was generally observed as a number of stained rootlets, which projected ventrally away from the hypoglossal nucleus of the ventral hindbrain. In several cases, some of the rootlets had converged to form a single hypoglossal nerve, which continued to extend caudally (figure 6.1, C and D). The two hypoglossal nerves of an embryo had not necessarily developed to the same extent, as reported previously for the hypoglossal nerves of chicken embryos (Rogers, 1965). There were no discernable differences between the hypoglossal nerves of heterozygous and homozygous embryos at this age.

6.3.2 The hypoglossal nerve in E11.5 mouse embryos carrying the *TAG-1* null allele

The majority of E11.5 embryos had distinct hypoglossal nerves extending away from the ventral hindbrain (figure 6.2 A and B). Often the nerve had turned to extend rostrally towards the developing tongue region (figure 6.2 A). Occasionally the hypoglossal nerve did not extend beyond the point of rootlet convergence (figure 6.2 C). In some cases, adjacent rootlets had developed to different extents (figure 6.2 D).

Many hypoglossal nerves were scored as having converged, extended ventrally and turned rostrally (as in figure 6.2 A; phenotype 1). Others were scored as having converged and extended ventrally but not turned rostrally (as in figure 6.2 B; phenotype 2), or as having converged but not extended beyond the point of rootlet convergence (as in figure 6.2 C; phenotype 3). If the rootlets on one side of an embryo had different phenotypes, fractions were attributed to the three categories as appropriate (figure 6.2 D). As indicated in figure

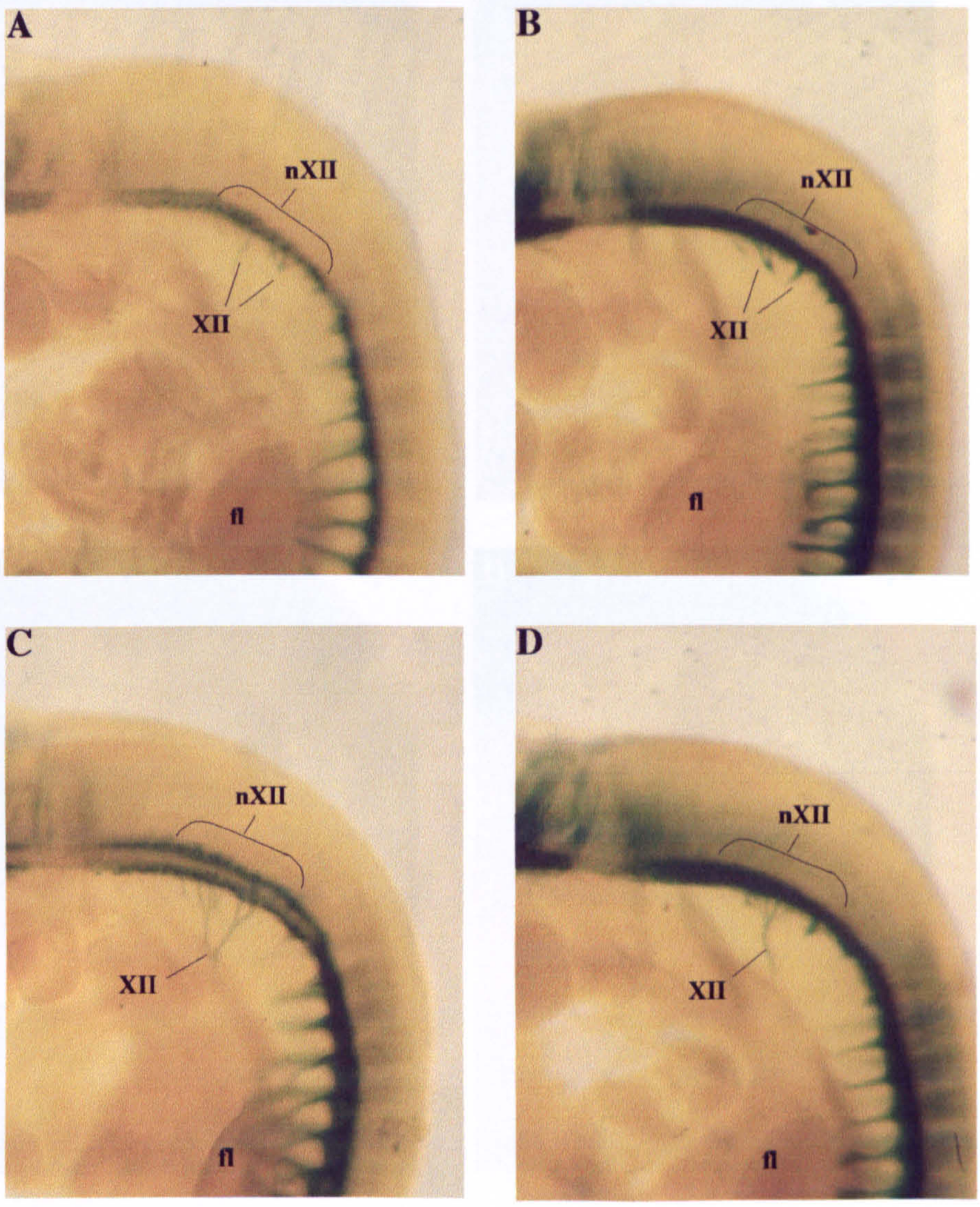

Figure 6.1 The hypoglossal nerves of E10.5 mouse embryos carrying the *TAG-1* null allele
The neck regions of E10.5 embryos (rostral is to the left, caudal to the bottom). A and C: examples of heterozygous embryos. B and D: examples of homozygous embryos. The extent to which the hypoglossal nerve rootlets had extended and/or converged varied, but this variation did not appear to be linked to genotype (n=16 heterozygous and n=56 homozygous hypoglossal "nerves"). The two rows of staining in C are the two hypoglossal nerves of this embryo: all embryos had been rendered transparent, but the other three photographs were taken with the two hypoglossal nuclei aligned. nXII- hypoglossal nerve nucleus, although it should be noted that the extent of the nucleus is estimated. XII- hypoglossal nerve (and/or rootlets); fl- fore limb.

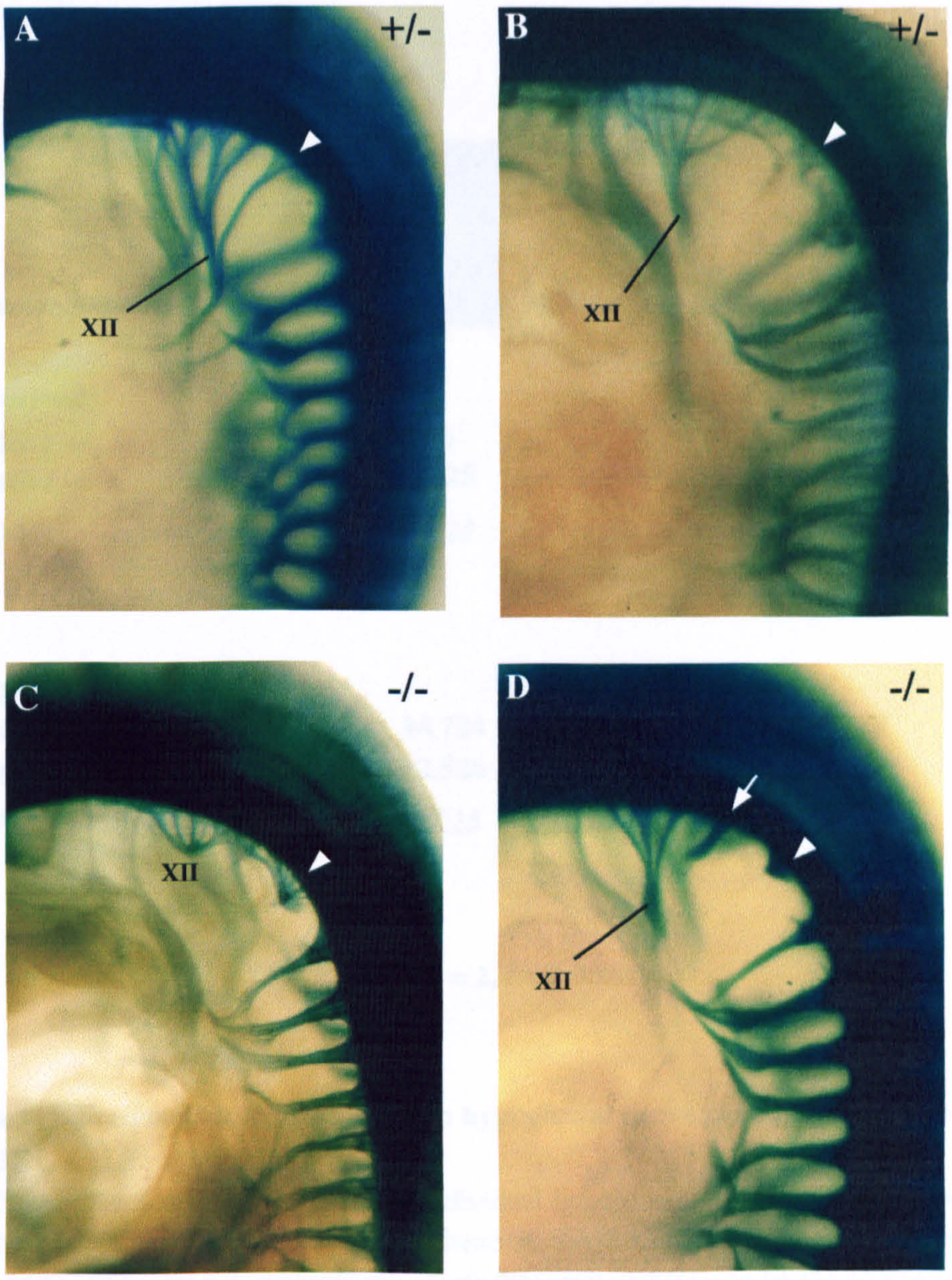

Figure 6.2 The hypoglossal nerves of E11.5 mouse embryos carrying the *TAG-1* null allele

Neck regions of E11.5 TAG-1 null mouse embryos (in each case rostral is to the left and caudal to the bottom), illustrating the different categories to which the stained hypoglossal nerves were assigned.

A: The hypoglossal nerve rootlets have converged, and are extending as a single nerve. This can be seen to extend back towards the developing tongue area (not actually shown; lies to the left of each picture)

B: A number of the hypoglossal nerve rootlets have converged. The resulting hypoglossal nerve extends caudally, but has not begun to extend rostrally towards the tongue region.

C: The hypoglossal nerve rootlets have converged, but no single nerve has extended beyond the point of convergence.

D: Occasionally rootlets of a single hypoglossal nerve would not all have the same fate. This example has three rootlets that seem to extended caudally after convergence, and a fourth that does not extend caudally with the others (arrowed). Arrowheads indicate staining of projections that were not included in the present analysis. It was not clear whether they were caudal hypoglossal nerve rootlets, or projections from the most rostral cervical spinal cord. The three distinct phenotypes shown in A, B and C were observed in both heterozygous and homozygous embryos, although the frequency with which each occurred differed significantly (see table 6.1).

The actual genotype of each embryo is indicated on the figure.

A

phenotype:	 *1*	 *2*	 *3*	*totals*
observed:				
TAG-1 +/-	31	44	4	*79*
TAG-1 -/-	34	23.25	16.75	*74*
total	*65*	*67.25*	*20.75*	*153*

B

expected:				
TAG-1 +/-	33.562	34.724	10.714	*79*
TAG-1 -/-	31.438	32.526	10.036	*74*
total	*65*	*67.25*	*20.75*	*153*

X^2= 14.227, *d.f.* = 2, *P*= 0.000814

Table 6.1 Frequencies with which each hypoglossal nerve phenotype was observed at E11.5, and X^2 analysis.

A: Numbers within the table represent individual hypoglossal nerves of the phenotypes illustrated at the head of each column. Phenotypes 1, 2 and 3 correspond to the embryos A, B and C of figure 6.2, respectively. Note that each embryo can be the source of two data points. Occasionally some of the rootlets of a nerve would have one fate, while other rootlets had another (see figure 6.2D). In such cases, fractions were assigned to categories as appropriate. For example, the nerve shown in figure 6.2 D would have been scored as 0.75 phenotype 2 and 0.25 phenotype 3. Damaged nerves were not scored.

The results were obtained from embryos that were either of a pure C57Bl/6 background (back-crossed for at least 6 generations), or that were on a mixed background of unknown composition.

B: X^2 analysis. "*expected*" values are those that would have been obtained if there was no difference between the heterozygous and homozygous nerves. These values were calculated as phenotype total x genotype total / grand total. The result of a X^2 test comparing the observed and expected frequencies is also shown. *d.f*: degrees of freedom; *P*: probability that the given X^2 statistic would have been obtained if there was no difference between heterozygous and homozygous hypoglossal nerves. Appendix 6.A presents the results of alternative classification of the above data (see discussion).

6.2, this analysis did not include "rootlets" that might in fact have been of cervical spinal origin. These did sometimes contribute to the hypoglossal nerve, as in figure 6.2 A, and as has been reported in chick embryos (Rogers, 1965), mouse embryos (Ericson *et al.*, 1997) and adult rats (O'Reilly and Fitzgerald, 1990). However, the contribution made by these projections varied, and did not appear to be linked to *TAG-1* genotype (data not shown).

Hypoglossal axons seemed to fail to extend beyond the point of rootlet convergence (i.e. they were of phenotype 3) more frequently in homozygote E11.5 embryos than in their heterozygote littermates (table 6.1 A). This difference was found to be statistically significant ($\chi^2 = 14.227$, $d.f. = 2$, $P < 0.001$; table 6.1 B), indicating that the hypoglossal nerves of homozygous embryos are more likely to be defective than those of heterozygotes.

6.3.3 The hypoglossal nerve in E12.5 mouse embryos carrying the *TAG-1* null allele

At E12.5, the majority of hypoglossal nerves had extended ventrally and also turned to grow towards the developing tongue (phenotype 1 in table 6.2). As shown in figure 6.3, some nerves had extended but not turned towards the tongue (phenotype 2), and others had not extended ventrally beyond rootlet convergence (phenotype 3). As at E11.5, failure to extend beyond the point of convergence was more common amongst the hypoglossal nerves of homozygous embryos (table 6.2). The difference between the two groups was found to be statistically significant ($\chi^2 = 8.701$, $d.f. = 2$, $P < 0.05$; table 6.2 B), indicating that a lack of TAG-1 protein also affects development of the hypoglossal nerve at E12.5.

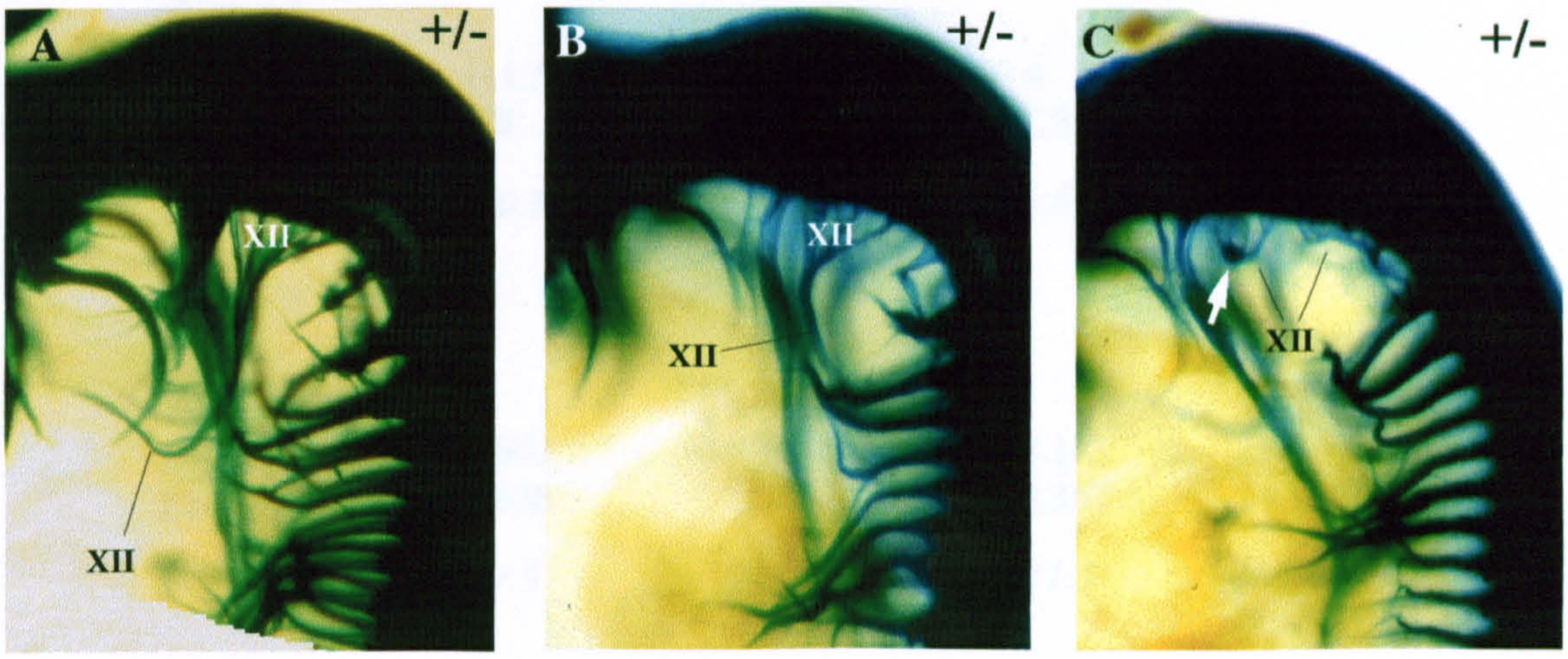

Figure 6.3 The hypoglossal nerves of E12.5 mouse embryos carrying the *TAG-1* null allele

Neck regions of E12.5 *TAG-1* null mouse embryos (rostral is to the left in each case), illustrating the different categories to which the stained hypoglossal nerves were assigned. A: Hypoglossal nerve rootlets have converged, and are extending as a single nerve that can be seen to extend back towards the developing tongue area. B: The hypoglossal nerve rootlets have converged, but the single nerve does not extend rostrally towards the tongue region. C: Hypoglossal nerve rootlets have converged, but no single nerve has extended beyond the point of convergence. The white arrow indicates a "knot-like" area at the point of rootlet convergence. This suggests that the hypoglossal axons are still able to grow, but that their ability to extend away from the "knot" is compromised. As at E11.5, projections that could not be confidently identified as being hypoglossal were not included in analyses. All three of the above phenotypes were observed in both heterozygous and homozygous embryos (see table 6.2)

The actual genotype of each embryo is indicated on the figure.

A

phenotype:	 *1*	 *2*	 *3*	*total*
observed:				
TAG-1 +/-	111.5	15.5	4	*131*
TAG-1 -/-	38	8.5	7.5	*54*
total	*149.5*	*24*	*11.5*	*185*

B

expected:				
TAG-1 +/-	105.862	16.995	8.143	*131*
TAG-1 -/-	43.638	7.005	3.357	*54*
total	*149.5*	*24*	*11.5*	*185*

X^2= 8.701, d.f. = 2, *P*= 0.0129

Table 6.2 Frequencies with which each hypoglossal nerve phenotype was observed at E12.5, and X^2 analysis. A: Numbers represent individual hypoglossal nerves of the phenotypes illustrated at the head of each column. Note that each embryo can be the source of two data points. Occasionally some of the rootlets of a nerve would have one fate, while other rootlets had another. In such cases, fractions were assigned to categories as appropriate. Damaged nerves were not scored. The results were obtained from embryos that were either of a pure C57Bl/6 background (back-crossed for at least 6 generations), or that were on a mixed background of unknown composition.
B: X^2 analysis. "e*xpected" value*s are those that would have been expected if there was no difference between the heterozygous and homozygous nerves. These values were calculated as phenotype total x genotype total / grand total. The result of a X^2 test comparing the observed and expected frequencies is also shown. *d.f.*: degrees of freedom; *P*: probability that the given X^2 statistic would have been obtained if there was no difference between heterozygous and homozygous hypoglossal nerves.

6.3.4 The hypoglossal nerve in E13.5 mouse embryos carrying the *TAG-1* null allele

At E13.5, the hypoglossal nerve appeared to be stained less strongly than at the younger ages examined. This was expected, as it has previously been reported that hypoglossal TAG-1 immunoreactivity begins to wane after E12 (Wolfer *et a*l., 1994). Intense staining of many other nerves meant that it was difficult to identify and trace the hypoglossal nerve. Of the E13.5 hypoglossal nerves that could be identified and traced, all extended ventrally, and all but one could be seen to turn to grow towards the tongue (figure 6.4; table 6.3). It was impossible to say whether the other hypoglossal nerves had turned rostrally, or had even extended beyond the point of convergence.

In view of the difficulty in tracing the hypoglossal nerve at E13.5, and the reported inadequacy of whole mount staining method at later ages (Whiting *et al.*, 1991), older embryos were not analysed.

6.3.5 The hypoglossal nerve in other mutant embryos

As an absence of TAG-1 appeared to have an effect upon the hypoglossal nerve, how TAG-1 might function was investigated using embryos with other mutations. Expression of the *TAG-1* null mutant allele was used as a marker for the hypoglossal nerve, and embryos that were heterozygous for this mutation, but otherwise wild type, were used as controls (see chapter 5). These embryos were compared with littermates that also had the TAG^{A} mutant allele, in order to establish whether the hypoglossal nerve developed normally in animals that expressed only truncated TAG-1. The control embryos were also compared with littermates that were in addition hemizygous for the *L1* mutation, to establish whether the nerve was affected by an absence of L1. Furthermore, embryos that were hemizygous for the *L1* mutation, and which *also* carried both *TAG-1* mutant alleles, were examined, in order to assess the effects of simultaneous deficiencies in both IgCAMs. It proved most

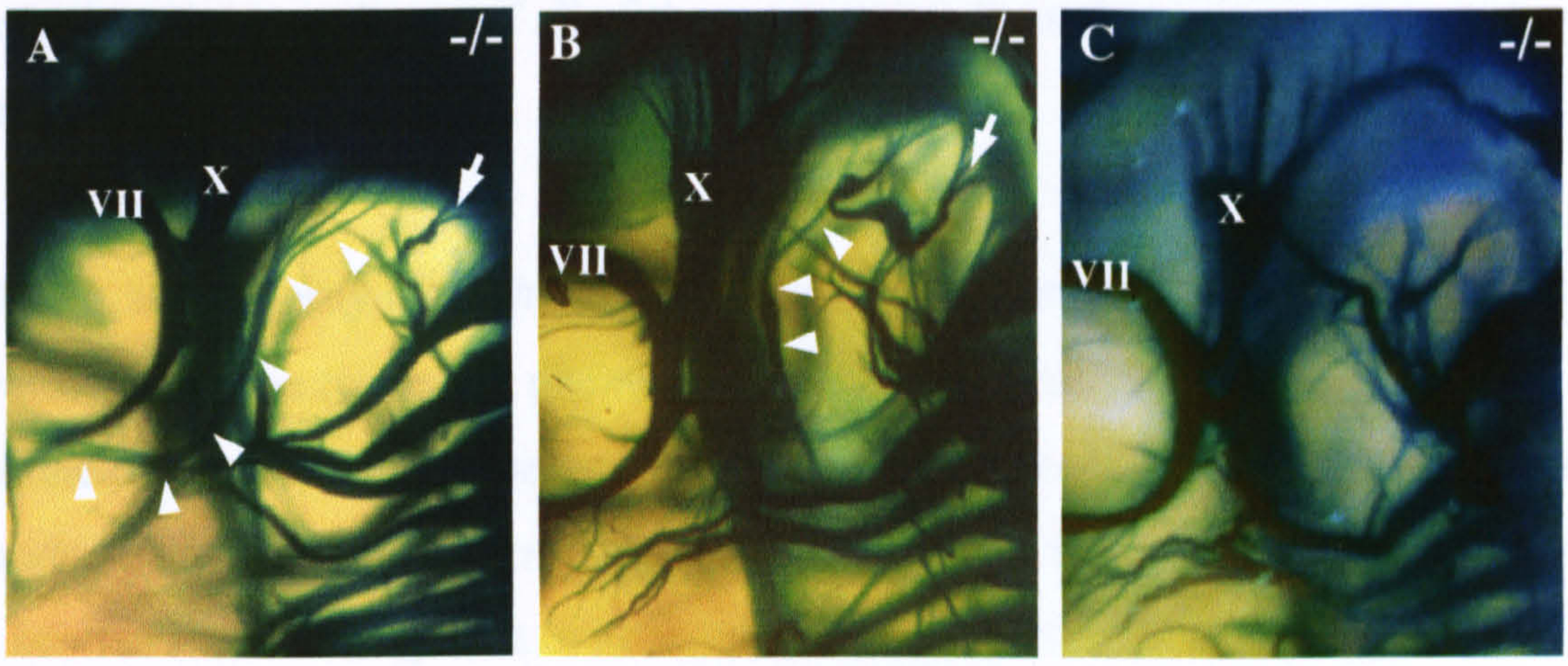

Figure 6.4 The hypoglossal nerves of E13.5 mouse embryos carrying the *TAG-1* null allele

Neck regions of E13.5 *TAG-1* null mouse embryos. Rostral is to the left in each case; the facial (VII) and vagal (X) nerves are labelled for orientation.

A: White arrowheads indicate a hypoglossal nerve that could be traced through a rostral turn and which definitely extended towards the tongue region.

B: White arrowheads indicate a hypoglossal nerve that extended beyond the point of convergence, but that could not be traced through a rostral turn with certainty.

C: In many cases, faint staining of the nerve relative to others around it meant that the hypoglossal nerve could not be identified at all.

White arrows indicate staining within what appeared to be the most rostral cervical spinal nerves. These projections varied considerably in the embryos studied, and their variation seemed to be independent of genotype (data not shown).

The actual genotype of each embryo is indicated on the figure.

phenotype:	 *1*	 *2*	*hypoglossal nerve was not positively identified*	*total*
TAG-1 +/-	15	0	3	*18*
TAG-1 -/-	5	1	4	*10*
total	*20*	*1*	*7*	*28*

Table 6.3 Frequencies with which each hypoglossal nerve phenotype was observe at E13.5.

Numbers represent individual hypoglossal nerves that could be traced through a rostral turn towards the tongue (phenotype 1), that could only be seen to extend ventrally but for which no rostral turn was apparent (phenotype 2), or that could not be identified at all.

The results were obtained from embryos of a mixed background of unknown composition.

A X^2 analysis could not be carried out as "expected" values were not large enough for such a test to be valid (data not shown; Dytham, 1999).

practical to obtain embryos of all of these genotypes from the same crosses, as shown in figure 2.4.

At E11.5, the majority of the hypoglossal nerves could be seen to have turned to extend towards the tongue (table 6.4, phenotype 1). This was true of all of the genotypes examined. The hypoglossal nerves that could not be traced through a rostral turn had all extended beyond the point of rootlet convergence (table 6.4, phenotype 2). Too few nerves had been examined for χ^2 tests to be valid (Dytham, 1999). However, the frequencies presented in table 6.4 were sometimes suggestive.

Row 1 of table 6.4 shows the results from control embryos; row 2 shows those from embryos that expressed wild type L1 protein, but only truncated forms of TAG-1. Within these groups, 17 out of 18, and 16 out of 18, hypoglossal nerves could be traced through a rostral turn respectively. This suggests that the hypoglossal nerve develops normally in embryos that have only truncated TAG-1 proteins.

The results from embryos devoid of wild type L1, but not wild type TAG-1 (table 6.4, row 5) were more ambiguous. 8 out of 10 of hypoglossal nerves had definitely made a rostral turn, but, as mentioned, the significance of this distribution could not be assessed statistically. Neither could the occurrence of the two phenotypes in the embryos that lacked L1 protein, and that expressed only truncated TAG-1 proteins (table 6.4, row 6). However, it is notable that 6 out of the 18 double mutant hypoglossal nerves could not be traced through a rostral turn. It is possible that this result reflects a delay in development of the hypoglossal nerves of embryos that lack L1 and express only truncated versions of TAG-1.

phenotype:	 *1*	 *2*	*total*
1. L1⁺, TAG-1 +/-	17 (94.4%)	1 (6%)	*18*
2. L1⁺, TAG-1A/-	16 (89%)	2 (11%)	*18*
3. L1+/-, TAG-1 +/-	8 (100%)	0	*8*
4. L1+/-, TAG-1A/-	4 (67%)	2 (33%)	*6*
5. L1-/Y, TAG-1 +/-	8 (80%)	2 (20%)	*10*
6. L1-/Y, TAG-1A/-	12 (67%)	6 (33%)	*18*
total	*65*	*13*	*78*

Table 6.4 The hypoglossal nerves of E11.5 *TAG-1/L1* double mutant embryos.
The hypoglossal nerves of *TAG-1/L1* mutant embryos were assigned to the first category if they could be seen to have turned to grow towards the tongue, and to the second if they could not. Hypoglossal nerves had always extended beyond the point of rootlet convergence. As previously, "*L1⁺*" refers to embryos of either the +/+ or +/*Y* genotype with regards to L1. All embryos have one *TAG-1* null allele, so that TAG-1 expressing cells could be stained for ß-galactosidase activity. Unfortunately the numbers of nerves were too low for valid X^2 analyses to be carried out (Dytham, 1999). Percentages show each frequency as a proportion of the total number of hypoglossal nerves of that genotype. Both of the nerves shown are from *L1⁺*, *TAG-1A/-* embryos.

6.4 Discussion

A general survey of the effects of the *TAG-1* null mutation upon neural development (chapter 5) raised the possibility that the hypoglossal nerve was affected by an absence of TAG-1 protein. Therefore the development of this nerve was investigated in more detail. As in the more general study, the *lacZ* reporter component of the *TAG-1* null mutation was used to study the nerves mouse embryos from E10.5 to E13.5 inclusive. The results presented support the idea that TAG-1 is indeed involved in hypoglossal nerve development.

6.4.1 E10.5 hypoglossal nerves

At E10.5, the hypoglossal nerve was seen as a number of rootlets. In several embryos, some of these rootlets had converged to form a single nerve. There did not appear to be a difference between the hypoglossal nerves of *TAG-1* null homozygous and heterozygous embryos at this age. This suggests that TAG-1 is not required for the initial stages of hypoglossal nerve formation. However, it would be necessary to examine more E10.5 embryos before the significance of these results could be tested statistically (Dytham, 1999).

6.4.2 E11.5 and E12.5 hypoglossal nerves

6.4.2.1 Effects of the *TAG-1* null mutation

At E11.5, all of the sets of hypoglossal nerve rootlets examined showed at least some convergence. Many of the resulting hypoglossal nerves extended beyond the point of

rootlet convergence, and a large proportion could also be traced through a rostral turn. χ^2 analysis of the occurrence of each phenotype showed that the hypoglossal nerves of *TAG-1* null homozygous embryos were significantly different from those of heterozygotes. The frequencies with which each phenotype was observed also differed significantly between heterozygous and homozygous hypoglossal nerves at E12.5. These results indicate that the E11.5 and E12.5 hypoglossal nerves are affected by an absence of TAG-1 protein.

To better understand the effects of the mutation, the E11.5 results were reclassified, and the significance of differences reassessed (appendix 6.A). When classified according to whether they had turned towards the tongue or not (i.e. when phenotypes 2 and 3 were combined), the hypoglossal nerves of the two genotypes did not differ significantly. When classified according to whether they had extended beyond convergence or not (i.e. when phenotypes 1 and 2 were combined), the genotypes did show a significant difference (χ^2 = 10.0640, *d.f.* = 1, P = 0.00151). This suggests that the main source of the difference between E11.5 heterozygous and homozygous hypoglossal nerves is their ability to extend beyond rootlet convergence. Thus if TAG-1 does in fact have a role in E11.5 hypoglossal axon development, it might act specifically at the stage of the post-convergence ventral extension. The fact that all *TAG-1* mutant hypoglossal nerves send rootlets ventrally to the point of convergence (see figures 6.2 and 6.3) supports the above suggestion that TAG-1 is not required for the earliest stages of extension away from the hindbrain.

At E12.5, the most obvious difference between hypoglossal nerves of the two genotypes was again in the frequency with which they failed to extend beyond rootlet convergence (table 6.2). This observation could not be tested for statistical significance, as regrouping of the phenotypes meant that the data were no longer suitable for χ^2 analysis. However, it was suggestive of TAG-1 also being specifically involved in post-convergence extension at E12.5.

6.4.2.2 How might TAG-1 be involved?

If TAG-1 is indeed involved in guidance of E11.5 and E12.5 hypoglossal nerves, it might function in any of a number of ways. It could be important for the growth of post-convergence hypoglossal axons, although the frequent occurrence of "knot-like" staining in affected nerves (as in figure 6.3 C) suggests that axons do continue to extend, and that it is the direction of their growth that is perturbed. TAG-1 could direct hypoglossal axons in association with activities that have previously been implicated in development of the nerve, such as HGF or Sema 3A, or in association with novel factors. Figure 6.5 summarises some of its possible modes of action.

Mid-gestation embryos homozygous for a mutation in the gene encoding Hepatocyte Growth Factor (HGF) displayed a similar phenotype to that described above. Hypoglossal nerve rootlets extended from the hindbrain and converged, but did not appear to extend further towards the tongue (Caton *et al.* 2000). The tongue regions of rat and chicken embryos express HGF mRNA, and mouse hypoglossal neurons express mRNA of the HGF receptor Met. These observations, and the fact that HGF is a chemoattractant for hypoglossal axons *in vitro*, led to the suggestion that HGF might normally attract hypoglossal axons *in vivo* (Caton *et al.*, 2000). It is conceivable that TAG-1 is involved in the ability of hypoglossal neurons to find HGF attractive. For instance, TAG-1 could interact with Met, affecting its ability to mediate attraction to HGF. As HGF can prevent the degeneration of adult rat hypoglossal motor neurons (Okura *et al.*, 1999), any alteration of its effects by TAG-1 could be of clinical importance.

TAG-1 could theoretically allow hypoglossal axons to respond to other attractive factors, such as those that attract cranial motor axons to branchial arches in the absence of HGF function (Caton *et al.*, 2000). Although its mid-gestation expression was not recorded, the developing tongue expresses Netrin-3 at E15.5 (Püschel, 1999), so it is conceivable that the failure to extend beyond convergence reflects an inability to find target netrins attractive. Chicken hypoglossal axons do not respond to Netrin-1 *in vitro* (Varela-Echavarría *et al.*, 1997), but their response to Netrin-3 does not appear to have been tested.

Allows hypoglossal axons to overcome a hindbrain chemoattractant?
e.g. netrin?

Allows hypoglossal axons to respond to a hindbrain chemorepellant?
e.g. Sema 3A (Varela-Echavarria *et al.*, 1997), netrin?, F-spondin?, Wnt-7b?

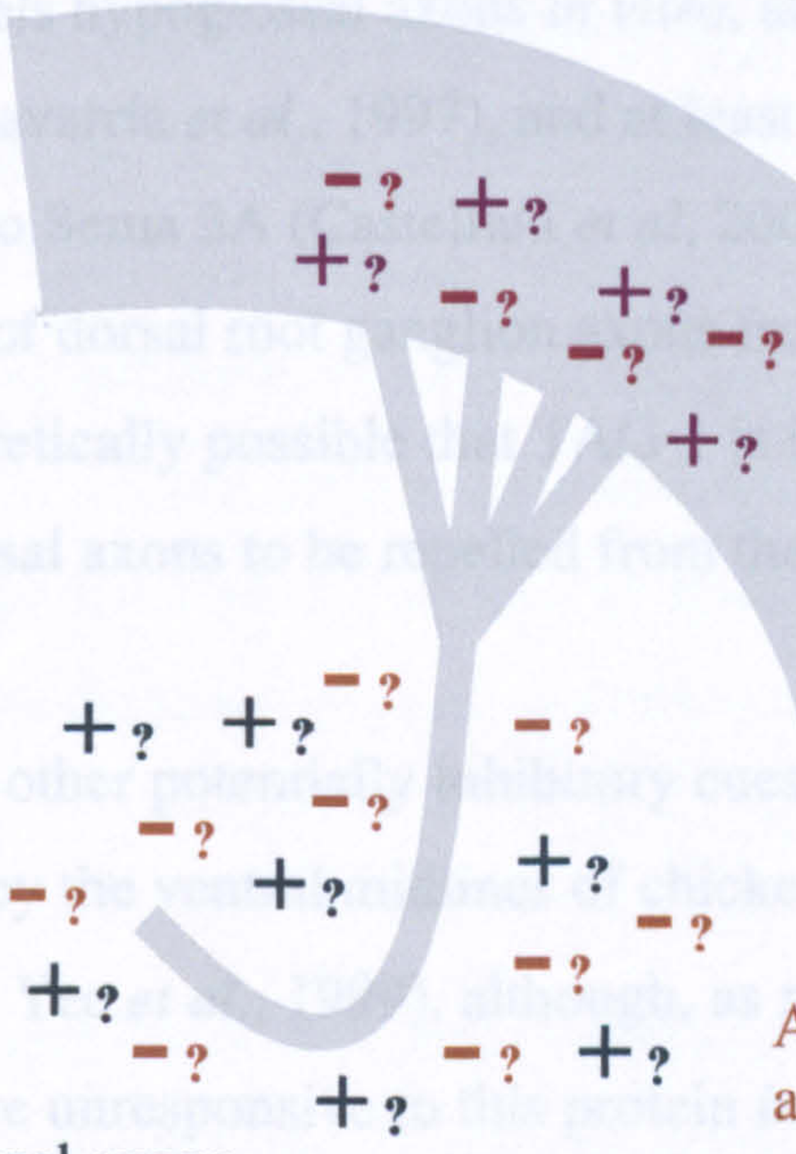

Allows hypoglossal axons to respond to a mesodermal chemoattractant?
e.g. HGF (Caton *et al.*, 2000), ephrins?

Allows hypoglossal axons to overcome an inhibitory factor within the mesoderm?
e.g. ephrins?

Figure 6.5 Summary of the ways in which TAG-1 may function during normal hypoglossal nerve development. Defects in extension of *TAG-1* null mutant hypoglossal nerves suggest that TAG-1 is important for both extension beyond rootlet convergence and the subsequent rostral turn. In both events, TAG-1 could allow hypoglossal axons to respond to repulsive signals from the hindbrain, to ignore attractive signals from the hindbrain, to respond to attractive signals from areas it usually enters, or to ignore repulsive signals from areas through which it must pass. Candidate molecules are mentioned above. Sema 3A and HGF have been shown to guide hypoglossal axons (for references, see diagram). All other factors are mentioned speculatively (for references, see text). The role of TAG-1 in response to factors could be tested *in vitro*.

Alternatively and/or additionally, TAG-1 could be important for the ability of hypoglossal axons to be repelled from the ventral hindbrain once they have converged. Semaphorin 3A (Sema 3A), which repels hypoglossal axons *in vitro*, and is expressed by the ventral hindbrain (Varela-Echavarría *et al.*, 1997), and at least one IgCAM can affect the way in which axons respond to Sema 3A (Castellani *et al*, 2000). Axonin-1 has been proposed to mediate the repulsion of dorsal root ganglion axons from the notochord (Masuda *et al.*, 2000). Thus it is theoretically possible that TAG-1 is involved in the ability of post-convergence hypoglossal axons to be repelled from the hindbrain by Sema 3A.

There are a number of other potentially inhibitory cues expressed by the ventral hindbrain. Netrin-1 is expressed by the ventral midlines of chicken and rat embryonic hindbrains (Kennedy *et al.*, 1994; Yee *et al.*, 1999), although, as mentioned above, chicken hypoglossal axons were unresponsive to this protein *in vitro* (Varela-Echavarría *et al.*, 1997). The ventral hindbrain expresses B ephrins (Gale *et al.*, 1996 b; Küry *et al.*, 2000; Yokoyama *et al.*, 2001): these ligands are known to repel limb motor axons (Wang and Anderson, 1997; Helmbacher *et al.*, 2000), a population of axons that shares other guidance mechanisms with those of the hypoglossal nerve (Ebens *et al.*, 1996; Arber *et al.*, 1999). A region that includes the hypoglossal nucleus has been reported to express at least one Eph B receptor at the time of hypoglossal nerve extension (Gale *et al.*, 1996 b; Henkemeyer *et al.*, 1998), and the TAG-1-related protein L1 can cause phosphorylation of at least one Eph receptor (Zisch *et al.*, 1997). Thus it is conceivable that TAG-1 could also interact with hypoglossal Eph receptors, in order to enable post-convergence axons to be repelled by hindbrain ephrins. Other candidate repellents include F-spondin and Wnt-7b. F-spondin is expressed in the floor plate of the hindbrain at E11.5 (Klar *et al.*, 1992), and this protein has been shown to repel other embryonic motor neurons (Tzarfti-Majar *et al.*, 2001). The signalling molecule Wnt-7b is also expressed in the caudal hindbrain (Osumi *et al.*, 1997): this protein has been implicated in the guidance of cerebellar axons (Salinas, 1999), and its

absence coincides with a failure of hypoglossal nerve extension in *Pax-6* mutant rat embryos (Osumi *et al.*, 1997).

Rather than simply allowing hypoglossal axons to respond to factors that cause their ventral extension, it is also possible that TAG-1 allows the axons to ignore factors that would otherwise prevent their ventral extension. TAG-1 has previously been suggested to act in such a way in other neurons. It seems to allow cerebellar granule neurites to overcome inhibitory effects of F3 (Buttiglione *et al.* 1998), and to render dorsal spinal commissural axons insensitive to the inhibitory activities of the floor plate (Stoeckli *et al.*, 1997; Stoeckli and Landmesser. 1998). A-class ephrins are expressed within the mesoderm ventral to the point of rootlet convergence, and also within the branchial arches (Gale *et al.*, 1996 b; Küry *et al.*, 2000), so it is conceivable that these are inhibitory for hypoglossal axons if TAG-1 is absent.

In vitro experiments could be used to establish whether any of the above speculations are valid. For example, the extent to which homozygous *TAG-1* null hypoglossal axons are repelled by a source of Sema 3A, or attracted by a source of HGF, could be investigated (as in Varela-Echavarría *et al.*, 1997 and Caton *et al.*, 2000 respectively).

The apparent defects in guidance of *TAG-1* null homozygote hypoglossal axons could be secondary to other effects of the mutation. For example, it is theoretically possible that TAG-1 is involved in the specification of hypoglossal motor neurons. Hypoglossal neurons were mis-specified in *Pax-6* and *Hb9* mutant animals (Ericson *et al.*, 1997; Osumi *et al.*, 1997; Arber *et al.*, 1999), and, in the *Hb9* mutant mice, what appeared to be the hypoglossal nerve was sometimes "severely misrouted" (Arber *et al.*, 1999). It seems that the hypoglossal nucleus is considered fully specified when it expresses mRNA of the transcription factor islet-2 (Varela-Echavarría *et al.*, 1996; Ericson *et al.*, 1997; Osumi *et al.*, 1997). This factor is not detected until after the onset of TAG-1 activity (Varela-Echavarría *et al.*, 1996; figure 6.1), so it could be that the above axon guidance defects reflect a change of neuron identity. This potential explanation could be further investigated by establishing whether the source of "hypoglossal" axons still expresses islet-2 and HB9.

It is also theoretically possible that TAG-1 is in fact important for the normal decussation of hypoglossal dendrites (described by Cajal, 1909, Kappers, 1936, Paxinos, 1985), and that failure of this somehow affects guidance of the axons. It would be interesting to establish whether hypoglossal dendrite decussation occurs normally in *TAG-1* null mutant embryos, for example by unilateral labelling of the hypoglossal nucleus with DiI.

However TAG-1 acts during hypoglossal axon guidance, the present results raise the possibility that its function does not require the first two Ig-like domains of the protein. The similarity between the phenotypes of $TAG^{+/-}$ and $TAG^{A/-}$ mutant hypoglossal nerves (table 6.4, rows 1 and 2) suggests that the absence of these domains of TAG-1 from an embryo does not affect hypoglossal nerve development. This is perhaps a surprising suggestion, as these domains are amongst those necessary for the interactions of axonin-1 with NgCAM and NrCAM (see Introduction; Rader *et al.*, 1996; Fitzli *et al.*, 2000). However, other domains of axonin-1 were both necessary and sufficient to promote neurite outgrowth *in vitro* (Rader *et al.*, 1996) and to mediate the homophilic interactions of its human homologue TAX-1 (Tsiotra *et al.*, 1996), so it is conceivable that such domains are also sufficient for the correct guidance of hypoglossal axons.

The first step in testing this idea would be to examine more TAG^{A} mutant embryos, so that the differences between $TAG^{+/-}$ and $TAG^{A/-}$ mutant hypoglossal nerves could be tested statistically. It would also be important to assess the effects of the TAG^{A} mutation on the same strain background used for the TAG-1 null analyses. *TAG-1* null embryos were either of the "pure" C57Bl/6 strain or of a mixed background of unknown composition, whereas the TAG^{A} mutants examined were obtained by mating mice of the mixed background with those of a pure 129/SvEv strain. Thus the TAG^{A} mutant embryos were of a background containing a substantially greater proportion of 129/SvEv genes than that used for *TAG-1* null embryos. As discussed in previous chapters, the *L1* null mutant phenotype is noticeably more severe in mice of the C57Bl/6 backgrounds (Dahme *et al.*, 1997), indicating that certain loci of the129/SvEv genome have alleles that can ameliorate effects of the *L1* mutation. The occurrence of cerebellar granule cell migration defects in C57Bl/6, but not 129/SvEv, mice suggests that 129/SvEv alleles might also lessen the effects of

TAG-1 mutations (K. Ohyama, R. Yoshida and A.J.W. Furley, personal communication). If so, it could be these that temper the TAG^{A} mutant hypoglossal nerve phenotype. Crossing both *TAG-1* mutations onto a single background would allow any differences between their effects to be studied more objectively.

6.4.2.3 Why are some homozygous mutant nerves unaffected?

Although E11.5 *TAG-1* null homozygous mutant hypoglossal nerves have been shown to be statistically more likely to stall at the point of convergence, many did extend further and turn towards the tongue. Often homozygous embryos had one stalled hypoglossal nerve and one that was apparently normal. Conversely, many heterozygous mutant hypoglossal nerves appeared to stall. Such incomplete penetrance of a mutation is a well-known phenomenon. The hypoglossal nerve was absent or misrouted in some *HB9* homozygous mutant embryos, but was unaffected in others (Arber *et al.*, 1999). Eph A4 null mutant mice were said to show agenesis of the anterior commissure "with high penetrance" when only seven out of thirteen brains were affected (Kullander *et al.*, 2001 a). Similarly, only 20% of *ephrin B3* mutant mice showed agenesis of the corpus callosum (Yokoyama *et al.*, 2001). Bolwig's nerve was defective in only around 55% of *Drosophila DSCAM* mutants (Schmucker *et al.*, 2000).

Why the *TAG-1* null mutation should show incomplete penetrance is unclear. It could reflect the heterogeneity of the genetic backgrounds used. Many of the embryos examined during the present study were of a mixed genetic background of unknown composition, such that siblings could have had different alleles at certain loci. As mentioned above, such differences can mean that a single mutation has different effects. However, some of the embryos studied were of a "pure" (back-crossed for at least six generations) C57Bl/6 background, and analysis of these embryos alone gave similar results to those from embryos of undefined strain (data not shown). This suggests that the apparent normality of some of the homozygous hypoglossal nerves cannot simply be attributed to the presence of modifying alleles in some embryos but not others.

It could be that TAG-1 acts in a subtle way, to increase the probability that a hypoglossal nerve extends, rather than forcing it to extend. For example, it could be that stochastically prevents the extension of a number of pioneer hypoglossal axons, which all other hypoglossal axons normally follow. TAG-1 could conceivably allow the pioneer axons to overcome such a factor, but levels of the factor might not always be high enough to be problematic. Alternatively, the levels of potentially redundant factors could vary stochastically. For instance, it might be that the activity that guides the pre-convergence hypoglossal rootlet extension is sometimes, but not always, sufficient to also rescue the effects of a lack of TAG-1 protein.

6.4.2.4 Possible inadequacies of the present results

As mentioned above, the some of the present results may reflect differences in the genetic backgrounds of embryos in addition to their *TAG-1* genotype. However, as also mentioned, the *TAG-1* null embryos of a mixed strain background showed a similar distribution of phenotypes to those of a pure strain (data not shown).

Another possible inadequacy is that the present results might actually underestimate the effects of the *TAG-1* null mutation. Although heterozygous mutants are often assumed to be essentially wild type (for example, by Leighton *et al.*, 2001), this is not necessarily the case. "Haplo-insufficiency" has been reported for other genes that encode axon guidance molecules. For example, mice heterozygous for a null mutation in the *Eph A4* gene had limb innervation defects that were of a severity intermediate to that of wild type and homozygote embryos (Helmbacher *et al.*, 2000). Around 12% of the flies heterozygous for a mutation in *DSCAM* had defects in Bolwig's nerve (Schmucker *et al.*, 2000). Aggression was markedly increased amongst mice either homozygous or heterozygous for an *NCAM* mutation (Stork *et al.*, 1997). Immunohistochemical labelling of wild type embryos does indicate that their hypoglossal nerves are similar to heterozygote hypoglossal nerves stained for ß-galactosidase activity (see appendices 5.B and 5.D). However, of the 16 wild type hypoglossal nerves labelled, all extended beyond convergence and made a rostral turn (see below; data not shown). This could indicate that a failure to extend beyond convergence is

not at all normal, and that a reduced amount of TAG-1 protein in heterozygous embryos can affect hypoglossal nerve development. This suggestion is supported by reports that cerebellar granule cell descent is impaired in mice that are either homozygous or heterozygous for *TAG-1* mutations (K. Ohyama, R. Yoshida and A.J.W. Furley, personal communication).

Thus the deviation of *TAG-1* null homozygous hypoglossal nerves from the norm could in fact be more pronounced than presented above. A direct comparison of wild type and homozygous embryos would require a technique such as immunohistochemistry or axon tracing. Preliminary attempts have shown that the E11.5 hypoglossal nerve can be labelled with DiI (data not shown) or antibodies (appendices 5.B and 5.D), although the success of these approaches was variable. The monoclonal anti-TAG-1 antibody 4D7 (Yamamoto *et al.*, 1986) often labelled the hypoglossal nerve strongly, but this would not be of use for the study of *TAG-1* null mutant nerves. 2H3, an anti-neurofilament antibody (Dodd *et al.*, 1988) that should label both wild type and mutant hypoglossal nerves, gave inconsistent results (data not shown). As appeared to be the case in previous studies, this antibody labels the hypoglossal nerve in some cases (as in Ericson *et al.*, 1997; Kitsukawa *et al.*, 1997; Osumi *et al.*, 1997), but not others (as in Van Maele-Fabry *et al.*, 1997; Giger *et al.*, 2000). This may reflect slight variations in the extent to which epitopes were fixed, or differences in the precise composition of the strain backgrounds used. Indeed, the 2H3 antibody seemed to label the hypoglossal nerves of pure 129/SvEv embryos, but not those of C57Bl/6 or mixed strain embryos (data not shown).

Immunohistochemistry would also allow TAG^{A} mutant embryos to be analysed in their own right. This would allow the importance of different regions of the TAG-1 protein to be examined without potential complications from other mutations. Immunohistochemical analysis might also provide a more reliable method of marking the hypoglossal nerves of E13.5 embryos. Generation of another *TAG-1* null mutation would allow the effects of an absence of TAG-1 to be studied independently of tau-ß-galactosidase. In one study, tau-GFP and tau-ß-galactosidase reporter proteins were shown to alter the fasciculation, morphology and survival of *Drosophila* sensory axons (Williams *et al.*, 2000), so it is

technically possible that tau-ß-galactosidase is responsible for the hypoglossal nerve defects of *TAG-1* null homozygotes. However, other studies have described the use of tau-containing reporter proteins to mark axons without detriment (for example, Callahan and Thomas, 1994; Mombaerts *et al.*, 1996). Many other nerves that were stained as strongly as the hypoglossal were not obviously different to those of wild type animals (compare figure 6.2 with appendices 5.B and 5.D). This implies that the tau-containing reporter protein did not adversely affect the development of *TAG-1* null mutant hypoglossal axons, although analysis of embryos with a different null mutation would be needed to confirm this.

6.4.3 Later development of the hypoglossal nerve

The results presented indicate that the *TAG-1* null mutation has a significant effect upon the projection of hypoglossal nerve at E11.5 and E12.5. At E13.5, faint staining of the hypoglossal nerve, and intense staining of many other nerves, meant that it was often difficult to trace hypoglossal projections. The hypoglossal nerves that were sufficiently strongly labelled could almost always be traced through a rostral turn, possibly reflecting a "recovery" of the hypoglossal nerve defects seen at earlier ages. However, it could equally reflect a greater tendency of defective nerves to lose their staining. Too few E13.5 hypoglossal nerves could be identified to distinguish between these possibilities with confidence. To increase the numbers of nerves examined, it might be better to identify hypoglossal nerves by application of the tracer DiI.

The idea that affected hypoglossal nerves recover is supported by other observations. The differences between heterozygous and homozygous hypoglossal nerves were not as significant at E12.5 as they were at E11.5, implying that nerves of the two genotypes become more similar as development proceeds. *TAG-1* null homozygous mice have no obvious defects of tongue function, and performed as well as heterozygous siblings in a test

of tongue extension (B.W. Kiernan, personal communication; after Kolb and Wishaw, 1983).

Recovery might occur in any of a number of ways. It could involve extension of hypoglossal axons that were previously stalled, for example if other factors begin to fulfil the role of TAG-1, or if a factor usually antagonised by TAG-1 ceases to function. Indeed, defects in the hypoglossal nerve extension of *HGF* mutant mouse embryos appear to be compensated for as development proceeds (Caton *et al.*, 2000). A detailed study of the expression of axon guidance molecules in the *TAG-1* mutant neck and hindbrain might identify factors that could mediate recovery.

Alternatively, recovery could involve innervation of the tongue by other neurons, as can occur after damage of the human hypoglossal nerve (Wilson *et al.*, 1994). Indeed, in *Pax-6* mutant rat embryos, which lack the hypoglossal nerve, the tongue is innervated by axons of the second cervical spinal nerve (Osumi *et al.*, 1997). Another possibility is that there is no recovery of tongue innervation, but that this is not detrimental. It was not uncommon for embryos to have one hypoglossal nerve that did extend towards the tongue and one that did not (data not shown), and it is possible that unilateral innervation allows adequate tongue movement. Indeed, injury of one hypoglossal nerve does not usually have a severe effect upon human patients (Wilson *et al.*, 1994).

Whether tongue innervation is restored could be investigated in a number of ways. While it is not practical to stain older embryos for ß-galactosidase activity (Whiting *et al.*, 1991), axons could be labelled with a tracer such as DiI. Application of DiI to the hypoglossal nucleus would allow the destination of hypoglossal axons to be determined. Application of DiI to the tongue itself would label any innervating axons retrogradely, and should show the location of their cell bodies. A marker of the hypoglossal nucleus, such as HB9 (Arber *et al.*, 1999), could be used to confirm whether a source of tongue innervation was indeed hypoglossal.

6.4.4 Hypoglossal nerve development and L1

L1, and *L1/TAG-1* double, mutant embryos were also analysed (table 6.4). The sample sizes were such that χ^2 tests would have been unreliable (Dytham, 1999), so it was not possible to say whether embryos lacking only L1 (row 5 of table 6.4*)* and controls (row 1*)* differed significantly. Neither was it possible to say whether the hypoglossal nerves of embryos lacking L1 and expressing only truncated TAG-1 (row 6) differed significantly from controls. The proportions of doubly deficient hypoglossal nerves that could not be traced through a rostral turn suggested that there is a difference between these and control nerves. However, the lack of an obvious rostral turn was often linked to paler staining for ß-galactosidase activity (table 6.4). This could reflect a delay in the general development of embryos that lack L1 and express only truncated TAG-1, rather than a specific effect upon hypoglossal axon guidance. More double mutant embryos would need to be analysed, and a purer genetic background used, before any conclusions could be made.

6.5 Conclusions

1. TAG-1 is involved in the correct development of the mid-gestation mouse hypoglossal nerve.

In the absence of TAG-1 protein, E11.5 and E12.5 hypoglossal nerves were significantly less likely to have extended beyond point of rootlet convergence, and turned towards the tongue, than if TAG-1 protein was present.

6.6 Appendices

Appendix 6.A: Analysis of E11.5 hypoglossal nerve results after reclassification.

Appendix 6.A Analysis of E11.5 hypoglossal nerve results after reclassification

A: Comparison of the numbers of hypoglossal nerves that had turned to grow rostrally (phenotype 1) with those of other phenotypes (2 + 3). When the rootlets of one nerve did not all have the same fate, fractions were assigned to categories as appropriate. "e*xpected*" values are those that would have been obtained if there was no difference between the heterozygous and homozygous nerves. The low X^2 value indicates that the heterozygote and homozygote hypoglossal nerves are not significantly different when compared in this way.

B: Comparison of the numbers of hypoglossal nerves that had extended beyond the point of convergence (phenotypes 1 + 2) with the numbers of those that had not (phenotype 3). The X^2 value of over 3.84 indicates that the heterozygote and homozygote hypoglossal nerves are do differ significantly in their ability to extend beyond the point of rootlet convergence.

d.f.: degrees of freedom; *P*: probability that the given X^2 statistic would have been obtained if there was no difference between the nerves.

A

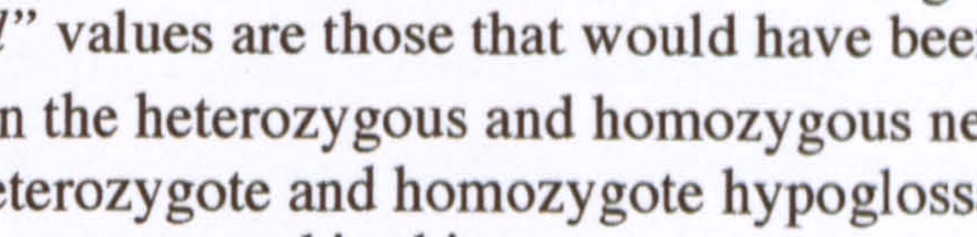

			total:
observed:			
TAG-1 +/-	31	48	79
TAG-1 -/-	34	40	74
total	65	88	153
expected:			
TAG-1 +/-	33.562	45.438	79
TAG-1 -/-	31.438	42.562	74
total	65	88	153

X^2= 0.703, *d.f.* = 1, *P*= 0.402

B

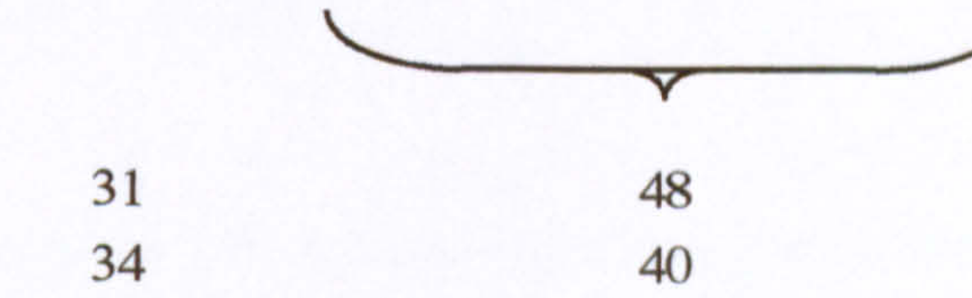

			total:
observed:			
TAG-1 +/-	75	4	79
TAG-1 -/-	57.25	16.75	74
total	132.25	20.75	153
expected			
TAG-1 +/-	68.286	10.714	79
TAG-1 -/-	63.964	10.036	74
total	132.25	20.75	153

X^2= 10.0640, *d.f.* = 1, *P*= 0.00151

7 General Discussion

During the development of a nervous system, axons extend from neuronal cell bodies to the targets on which they will synapse. This extension is guided by a variety of molecular cues within the axons' environment, and by axonal receptors for these cues. Proteins that might act as such cues and/or receptors include certain members of the immunoglobulin-like super-family (IgCAMs). A number of IgCAMs have been shown to influence the guidance of axons *in vitro*, and to have expression patterns suggestive of roles in axon guidance. Whether the proteins do in fact guide axons *in vivo* is perhaps best tested using animals in which IgCAM function has been perturbed. The majority of this thesis describes what is to date the most comprehensive analysis of neural development in mice with mutated *TAG-1* alleles. It also provides novel information on the roles of other cell surface proteins in the development of TAG-1-expressing neurons.

The work conducted falls into one of two main categories. Particular attention was paid to dorsal spinal commissural neurons, because the IgCAMs TAG-1, L1 and NrCAM have previously been implicated in their development. In addition, developing *TAG-1* null mutant mice were examined for gross defects in other aspects of their neuroanatomy. The results obtained are summarised below, along with brief discussions of their potential implications, suggestions for further research. Positive and negative aspects of the study are also considered.

7.1 The development of dorsal spinal commissural axons

7.1.1 Wild type dorsal spinal projections do not all decussate and turn rostrally

The present study provides a detailed description of the dorsal spinal projections of the mid-gestation wild type mouse. The dorsal spinal projections of mid-gestation wild type rats (Bovolenta and Dodd, 1990) and mice (Burstyn-Cohen *et al.*, 1999; Matise *et al.*, 1999; Imondi *et al.*, 2000; Zou *et al.*, 2000) have been described previously. However, little attention had been paid to axons that did anything other than extend across the floor plate and turn rostrally. The results presented here confirm that between 3 and 4% of wild type mouse dorsal spinal axons normally turn caudally after decussation, and that a further 1 to 2% continues to extend laterally rather than making any longitudinal turn. They also show that the trajectory taken by dorsal spinal commissural axons can depend upon the dorso-ventral level of DiI application, and upon mouse genetic background. For example, the axons of E13.5 C57Bl/6 embryos were significantly more likely to have left the floor plate and turned rostrally than those of 129/SvEv embryos, possibly reflecting an inherent difference between these mouse strains. Such findings could prove to be important for the interpretation of other work.

7.1.2 Dorsal spinal commissural projections seem to develop normally in the absence of wild type TAG-1, L1 or NrCAM proteins

Previous studies have implicated the chicken homologues of TAG-1, L1 and NrCAM in the ability of dorsal spinal commissural axons to extend into the floor plate (Stoeckli and Landmesser, 1995; Stoeckli *et al.*, 1997; Fitzli *et al.*, 2000). The present work found there to be no significant differences between the ways in which these axons projected in wild type and *TAG-1* mutant mouse embryos. This indicates that TAG-1 is not required for the

normal guidance of mouse dorsal spinal neurons. Similarly, there were no significant differences between the dorsal spinal projections of embryos that lacked L1 and those of their wild type littermates. In *NrCAM* homozygous mutant embryos, a significantly greater proportion of dorsal spinal projections made a caudal turn after decussation, but the dorsal spinal axons of wild type and *NrCAM* mutant animals were otherwise identical.

These results all appear to be in contrast to those from chicken embryos (Stoeckli and Landmesser, 1995; Stoeckli *et al.*, 1997; Fitzli *et al.*, 2000). One possible explanation for such discrepancies is that the antibodies and soluble proteins applied to chick spinal cord did not simply perturb IgCAM function, as had been assumed. Another possibility is that there are differences between the ways in which the dorsal spinal axons of mouse and chicken are guided.

The reported absence of defects indicates that TAG-1, L1 and/or NrCAM are individually unnecessary for mouse dorsal spinal axon development. However, it does not exclude the possibility that these proteins are involved in the development of these projections. It might be that other factors can compensate for their absence. This possibility could be investigated by comparing the responses of wild type and mutant axons to floor plate tissue *in vitro*. Perturbation of axonin-1 or NrCAM function had more pronounced effects upon chick dorsal spinal axons *in vitro* than *in vivo* (Stoeckli and Landmesser, 1995; Stoeckli *et al.*, 1997), so it is conceivable that the effects of IgCAM mutations would also be more evident *in vitro*. If this proved to be the case, *in vitro* experiments could also be used to better understand IgCAM function. For example, dorsal spinal explants could be confronted with cells that express just one floor plate factor, for comparison of the responses of mutant and wild type axons to this factor alone.

7.1.3 Dorsal spinal commissural projections are abnormal in *TAG-1/L1* double mutant embryos

The possibility that other factors compensate for TAG-1, L1 or NrCAM can also be investigated by analyses of embryos that carry more than one mutation. The present study included such an examination of the dorsal spinal projections of *TAG-1/L1* double mutant embryos. The apparent reticence of double mutant axons to extend out of the E12.5 floor plate suggested that TAG-1 and L1 might indeed be partially redundant in floor plate exit. This is conceivable, as these proteins are co-expressed on the regions of dorsal spinal commissural axons that lie within the floor plate (Dodd *et al.*, 1988), and are known to interact physically (Felsenfeld *et al.*, 1994; Malhorta *et al.*, 1998). At E13.5, double mutant axons were *less* likely to be in or at the floor plate than those of wild type embryos. This could have any of a number of explanations. There might be some sort of over compensation for the absence of TAG-1 and L1, such as the up-regulation of factors that have similar roles, or the down-regulation of factors with antagonistic roles. Alternatively, the relative increase in the proportion of contra-rostral axons could reflect the death of axons that were in other categories. For instance, the "in/at floor plate" neurons might have an impaired ability to respond to trophic factors from the midline (Wang and Tessier-Lavigne, 1999), and so be more likely to die. Whether there is selective death of the stalled axons could be tested using TUNEL (Gavrieli *et al.*, 1992). As this double mutant analysis has indicated that TAG-1 and L1 might be functionally redundant, it would also be interesting to examine the dorsal spinal projections of *TAG-1/NrCAM* and *L1/NrCAM* double mutant embryos.

7.1.4 Dorsal spinal commissural projections are abnormal in *ephrin B3* mutant embryos

This thesis also includes direct evidence for the involvement of ephrin B3 in dorsal spinal commissural axon development. Expression patterns and *in vitro* experiments had previously led to the suggestion that ephrin B3 might repel these axons from the ventral midline (Imondi *et al.*, 2000). Indeed, ephrin B3 appears to have such an effect upon corticospinal axons (Kullander *et al.*, 2001 b; Yokoyama *et al.*, 2001). At E12.5, the dorsal spinal commissural axons of *ephrin B3* homozygous mutant embryos were found to be significantly more likely to be in or at the floor plate than those of heterozygous littermates. Thus the present work indicates that ephrin B3 does indeed repel dorsal spinal commissural axons from the mouse floor plate. It also implies that other factors can subsequently compensate for an absence of ephrin B3. There were no significant differences between homozygous and heterozygous dorsal spinal projections at E13.5, when ephrins B1 and B2 are first expressed (Imondi *et al.*, 2000). The possibility that these factors compensate for an absence of ephrin B3 could be investigated by the analysis of double mutant embryos.

7.2 A general survey of other aspects of neural development

7.2.1 Description of the regions in which *TAG-1* gene regulatory sequences are active

This thesis also describes investigations into the roles that TAG-1 might have in other aspects of neural development. Part of this work involved a detailed account of *TAG-1* promoter sequence activity at certain developmental stages, as determined by its ability to drive expression of a *lacZ* reporter gene. The distribution of TAG-1 immunoreactivity in the developing mouse nervous system has been described previously (Yamamoto *et al.*, 1986; Wolfer *et al.*, 1994). However, this does not necessarily reflect all instances of TAG-1 protein expression or *TAG-1* gene activity. For example, TAG-1 is often secreted (Ruegg *et al.*, 1989; Furley *et al.*, 1990; Karagogeos *et al.*, 1991), and it could be that the soluble protein is too readily lost from tissue to be labelled by immunohistochemistry. *In situ* hybridisation has been used to determine the extent of *TAG-1* transcription in the adult mouse (Yoshihara *et al.*, 1995; Wolfer *et al.*, 1998), but the present work constitutes the first description of *TAG-1* gene activity in the developing murine nervous system.

The results presented here are largely in agreement with reports of TAG-1-immunoreactivity, although some novel staining was also observed. This could sometimes be attributed to a structure not having been examined in previous studies, or to the ability of the *lacZ* gene product to perdure. In other cases, such as those of limb and mandibular mesenchyme, staining was suggestive of novel *TAG-1* gene activity. This might reflect the presence of previously uncharacterised regulatory elements, which normally repress TAG-1 expression, but that had been deleted in the *TAG-1* null allele. Alternatively, it could represent normal expression of TAG-1 protein that is not detectable by antibody labelling. *In situ* hybridisation of embryos for TAG-1 mRNA would establish whether TAG-1 is indeed transcribed in the developing limbs and/or mandible.

7.2.2 Most neurons seem to be unaffected by a lack of TAG-1 protein

The results presented demonstrate significant agreement between patterns of ß-galactosidase activity and TAG-1 immunoreactivity. This means that the *TAG-1* null allele is a valuable tool for studying the effects of mutations upon structures that normally express TAG-1.

There were few differences between the patterns of ß-galactosidase staining in *TAG-1* null heterozygous and homozygous embryos or immature brains. Structures whose development might have been expected to involve TAG-1 often appeared to be unaffected by an absence of the protein. For example, axonin-1 has been implicated in correct innervation of chicken hind limb (Landmesser and Honig, 1986; Honig *et al.*, 1998; Xue and Honig, 1999), but the limbs of *TAG-1* null homozygous mouse embryos appeared to be innervated normally. TAG-1 is expressed by the facial nerve nucleus, and has been suggested to have a role in the migration of its cell bodies (Garel *et al.*, 2000). However, this migration also seemed to be unaffected by an absence of the protein.

These results demonstrate that TAG-1 is not essential for the gross development of most of the neurons that normally express it. However, they do not exclude the possibility that TAG-1 is involved in their development in some way. For instance, the *TAG-1* null mutation might have more subtle effects than were evident here: this could be investigated if mutant embryos and brains were sectioned and examined at higher magnifications. Alternatively, other factors might compensate for the lack of TAG-1. Whether L1 and NrCAM are such factors could be investigated by analysis of double mutant null embryos.

7.2.3 TAG-1 could be important for development of the hypoglossal nerve

Two populations of neurons that may have been affected by the *TAG-1* null mutation are those of the habenulointerpeduncular tract (HIPT) and those of the hypoglossal nerve. Further sectioning of brains would be required to confirm whether development of the HIPT had in fact been compromised. Application of DiI to the habenula nucleus would give a better idea of the nature of any HIPT disruption.

Hypoglossal nerve defects were less ambiguous. In the absence of TAG-1 protein, E11.5 hypoglossal nerves were significantly more likely to stall at the point of rootlet convergence than if TAG-1 was present. The nerves also differed significantly between homozygous and heterozygous embryos at E12.5.
Thus TAG-1 might be important for the ability of mid-gestation hypoglossal nerve axons to extend correctly. The present work also provides evidence that the defects are either not detrimental, or subsequently repaired. Applications of DiI to the hypoglossal nerve, or to the tongue, at later stages would help to distinguish between these possibilities. So too might immunohistochemical labelling of the axons. This would also allow the hypoglossal nerves of homozygous mutant embryos to be compared directly with those of wild type embryos. In addition, it would allow the hypoglossal nerve to be studied in mice that do not carry a *lacZ*-containing allele.

7.3 Positive and negative aspects of the study

This thesis describes the use of genetically modified mice to better understand the roles of particular proteins in mouse neural development. This approach has several benefits. In contrast to the experiments performed in chicken embryos (Stoeckli and Landmesser, 1995; Lustig *et al.*, 2001), the mouse embryos used here actually lacked the proteins of interest (A.J.W. Furley, personal communication; Cohen *et al.*, 1997; Sakurai *et al.*, 2001; Kullander *et al.*, 2001 b). Thus experimental animals could be compared with controls without the possibility that injected factors might have blocked protein function incompletely, or have had effects upon other proteins.

The use of mutant mice also had drawbacks. As reported previously, the effects of mutations can vary depending upon mouse genetic background (Dahme *et al.*, 1997; Kitsukawa *et al.*, 1997; Guo *et al.*, 2000). When mice of mixed strain backgrounds are mated, the resulting embryos can differ from one another genetically, and littermates with a single mutation can theoretically have different phenotypes. Thus the effects of mutations are best studied using mice of a homogenous genetic strain. As such mice were not available at the beginning of the study, the effects of *TAG-1* mutations were initially analysed using mice of mixed strains. Subsequently "pure" genetic strains were also generated. In the present study this involved at least 6 "back-crosses", which required approximately one year's worth of breeding (Gerlai, 1996). This delayed the investigation, with consequences such as there being insufficient time to generate ideal numbers of embryos for the E12.5 hypoglossal nerve analysis. A further concern is that such back-crossing is possibly an inadequate measure. It has been calculated that, even after 12 generations of back-crossing, as much as 1% of the mouse genome could remain linked to a gene of interest (Gerlai, 1996). Thus a relatively large number of genes might be so close to the *TAG-1* locus as to be effectively inseparable from it, and the phenotypes of *TAG-1* mutant mice might actually be reflecting the presence of a particular allele at a different locus (Gerlai, 1996; Lathe, 1996). This possibility could be investigated by rescue experiments. For instance, if *TAG-1* null mutant mice were caused to express TAG-1

protein, correct development of all hypoglossal nerves would indicate that defects were a direct result of the *TAG-1* mutation. *TAG-1* null mutant mice could be caused to specifically express TAG-1 by introduction of a *TAG-1*-containing transgene (Gerlai, 1996), either by the microinjection of transgenic DNA into pronuclei (Hogan *et al.*, 1994), or infection by a transgene-containing virus (Slack and Miller, 1996; Vogt *et al.*, 1996; Giger *et al.*, 1997).

A further drawback of using mutant mice is that the approach can rarely prove that a protein is *not* involved in a process. Overlap between the functions of proteins can often mean that other molecules fill the roles of one that is targeted. For example, the HIPT was unaffected by mutations in either *eph B2* or *eph B3*, but was defasciculated in mice that were homozygous for both mutations. This suggests that the Eph B2 and B3 receptors can affect development of the tract, but that the presence of either one is sufficient for development to proceed normally (Orioli *et al.*, 1996). Similarly, *NrCAM/L1* double mutant mice have more severe defects in the morphology of their cerebella than mice with only one of the mutations. This indicates that NrCAM and L1 have partially redundant functions in cerebellar development (Sakurai *et al.*, 2001). Thus it is possible that TAG-1, L1 and NrCAM are involved in many more processes than are affected by the absence of these proteins individually.

As discussed above, the effects of perturbing chicken IgCAM function were more pronounced *in vitro* than *in vivo* (Stoeckli and Landmesser, 1995; Stoeckli *et al.*, 1997). Thus the present study might have benefited from an *in vitro* comparison of mutant and wild type axons. It is also possible that more pronounced effects would have been observed if animals with multiple mutations had also been used. *TAG^{A}/L1* double mutant embryos were examined, but *TAG-1* null/*L1* double mutant embryos were not, so the possibility that L1 has some overlap of function with the truncated TAG-1 proteins remains untested. However, it is costly in both time and money to generate animals with multiple mutations, particularly if the mutations are not already being maintained on a single strain background (see above).

Some aspects of the present study would have benefited from analysis of greater numbers of samples. Had more animals been available in the time allowed, it would also have been better to examine certain things more thoroughly. For example, injection of DiI into transverse sections of spinal cord would have allowed the fasciculation of dorsal commissural interneurons to be assessed, as in the chicken experiments (Stoeckli and Landmesser, 1995). A more detailed immunohistochemical analysis of *TAG-1* mutant animals would have allowed structures that do not normally express TAG-1 to be studied. This might have proved interesting as the secretion of TAG-1 protein (Ruegg *et al.*, 1989; Furley *et al.*, 1990; Karagogeos *et al.*, 1991) means that the *TAG-1* null mutation could theoretically have non-cell-autonomous effects.

7.4 Conclusions

This thesis describes an investigation into the roles of certain proteins in development of the mouse nervous system. It reports the use of a *lacZ* reporter gene to confirm, and extend, what is known about expression of TAG-1 in the developing mouse. It also describes use of this reporter to study the development of structures that normally express TAG-1. It provides the first evidence that an absence of TAG-1 protein is detrimental for hypoglossal nerve development. The results presented also demonstrate that TAG-1 is not essential for the gross development of many of the other the neural structures that ordinarily express it. This includes some of those that TAG-1 has previously been suggested to affect, such as the facial nerve nucleus (Garel *et al.*, 2000) and axons that innervate the limbs (Landmesser and Honig, 1986; Honig *et al.*, 1998; Xue and Honig, 1999).

In contrast to what may have been expected from chicken experiments (Stoeckli and Landmesser. 1995; Stoeckli *et al.*, 1997), the commissural axons of dorsal spinal interneurons also appeared to develop normally in the absence of TAG-1. This was verified using axon-tracing methods. Such analyses also provided evidence to support previous suggestions that dorsal spinal commissural axons are unaffected by the *L1* null mutation (Cohen *et al.*, 1997), and confirmed independent findings that their development does not require NrCAM (Moré *et al.*, 2001). In addition, the results presented provide evidence for functional redundancy between TAG-1 and L1, and for a role for ephrin B3, in the ability of commissural axons to extend out of the E12.5 floor plate.

References

Altman, J. and Bayer, S.A. (1984). The Development of the Rat Spinal Cord. *Advances in Anatomy, Embryoloy and Cell Biology volume* **85**, Springer Verlag, Berlin.

Altman, J. and Bayer, S.A. (1995). *Atlas of Prenatal Rat Brain Development.* CRC Press Inc., Florida.

Altman, J. and Bayer, S.A. (1997). *Development of the Cerebellar System: in Relation to its Evolution, Structure and Functions.* CRC Press Inc., Florida.

Alvarez-Dolado, M., Figueroa, A., Kozlov, S., Sonderegger, P., Furley, A.J. and Muñoz, A. (2001). Thyroid hormone regulates TAG-1 expression in the developing ratbrain. *Eur-J-Neurosci.* **14,** (1209-1218).

Arber, S., Han, B., Mendelsohn, M., Smith, M., Jessell, T.M. and Sockanathan, S. (1999). Requirement for the homeobox gene *Hb9* in the consolidation of motor neuron identity. *Neuron* **23,** 659-674.

Augsburger, A., Schuchardt, A., Hoskins, S., Dodd, J., Butler, S. (1999). BMPs as mediators of roof plate repulsion of commissural neurons. *Neuron* **24,** 127-141.

Bagnard, D., Thomasset, N., Lohrum, M., Püschel, A.W. and Bolz, J. (2000). Spatial distributions of guidance molecules regulate chemorepulsion and chemoattraction of growth cones. *J-Neurosci* **20** (3), 1030-1035.

Bastiani, M.J., Raper, J.A., and Goodman, C.S. (1984). Pathfinding by neuronal growth cones in grasshopper embryos III. Selective affinity of the G growth cone for the P cells within the A/P fascicle. *J-Neurosci* **4,** 2311-2328.

Becker, T., Bernhardt, R.R., Reinhard, E., Wuillimann, M.F., Tongiori, E. and Schachner, M. (1998). Readiness of zebrafish brain neurons to regenerate a spinal axon correlates with differential expression of specific cell recognition molecules. *J-Neurosci.* **18** (15), 5789-5803.

Beer, S., Oleszewski, M., Gutwein, P., Geiger, C. and Altevogt, P. (1999). Metalloproteinase-mediated release of the ectodomain of L1 adhesion molecule. *J-Cell-Sci.* **112,** 2667-2675.

Bently, D. and Caudy, M. (1983). Pioneer axons lose directed outgrowth after selective killing of guidepost cells. *Nature* **304,** 62-65.

Bergemann, A.D., Zhang, L., Chiang, M.K., Brambrilla, R., Klein, R. and Flanagan, J.G. (1998). Ephrin-B3, a ligand for the receptor EphB3, expressed at the midline of the developing neural tube. *Oncogene* **16,** 471-480.

Berglund, E.O. and Ranscht, B. (1994). Molecular cloning and in situ localization of the human contactin gene (CNTN1) on chromosome 12q11-q12. *Genomics* **21** (3), 571-582.

Berglund, E.O., Murai, K.K., Fredette, B., Sekerková, G., Marturano, B., Weber, L., Mugnaini, E. and Ranscht, B. (1999). Ataxia and abnormal cerebellar microorganization in mice with ablated contactin gene expression. *Neuron* **24,** 739-750.

Bermingham, N.A., Hassan, B.A., Wang, V.Y., Fernandez, M., Banfi, S., Bellen, H.J., Fritzch, B. and Zoghbi, H.Y. (2001). Proprioceptor pathway development is dependent on MATH1. *Neuron* **30,** 411-422.

Bieber, A.., Snow, P.M., Hortsch, M., Patel, N.H., Jacobs, .R., Traquina, Z.R., Schilling, J. and Goodman, C.S. (1989). *Drosophila* neuroglian: a member of the immuoglobulin superfamily with extensive homology to the vertebrate neural adhesion molecule L1. *Cell* **59**, 447-460.

Birgbauer, E., Oster, S.F., Severin, C.G. and Stretevan, D.W. (2001). Retinal axon growth cones respond to EphB extracellular domains as inhibitory axon guidance cues. *Development* **128**, 3041-3048.

Bock, E., Richter-Landsberg, C., Faissner, A. and Schachner, M. (1985). Demonstration of immunochemical identity between the nerve growth factor-inducible large external (NILE) glycoprotein and the cell adhesion molecule L1. *EMBO* **4** (11), 2765-2768.

Booth, G.E., Kinrade, E.F.V. and Hidalgo, A. (2000). Glia maintain follower neuron survival during Drosophila CNS development. *Development* **127**, 237-244.

Bork, P., Holm, L. and Sander, C. (1994). The immunoglobulin fold: structural classification, sequence patterns and common core. *J-Mol-Bio.l* **242**, 309-320.

Bovolenta, P. and Dodd, J. (1990). Guidance of commissural growth cones at the floor plate in embryonic rat spinal cord. *Development* **109**, 435-437.

Bovolenta, P. and Dodd, J. (1991). Perturbation of neuronal differentiation and axon guidance in the spinal cord of mouse embryos lacking a floor plate: analysis of Danforth's short tail mutation. *Developmen*t **113**, 625-629.

Boyle, M.E.T., Berglund, E.O., Murai, K.K., Weber, L., Peles, E. and Ranscht, B. (2001). Contactin orchestrates assembly of the septate-like junctions at the paranode in myelinated nerves. *Neuron* **30**, 385-397.

Bras, H., Cavallari, P., Jankowska, E. and Kubin, L. (1989). Morphology of midlumber interneurons relaying information from group II muscle afferents in the cat spinal cord. *J-Comp-Neurol.* **290**, 1-12.

Briscoe, J., Sussel, L., Serup., P., Hartigan-O'connor, D., Jessell, T.M., Rubenstein, L.R. and Ericson, J. (1999). Homeobox gene *Nkx2.2* and specification of neuronal identity by graded sonic hedgehog signalling. *Nature* **398**, 622-627.

Briscoe, J., Pierani, A., Jessell, T.M. and Ericson, J. (2000). A homeodomain protein code specifies progenitor cell identity and neuronal fate in the ventral neural tube. *Cell* **101**, 435-445.

Brose, K., Bland, K.S., Wang, K.H., Arnott, D., Henzel, W., Goddman, C.S., Tessier-Lavigne, M. and Kidd, T. (1999). Slit proteins bind Robo receptors and have an evolutionarily conserved role in repulsive axon guidance. *Cell* **96**, 795-806.

Brown, A.G. (1981). *Organisation in the spinal cord: the anatomy and physiology of identified neurons.* Springer-Verlag, Berlin and Heidelburg.

Brückner, K., Pasquale, E.B. and Klein, R. (1997). Tyrosine phosphorylation of transmembrane ligands for Eph receptors. *Science* **275**, 1640-1643.

Brückner, K. and Klein, R. (1998). Signalling by Eph receptors and their ephrin ligands. *Curr-Biol.* **8**, 375-382.

Brückner, K., Labrador, J.P., Scheiffele, P., Herb, A., Seeburg, P.H. and Klein, R. (1999). Ephrin B ligands recruit GRIP family PDZ adaptor proteins into raft membrane microdomains. *Neuron* **22**, 511-524.

Brümmendorf, T., Wolff, .M., Frank, R and Rathjen, F.G. (1989). Neural cell recognition molecule F11: homology with fibronectin type III and immunoglobulin type C domains. *Neuron* **2** (4), 1351-1361.

Brümmendorf, T., Hubert, U., Treubert, R., Leuschner, A., Tarnok, A. and Rathjen, F.G. (1993). The axonal recognition molecule F11 is a multifunctional protein: specific domains mediate interactions with Ng-CAM and restrictin. *Neuron* **10**, 711-727.

Brümmendorf, T and Rathjen, F.G. (1995). Cell Adhesion I: the Immunoglobulin-like Superfamily. *Protein Profile* **2**, 963-1108

Brümmendorf, T., Kenwrick, S. and Rathjen, F.G. (1998). Neural cell recognition molecule L1: from cell biology to human hereditary brain malformations. *Curr-Biol* **8**, 87-97.

Brümmendorf, T and Lemmon, V. (2001). Immunoglobulin superfamily receptors: cis-interactions, intracellular adaptors and alternative splicing regulate adhesion. *Curr-Op-Cell-Biol* **13**, 611-618.

Buchstaller, A., Kunz, S., Berger, P., Kunz, B., Ziegler, U., Rader, C., and Sonderegger, P. (1996). Cell adhesion molecules NgCAM and axonin-1 form heterodimers in the neuronal membrane and co-operate in neurite outgrowth promotion. *J-Cell-Biol.* **135**, 1593-607.

Burgoon, M. P., Grumet, M., Mauro, V., Edelman, G. M., and Cunningham, B. A. (1991). Structure of the chicken neuron-glia cell adhesion molecule, Ng-CAM: origin of the polypeptides and relation to the Ig superfamily. *J-Cell-Biol.* **112**, 1017-29.

Burgoon, M.P., Hazan, R.B., Phillips, G.R., Crossin, K.L., Edelman, G.M. and Cunningham, B.A. (1995). Functional analysis of posttranslational cleavage products of the neuron-glia cell adhesion molecule NgCAM. *J-Cell-Biol.* **130**, 733-744.

Burrill, J.D., Moran, L., Goulding, M.D. and Saueressig, H. (1997). PAX2 is expressed in multiple spinal cord interneurons, including a population of EN1$^+$ interneurons that require PAX6 for their development. *Development* **124**, 4493-4503.

Burns, F.R., von Kannen, S., Guy, L., Raper, J.A., Kamholz, J. and Chang, S. (1991). DM-GRASP, a novel immunoglobulin superfamily axonal surface protein that supports neurite extension. *Neuron* **7**, 209-220.

Burstyn-Cohen, T., Tzarfaty, V., Frumkin, A., Feinstein, Y., Stoeckli, E. and Klar, A. (1999). F-Spondin is required for accurate pathfinding of commissural axons at the floor plate. *Neuron* **23**, 233-246.

Buttiglione, M., Revest, J-M., Rougon, G. and Faivre-Sarrailh, C. (1996). F3 neuronal adhesion molecule controls outgrowth and fasciculation of cerebellar granule cell neurites: a cell-type-specific effect mediated by the Ig-like domains. *Mol-Cell-Neurosci.* **8**, 53-69.

Buttiglione, M., Revest, J-M., Pavlou, O., Karagogeos, D., Furley, A., Rougon, G. and Faivre-Sarrailh, C. (1998). A functional interaction between the neuronal adhesion molecules TAG-1 and F3 modulates neurite outgrowth and fasciculation of cerebellar granule cells. *J-Neurosci.* **18** (17), 6853-6870.

Cajal, S.Ramón Y. (1909), *Histology of the Nervous System, Volume I: General Principles, Spinal Cord, Spinal Ganglia, Medulla and Pons*, translated by N. Swanson and L.W. Swanson. Oxford University Press, New York.

Callahan, C.A. and Thomas, B. (1994). Tau-ß-galactosidase, an axon-targeted fusion protein. *PNAS* **91**, 5972-5976.

Campbell, R.M., Peterson, A.C. (1993). Expression of a *lacZ* transgene reveals floor plate morphology and macromolecular transfer to commissural axons. *Development* **119**, 1217-1228

Capecchi, M.R. (2001). Generating mice with targeted mutations. *Nat-Medicine* **7** (10), 1086-1090.

Castellani, V., Yue, Y., Gao, P-P., Zhou, R. and Bloz, J. (1998). Dual action of a ligand for Eph receptor tyrosine kinases on specific populations of axons during the development of cortical circuits. *J-Neurosci.* **18** (12), 4663-4672.

Castellani, V., Chédotal, A., Schachner, M., Faivre-Sarrailh, C. and Rougon, G. (2000). Analysis of the L1-deficient mouse phenotype reveals cross-talk between Sema 3A and L1 signalling pathways in axonal guidance. *Neuron* **27**, 237-249.

Caton, A., Hacker, A., Naeem, A., Livet, J., Maina, F., Bladt, F., Klein, R., Birchmeier, C. and Guthrie, S. (2000). The branchial arches and HGF are growth-promoting and chemoattractant for cranial motor axons. *Development* **127**, 1751-1760.

, H., Chédotal, A., He, Z., Goodman, C.S. and Tessier-Lavigne, M. (1997). Neuropili-2, a novel member of the neuropilin family, is a high affinity receptor for the semaphorins Sema E and IV but not Sema III. *Neuron* **19**, 547-559.

Chen, H., Bagri, A., Zupicich, J.A., Zou, Y., Stoeckli, E., Pleasure, S.J., Lowenstein, D.H., Skarnes, W.C., Chedotal, A., Tessier-Lavigne, M. (2000). Neuropilin-2 regulates the development of select cranial and sensory nerves and hippocampal mossy fibre projections. *Neuron* **25**, 43-56.

Chen, L., Ong, B. and Bennet, V. (2001). LAD-1, the Caenorhabditis elegans L1CAM homologue, participates in embryonic and gonadal morphogenesis and is a substrate for fibroblast growth factor receptor pathway-dependent phosphotyrosine-based signalling. *J-Cell-Biol.* **154** (4), 841-856.

Cheng, H-J., Nakamoto, M., Bergemann, A.D. and Flanagan, J.G. (1995). Complementary gradients in expression and binding of ELF-1 and Mek4 in development of the topographic retinotectal projection map. *Cell* **82**, 371-381.

Cheng, Y., Endo, K., Wu, K., Rodan, A.R., Heberlein, U. and Davis, R. (2001). Drosophila fasciclin II is required for the formation of odour memories and for normal sensitivity to alcohol. *Cell* **105**, 757-768.

Chien, C. B. (1998). Why does the growth cone cross the road? *Neuron* **20**, 3-6.

Chothia, C.and Jones, E.Y. (1997). The molecular structure of cell adhesion molecules. *Ann-Rev-Biochem.* **66**, 823-862.

Cohen, N. R., Taylor, J. S. H., Scott, L. B., Guillery, R. W., Soriano, P., and Furley, A. J. W. (1997). Errors in corticospinal axon guidance in mice lacking the neural cell adhesion molecule L1. *Curr-Biol.* **8**, 26-33.

Colamarino, S.A. and Tessier-Lavigne, M. (1995). The axonal chemoattractant netrin-1 is also a chemorepellant for trochlear motor axons. *Cell* **81**, 621-629.

Cole, G.J., Schubert, D. and Glaser, L. (1985). Cell-substratum adhesion in chick neural retina depends upon protein-heparan sulfate interactions. *J-Cell-Biol.* **100**, 1192-1199.

Cole, G.J. and Glaser, L. (1986). A heparin-binding domain from NCAM is involved in neural cell-substratum adhesion. *J-Cell-Biol.* **102**, 403-412.

Coonan, J.R., Greferath, U., Messenger, J., Hartley, Murphy, M., Boyd, A.W., Dottori, M. Galea, M.P. and Bartlett, P.F. (2001). Development and reorganization of corticospinal projections in Eph A4 deficient mice. *J-Comp-Neurol.* **436** (2), 248-262.

Cordes, S.P. (2001). Molecular genetics of cranial nerve development in mouse. *Nat-Rev-Neurosci.* **2**, 611.

Cota, E., Steward, A., Fowler, S.B. and Clarke, J. (2001). The folding nucleus of a fibronectin type III domain is composed of core residues of the immunoglobulin-like fold. *J-Mol-Biol.* **305** (5), 1185-1194.

Cowan, C.A., Yokoyama, N., Bianhci, L.M., Henkemeyer, M. and Fritzsch, B. (2000). EphB2 guides axons at the midline and is necessary for normal vestibular function. *Neuron* **26**, 417-430.

Cowan, C.A. and Henkemeyer, M. (2001). The SH2/SH3 adaptor Grb4 transduces B-ephrin reverse signals. *Nature* **413**, 174-179.

Cremer, H., Lange, R., Christoph, A., Plomann, M., Vopper, G., Roes, J., Brown, R., Baldwin, S., Kraemer, P., Scheff, S., Barthels, D., Rajewsky, K. and Wille, W. (1994). Inactivation of the NCAM gene in mice results in size reduction of the olfactory bulb and deficits in spatial learning. *Nature* **367**, 455-459.

Cremer, H., Cazal, G., Goridis, C. and Represa, A. (1997). NCAM is essential for axonal growth and fasciculation in the hippocampus. *Mol-Cell-Neurosci.* **8**, 323-335.

Dahme, M., Bartsch, U., Martini, R., Anliker, B., Schachner, M. and Mantei, N. (1997). Disruption of the mouse L1 gene leads to malformations of the nervous system. *Nat-Genet.* **17**, 346-349.

Dale, J.K., Vesque, C., Lints, T.J., Sampath, T., Furley, A., Dodd, J and Placek, M. (1997). Cooperation of BMP7 and SHH in the induction of forebrain ventral midline cells. *Cell* **90**, 257-269.

Davis, J.Q., McLaughlin, T. and Bennet, V. (1993). Ankyrin-binding proteins related to nervous system cell adhesion molecules: Candidates to provide transmembrane and intercellular connections in adult brain. *J-Cell-Biol.* **121** (1), 121-133.

Davis, G.W., Schuster, C.M. and Goodman, C.S. (1997). Genetic analysis of the mechanisms controlling target selection: target-derived fasciclin II regulates the pattern of synapse formation. *Neuron* **19**, 561-573.

De Angelis, E., MacFarlane, J., Du, J., Yeo, G., Hicks, R., Rathjen, F.G., Kenwrick, S. and Brümmendorf, T. (1999). Pathological missense mutations of neural cell adhesion molecule L1 affect homophilic and heterophilic binding activities. *E-M-B-O* **18** (17), 4744-4753.

DeBernardo, A. P., and Chang, S. (1996). Heterophilic interactions of DM-GRASP: GRASP-NgCAM interactions involved in neurite extension. *J-Cell-Biol.* **133**, 657-66.

Demyanenko, G.P., Tsai, A.Y. and Maness, P.F. (1999). Abnormalities in neuronal process extension, hippocampal development and the ventricular system of L1 knockout mice. *J-Neurosci.* **19** (12), 4907-4920.

Denburg, J.L., Caldwell, R.T. and Marner, J.M. (1995). Developmental changes in epitope accessibility as an indicator of multiple states of an immunoglobulin-like neural cell adhesion molecule. *J-Comp-Neurol.* **354** (4), 533-550.

Desai, C.J., Sun, Q. and Zinn, K (1997). Tyrosine phosphorylation and axon guidance: of mice and flies. *Curr-Op-Neurobiol* **7**, 70-74.

Dickson, B.J. (2001). Moving On. *Science* **291**, 1910

Dodd, J., Morton, S. B., Karagogeos, D., Yamamoto, M., and Jessell, T. M. (1988). Spatial regulation of axonal glycoprotein expression on subsets of embryonic spinal neurons. *Neuron* **1**, 105-16.

Doherty, P., and Walsh, F. S. (1994). Signal transduction events underlying neurite outgrowth stimulated by cell adhesion molecules. *Curr- Op-Neurobiol* **4**, 49-55.

Doherty, P., Williams, E., and Walsh, F. S. (1995). A soluble chimeric form of the L1 glycoprotein stimulates neurite outgrowth. *Neuron* **14**, 57-66.

Dottori, M., Hartley, L., Galea, M., Paxinos, G., Polizzotto, M., Kilpatrick, T., Bartlett, P.F., Murphy, M., Köntgen, F. and Botd, A.W. (1998). EphA4 (Sek1) receptor tyrosine kinase is required for the dvelopment of the corticospinal tract. *PNAS* **95**, 13248-13253.

Drescher, B., Spiess, E., Schachner, M., and Probstmeier, R. (1996). Structural analysis of the murine cell adhesion molecule L1 by electron microscopy and computer-assisted modelling. *Eur-J-Neurosci.* **8**, 2467-78.

Drescher, U., Kremoser, C., Handwerker, C., Löschinger, J., Noda, M. and Bonhoeffer, F. (1995). In vitro guidance of retinal ganglion cell axons by RAGS, a 25kDa tectal protein related to ligands for Eph receptor tyrosine kinases. *Cell* **82**, 359-370.

Drescher, U. (1997). The Eph family in the patterning of neural development. *Curr-Biol.* **7**, R799-R807.

Durbec, P., Gennarini, G., Goridis, C. and Rougon, G. (1992). A soluble form of the F3 neuronal cell adhesion molecule promotes neurite outgrowth. *J-Cell-Biol* **117**, 877-887.

Dütting, D., Handwerker, C. and Drescher, U. (1999). Topographic targeting and pathfinding errors of retinal axons following overexpression of EphrinA ligand on retinal ganglion cell axons. *Dev-Biol.* **216**, 297-311.

Dytham, C. (1999). *Choosing and Using Statistics: a Biologist's Guide.* Blackwell Science, Oxford, UK.

Ebens, A., Brose, K., Leonardo, E.D., Gartz Hanson Jr, M., Bladt, F., Birchmeier, C., Barres, B.A. and Tessier-Lavigne, M. (1996). Hepatocyte Growth Factor/Scatter Factor is an axonal chemoattractant and a neurotrophic factor for spinal motor neurons. *Neuron* **17**, 1157-1172.

Echelard, Y., Vassileva, G. and McMahon, A.P. (1994). *Cis*-acting regulatory sequences governing *Wnt-1* expression in the developing mouse CNS. *Development* **120**, 2213-2224.

Eide, A-L., Glover, J., Kjaerulff, O. and Kiehn, O. (1999). Characterisation of commissural interneurons in the lumbar region of the neonatal rat spinal cord. *J-Comp-Neurol.* **403**, 332-345.

Eisele, D.W., Smith, P.L., Alam, D.S. and Schwartz, A.R. (1997). Direct hypoglossal nerve stimulation in sleep apnea. *Arch-Otolaryngol-Head-Neck-Surg.* **123** (1), 57-61.

El-Deeb, S., Thompson, S.C. and Covault, J. (1992). Characterisation of a cell surface adhesion molecule expressed by a subset of developing chick neurons. *Dev-Biol.* **149**, 213-227.

Eph Nomenclature Committee (1997). Unified nomenclature for Eph family receptors and their ligands, the ephrins. *Cell* **90**, 403-404.

Ericson, J., Rashbass, P., Schedl, A., Brenner-Morton, S., Kawakami, A., van Heyningen, V., Jessel, T.M. and Briscoe, J. (1997). Pax6 controls progenitor cell identity and neuronal fate in reponse to graded Shh signalling. *Cell* **90**, 169-180.

Fambrough, D. and Goodman, C.S. (1996). The Drosophila beaten path gene encodes a novel secreted protein that regulates defasciculation at motor axon choice points. *Cell* **87**, 1049-1058.

Fearon, E.R., Cho, K.R., Nigro, J.M., Kern, S.E., Simons, J.W., Ruppert, J.M., Hamilton, S.R.; Preisinger, A.C., Thomas, G, Kinzler, K.W. and Vogelstein, V. (1990). Identification of a chromosome 18q gene that is altered in colorectal cancers. *Science* **247**, 49-56.

Feng, G., Laskowski, m.B., Feldheim, D.A., Wang, H., Lewis, R., Frisén, J., Flanagan, J.G. and Sanes, J.R. (2000). Roles for ephrins in positionally selective synaptogenesis between motor neurons and muscle fibers. *Neuron* **25**, 295-306.

Felsenfeld, D. P., Hynes, M. A., Skoler, K. M., Furley, A. J., and Jessell, T. M. (1994). TAG-1 can mediate homophilic binding, but neurite outgrowth on TAG-1 requires an L1-like molecule and beta 1 integrins. *Neuron* **12**, 675-90.

Fitzgerald, M.J.T. (1992). *Neuroanatomy: Basic and Clinical (2nd Edition).* Baillière Tindall, London.

Fitzli, D., Stoeckli, E.T., Kunz, S., Siribour, K., Rader, C., Kunz, B., Kozlov, S.V., Buchstaller, A., Lane, R.P.; Suter, D.M., Dreyer, W.J. and Sonderegger, P. (2000). A dirct interaction of axonin-1 with NgCAM-related cell adhesion molecule (NrCAM) results in guidance, but not growth of commissural axons. *J-Cell-Biol.* **149**, 951-968.

Fraboulet, S., Schmidt-Petri, T., Dhouailly, D. and Pourquié, O. (2000). Expression of DM-GRASP/BEN in the developing mouse spinal cord and various epithelia. *Mech-Dev.* **95**, 221-224.

Flanagan, J.G. and Vanderhaeghen, P. (1998). The ephrins and Eph receptors in neural development. *Ann-Rev-Neurosci.* **21**, 309-345.

Fransen, E., D'Hooge, R., Van Camp, G., Verhoye, M., Sijbers, J., Reyniers, E., Soriano, P., Kamiguchi, H., Willemsen, R., Koekkoek, S.K.E., De Zeeuw, C.I., De Deyn, P.P., Van der Linden, A., Lemmon, V., Kooy, R.F. and Willems, P.J. (1998). Li knockout mice show dilated ventricles, vermis hypoplasia and impaired exploration patterns. *Hum-Mol-Genet.* **7**, 999-1009.

Freigang, J., Proba, K., Leder, L., Diederichs, K., Sonderegger, P. and Welte, W. (2000). The crystal structure of the ligand binding module of axonin-1/TAG-1 suggests a zipper mechanism for neural cell adhesion. *Cell* **101**, 425-433.

Friedland, D.R., Eden, A.R. and Laitman, J.T. (1995). Naturally occuring motoneuron cell death in rat upper respiratory tract motor nuclei: a histological, fast DiI and immunocytochemical study in the hypoglossal nucleus. *J-Neurobiol.* **27** (4), 520-534.

Friedlander, D.R., Milev, P., Karthikeyan, L., Margolis, R.K., Margolis, R.U. and Grumet, M. (1994). The neuronal chondroitin sulfate proteoglycan neurocan binds to the neural cell adhesion molecules NgCAM/NILE and NCAM, and inhibits neuronal adhesion and outgrowth. *J-Cell-Biol.* **125** (3), 669-680.

Frisén, J., Yates, P.A., McLaughlin, T., Friedman, G.C., O'Leary, D.D.M. and Barbacid, M. (1998). Ephrin-A5 (Al-1/RAGS) is essential for proper retinal axon guidance and topographic mapping in the mammalian visual system. *Neuron* **20**, 235-243.

Frisén, J., Holmberg, J. and Barbacid, M. (1999). Ephrins and their Eph receptors: multitalented directors of embryonic development. *EMBO* **18** (19), 5159-5165.

Fukamauchi, F., Aihara, O., Wang, Y-J., Akasaka, K., Takeda, Y., Horie, M., Kawano, H., Sudo, K., Asano, M., Watanabe, K. and Iwakurta, Y. (2001). TAG-1 deficient mice have marked elevation of adenosine A1 receptors in the hippocampus. *Biochem-Biophys-Res-Commun.* **281**, 220-226.

Funato, H., Saito-Nakazato, Y. and Takahaski, H. (2000). Axonal growth from the habenular nucleus along the neuromere boundary region of diencephalon is regulated by semaphorin 3F and netrin-1. *Mol-Cell-Neurosci.* **16**, 206-220.

Furley, A.J., Morton, S.B., Manalo, D., Karagogeos, D., Dodd, J. and Jessel, T.M. (1990). The axonal glycoprotein TAG-1 is an immunoglobulin superfamily member with neurite outgrowth-promoting activity. *Cell* **61**, 157-170.

Gale, N.W., Flenniken, A., Compton, D.C., Jenkins, N., Copeland, N.G., Gilbert, D.J., Davis, S., Wilkinson, D.G. and Yancopoulos, G.D. (1996 a). Elk-L3, a novel transmembrane ligand for the Eph family of receptor

tyrosine kinases, expressed in embryonic floor plate, roof plate and hindbrain segments. *Oncogene* **13**, 1343-1352.

Gale, N.W., Holland, S.J., Valenzuela, D.M., Flenniken, A., Pan, L., Ryan, T.E., Henkemeyer, M., Strebhardt, K., Hirai, H., Wilkinson, D.G., Pawson, T., Davies, S. and Yancopoulos, G.D. (1996 b). Eph receptors and ligands comprise two major specificity subclasses and are reciprocally compartmentalized during embryogenesis. *Neuron* **17**, 9-19.

Gao, P-P., Zhang, J-H., Yokoyama, M., Racey, B., Dreyfus, C.F., Black, I.B. and Zhou, r. (1996). Regulation of topographic projection in the brain: Elf-1 in the hippocamposeptal system. *PNAS* **93**, 11161-11166.

Gao, P-P., Yue, Y., Cerretti, D.P., Dreyfus, C. and Zhou, R. (1999). Ephrin-dependent growth and pruning of hippocampal axons. *PNAS* **96**, 4073-4077.

García-Alonso, L., Romani, S. and Jiménez, F. (2000). The EGF and FGF receptors mediate neuroglian function to control growth cone decisions during sensory axon guidance in *Drosophila*. *Neuron* **28**, 741-752.

Garel, S., Garcia-Domingue, M. and Charnay, P. (2000). Control of the migratory pathway of facial branchiomotor neurones. *Development* **127**, 5297-5307.

Garrity, P. A., and Zipursky, S. L. (1995). Neuronal target recognition. *Cell* **83**, 177-185.

Gavrieli, Y., Sherman, Y. and Ben-Sasson, S.A. (1992). Identification of programmed cell death via specific labelling of nuclear fragmentation. *J-Cell-Biol.* **119** (3), 493-501.

Gennarini, G., Cibelli, G., Rougon, G, Mattei, M.G. and Goridis, C. (1989). The mouse neuronal cell surface protein F3: a phosphatidylinositol-anchored member of the immunoglobulin superfamily related to chicken contactin. *J-Cell-Biol.* **109** (2), 775-788.

Gennarini, G., Durbec, P., Boned, A., Rougon, G and Goridis, C. (1991). Transfected F3/F11 neuronal cell surface protein mediates intercellular adhesion and promotes neurite outgrowth. *Neuron* **6** (4), 595-606.

Gerlai, R. (1996). Gene-targeting studies of mammalian behaviour: is it the mutation or the background genotype? *Trends-Neurosci.* **19**, 177-181.

Giger, R.J., Ziegler, U., Hermens, W.T.J.M.C., Kunz, B., Kunz, S. and Sonderegger, P. (1997). Adenovirus-mediated gene transfer in neurons: construction and characterization of a vector for heterologous expression of the axonal cell adhesion molecule axonin-1. *J-Neurosci-Methods* **71**, 99-111.

Giger, R.J., Cloutier, J-F., Sahay, A., Prinjha, R.K., Levengood, D.V., Moore, S.E., Pickering, S., Simmons, D., Rastan, S., Walsh, F.S., Kolodkin, A.L., Ginty, D.D. and Geppert, M. (2000). Neuropilin-2 is required in vivo for selective axon guidance responses to secreted semaphorins. *Neuron* **25**, 29-41.

Giger, R.J. and Kolodkin, A.L. (2001). Silencing the siren: guidance cue hierarchies at the CNS midline. *Cell* **105**, 1-4.

Giuffrida, S., Lo Bartolo, M.L., Nicoletti, A., Reggio, E., Lo Fermo, S., Restivo, D.A., Domina, E. and Reggio, A. (2000). Isolated, unilateral, reversible palsy of the hypoglossal nerve. *Eur-J-Neurol.* **7**, 347-349.

Godement, P., Vanselow, J., Thanos, S. and Bonhoeffer, F. (1987). A study in developing visual systems with a new method of staining neurones and their processes in fixed tissue. *Development* **101**, 697-713.

Gomez. T.M., Robles, E., Poo, M-m. and Spitzer, N.C. (2001). Filopodial calcium transients promote substrate-dependent growth cone turning. *Science* **291**, 1983-1987.

Goodman, C. S., Bastiani, M. J., Doe, C. Q., du Lac, S., Helfand, S. L., Kuwada, J. Y., and Thomas, J. B. (1984). Cell recognition during neural development. *Science* **225**, 1271-1279.

Goodman, C.S. and Shatz, C.J. (1993). Developmental mechanisma that generate precise patterns of neuronal connectivity. *Cell* **77** (suppl.), 77-98.

Gowan, K., Helms, A.W., Hunsaker, T.L., Collisson, T., Ebert, P.J., Odom, R. and Johnson, J.E. (2001). Crossinhibitory activities of Ngn1 and Math1 allow specification of distinct dorsal interneurons. *Neuron* **31**, 219-232.

Grenningloh, G., Rehm, J.E. and Goodman, C.S. (1991). Genetic analysis of growth cone guidance in Drosophila: Fasciclin II functions as a neuronal recognition molecule. *Cell* **67**, 45-57.

Grenningloh, G. and Goodman, C.S. (1992). Pathway recognition by neural growth cones: genetic analysis of neural cell adhesion molecules in *Drosophila. Curr-Op-Neurobiol.* **2**, 42-47.

Gribnau, A.A.M., de Kort, E.J.M., Dederen, P.J.W.C. and Nieuwenhuys, R. (1986). On the development of the pyramidal tract in the rat II: an anterograde tracer study of the outgrowth of corticospinal fibres. *Anat-Embryol.* **175**, 101-110.

Grumet, M. and Edelman, G.M. (1988). Neuon-glia cell adhesion molecule interacts with neurons and astroglia via different binding mechanisms. *J-Cell-Biol.* **106**, 487-503.

Grumet, M., Mauro, V., Burgoon, M.P., Edelman, G.M. and Cunningham, B.A. (1991). Structure and characterization of NrCAM, a new member of the Ig superfamily that is closely related to NgCAM. *J-Cell-Biol.* **113**, 1399-1412.

Grumet, M. (1992). Structure, expression and function of NgCAM, a member of the immunoglobulin superfamily involved in neuron-neuron and neuron-glia adhesion. *J-Neurosci-Res.* **31** (1), 1-13.

Grumet, M., Friedlander, D.R. and Edelman, G.M. (1993 a). Evidence for the binding of NgCAM to laminin. *Cell-Adhes-Commun.* **1** (2), 177-190.

Grumet, M., Flaccus, A. and Margolis, R.U. (1993 b). Functional characterisation of chondroitin sifate proteoglycans of brain: interactions with neurons and neural cell adhesion molecules. *J-Cell-Biol* **120** (3), 815-824.

Grumet, M. and Sakurai, T. (1996). Heterophilic interactions of the neural cell adhesion molecules NgCAM and NrCAM with neural receptors and extracellular matrix proteins. *Sem-Neurosci.* **8**, 379-389.

Guo, H., Christoff, J.M., Campos, V.E. and Li, Y (2000). Normal corpus callosum in Emx1 mutant mice with C57BL/6 background. *Biochem-Biophys-Res-Comm.* **276**, 649-653.

Gutwein, P., Oleszewski, M., Mechtersheimer, S., Agmon-Levin, N., Krauss, K. and Altevogt, P. (2000). Role of Src kinases in the ADAM-mediated release of L1 adhesion molecule from human tumour cells. *J-Biol-Chem.* **275** (20), 15490-15497.

Hall, S.G. and Bieber, A.J. (1998). Mutations in the *Drosophila* neuroglian cell adhesion molecule affect motor neuron pathfinding and peripheral nervous system patterning. *J-Neurobiol.* **32** (3), 325-340.

Hall, H., Bozic, D., Fauser, C. and Engel, J. (2000). Trimerization of cell adhesion molecule L1 mimics clustered expression on the cell surface: influence on L1-ligand interactions and on promotion of neurite outgrowth. *J-Neurochem.* **75**, 336-346

Hamburger V. and Hamilton, H.L. (1951). A series of normal stages in the development of the chick embryo. *J-Morph.* **88**, 49-92; published in an abridged form as an appendix to Stern and Holland, 1993.

Harpaz, Y. and Chothia, C. (1994). Many of the immunoglobulin superfamily domains in cell adhesion molecules and surface receptors belong to a new structural set which is close to that containing variable domains. *J-Mol-Biol* **238**, 528-539.

Harris, W.A, and Holt, C.E. (1999). Slit, the midline repellent. *Nature* **398**, 462-463.

Harris, W.A, and Holt, C.E. (2001). Stimulating new turns. *Neuron* **29**, 311--312.

Harrison, R.G. (1910). *J-Exp-Zool* **9**, 787 - as referred to in Goodman *et al.*, 1984.

Hasler, T.H., Rader, C., Stoeckli, E.T., Zuellig, R.A. and Sonderegger, P. (1993). cDNA cloning, structural features, and eucaryotic expression of human TAG-1/axonin-1. *Eur-J-Biochem.* **211** (1-2), 329-339.

Hassel, B., Rathjen, F.G. and Volkmer, H. (1997). Organization of the neurofascin gene and analysis of developmentally regulated alternative splicing. *J-Biol-Chem.* **272**, 28742-28749.

He, Z. (2000). Crossed wires: L1 and Neuropilin interactions. *Neuron* **27**, 191-196.

Hedrick, L., Cho, K.R., Fearon, E.R., Wu, T., Kinler, H.W. and Vogelstein, B. (1994). The DCC gene product in cellular differentiation and colorectal tumorigenesis. *Genes-Dev.* **8**, 1174-1183.

Helmbacher, F., Schneider-Maunoury, Topilko, P., Tiret, L. and Charnay, P. (2000). Targeting of the EphA4 tyrosine kinase receptor affects dorsal/ventral pathfinding of limb motor axons. *Development* **127**, 3313-3324.

Helms, A.W. and Johnson, J.E. (1998). Progenitors of dorsal commissural interneurons are defined by MATH-1 expression. *Development* **125**, 919-928.

Henkemeyer, M., Orioli, D., Henderson, .T., Saxton, T.M., Roder, J., Pawson, T. and Klein, R. (1996). Nuk controls pathfinding of commissural axons in the mammalian central nervous system. *Cell* **86**, 35-46.

Hillenbrand, R., Molthagen, M., Montag, D. and Schachner, M. (1999). The close homologue of the neural cell adhesion molecule L1 (CHL1): Patterns of expression and promotion of neurite outgrowth by heterophilic interactions. *Eur-J-Neurosci.* **11**, 813-826.

Hoffman, S., Sorkin, B.C., White, P.C., Brackenbury, R., Mailhammer, R., Rutishauser, U., Cunningham, B.A. and Edelman, G.M. (1982). Chemical characterisation of a neural cell adhesion molecule purified from embryonic brain membranes. *J-Biol-Chem.* **257**, 7720-7729.

Hoffman, S. and Edelman, G.M. (1983). Kinetics of homophilic binding by embryonic and adult forms of the neural cell adhesion molecule. *PNAS* **80**, 5762-5766.

Hogan, B., Beddington, R., Constantini, F. and Lacy, E. (1994). *Manipulating the Mouse Embryo, A Laboratory Manual (2nd edition).* Cold Spring Harbor Laboratory Press, New York.

Holder, N. and Klein, R. (1999). Eph receptors and ephrins: effectors of morphogenesis. *Development* **126**, 2033-2044.

Holland, S.J., Gale, N.W., Mbamalu, G., Yancopoulos, G.D., Henkemeyer, M and Pawson, T. (1996). Bidirectional signalling through the EPH-family receptor Nuk and its transmembrane ligands. *Nature* **383**, 722-725.

Holland, S.J., Peles, E., Pawson, T. and Schlessinger, J. (1998). Cell-contact-dependent signalling in axon growth and guidance: Eph receptor tyrosine kinases and receptor protein tyrosine phosphatase ß. *Curr-Op-Neurobiol.* **8**, 117-127.

Holley, J.A. (1982). Early development of the circumferential axonal pathway in mouse and chick spinal cord. *J-Comp-Neurol.* **205**, 371-382.

Holm, J., Hillenbrand, R., Steuber, V., Bartsch, U., Moos, M., Lubbert, H., Montag, D., and Schachner, M. (1996). Structural features of a close homologue of L1 (CHL1) in the mouse: a new member of the L1 family of neural recognition. *Eur-J-Neurosci.* **8**, 1613-1629.

Hong, K.S., Hinck, L., Nishiyama, M., Poo, M.M., Tessier-Lavigne, M. and Stein, E. (1999). A ligand-gated association between cytoplasmic domains of UNC5 and DCC family receptors converts netrin-induced growth cone attraction to repulsion. *Cell* **97** (7), 927-941.

Honig, M.G., Frase, P.A. and Camilli, S.J. (1998). The spatial relationships among cutaneous, muscle sensory and motoneuron axons during development of the chick hindlimb. *Development* **125**, 995-1004.

Honig, M.G. and Rutishauser, U.S. (1996). Changes in the segmental pattern of sensory neuron projections in the chick hindlimb under conditions of altered cell adhesion molecule function. *Dev-Biol.* **175**, 325-337.

Höpker, V.H., Shewan, D., Tessier-Lavigne, M., Poo, M. and Holt, D. (1999). Growth-cone attraction is converted to repulsion by laminin-1. *Nature* **401** (6748): 69-73.

Hortsch, M. (2000). Structural and functional evolution of the L1 family: are four adhesion molecules better than one? *Mol-Cell-Neurosci.* **15**, 1-10.

Huang, Y., Jellies, J., Johansen, K.M. and Johansen, J. (1997). Differential glycosylation of Tractin and LeechCAM, two novel Ig superfamily members, regulates neurite extension and fascicle formation. *J-Cell-Biol.* **138** (1), 143-157.

Hummel, T., Schimmelpfeng, K. and Klämbt, C. (1999). Commissure formation in the embryonic CNS of Drosophila II. Function of the different midline cells. *Development* **126**, 771-779.

Imondi, R., Wideman, C. and Kaprielian, Z. (2000). Complementary expression of transmembrane ephrins and their receptors in the mouse spinal cord: a possible role in constraining the orientation of longitudinally projecting axons. *Development* **127**, 1397-1410.

International Human Genome Sequencing Consortium (2001). Initial sequencing and analysis of the human genome. *Nature* **409** (6822), 860-921.

Izumoto, S., Ohnishi, T., Arita, N., Hiraga, S., Taki, T. and Hayakawa, T. (1996). Gene expression of neural cell adhesion molecule L1 in malignant gliomas ands biological significance of L1 in glioma invasion. *Cancer Res.* **56** (6), 1440-1444.

Jacobowitz, D.M. and Abbott, L.C. (1997). *Chemoarchitectonic Atlas of the Developing Mouse Brain.* CRC Press, Florida.

Jankowska, E. and Lundberg, A. (1981). Interneurons in the spinal cord. *Trends-Neurosci.* **4**, 230-233.

Jessell and Sanes, 2000. The decade of the developing brain. *Curr-Op-Neurobiol.* **10**, 599-611.

Kadmon, G., Kowitz, A., Altevogt, P., and Schachner, M. (1990). The neural cell adhesion molecule N-CAM enhances L1-dependent cell-cell interactions. *J-Cell-Biol.* **110**, 193-208.

Kalil, K. (1984). Development and regrowth of the rodent pyramidal tract. *Trends-Neurosci.* **7**, 394-398.

Kallunki, P., Jenkinson, S., Edelman, G.M. and Jones, F.S. (1995). Silencer elements modulate the expression of the gene for the neuron-glia cell adhesion molecule NgCAM. *J-Biol-Chem.* **270** (36), 21291-21298.

Kallunki, P., Edelman, G.M. and Jones, F.S. (1997). Tissue-specific expression of the L1 cell adhesion molecule is modulated by the neural restrictive silencer element. *J-Cell-Biol.* **138** (6), 1343-1354.

Kallunki, P., Edelman, G.M. and Jones, F.S. (1998). The neural restrictive silencer element can act as both a repressor and enhancer of L1 cell adhesion molecule gene expression during postnatal development. *PNAS* **95**, 3233-3238.

Kamei, Y., Tsutsumi, O., Taketni, Y. and Watanabe, K. (1998). CDNA cloning and chromosomal localization of neural adhesion molecule NB-3 in human. *J-Neurosci-Re.s* **51** (3), 275-283.

Kamei, Y., Takeda, Y., Teramoto, K., Tsutsumi, O, Taketani, Y and Watanabe, K. (2000). Human NB-2 of the contactin subgroup molecules: chromosomal localization of the gene (*CNTN5*) and distinct expression pattern from other subgroup members. *Genomics* **69**, 113-119.

Kamiguchi, H., Hlavin, M.L. and Lemmon, V. (1998). Role of L1 in neural development: what the knockouts tell us. *Mol-Cell-Neurosci.* **12**, 48-55.

Kamiguchi, H and Lemmon, V. (2000). IgCAMs: bidirectional signals underlying neurite growth. *Curr-Op-Cell-Biol.* **12**, 598-605.

Kappers, A., Huber, C. and Crosby, E.C. (1936). *The comparative anatomy of the nervous system of vertebrates, including man (volume 1).* MacMillan, New York.

Karagogeos, D., Morton, S. B., Casano, F., Dodd, J., and Jessell, T. M. (1991). Developmental expression of the axonal glycoprotein TAG-1: differential regulation by central and peripheral neurons *in vitro*. *Development* **112**, 51-67.

Karagogeos, D., Pourquié, C., Kyriakopoulou, K., Tavian, M., Stallcup, W., Péault, B. and Pourquié, O. (1997). Expression of the cell adhesion proteins BEN/SC1/DM-GRASP and TAG-1 defines early steps of axonogenesis in the human spinal cord. *J-Comp-Neurol.* **379**, 415-427.

Kaufman, M.H. (1992). *The Atlas of Mouse Development.* Academic Press Limited, London.

Kayyem, J. F., Roman, J. M., Delarosa, E. J., Schwarz, U., and Dreyer, W. J. (1992). Bravo/nr-cam is closely related to the cell-adhesion molecules L1 and Ng-cam and has a similar heterodimer structure. *J-Cell-Biol.* **118**, 1259-1270.

Keino-Masu, K., Masu, M., Hinck, L., Leonardo, E.D., Chan, S.S., Culotti, J.G. and Tessier-Lavigne, M. (1996). Deleted in colorectal cancer (DCC) encodes a netrin receptor. *Cell* **87** (2), 175-185.

Kennedy, T.E., Serafini, T., de la Torre, J.R. and Tessier-Lavigne, M. (1994). Netrins are diffusible chemotropic factors for commissural axons in the embryonic spinal cord. *Cell* **78**, 425-435.

Kidd, T., Brose, K., Mitchell, K.J., Fetter, R.D., Tessier-Lavigne, M., Goodman, C.S. and Tear, G. (1998a). Roundabout controls axon crossing of rhe CNS midlineand defines a novel subfamily of evolutionarily conserved guidance receptors. *Cell* **92**, 205-215.

Kidd, T., Russell, C., Goodman, C. S., and Tear, G. (1998b). Dosage-sensitive and complementary functions of roundabout and commissureless control axon crossing of the CNS midline. *Neuron* **20**, 25-33.

Kidd, T., Bland, K.S. and Goodman, C.S. (1999). Slit is the midline repellent for the robo receptor in *Drosophila. Cell* **96**, 785-794.

Kitsukawa, T., Shimizu, M., Sanbo, M., Hirata, T., Taniguchi, M., Bekku, Y., Yagi, T. and Fujisawa, H. (1997). Neuropilin-Semaphorin III/D-mediated chemorepulsive signalsplay a crucial role in peripheral nerve projections in mice. *Neuron* **19**: 995-1005.

Klar, A., Baldassare, M. and Jessell, T. (1992). F-Spondin: a gene expressed at high levels in the floor plate encodes a secreted protein that promotes neural cell adhesion and neurite extension. *Cell* **69**, 95-110.

Kolb, B. and Whishaw, I.Q. (1983). Dissociation of the contributions of the prefrontal, motor and parietal cortex to the control of movement in the rat: an expreimental review. *Can-J-Psych.* **37** (2), 211-232.

Kolodkin, A.L., Levengood, D.V., Rowe, E.G., Tai, Y., Giger, R.J. and Ginty, D.D. (1997). Neuropilin is a semaphorin III receptor. *Cell* **90**, 753-762.

Kolodziej, P.A., Timpe, L.C., Mitchell, K.J., Fried, S.R., Goodman, C.C., Jan, L.Y. and Jan, Y.N. (1996). *frazzled* encodes a *Drosophila* member of the DCC immunoglobulin-superfamily and is required for CNS and motor axon guidance. *Cell* **87**, 197-204.

Kose, H., Rose, D., Zhu, X. and Chiba, A. (1997). Homophilic synaptic target recognition mediated by immunoglobulin-like cell adhesion molecule Fasciclin III. *Development* **124**, 4143-4152.

Kuhn, T. B., Stoeckli, E. T., Condrau, M. A., Rathjen, F. G., and Sonderegger, P. (1991). Neurite outgrowth on immobilized axonin-1 is mediated by a heterophilic interaction with L1 (G4). *J-Cell-Biol.* **115**, 1113-1126.

Kullander, K., Mather, N.K., Diella, F., Dottori, M., Boyd, A.W. and Klein, R. (2001 a). Kinase-dependent and kinase independent functions of EphA4 receptors in major axon tract formation *in vivo*. *Neuron* **29**, 73-84.

Kullander, K., Croll, S.D., Zimmer, M., Pan, L., McClain, J., Hughes, V., Zabski, S., DeChiara, T., Klein, R., Yancopoulos, G. and Gale, N.W. (2001 b). Ephrin-B3 is the midline barrier that prevents corticospinal tract axons from recrossing, allowing for unilateral motor control. *Genes-Dev.* **15**, 877-888.

Kunz, S., Ziegler, U., Kunz, B., and Sonderegger, P. (1996). Intracellular signaling is changed after clustering of the neural cell adhesion molecules axonin-1 and NgCAM during neurite fasciculation. *J-Cell-Biol* **135**, 253-67.

Kunz, S., Spirig, M., Ginsburg, C., Buchstaller, A., Berger, P., Lanz, R., Rader, C., Vogt, L., Kunz, B and Sonderegger, P. (1998). Neurite fasciculation mediated by complexes of axonin-1 and Ng cell adhesion molecule. *J-Cell-Biol.* **143** (6), 1673-1690.

Küry, P., Gale, N., Connor, R., Pasquale, E. and Guthrie, S. (2000). Eph receptors and ephrin expression in cranial motor neurons and the branchial arches of the chick embryo. *Mol-Cell-Neurosci.* **15**, 123-140.

Landmesser, L. and Honig, M. (1986). Altered sensory projections in the chick hind limb following the early removal of motoneurons. *Dev-Biol.* **118**, 511-531.

Lane, R.P.; Chen, X-N., Yamakawa, K., Vielmetter, J., Korenberg, J.R. and Dreyer, W.J. (1996). Characterization of a highly conserved human homolog to the chicken neural cell surface protein Bravo/NrCAM that maps to chromosome band 7q31. *Genomics* **35**, 456-465.

Lathe, R. (1996). Mice, gene targeting and behaviour: more than just genetic background. Trends-Neurosci. **19**, *183-186*.

Leber, S.M. and Sanes, J.R. (1995). Migratory paths of neurons and glia in the embryonic chick spinal cord. *J-Neurosci.* **15** (2), 1236-1248.

Lee, K.J., Mendelsohn, M. and Jessell, T.M. (1998). Neuronal patterning by BMPs: a requirement for GDF7 in the generation of a discrete class of commissural interneurons in the mouse spinal cord. *Genes-Dev.* **12**, 3394-3407.

Lee, K.J. and Jessell, T.M. (1999). The specification of dorsal cell fates in the vertebrate central nervous system. *Annu-Rev-Neurosci.* **22**, 261-94.

Leighton, P.A., Mitchell, K.J., Goodrich, L.V., Lu, X., Pinson, K., Scherz, P., Skarnes, W.C. and Tessier-Lavigne, M. (2001). Defining brain wiring patterns and mechanisms through gene trapping in mice. *Nature* **410**, 174-179.

Lemmon, V., Burden, S. M., Payne, H. R., Elmslie, G. J., and Hlavin, M. L. (1992). Neurite growth on different substrates: Permissive versus instructive influences and the role of adhesive strength. *J-Neurosci.* **12**, 818-826.

Lemmon, V., Farr, K. L., and Lagenaur, C. (1989). L1-mediated axon outgrowth occurs via a homophilic binding mechanism. *Neuron* **2**, 1597-603.

Li, H., Chen, J., Wu, W., Fagaly, T., Zhou, L., Yuan, W., Dupuis, S., Jaing, Z., Nash, W., Gick, C., Ornitz, D.M., Wu, J.Y. and Rao, Y. (1999). Vertebrate slit, a secreted ligand for the transmembrane protein roundabout, is a repellent for olfactory bulb axons. *Cell* **96**, 807-818.

Liem, K.F.Jr., Tremml, G. and Jessell, T.M. (1997). A role for the roof plate and its resident TGFß-related proteins in neuronal patterning in the dorsal spinal cord. *Cell* **91**, 127-138.

Lierheimer, R., Kunz, B., Vogt, L., Savoca, R., Brodbeck, U., and Sonderegger, P. (1997). The neuronal cell-adhesion molecule axonin-1 is specifically released by an endogenous glycosylphosphatidylinositol-specific phospholipase D. *Eur-J-Biochem.* **243**, 502-10.

Lin, D.M. and Goodman, C.S. (1994). Ectopic and increased expression of fasciclin II altes motoneuron growth cone guidance. *Neuron* **13**, 507-523.

Lin, D.M., Fetter, R.D., Kopczynski, C., Grenningloh, G. and Goodman, C.S. (1994). Genetic analysis of Fasciclin II in Drosophila: Defasciculation, re-fasciculation, and altered fasciculation. *Neuron* **13**, 1055-1069

Long, K.E., Asou, H., Snider, M.D. and Lemmon, V. (2001). The role of endocytosis in regulating L1-mediated adhesion. *J-Biol-Chem.* **276** (2), 1285-1290.

Lowrie, M.B. and Lawson, S.. (2000). Cell death of spinal interneurons. *Prog-Neurobiol.* **61**, 543-555.

Lumsden, A.G.S. and Davies, A.M. (1983). Earliest sensory nerve fibres are guided to peripheral targets by attractants other than nerve growth factor. *Nature* **306**, 786-788.

Lustig, M., Sakurai, T. and Grumet, M. (1999). NrCAM promotes neurite outgrowth from peripheral ganglia by a mechanism involving Axonin-1 as a neuronal receptor. *Dev-Biol.* **209**, 340-351.

Lustig, M., Erskine, L., Mason, C.A., Grumet, M and Sakurai, T. (2001). NrCAM expression in the developing mouse nervous system: ventral midline structures, specific fiber tracts, and neuropilar regions. *J-Comp-Neurol.* **434** (1), 13-28.

Malhorta, J.D., Tsiotra, P., Karagogoes, D. and Hortsch, M. (1998) Cis-activation of L1-mediated ankyrin recruitment by TAG-1 homophilic cell adhesion. *J-Biol-Chem.* **273**, 33354-33359.

Mansour, S.L., Thomas, K.R., Deng, C. and Capecchi, M.R. (1990). Introduction of a lacZ reporter gene into the mouse *int-2* locus by homologous recombination. *P-N-A-S* **87**, 7688-7692.

Masuda, T., Okado, N. and Shiga, T. (2000). The involvement of axonin-1/SC2 in mediating notochord-derived chemorepulsive activities for dorsal root ganglion neurites. *Dev-Biol.* **224**, 112-121.

Matise, M.P. and Joyner, A.L. (1997). Expression patterns of developmental control genes in normal and *engrailed-1* mutant mouse spinal cord reveal early diversity in developing interneurons. *J-Neurosci.* **17** (20), 7805-7816.

Matise, M.P., Lustig, M., Sakurai, T., Grumet, M. and Joyner, A.L. (1999). Ventral midline cells are required for local control of commissural axon guidance in the mouse. *Development* **126**, 3649-3659.

Mauro, V.P., Krushel, L.A., Cunningham, B.A. and Edelman, G.M. (1992). Homophilic and heterophilic binding activities of Nr-CAM, a nervous system cell adhesion molecule. *J-Cell-Biol.* **119**, 191-202.

Messersmith, E., Leonardo, E.D., Shatz, C.J., Tessier-Lavigne, M., Goodman, C.S. and Kolodkin, A.L. (1995). Semaphorin III can function as a selective chemorepellant to pattern sensory projections in the spinal cord. *Neuron* **14**, 949-959.

Meyers, E.N. and Martin, G.R. (1999). Differences in left-right axis pathways in mouse and chick: functions of FGF8 and SHH. *Science* **285**, 403-406.

Milev, P., Friedlander, D.R., Sakurai, T., Karthikeyan, L., Flad, M., Margolis, R.K., Grumet, M. and Margolis, R.U. (1994). Interactions of the chondroitin sulfate proteoglycan phosphacan, the extracellular domain of a receptor-type protein tyrosine phosphatase, with neurons, glia, and neural cell adhesion molecules. *J-Cell-Biol.* **127**, 1703-1715.

Milev, P., Maurel, P., Haring, M., Margolis, R.K., Margolis, R.U. (1996). TAG-1/axonin-1 is a high affinity ligand of neurocan, phosphacan/protein tyrosine phosphatase-ß and N-CAM. *J-Biol-Chem.* **271**, 15716-15723.

Ming, G-L., Song, H-J., Berninger, B., Holt, C.E., Tessier-Lavigne, M and Poo, M-M. (1997). cAMP-dependent growth cone guidance by netrin-1. *Neuron* **19**, 1225-1235.

Ming, G-L., Henley, J., Tessier-Lavigne, M., Song, H-J. and Poo, M-M. (2001). Electrical activity modulates growth cone guidance by diffusible factors. *Neuron* **29**, 441-452.

Mock, B.A., Connely, M.A., McBride, O.W., Kozak, C.A. and Marcu, K.B. (1996). Plasmacytome-associated neuronal glycoprotein, P*ang*, maps to mouse chromosome 6 and human chromosome 3. *Genomics* **34**, 226-228.

Mombaerts, P., Wang, F., Dulac, C., Chao, S.K., Nemes, A., Mendelsohn, M., Edmundson, J. and Axel, R. (1996). Visualising an olfactory sensory map. *Cell* **87**, 675-686.

Monschau, B., Kremoser, C., Ohta, K., Tanaka, H., Kaneko, T., Yamada, T., Handwerker, C., Hornberger, M.R., Löschinger, J., Pasquale, E.B., Siever, D.A., Verderame, M.F., Müller, B.K., Bonhoeffer, F. and Drescher, U. (1997). Shared and distinct functions of RAGS and ELF-1 in guiding retinal axons. *EMBO* **16** (6), 1258-1267.

Montgomery, A. M., Becker, J. C., Siu, C. H., Lemmon, V. P., Cheresh, D. A., Pancook, J. D., Zhao, X., and Reisfeld, R. A. (1996). Human neural cell adhesion molecule L1 and rat homologue NILE are ligands for integrin alpha v beta 3. *J-Cell-Biol.* **132**, 475-85.

Morales, G., Sanchez Puelles, J. M., Schwarz, U., and de la Rosa, E. J. (1996). Synergistic neurite-outgrowth promoting activity of two related axonal proteins, Bravo/Nr-CAM and G4/Ng-CAM in chicken retinal explants. *Eur-J-Neurosci.* **8**, 1098-105.

Moran-Rivard, L., Kagawa, T., Saueressig, H., Gross, M.K., Burrill, J. and Goulding, M. (2001). *Evx1* is a postmitotic determinant of V0 interneuron identity in the spinal cord. *Neuron* **29**, 385-399.

Moré, M.I., Kirsch, F.P. and Rathjen, F.G. (2001). Targeted ablation of NrCAM or ankyrin-B results in disorganized lens fibers leading to cataract formation. *J-Cell-Biol.* **154**, 187-196.

Morini, A., Rozza, L., Manera, V., Buganza, M., Tranquillini, E. and Orrico, D. (1998). Isolated hypoglossal nerve palsy due to an anomalous vertebral artery course: report of two cases. *Ital-J-Neurol-Sci.* **19** (6), 379-382.

Moscoso, L.M., and Sanes, J.R. (1995). Expression of four immunoglobulin-superfamily adhesion molecules (L1, NrCAM/Bravo, Neurofascin/ABGP and NCAM) in the developing mouse spinal cord. *J-Comp-Neurol.* **352**, 321-334.

Mu, L. and Sanders, I. (1999). Neuromuscular organization of the canine tongue. *Anat-Rec.* **256** (4), 412-424.

Mueller, B.K. (1999). Growth cone guidance: first steps towards a deeper understanding. *Ann-Rev-Neurosci.* **22**, 351.

Nakagawa, S., Brennan, C., Johnson, K.G., Shewan, D., Harris, W.A. and Holt, C.E. (2000). Ephrin-B regulates the ipsilateral routing of retinal axons at the optic chiasm. *Neuron* **25**, 599-610.

Neugebauer, K. M., and Reichardt, L. F. (1991). Cell-surface regulation of beta1-integrin activity on developing retinal neurons. *Nature* **350**, 68-71.

Nguyen Ba-Charvet, K.T., Brose, K., Marillat, V., Kidd, T., Goodman, C.S., Tessier-Lavigne, M., Sotelo, C. and Chédotal, A. (1999). Slit2-mediated chemorepulsion and collapse of developing forebrain axons. *Neuron* **22**, 463-473.

Nguyen Ba-Charvet, K.T., Brose, K., Marillat, V., Sotelo, C., Tessier-Lavigne, M. and Chédotal, A. (2001). Sensory axon response to substrate-bound slit2 is modulated by laminin and cyclic GMP. *Mol-Cell-Neurosci.* **17**, 1048-1058.

Nörenberg, U., Hubert, M., Brummendorf, T., Tarnok, A., and Rathjen, F. G. (1995). Characterization of functional domains of the tenascin-R (restrictin) polypeptide: cell attachment site, binding with F11, and enhancement of F11-mediated neurite outgrowth by tenascin-R. *J-Cell-Biol.* **130**, 473-84.

Nose, A., Mahajan, V.B. and Goodman, C.S. (1992). Connectin: a homophilic cell adhesion molecule expressed on a subset of muscles and the motoneurons that innervate them in Drosophila. *Cell*, **70**, 553-567.

Nose, A., Umeda, T. and Takeichi, M. (1997). Neuromuscular target recognition by a homophilic interaction of connectin cell adhesion molecules in Drosophila. *Development* **124**, 1433-1441.

Ogawa, J., Kaneko, H., Masuda, T., Nagata, S., Hosoya, H. and Watanabe, K. (1996). Novel neural adhesion molecules in the contactin/F3 subgroup of the immunoglobulin superfamily: isolation and characterisation of cDNAs from rat brain. *Neurosci-Lett.* **218**, 173-176.

Okura, T., Arimoto, H., Tanuma, N., Matsumoto, K., Nakamura, T., Yamashima, T., Miyawza, T. and Matsumoto, Y. (1999). Analysis of neurotrophic effects of Hepatocyte growth factor in the adult hypoglossal nerve axotomy model. *Eur-J-Neurosci. 11* (11), 4139-4144.

O'Leary, D.D.M. and Wilkinson, D.G. (1999). Eph receptors and ephrins in neural development. *Curr-Biol-Neurobiol.* **9**, 65-73.

Oleszewski, M., Beer, S., Katich, S., Geiger, C., Zeller, Y., Rauch, U. and Altevogt, P. (1999). Integrin and neurocan binding to L1 involves distinct Ig domains. *J-Biol-Chem.* **274** (35), 24602-24610.

Oleszewski, M., Gutwein, P., von der Lieth, W., Rauch, U. and Altevogt, P. (2000). Characterization of the L1-neurocan-binding site: implications for L1-L1 homophilic binding. *J-Biol-Chem.* **275** (44), 34478-34485.

Olive, S., Dubois, C., Schachner, M. and Rougon, G. (1995). The F3 neuronal glyscophosphatidylinositol-linked molecule is localized to glycolipid-enriched membrane subdomains and interacts with L1 and fyn kinase in cerebellum. *J-Neurochem.* **65** (5), 2307-2317.

Oppenheim, R.W., Shneiderman, A., Shmizu, I. And Yaginuma, H. (1988). Onset and development of intersegmental projections in the chick embryo. *J. Comp. Neurol.* **275**, 159-180.

Orioli, D., Henkemeyer, M., Lemke, G., Klein, R. and Pawon, T. (1996). Sek4 and Nuk receptors cooperate in guidance of commissural axons and palate formation. *EMBO* **15** (22), 6035-6049.

Orlino, E.N., Wong, C.M. and Phelps, P.E. (2000). L1 and GAD65 are expressed on dorsal commissural axons in embryonic rat spinal cord. *Dev-Brain-Res.* **125**, 117-130.

Osumi, N., Hirota, A., Ohuchi, H., Nakafuku, M., Iimura, T., Kuatani, S., Fujiwara, M., Noji, S. and Eto, K. (1997). *Pax-6* is involved in the specification of hindbrain motor neuron subtype. *Development* **124**, 2961-2972.

Park, S., Frisén, J. and Barbacid, M. (1997). Aberrant axonal projections in mice lacking EphA8 (Eek) tyrosine protein kinase receptors. *EMBO* **16** (11), 3106-3114.

Paxinos, G. (1985). *The Rat Nervous System Volume 1: Forebrain and Midbrain.* Academic Press Inc., San Diego.

Paxinos, G., Törk, I., Tecott, L.H. and Valentino, K.L. (1991). *Atlas of The Developing Rat Brain.* Academic Press Inc., San Diego.

Peles, E., Nativ, M., Campbell, P. L., Sakurai, T., Martinez, R., Lev, S., Clary, D. O., Schilling, J., Barnea, G., Plowman, G. D., Grumet, M., and Schlessinger, J. (1995). The carbonic anhydrase domain of receptor tyrosine phosphatase beta is a functional ligand for the axonal cell recognition molecule contactin. *Cell* **82**, 251-60.

Peles, E., Nativ, M., Lustig, M., Grumet, M., Schilling, J., Martinez, R., Plowman, G. D., and Schlessinger, J. (1997). Identification of a novel contactin-associated transmembrane receptor with multiple domains implicated in protein-protein interactions. *EMBO* **16**, 978-88.

Perez-Castillo, A., Martin-Lucas, M.A. and Abrisqueta, J.A. (1984). Is a gene for microcephaly located on chromosome 1? *Hum-Genet.* **67** (2), 230-232.

Pesheva, P., Gennarini, G., Goridis, C. and Schachner, M. (1993). The F3/F11 cell adhesion molecule mediates the repulsion of neurons by the extracellular matrix glycoprotein J1-160/180. *Neuron* **10**, 69-82.

Pierani, A., Brenner-Morton, S., Chiang, C and Jessell, T.M. (1999). A sonic hedgehog-independent, retinoid-activated pathway of neurogenesis in the ventral spinal cord. *Cell* **97**, 903-915.

Pierani, A., Moran-Rivard, L., Sunshine, M.., Littman, D.R., Goulding, M. and Jessell, T.M. (2001). Control of interneuron fate in the developing spinal cord by the progenitor homeodomain protein Dbx1. *Neuron* **29**, 367-384.

Placzek, M., Tessier-Lavigne, M., Jessell, T.M. and Dodd, J. (1990a). Orientation of commissural axons in vitro in response to a floor plate derived chemoattractant. *Development* **110**: 19-30.

Placzek, M., Tessier-Lavigne, M., Yamada, T., Dodd, J. and Jessell, T.M. (1990). Guidance of developing axons by diffusible chemoattractants. *CSH-Symp-Quant-Biol.* **LV**, 279-289.

Placzek, M., Jessell, T.M. and Dodd, J. (1993). Induction of floor plate differentiation by contact-dependent, homeogenetic signals. *Development* **117**, 205-218.

Plagge, A., Sendtner-Voelderndorff, L., Sirim, P., Freigang, J., Rader, C., Sonderegger, P. and Brümmendorf, T. (2001). The contactin-related protein FAR-2 defines purkinje cell clusters and labels subpopulations of climbing fibers in the developing cerebellum. *Moll-Cell-Neurosci.* **18**, 91-107.

Pollerberg, E., Burridge, K. Krebs, K., Goodman, S., and Schachner, M. (1987). The 180 kD component of the neural cell adhesion molecule N-CAM is involved in cell-cell contacts and cytoskeleton-membrane interactions. *Cell-Tiss-Res.* **250**, 227-236.

Probstmeier, R., Kuhn, K. and Schachner, M. (1989). Binding properties of the neural cell adhesion molecule to different components of the extracellular matrix. *J-Neurochem.* **53**, 1794-1801.

Püschel, A.W., Adams, R.H. and Betz, H. (1995). Murine Semaphorin D/ Collapsin is a member of a diverse gene family and creates domains inhibitory for axonal extension. *Neuron* **14**, 941-948.

Püschel, A.W. (1999). Divergent properties of mouse netrins. *Mech-Dev.* **83**, 65-75.

Purves, D. and Lichtman, J.W. (1980). Elimination of synapses in the developing nervous system. *Science* **210**, 153-157.

Rader , C., Stoeckli, E.T., Zeigler, U., Osterwalder, T., Kunz, B. and Sonderegger, P. (1993). Cell-cell adhesion by homophilic interaction of the neuronal recognition molecule axonin-1. *Eur-J-Biochem.* **215**, 133-141.

Rader, C., Kunz, B., Lierheimer, R., Giger, R. J., Berger, P., Tittmann, P., Gross, H., and Sonderegger, P. (1996). Implications for the domain arrangement of axonin-1 derived from the mapping of its NgCAM binding site. *EMBO* **15**, 2056-68.

Raper, J.A., Bastiani, M. and Goodman, C.S. (1983a). Pathfinding by neuronal growth cones in grasshopper embryos I. Divergent choices made by the growth cones of sibling neurons. *J-Neurosci.* **3**, 20-30

Raper, J.A., Bastiani, M. and Goodman, C.S. (1983b). Pathfinding by neuronal growth cones in grasshopper embryos II. Selective fasciculation onto specific axonal pathways. *J-Neurosci.* **3**, 31-41

Raper, J.A., Bastiani, M. and Goodman, C.S. (1984). Pathfinding by neuronal growth cones in grasshopper embryos IV. The effects of ablating the A and P axons upon the behaviour of the G growth cone. *J-Neurosci.* **4**, 2329-2345

Rathjen, F.G. and Schachner, M. (1984). Immunocytological and biochemical characterisation of a new neuronal cell surface component (L1 antigen) which is involved in cell adhesion. *EMBO* **3** (1), 1-10.

Rathjen, F.G., Wolff, J.M., Frank, R., Bonhoeffer, F., Rutishauser, U. and Schoeffski, A. (1987 a). Membrane glycoproteins involved in neurite fasciculation. *J-Cell-Biol.* **104**, 343-353.

Rathjen, F.G., Wolff. J.M., Chang, S., Bonhoeffer, F. and Raper, J.A. (1987 b). Neurofascin: a novel chick cell-surface glycoprotein involved in neurite-neurite interactions. *Cell* **51**, 841-849.

Rathjen, F.G., Wolff, J.M. and Chquet-Ehrismann, R. (1991). Restrictin: a chick neural extracellular matrix protein involved in cell attachment co-purifies with the cell recognition molecule F11. *Development* **113**, 151-164.

Reid, R.A., Bronson, D.D., Young, K.M. and Hemperly, J.. (1994). Identification and characterization of the human cell adhesion molecule contactin. *Brain-Res-Mol-Brain-Res.* **21** (1-2), 1-8.

Rickman, D.S., Tyagi, R., Zhu, X-X., Bobek, M.P., Song, S., Blaivas, M., Misek, D.E., Israel, M.A., Kurnit, D.M., Ross, D.A., Kish, P.E. and Hanah, S.M. (2001). The gene for axonal cell adhesion molecule *TAX-1* is amplified and aberrantly expressed in malignant gliomas. *Cancer-Res.* **61**, 2162-2168.

Rogers, K.T. (1965). Development of the XIth or spinal accessory nerve in the chick, with some notes on the hypoglossal and upper cervical nerves. *J-Comp-Neurol.* **125**, 273-286.

Rogers, J.H., Ciossek, T., Menzel, P. and Pasquale, E.B. (1999). Eph receptors and ephrins demarcate cerebellar lobules before and during their formation. *Mech-Dev.* **87**, 119-128.

Rougon, G., Olive, S., Durbec, P., Faivre-Sarrailh, C. and Gennarini, G. (1994). Functional studies and cellular distribution of the F3 GPI-anchored adhesion molecule. *Braz-J-Med-Biol-Res.* **27** (2), 409-414.

Ruegg, M.A., Stoeckli, E.T., Lanz, R.B., Streit, P. and Sonderegger, P. (1989). A homologue of the axonally secreted protein axonin-1 is an integral membrane protein of nerve fibre tracts involved in neurite fasciculation. *J-Cell-Biol.* **109**, 2363-2378.

Runko, E., Wideman, C. and Kaprielian, Z. (1999). Cloning and expression of VEMA: a novel ventral midline antigen in the rat CNS. *Mol-Cell-Neurosci.* **14**, 428-443.

Rusch,J. and Van Vactor, D. (2000). New roundabouts send axons into the Fas lane. *Neuron* **28**, 637-640.

Saffell, J. L., Williams, E. J., Mason, I. J., Walsh, F. S., and Doherty, P. (1997). Expression of a dominant negative FGF receptor inhibits axonal growth and FGF receptor phosphorylation stimulated by CAMs. *Neuron* **18**, 231-42.

Sakurai, T., Lustig, M., Nativ, M., Hemperly, J.J., Schlessinger, J., Peles, E. and Grumet, M. (1997). Induction of neurite outgrowth through contactin and Nr-CAM by extracellular regions of glial receptor tyrosine phosphatase ß. *J-Cell-Biol.* **136**, 907-918.

Sakurai, T., Lustig, M., Babiarz, J., Furley, A.J.W., Tait, S., Brophy, P.J., Brown, S.A., Brown, L.Y., Mason, C.A. and Grumet, M. (2001). Overlapping functions of the cell adhesion molecules NrCAM and L1 in cerebellar development. *J-Cell-Biol.* **154** (6), 1259-1273.

Salinas, P. (1999). Wnt factors in axonal remodelling and synaptogenesis. *Biochem-Soc-Symp.* **65**, 101-109.

Saueressig, H., Burrill, J. and Goulding, M. (1999). Engrailed-1 and netrin-1 regulate axon pathfinding by association interneurons that project to motor neurons. *Development* **126**, 4201-4212.

Schlessinger, J., Axelrod, D., Koppel, D.E., Webb, W.W. and Elson, E.L. (1977). Lateral transport of a lipid probe and labelled proteins on a cell membrane. *Science* **195**, 307-309.

Schmucker, D., Clemens, J., Shu, H., Worby, C.A., Xiao, J., and Zipursky, S.L. (2000). Drosophila Dscam is an axon guidance receptor exhibiting extraordinary molecular diversity. *Cell* **101**, 671-684.

Schneider, B.F. and Norton, S. (1979). Equivalent ages in rat, mouse and chick embryos. *Teratology* **19**, 273-278.

Schoenher, C.J., Paquette, A.J. and Anderson, D.J. (1996). Identification of potential target genes for the neuron-restrictive silence factor. *PNAS* **93**, 9881-9886.

Schott, G.D. and Wyke, M.A. (1981). Congenital Mirror Movements. *J-Neurol-Neurosurg-Psychiatry* **44** (7), 586-599.

Schuch, U., Lohse, M.J. and Schachner, M. (1989). Neural cell adhesion molecules influence second messenger systems. *Neuron* **3**, 13-20.

Schürmann, G., Haspel, J., Grumet, M. and Erickson, H.P. (2001). Cell adhesion molecule L1 in folded (horseshoe) and extended conormations. *Mol-Biol-Cell.* **12**, 1765-1773).

Schuster, C.M., Davis, G.W., Fetter, R.D. and Goodman, C.S. (1996). Genetic dissection of structural and functional components of synaptic plasticity. I. Fasciclin II controls synaptic stabilization and growth. *Neuron* **17**, 641-654.

Seeger, M., Tear, G., Ferres-Marco, D. and Goodman, C.S. (1993). Mutations affecting growth cone guidance in Drosophila: genes necessary for guidance toward or away from the midline. *Neuron* **10**, 409-426.

Sehgal, A., Boynton, A.L., Young, R.F., Vermeulen, S.S., Yonemura, K.S., Kohler, E.P., Aldape, H.C. Simrell, C.R. and Murphy, G.P. (1998). Cell adhesion molecule NrCAM is over-expressed in human brain tumours. *Int-J-Cancer* **76**, 451-458.

Serafini, T., Kennedy, T.E., Galko, M.J., Mirzayan, C., Jessell, T.M. and Tessier-lavigne, M. (1994). The netrins define a family of axon outgrowth promoting proteins homologous to *C. elegans* UNC-6. *Cell* **78**: 409-424

Serafini, T., Colamarino, S.A., Leonardo, E.D., Wang, H., Beddington, R., Skarnes, W.C. and Tessier-lavigne, M. (1996). Netrin-1 is required for commissural axon guidance in the developing vertebrate nervous sytem. *Cell* **87**, 1001-1014.

Shen, H.; Watanabe, M., Tomasiewicz, H., Rutishauser, U., Magnuson, T. and Glass, J.D. (1997). Role of 409-424 neural cell adhesion molecule and polysialic acid in mouse circadian clock function. *J-Neurosci.* **17** (13), 5221-5229.

Shiga, T. and Oppenheim, R.W. (1991). Immunolocalization studies of putative guidance molecules used by axons and gowth cones of intersegmental interneurons in the chick embryo spinal cord. *J-Comp-Neurol.* **310**, 234-252.

Shirasaki, R., Tamada, A., Katsumata, R and Murakami, F. (1995). Guidance of cerebellofugal axons in the rat embryo: directed growth toward the floor plate and subsequent elongation alongthe longitudinal axis. *Neuron* **14**, 961-972.

Shirasaki, R., Mirzayan, C., Tessier Lavigne, M., and Murakami, F. (1996). Guidance of circumferentially growing axons by netrin-dependent and -independent floor plate chemotropism in the vertebrate brain. *Neuron* **17**, 1079-88.

Shirasaki, R., Katsumata, R. and Murakami, F. (1998). Change in chemoattractant responsiveness of developing axons at an intermediate target. *Science* **279**, 105-107.

Shoji, H., Ito, T., Wakamatsu, Y., Hayasaka, N., Ohsaki, K., Oyanagi, M., Kominami, R., Kondoh, H. and Takahashi, N. (1996). Regionalised expression of the *Dbx* family homeobox genes in the embryonic CNS of mouse. *Mech-Dev.* **56**, 25-39.

Silos- Santiago, I. and Snider, W.D. (1992). Development of commissural neurons in the embryonic rat spinal cord. *J-Comp-Neurol.* **325**, 514-526.

Silos- Santiago, I. and Snider, W.D. (1994). Development of interneurons with isplateral projections in embryonic rat spinal cord. . *J-Comp-Neurol.* **342**, 221-231.

Simpson, J.H., Bland, K.S., Fetter, R.D. and Goodman, C.S. (2000). Short range and long range guidance by slit and its robo receptors: a combinatorial code of robo receptors controls lateral position. *Cell* **103**, 1019-1032.

Skynner, M.J., Slater, R., Sim, J.A., Allen, N.D. and Herbison, A.E. (1999). Promoter transgenics reveal multiple gonadotrophin-releasing-hormone-I-expxpressing cell populations of different embryological origin in mouse brain. *J-Neurosci.* **19** (14), 5955-5966.

Slack, J. (2001). *Essential Developmental Biology*. Blackwell Science, Oxford.

Slack, R.S. and Miller, F.D. (1996). Viral vectors for modulating gene expression in neurons. *Curr-Op-Neurobiol.* **6**, 576-583.

Small, S.J., Haines, S.L. and Akeson, R.A. (1988). Polypeptidevariation in an N-CAM extracellular immunoglobulin-like fold is developmentally regulated through alternative splicing. *Neuron* **1**, 1007-1017.

Sokoloff, A.J. (2000). Localization and contractile properties of intrinsic longitudinal motor units of the rat tongue. *J-Neurophysiol.* **84** (2), 827-835.

Sonderegger, P., and Rathjen, F. G. (1992). Regulation of axonal growth in the vertebrate nervous-system by interactions between glycoproteins belonging to two subgroups of the immunoglobulin superfamily. *J-Cell-Biol.* **119**, 1387-1394.

Song, H., Ming, G., He, Z., Lehmann, M., McKerracher, L., Tessier-Lavigne, M. and Poo, M. (1998). Conversion of neuronal growth cone responses from repulsion to attraction by cyclic nucleotides. *Science* **281**, 1515-1518.

Sperry, R.W. (1963). Chemoaffinity in the orderly growth of nerve fibre patterns and connections. *PNAS* **50**, 703-710.

Stein, E. and Tessier-Lavigne, M. (2001). Hierarchical organization of guidance receptors: silencing of netrin attraction by slit through a robo/DCC receptor complex. *Science* **291**, 1928-1938.

Stein, E., Zou, Y., Poo, M-M and Tessier-Lavigne, M. (2001). Binding of DCC by netrin-1 to mediate axon guidance independent of adenosine A2B receptor activation. *Science* **291**, 1976-1982.

Stoeckli, E.T., Kuhn, T.B., Duc, C.O., Ruegg, M.A. and Sonderegger, P. (1991). The axonally secreted protein axonin-1 is a potent substratum for neurite outgrowth. *J-Cell-Biol.* **112** (3), 449-455.

Stoeckli, E. T., and Landmesser, L. T. (1995). Axonin-1, Nr-CAM, and Ng-CAM play different roles in the in vivo guidance of chick commissural neurons. *Neuron* **14**, 1165-1179.

Stoeckli, E. T., Ziegler, U., Bleiker, A. J., Groscurth, P., and Sonderegger, P. (1996). Clustering and functional cooperation of Ng-CAM and axonin-1 in the substratum-contact area of growth cones. *Dev-Biol.* **177**, 15-29.

Stoeckli, E. T., Sonderegger, P., Pollerberg, G.E. and Landmesser, L.T. (1997). Interference with axonin-1 and Nr CAM interactions unmasks a floor plate activity inhibitory for commissural axons. *Neuron* **18**: 209-221.

Stoeckli, E. T., and Landmesser, L. T. (1998). Axon Guidance at choice points. *Curr-Op-Neurobiol.* **8**, 73-79.

Stoeckli, E.T. (2000). Waltzing mice add a new twist to the function of Eph B2. *Neuron* **25**, 276-286.

Stork, O., Welzel, H., Cremer, H and Schachner, M. (1997). Increased male aggression and neuroendocrine response in mice deficient for the neural cell adhesion molecule (NCAM). *Eur-J-Neurosci.* **9** (6), 1117-1125.

Stoker, A. and Dutta, R. (1998). Protein tyrosine phosphatases and neural development, *Bioessays* **20**, 463-472.

Su, X-D., Gastinel, L.N., Vaughn, D.E., Faye, I., Poon, P. and Bjorkman, P. (1998). Crystal structure of hemolin: a horseshoe shape with implications for homophilic adhesion. *Science* **281**, 991-995.

Sugawa, M., Ono, K., Yasui, Y., Kishi, T. and Tsumori, T. (1997). Enhancement of neurite outgrowth by the soluble form of human L1 (neural cell adhesion molecule). *Neuroreport* **8** (14), 3157-3162.

Sun, Q., Bahri, S., Schmid, A., Chia, W. and Zinn, K. (2000). Receptor tyrosine phosphatases regulate axon guidance across the midline of the Drosophila embryo. *Development* **127**, 801-812.

Suter, D.M., Pollerberg, G.E., Buchstaller, A ., Giger, R.J., Dreyer, W.J. and Sonderegger, P. (1995). Binding between the neural cell adhesion molecules axonin-1 and Nr-CAN/Bravo is involved in neuron-glia interactions. *J-Cell-Biol.* **131**, 1067-1081.

Tait, S., Gunn-Moore, F., Collinson, J.M., Huang, J., Lubetzki, C., Pedraza, L., Sherman, D.L., Colman, D.R. and Brophy, P.J. (2000). An oligodendrocyte cell adhesion molecule at the site of assembly of the paranodal axo-glial junction. *J-Cell-Biol* **150** (3), 657-666.

Takahashi, T. and Strittmatter, S.M. (2001). PlexinA1 autoinhibition by the plexin sema domain. *Neuron* **29**, 429-439.

Tanaka, H., Matsui, T., Agata, A., Tomura, M., Kubota, I., McFarland, K.C., Khor, B., Lee, A., Phillips, H.S. and Shelton, D.L. (1991). Molecular cloning and expression of a novel adhesion molecule, SC1. *Neuron* **7**, 535-545.

Taniguchi, M., Yuasa, S., Fujisawa, H., Naruse, I., Saga, S., Mishina, M. and Yagi, T. (1997). Disruption in the Semaphorin III/D gene causes severe abnormality in peripheral nerve projection. *Neuron* **19**, 519-530.

Tear, G., Harris, R., Sutaria, S., Kilomanski, K., Goodman, C.S. and Seeger, M.A. (1996). Commissureless controls growth cone guidance across the CNS midline in Drosophila and encodes a novel membrane protein. *Neuron* **16**, 501-514.

Tessier-Lavigne, M., Placzek, M., Lumsden, A.G.S., Dodd, J. and Jessell, T.M. (1988). Chemotropic guidance of developing axons in the mammalian central nervous system. *Nature* **336**, 775-778.

Tessier Lavigne, M., and Goodman, C. S. (1996). The molecular biology of axon guidance. *Science* **274**, 1123-33.

Thanos, S., Bonhoeffer, F. and Rutishauser, U. (1984). Fiber-fiber interaction and tectal cues influence the development of the chicken retinotectal projection. *PNAS* **81** (6), 1906-1910.

Togari, A., Mogi, M., Arai, M., Yamamoto, S. and Koshihara, Y. (2000). Expression of mRNA for axon guidance molecules, such as semaphorin-III, netrins and neurotrophins, in human osteoblasts and osteoclasts. *Brain Res.* **878**, 204-209.

Tongiorgi, E., Bernhardt, R.R. and Schachner, M. (1995). Zebrafish neurons express two L1-related molecules during early axonogenesis. *J-Neurosci-Res.* **42** (4), 547-561.

de la Torre, J.R., Höpker, V.H., Ming, G., Poo, M., Tessier-Lavigne, M., Hemmati-Brivanlou, A. and Holt, C.E. (1997). Turning of retinal growth cones in a netrin-1 gradient mediated by the netrin receptor DCC. *Neuron* **19**, 1211-1224.

Tracey, D.J. (1985). Chapter 7: Somatosensory System, in Paxinos, G., *The Rat Nervous System 2: Hindbrain and Spinal Cord.* Academic Press, Sydney, Australia.

Tran, T.S. and Phelps, P.E. (2000). Axons crossing in he ventral commissure express L1 and GAD65 in the ceveloping rat spinal cord. *Dev-Neurosci.* **22**, 228-236.

Treubert, U., and Brummendorf, T. (1998). Functional cooperation of beta1-integrins and members of the Ig superfamily in neurite outgrowth induction. *J-Neurosci.* **18**, 1795-805.

Tsiotra, P.C., Karagogeos, D., Theodorakis, K., Michaelidis, T.M., Modi, W.S., Furley, A.J., Jessell, T.M. and Papamatheakis, . (1993). Isolation of the cDNA and chromosomal localization of the gene (*TAX-1*) encoding the human axonal glycoprotein TAG-1. *Genomics* **18**, 562-567.

Tsiotra, P.C., Theodorakis, K., Papamatheakis, J. and Karagogeos, D. (1996). The fibronectin domains of the neural cell adhesion molecule TAX-1 are necessary and sufficient for homophilic binding. *J-Biol-Chem* **271** (46), 29216-29222.

Tuttle, R. and O'Leary, D.M. (1998). Neurotrophins rapidly modulate growth cone response to the axon guidance molecule, collapsin-1. *Mol-Cell-Neurosci.* **11**, 1-8.

Tzarfati-Majar, V., Burstyn-Cohen, T. and Klar, A. (2001). F-spondin is a contact-repellent molecule for embryonic motor neurons. *PNAS* **98** (8), 4722-4727.

Van Maele-Fabry, G., Clotman, F., Gofflot, F., Bosschaert, .J. and Picard, J.J. (1997). Postimplantation mouse embryos cultures *in vitro*: assessment with whole-mount immunostaining and *in situ* hybridization. *Int-J-Dev-Biol.* **41**, 365-374.

Varela-Echavarría, A., Pfaff, S.L. and Guthrie, S. (1996). Differential expression of LIM homeobox genes among motor neuron subpopulations in the developing chick brain stem. *Mol-Cell-Neurosci.* **8**, 242-257.

Varela-Echavarría and Guthrie, S. (1997). Molecules making waves in axon guidance. *Genes-Dev.* **11**, 545-557.

Varela-Echavarría, A., Tucker, A., Püschel, A.W. and Guthrie, S. (1997). Motor axon subpopulations respond differentially to the chemorepellents netrin-1 and semaphorin D. *Neuron* **18**, 193-207.

Vargesson, N., Luria, V., Messine, I., Erskine, L. and Laufer, E. (2001). Expression of Slit and Robo family members during vertebrate limb development. *Mech-Dev.* **106**, 175-180.

Vaughn, J.E., Phelps, P.E., Yamamoto, M. and Barber, R.P. (1992). Association interneurons of embryonic rat spinal cord transiently express the cell surface glycoprotein SNAP/TAG-1. *Dev-Dyn.* **194**, 43-51.

Vaughn, D.E. and Bjorkman, P.J. (1996). The (Greek) key to structures of neural adhesion molecules. *Neuron* **16**, 261-273.

Virgintino, D., Ambrosini, M., D'errico, P., Bertossi, M., Papadaki, C., Karagogeos, D. and Gennerini, G. (1999). Regional distribution and cell type-specific expression of the mouse F3 axonal glycoprotein: a developmental study. *J-Comp-Neurol.* **413**, 357-372.

Vogt, L., Giger, R.J., Ziegler, U., Kunz, B., Buchstaller, A., Hermens, W.T.J.M.C., Kaplitt, M.G., Rosenfeld, M.R., Pfaff, D.W., Verhaagen, J. and Sonderegger, P. (1996). Continuous renewal of the axonal pathway

sensor apparatus by insertion of new sensor molecules into the growth cone membrane. *Curr-Biol.* **6** (9), 1153-1158.

Volkmer, H., Leuschner, R., Zacharias, U., and Rathjen, F. G. (1996). Neurofascin induces neurites by heterophilic interactions with axonal NrCAM while NrCAM requires F11 on the axonal surface to extend neurites. *J-Cell-Biol.* **135**, 1059-1069.

Volkmer, H., Zacharias, U., Norenberg, U., and Rathjen, F., G. (1998). Dissection of complex molecular interactions of neurofascin with axonin-1, F11 and tenascin-R which promote attachment and neurite formation of tectal cells. *J-Cell-Biol.* **142**, 1083-1093.

Wang, H.U. and Anderson, D.J. (1997). Eph family transmembrane ligands can mediate repulsive guidance of trunk neural crest migration and motor axon outgrowth. *Neuron* **18**, 383-396.

Wang, H.U., Chen, Z-F. and Anderson, D.J. (1998). Molecular distinction and angiogenic interaction between embryonic arteries and veins revealed by ephrin-B2 and its receptor Eph-B4. *Cell* **93**, 741-753.

Wang, H. and Tessier-Lavigne, M. (1999). En Passant neurotrophic action of an intermediate axonal target in the developing mammalian CNS. *Nature* **401**, 765-769.

Wang, K.H., Brose, K., Arnott, D., Kidd, T., Goodman, C.S., Henzel, W. and Tessier-Lavigne, M. (1999 a). Biochemical purification of a mammalian slit protein as a positive regulator of sensory axon elongation and branching. *Cell* **96**, 771-784.

Wang, H., Copeland, N.G., Gilbert, D.J., Jenkins, N.A. and Tessier-Lavigne, M. (1999 b). Netrin-3, a mouse homolog of human NTN2L, is highly expressed in sensory ganglia and shows differential binding to netrin receptors. *J-Neurosci.* **19** (12), 4938-4947.

Wang, S-L., Kutsche, M., DiSciullo, G., Schachner, M. and Bogen, S.A. (2000). Selective malformation of the splenic white pulp border in L1-deficient mice. *J-Immunol.* **165**, 2465-2473.

Warren, T., Chandrasekhar, A., Kanki, J.P., Rangarajan, R., Furley, A.J. and Kuwada, J.Y. (1999). Molecular cloning and developmental expression of a zebrafish axonal glycoprotein similar to TAG-1. *Mech-Dev.* **80** (2), 197-201.

Wei, M-H., Karavanova, I., Ivanov, S.V., Popescu, N.C., Keck, C.L., Pack, S., Eisen, J.A. and Lerman, M.I. (1998). In silico- initiated cloning and molecular characterisation of a novel human member of the L1 gene family of neural cell adhesion molecules. *Hum-Genet.* **103** (3), 355-364.

Weiss, P. (1936). Selectivity controlling the central-peripheral relations in the nervous system. *Biol-Rev.* **11**, 494-531.

Wentworth, L. (1984). The development of the cervical spinal cord of the mouse embryo. II. A golgi analysis of sensory, commissural, and association cell differentiation. *J-Comp-Neurol.* **222**, 96-115.

White, F.A. and Behar, O. (2000). The development and subsequent elimination of aberrant peripheral axon projections in *Semaphorin 3A* null mutant mice. *Dev-Biol.* **225**, 79-86.

Whiting, J., Marshall, H., Cook, M., Krumlauf, R., Rigby, P.W.J., Stott, D. and Allemann, R.K. (1991). Multiple spatially specific enhancers are required to reconstruct the pattern of Hox-2.6 gene expression. *Genes & Development* **5**, 2048-2059.

Williams, A.F. and Barclay, A.N. (1988). The immunoglobulin superfamily- domains for cell surface recognition. *Ann-Rev-Immunol.* **6**, 381-405.

Williams, D.W., Tyrer, M. and Shepherd, D. (2000). Tau and tau reporters disrupt central projections of sensory neurons in Drosophila. *J-Comp-Neurol.* **428** (4), 630-640.

Wilson, J.R., Summer, A.J. and Eichelman, J. (1994). Abberant reinnervation following hypoglossal nerve damage. *Musc-Nerve* **17** (8), 931-935.

Winberg, M.L., Mitchell, K.J. and Goodman, C.S. (1998). Genetic analysis of the mechanisms controlling target selection: complementary and combinatorial functions of netrins, semaphorins and IgCAMs. *Cell* **93**, 581-591.

Winberg, M.L., Tamagnone, L., Bai, J., Comoglio, P.M., Montell, D. and Goodman, C.S. (2001). The transmembrane protein Off-Track associates with plexins and functions downstream of semaphorin signalling during axon guidance. *Neuron* **32**, 53-62.

Wolfer, D.P., Henehan-Beatty, A., Stoeckli, E. T., Sonderegger, P. and Lipp, H-P (1994). Distribution of TAG-1/Axonin-1 in fibre tracts and migratory streams of the developing mouse nervous system. *J-Comp-Neurol.* **345**: 1-32.

Wolfer, D.P., Giger, R.J., Stagliar, M., Sonderegger, P. and Lipp, H.P. (1998). Expression of the axon growth-related neural adhesion molecule TAG-1/axonin-1 in the adult mouse brain. *Anat-Embryol.* **197** (3), 177-185.

Wolff, J.M., Brummendorf, T. and Rathjen, F.G. (1989). Neural cell adhesion molecule F11: membrane interaction by covalently attached phosphatidylinositol. *Biochem-Biophys-Res-Comm.* **161** (2), 931-938.

Wong, E.V., Kenwrick, S., Willems, P. and Lemmon, V. (1995). Mutations in the cell adhesion molecule L1 cause mental retardation. *Trends Neurosci.* **18**, 168-172.

Wong, J.T.W., Yu, W.T.C. and O'Connor, T.P. (1997). Transmembrane grasshopper semaphorin I promotes axon outgrowth *in vivo*. *Development* **124**, 3597-3607.

Wright, D.E., White, F.A., Gerfen, R.W., Silos-Santiago, I. And Snider, W.D. (1995). The guidance molecule semaphorin III is expressed in regions of spinal cord and periphery avoided by growing sensory axons. *J-Comp-Neurol.* **361** (2), 321-333.

Xu, Q., Mellitzer, G., Robinson, V. and Wilkinson, D.G. (1999). *In vivo* cell sorting in complementary segmental domains mediated by Eph receptors and ephrins. *Nature* **399**, 267-271.

Xue, Y. and Honig, M.G. (1999). Ultrastructural observations on the expression of axonin-1: Implications for the fasciculation of sensory axons during outgrowth into the chick hindlimb. *J-Comp-Neuro.* **408**, 299-317.

Yamakawa, K., Huo, Y.K., Haendal, M.A., Hubert, R., Chen, X.N., Lyons, G.E. and Korenburg, J.R. (1998). DSCAM: a novel member of the immunoglobulin superfamily maps in a Down syndrome region and is involved in the development of the nervous system. *Hum-Mol-Genet.* **7** (2), 227-237.

Yamamoto, M., Bowyer, A.M., Crandell, J.E., Edwards, M. and Tanaka, H. (1986). Distribution of stage-specific neurite-associated proteins in the developing murine nervous system recognized by a monoclonal antibody. *J-Neurosci.* **6** (12), 3576-3594.

Yamamoto, M., Hassinger, L. and Crandell, J.E. (1990). Ultrastructural localization of stage-specific associated proteins in the developing rat cerebral and cerebellar cortices. *J-Neurocyto.* **19**, 619-627.

Yee, K.T., Simon, H.H., Tessier-Lavigne, M. and O'Leary, D.D.M. (1999). Extension of long leading processes and neuronal migration in the mammalian brain directed by the chemoattractant Netrin-1. *Neuron* **24**, 607-622.

Yokoyama, N., Romero, M.I., Cowan, C.A., Galvan, P., Helmbacher, F., Charnay, P., Parada, L.F. and Henkemeyer, M. (2001). Forward signalling mediated by Ephrin-B3 prevents contralateral corticospinal axons from r-crossing the spinal cord midline. *Neuron* **29**, 85-97.

Yoshihara, Y., Kawasaki, M., Tani, A., Tamada, A., Nagata, S., Kagamiyama, H. and Mori, K. (1994). BIG-1: a new TAG-1/F3-related member of the immunoglobulin superfamily with neurite outgrowth promoting activity. *Neuron* **13** (2), 415-426.

Yoshihara, Y., Kawasaki, M., Tamade, A., Nagata, S., Kagamiyama, H. and Mori, K. (1995). Overlapping and differential expression of BIG-2, BIG-1, TAG-1 and F3: four members of an axon-associated call adhesion molecule subgroup of the immunoglobulin superfamily. *J-Neurobiol.* **28**, 51-69.

Yu, H., Araj, H.H., Ralls, S.A. and Kolodkin, A.L. (1998). The transmembrane semaphorin Sema I is required in Drosophila for embryonic motor and CNS axon guidance. *Neuron* **20**, 207-220.

Yuan, W., Zhou, L., Chen, J., Wu, J.Y., Rao, Y. and Ornitz, D.M. (1999). The mouse SLIT family: secreted ligands for ROBO expressed in patterns hat suggest a role in morphogenesis and axon guidance. *Dev-Biol.* **212**, 290-306.

Yue, Y., Su, J., Cerretti, D.P., Fox, G.M., Jing, S. and Zhou, R. (1999). Selective inhibition of spinal cord neurite outgrowth and cell survival buy the Eph family ligand Ephrin-A5. *J-Neurosci.* **19**, 10026-10035.

Zallen, J. A., Yi, B. A., and Bargmann, C. I. (1998). The conserved immunoglobulin superfamily member SAX-3/Robo directs multiple aspects of axon guidance in *C. elegans*. *Cell* **92**, 217-27.

Zinn, K. and Sun, Q. (1999). Slit branches out: a secreted protein mediates both attractive and repulsive axon guidance. *Cell* **97**, 1-4.

Zisch, A.H., D'Alessandri, L., Ranscht, B., Falchetto, R., Winterhalter, K.H. and Vaughn, L. (1992). Neuronal cell adhesion molecule contactin/F11 binds to tenascin via its immunoglobulin-like domains. *J-Cell-Biol.* **119** (1), 203-213.

Zisch, A.H., Stallcup, W.B., Chong, L.D., Dahlin Huppe, K., Voshol, J., Schachner, M. and Pasquale, E.B. (1997). Tyrosine phosphorylation of L1 family adhesion molecules: implication of the Eph kinase Cek5. *J-Neurosci-Res.* **47**, 655-665.

Zou, Y Stoeckli, E., Chen, H. and Tessier-Lavigne, M. (2000). Squeezing axons out of the gray matter: a role for slit and semaphorin proteins from midline and ventral spinal cord. *Cell* **102**, 363-375.

Zuellig, R.A., Rader, C., Schroeder, A., Kalousek, M.B., Von Bohlen und Halbach, F., Osterwalder, T., Inan, C., Stoeckli, E.T., Affolter, H.U., Fritz, A., et al. (1992). The axonally secreted cell adhesion molecule axonin-1. Primary structure, immunoglobulin-like and fibronectin-type-III-like domains and glycosyl-phosphatidylinositol anchorage. *Eur-J-Biochem.* **204** (2), 453-463.